

UNCLASSIFIED

AD NUMBER: AD0876496

LIMITATION CHANGES

TO:

Approved for public release; distribution is unlimited.

FROM:

This document is subject to special export controls and each transmittal to foreign governments or foreign nationals may be made only with prior approval of AFRPL (RPPR/STINFO), Edwards, CA 93523.

AUTHORITY

ST-A AFRPL LTR, 29 SEP 1971

AFRPL-TR-70-115

AD876496

FINAL REPORT ON THE
DEVELOPMENT OF THE TILT-EDGE BELLOWS CONCEPT

L. E. Hulbert, T. M. Trainer, N. D. Ghadiali

Battelle Memorial Institute
Columbus Laboratories

TECHNICAL REPORT AFRPL-TR-70-115

October 1970

[Handwritten signature]
[Handwritten "70"]
[Handwritten "CB"]

AD No. _____
DDC FILE COPY

DDC
RECORDED
NOV 13 1970
INDEXED
[Handwritten "B"]

This document is subject to special export controls and each transmittal to foreign governments or foreign nationals may be made only with prior approval of AFRPL (RPPR/STINFO), Edwards, California 93523

Air Force Rocket Propulsion Laboratory
Directorate of Laboratories
Air Force Systems Command
Edwards Air Force Base
California

NOTICES

Qualified users may obtain copies of this report from the Defense Documentation Center.

When U. S. Government drawings, specifications, or other data are used for any purpose other than a definitely related Government procurement operation, the Government thereby incurs no responsibility nor any obligation whatsoever, and the fact that the Government may have formulated, furnished, or in any way supplied the said drawings, specifications, or other data, is not to be regarded by implication or otherwise, or in any manner licensing the holder or any other person or corporation, or conveying any rights or permission to manufacture use, or sell any patented invention that may in any way be related thereto.

If this copy is not needed, return to AFRPL (RPRPD), Edwards, California 93523.

This document is subject to special export controls and each transmittal to foreign governments or foreign nationals may be made only with prior approval of AFRPL (RPPR/STINFO), Edwards, California 93523.

ACCESSION FOR	
CFPTI	WRITE SECTION <input type="checkbox"/>
DDR	DIFF SECTION <input type="checkbox"/>
UNANNOUNCED	<input type="checkbox"/>
JUSTIFICATION	
BY	
DISTRIBUTION/AVAILABILITY CODES	
DIST.	AVAIL. and/or SPECIAL

[Handwritten signature]

AFRPL-TR-70-115

FINAL REPORT ON THE
DEVELOPMENT OF THE TILT-EDGE BELLOWS CONCEPT

L. E. Hulbert, T. M. Trainer, N. D. Ghadiali

Battelle Memorial Institute
Columbus Laboratories

TECHNICAL REPORT AFRPL-TR-70-115

October 1970

This document is subject to special export controls and each transmittal to foreign governments or foreign nationals may be made only with prior approval of AFRPL (RPPR/STINFO), Edwards, California 93523

Air Force Rocket Propulsion Laboratory
Directorate of Laboratories
Air Force Systems Command
Edwards Air Force Base
California

FORWORD

This report summarizes research conducted under USAF Contract No. F04611-68-C-0031 from January 1, 1968, through September, 1970. The Contract was established under Air Force Budget Program Structure No 623058, AFSC Project No. 3058, Program Element No. 6.24.05.18.F. The work was performed by the Battelle Memorial Institute, Columbus Laboratories for the Air Force Rocket Propulsion Laboratory, Directorate of Laboratories, Edwards Air Force Base, with Captain A. B. Spencer and Lt. E. Lantzer serving as contract managers. The principal contributors to the report were Mr. T. M. Trainer, Program Manager, Dr. L. E. Hulbert, Division Chief, and Dr. D. T. Hunter and Mr. N. D. Ghadiali, Research Engineers.

This technical report has been reviewed and is approved.

Edwin L. Lantzer
1st Lt., USAF
Project Engineer

ABSTRACT

A two and one-half year program was conducted to investigate the tilt-edge bellows concept. This involved the idea that the stresses at the convolution root and crown welds of a welded bellows could be minimized by appropriately tilting the convolution midsurfaces near the root and crown. The research program involved an extensive theoretical analysis of various convolution cross-sectional shapes to optimize the shape with respect to the maximum stress as well as the weld bead stresses. A particular optimized bellows with a 3.5-inch OD was fabricated and tested. The results of the tests verified that the tilt-edge bellows had superior fatigue resistance. Further, the fatigue failures occurred at positions away from the welds which verified that the weld bead stresses were small. Elimination of fatigue failures at the convolution and end fitting welds also resulted in reduced scatter in bellows fatigue life. This should allow fatigue life predictions to be made with greater confidence for tilt-edge bellows than for conventional welded bellows designs.

TABLE OF CONTENTS

	<u>Page</u>
INTRODUCTION	1
ANALYSIS OF GEOMETRIC PARAMETER VARIATIONS	3
Nomenclature for Tilt-Edge Welded Bellows	3
Determination of Optimum Tilt Angles for Tilt-Edge Welded Bellows	6
Effects of Variations in Span	14
Investigation of Sweep Radius Variation	24
Effects of Variations in Convolution Pitch.	36
OPTIMIZATION OF BELLOWS CONVOLUTION CROSS SECTIONS	48
Selection of Optimum Convolution Shapes	48
Study of End Fitting Stresses	58
ANALYSIS, FABRICATION, AND EVALUATION OF TILT-EDGE BELLOWS DESIGNS.	66
Fabrication and Evaluation of an Interim Tilt-Edge Bellows Design	66
Preliminary Fabrication Investigation	66
Bellows Manufacturer Selection	67
Interim Bellows Fabrication	68
Interim Bellows Inspection	68
Interim Bellows Tests	68
Interim Bellows Conclusions	79
Design, Fabrication, and Evaluation of an Optimum Bellows Configuration in Comparison With an Conventional Welded Bellows	79
Satisfactory Bellows Fabrication	82
Optimized Bellows Inspection	90
Optimized Bellows Evaluation	90
CONCLUSIONS	100
Theoretical Design Study	100
Fabrication	101
Experimental Program	101
RECOMMENDATIONS	103
APPENDIX A - ANALYSIS OF WELD AREA OF BELLOWS	105
APPENDIX B - ADDITIONAL SUBROUTINES TO AID IN THE INVESTIGATION OF WELDED BELLOWS	131
REFERENCES	254

LIST OF ILLUSTRATIONS

	<u>Page</u>
FIGURE 1. CROSS SECTION OF ONE CONVOLUTION OF A TYPICAL TILT-EDGE WELDED BELLOWS	4
FIGURE 2. CONFIGURATION OF ONE CONVOLUTION OF A TYPICAL TILT-EDGE BELLOWS. NUMBERS IN CIRCLES REFER TO THE PART NUMBERS OF THE MATHEMATICAL MODEL	5
FIGURE 3. TYPICAL MATHEMATICAL MODEL USED IN STUDY OF OPTIMUM TILT-EDGE WELDED BELLOWS	7
FIGURE 4. MATHEMATICAL MODEL OF INSIDE DIAMETER WELD AREA FOR TILT ANGLE STUDY OF 4-INCH BELLOWS	8
FIGURE 5. MATHEMATICAL MODEL OF OUTSIDE DIAMETER WELD AREA FOR TILT ANGLE STUDY OF 4-INCH BELLOWS	8
FIGURE 6. INSIDE DIAMETER MERIDIONAL WELD STRESS RATIOS FOR VARIOUS ID TILT ANGLES, 4-INCH WELDED BELLOWS, DEFLECTION LOADING	9
FIGURE 7. INSIDE DIAMETER MERIDIONAL WELD STRESS RATIOS FOR VARIOUS ID TILT ANGLES, 4-INCH WELDED BELLOWS, PRESSURE LOADING	9
FIGURE 8. OUTSIDE DIAMETER MERIDIONAL WELD STRESS RATIOS FOR VARIOUS OD TILT ANGL'S, 4-INCH WELDED BELLOWS, DEFLECTION LOADING	10
FIGURE 9. OUTSIDE DIAMETER MERIDIONAL WELD STRESS RATIOS FOR VARIOUS OD TILT ANGLES, 4-INCH WELDED BELLOWS, PRESSURE LOADING	10
FIGURE 10. OUTER SURFACE MERIDIONAL STRESSES IN AN AXIALLY COMPRESSED 3.5-INCH BELLOWS WITH 45° ID, 50° OD TILT ANGLES, ±5° CHORD ANGLES, 0.10-INCH SWEEP RADII AND 0.5304-INCH SPAN (Unit Deflection Per Unit Bellows Length)	20
FIGURE 11. OUTER SURFACE MERIDIONAL STRESSES IN AN AXIALLY COMPRESSED 3.5-INCH BELLOWS WITH 45° ID, 50° OD TILT ANGLES, ±5° CHORD ANGLES, 0.15373-INCH SWEEP RADII AND 0.6188-INCH SPAN (Unit Deflection Per Unit Bellows Length)	
FIGURE 12. OUTER SURFACE MERIDIONAL STRESSES IN AN INTERNALLY PRESSURIZED 3.5-INCH BELLOWS WITH 45° ID, 50° OD TILT ANGLES, ±5° CHORD ANGLES, 0.10-INCH SWEEP RADII AND 0.378-INCH SPAN (Pressure = 1 psi)	22

LIST OF ILLUSTRATIONS (Continued)

Page

- FIGURE 13. OUTER SURFACE MERIDIONAL STRESSES IN AN INTERNALLY PRESSURIZED 3.5-INCH BELLOWS WITH 45° ID, 50° OD TILT ANGLES, ±5° CHORD ANGLES, 0.15373-INCH SWEEP RADII AND 0.6188-INCH SPAN (Pressure = 1 psi) 23
- FIGURE 14. OUTER SURFACE MERIDIONAL STRESSES IN AN AXIALLY COMPRESSED 3-INCH BELLOWS WITH 45° ID, 50° OD TILT ANGLES, ±5° CHORD ANGLES, 0.11859-INCH SWEEP RADII, AND 0.5304-INCH SPAN (Unit Deflection Per Unit Bellows Length) 26
- FIGURE 15. OUTER SURFACE MERIDIONAL STRESSES IN AN AXIALLY COMPRESSED 3-INCH BELLOWS WITH 45° ID, 50° OD TILT ANGLES, ±5° CHORD ANGLES, 0.14495-INCH SWEEP RADII AND 0.5304-INCH SPAN (Unit Deflection Per Unit Bellows Length) 27
- FIGURE 16. OUTER SURFACE MERIDIONAL STRESSES IN AN INTERNALLY PRESSURIZED 3-INCH BELLOWS WITH 45° ID, 50° OD TILT ANGLES, ±5° CHORD ANGLES, 0.11859-INCH SWEEP RADII, AND 0.5304-INCH SPAN (Pressure = 1 psi) 28
- FIGURE 17. OUTER SURFACE MERIDIONAL STRESSES IN AN INTERNALLY PRESSURIZED 3-INCH BELLOWS WITH 45° ID, 50° OD TILT ANGLES, ±5° CHORD ANGLES 0.14495-INCH SWEEP RADII AND 0.5304-INCH SPAN (Pressure = 1 psi) 29
- FIGURE 18. OUTER SURFACE MERIDIONAL STRESSES IN AN AXIALLY COMPRESSED 3.5-INCH BELLOWS WITH 60° ID, 60° OD TILT ANGLES, ±5° CHORD ANGLES, 0.07-INCH SWEEP RADII AND 0.378-INCH SPAN (Unit Deflection Per Unit Bellows Length) 30
- FIGURE 19. OUTER SURFACE MERIDIONAL STRESSES IN AN AXIALLY COMPRESSED 3.5-INCH BELLOWS WITH 60° ID, 60° OD TILT ANGLES, ±5° CHORD ANGLES, 0.10-INCH SWEEP RADII AND 0.378-INCH SPAN (Unit Deflection Per Unit Bellows Length) 31
- FIGURE 20. OUTER SURFACE MERIDIONAL STRESSES IN AN INTERNALLY PRESSURIZED 3.5-INCH BELLOWS WITH 60° ID, 60° OD TILT ANGLES, ±5° CHORD ANGLES, 0.07-INCH SWEEP RADII AND 0.378-INCH SPAN (Pressure = 1 psi) 32
- FIGURE 21. OUTER SURFACE MERIDIONAL STRESSES IN AN INTERNALLY PRESSURIZED 3.5-INCH BELLOWS WITH 60° ID, 60° OD TILT ANGLES, ±5° CHORD ANGLES, 0.10-INCH SWEEP RADII AND 0.378-INCH SPAN (Pressure = 1 psi) 33
- FIGURE 22. INNER SURFACE MERIDIONAL STRESSES IN AN AXIALLY COMPRESSED 2-INCH BELLOWS WITH 50° ID, 55° OD TILT ANGLES, ±2.5° CHORD ANGLES, 0.08635-INCH SWEEP RADII AND 0.3476-INCH SPAN (Unit Deflection Per Unit Bellows Length) 39

LIST OF ILLUSTRATIONS (Continued)

	<u>Page</u>
FIGURE 23. OUTER SURFACE MERIDIONAL STRESSES IN AN AXIALLY COMPRESSED 2-INCH BELLOWS WITH 50° ID, 55° OD TILT ANGLES, ±2.5° CHORD ANGLES, 0.08635-INCH SWEEP RADII AND 0.3476-INCH SPAN (Unit Deflection Per Unit Bellows Length)	40
FIGURE 24. INNER SURFACE MERIDIONAL STRESSES IN AN AXIALLY COMPRESSED 2-INCH BELLOWS WITH 50° ID, 55° OD TILT ANGLES, ±5° CHORD ANGLES, 0.08785-INCH SWEEP RADII AND 0.3536-INCH SPAN (Unit Deflection Per Unit Bellows Length)	41
FIGURE 25. OUTER SURFACE MERIDIONAL STRESSES IN AN AXIALLY COMPRESSED 2-INCH BELLOWS WITH 50° ID, 55° OD TILT ANGLES, ±5° CHORD ANGLES, 0.08785-INCH SWEEP RADII AND 0.3536-INCH SPAN (Unit Deflection Per Unit Bellows Length)	42
FIGURE 26. INNER SURFACE MERIDIONAL STRESSES IN AN INTERNALLY PRESSURIZED 2-INCH BELLOWS WITH 50° ID, 55° OD TILT ANGLES, ±2.5° CHORD ANGLES, 0.08635 INCH SWEEP RADII AND 0.3476-INCH SPAN (Pressure = 1 psi)	43
FIGURE 27. OUTER SURFACE MERIDIONAL STRESSES IN AN INTERNALLY PRESSURIZED 2-INCH BELLOWS WITH 50° ID, 55° OD TILT ANGLES, ±2.5° CHORD ANGLES, 0.08635-INCH SWEEP RADII AND 0.3476-INCH SPAN (Pressure = 1 psi)	44
FIGURE 28. INNER SURFACE MERIDIONAL STRESSES IN AN INTERNALLY PRESSURIZED 2-INCH BELLOWS WITH 50° ID, 50° OD TILT ANGLES, ±5° CHORD ANGLES, 0.08785-INCH SWEEP RADII AND 0.3536-INCH SPAN (Pressure = 1 psi)	45
FIGURE 29. OUTER SURFACE MERIDIONAL STRESSES IN AN INTERNALLY PRESSURIZED 2-INCH BELLOWS WITH 50° ID, 55° OD TILT ANGLES, ±5° CHORD ANGLES, 0.08785-INCH SWEEP RADII AND 0.3536-INCH SPAN (Pressure = 1 psi)	46
FIGURE 30. OUTER SURFACE MERIDIONAL STRESSES IN AN AXIALLY COMPRESSED 1-INCH BELLOWS WITH 60° ID, 60° OD TILT ANGLES, ±5° CHORD ANGLES, 0.04392-INCH SWEEP RADII AND 0.1868-INCH SPAN (Unit Deflection Per Unit Bellows Length)	52
FIGURE 31. OUTER SURFACE MERIDIONAL STRESSES IN AN INTERNALLY PRESSURIZED 1-INCH BELLOWS WITH 60° ID, 60° OD TILT ANGLES, ±5° CHORD ANGLES, 0.04392-INCH SWEEP RADII AND 0.1868-INCH SPAN (Pressure = 1 psi)	53

LIST OF ILLUSTRATIONS (Continued)

Page

FIGURE 32. OUTER SURFACE MERIDIONAL STRESSES IN AN AXIALLY COMPRESSED 2-INCH BELLOWS WITH 55° ID, 60° OD TILT ANGLES, ±2.5° CHORD ANGLES, 0.08635-INCH SWEEP RADII AND 0.3546-INCH SPAN (Unit Deflection Per Unit Bellows Length)	54
FIGURE 33. OUTER SURFACE MERIDIONAL STRESSES IN AN INTERNALLY PRESSURIZED 2-INCH BELLOWS WITH 55° ID, 60° OD TILT ANGLES, ±2.5° CHORD ANGLES, 0.08635-INCH SWEEP RADII AND 0.3546-INCH SPAN (Pressure = 1 psi)	55
FIGURE 34. A TYPICAL UPPER END FITTING FOR A 3.5-INCH TILT-EDGE WELDED BELLOWS	59
FIGURE 35. A TYPICAL LOWER END FITTING FOR A 3.5-INCH TILT-EDGE WELDED BELLOWS	60
FIGURE 36. SETUP FOR MAKING AN INNER CONVOLUTION WELD	69
FIGURE 37. SETUP FOR MAKING AN OUTER CONVOLUTION WELD	70
FIGURE 38. PARTIAL DISASSEMBLY OF THE INNER-CONVOLUTION-WELD TOOLING	71
FIGURE 39. PARTIAL DISASSEMBLY OF THE OUTER-CONVOLUTION-WELD TOOLING	72
FIGURE 40. COMPLETE DISASSEMBLY OF THE OUTER -CONVOLUTION-WELD TOOLING	73
FIGURE 41. CROSS SECTION OF FIRST INTERIM BELLOWS SHOWING END-FITTING FAILURE AND END-FITTING INTERFERENCE	76
FIGURE 42. CROSS SECTION OF FATIGUE FRACTURE IN INNER TOROIDAL SEGMENT OF FOURTH CONVOLUTION OF INTERIM BELLOWS KT-1	77
FIGURE 43. FATIGUE FRACTURE IN FIGURE 42 AT HIGHER MAGNIFICATION	77
FIGURE 44. FATIGUE RESULTS OF STAINLESS STEEL FORMED BELLOWS AND STAINLESS STEEL COUPONS	78
FIGURE 45. CROSS SECTION OF UNSATISFACTORILY FABRICATED BELLOWS SPECIMEN	81
FIGURE 46. INNER-SURFACE MERIDIONAL STRESS IN UPPER LEAF OF 3.5-INCH WELDED BELLOWS AS DESIGNED, (Unit Axial Compression Per Unit Bellows Length)	83

LIST OF ILLUSTRATIONS (Continued)

	<u>Page</u>
FIGURE 47. INNER-SURFACE MERIDIONAL STRESS IN UPPER LEAF OF 3.5-INCH WELDED BELLOWS AS DESIGNED (Internal Pressure = 1 psi)	84
FIGURE 48. INNER-SURFACE MERIDIONAL STRESS IN UPPER LEAF OF 3.5-INCH WELDED BELLOWS AS FABRICATED (Unit Axial Compression Per Unit Bellows Length)	85
FIGURE 49. INNER-SURFACE MERIDIONAL STRESS IN UPPER LEAF OF 3.5-INCH WELDED BELLOWS AS FABRICATED, (Internal Pressure = 1 psi)	86
FIGURE 50. CROSS SECTION OF MODIFIED OPTIMIZED BELLOWS SPECIMEN	87
FIGURE 51. CONVOLUTION OF MODIFIED OPTIMIZED BELLOWS SPECIMEN SELECTED FOR MEASUREMENT	87
FIGURE 52. OUTER SURFACE MERIDIONAL STRESSES FOR INTERNAL PRESSURE IN AN EXACT MATHEMATICAL MODEL OF FABRICATED 3.5-INCH BELLOWS WITH 43° ID, 51.5° OD TILT ANGLES, 0.086-INCH PITCH AND 0.5950-INCH SPAN, (Internal Pressure = 1 psi)	88
FIGURE 53. OUTER SURFACE MERIDIONAL STRESSES FOR AXIAL TENSION OF AN EXACT MATHEMATICAL MODEL OF FABRICATED 3.5-INCH BELLOWS WITH 43° ID, 51.5° OD TILT ANGLES, 0.086-INCH PITCH AND 0.5950-INCH SPAN, (Unit Deflection Per Unit Bellows Length)	89
FIGURE 54. POOR END-FITTING WELD OF BELLOWS THAT WAS RETURNED FOR REWELDING	91
FIGURE 55. FATIGUE FAILURE COMPARISON OF OPTIMIZED TILT-EDGE BELLOWS WITH STANDARD BELLOWS	98
FIGURE A-1 MESH CONFIGURATION FOR MATHEMATICAL MODEL OF OD WELD OF 4-INCH WELDED BELLOWS WITH 35° EDGE TILT	109
FIGURE A-2 CONTOURS OF PRINCIPAL STRESS IN MATHEMATICAL MODEL OF OD WELD OF 4-INCH WELDED BELLOWS WITH 35° EDGE TILT DUE TO AN AXIAL DEFLECTION OF $\delta = 0.09838$ INCH PER CONVOLUTION	114
FIGURE A-3 CONTOURS OF PRINCIPAL STRESS IN MATHEMATICAL MODEL OF OD WELD OF 4-INCH WELDED BELLOWS WITH 15° EDGE TILT DUE TO AN AXIAL DEFLECTION OF $\delta = 0.09839$ INCH PER CONVOLUTION	115
FIGURE A-4 CONTOURS OF HOOP STRESS IN MATHEMATICAL MODEL OF OD WELD OF 4-INCH WELDED BELLOWS WITH 35° EDGE TILT DUE TO AN AXIAL DEFLECTION OF $\delta = 0.09838$ INCH PER CONVOLUTION	116

LIST OF ILLUSTRATIONS (Continued)

	<u>Page</u>	
FIGURE A-5	CONTOURS OF HOOP STRESS IN MATHEMATICAL MODEL OF OD WELD OF 4-INCH WELDED BELLOWS WITH 15° EDGE TILT DUE TO AN AXIAL DEFLECTION OF $\delta = 0.09838$ INCH PER CONVOLUTION	117
FIGURE A-6	CONTOURS OF PRINCIPAL STRESS IN MATHEMATICAL MODEL OF ID WELD OF 4-INCH WELDED BELLOWS WITH 35° EDGE TILT DUE TO AN AXIAL DEFLECTION OF $\delta = 0.09838$ INCH PER CONVOLUTION	118
FIGURE A-7	CONTOURS OF PRINCIPAL STRESS IN MATHEMATICAL MODEL OF ID WELD OF 4-INCH WELDED BELLOWS WITH 15° EDGE TILT DUE TO AN AXIAL DEFLECTION OF $\delta = 0.09838$ INCH PER CONVOLUTION	119
FIGURE A-8	CONTOURS OF PRINCIPAL STRESS IN MATHEMATICAL MODEL OF OD WELD OF 4-INCH WELDED BELLOWS WITH 35° EDGE TILT DUE TO AN INTERNAL PRESSURE OF 10.0 PSI	120
FIGURE A-9	CONTOURS OF PRINCIPAL STRESS IN MATHEMATICAL MODEL OF OD WELD OF 4-INCH WELDED BELLOWS WITH 15° EDGE TILT DUE TO AN INTERNAL PRESSURE OF 10.0 PSI	121
FIGURE A-10	CONTOURS OF PRINCIPAL STRESS IN MATHEMATICAL MODEL OF ID WELD OF 4-INCH WELDED BELLOWS WITH 35° EDGE TILT DUE TO AN INTERNAL PRESSURE OF 10.0 PSI	122
FIGURE A-11	CONTOURS OF PRINCIPAL STRESS IN MATHEMATICAL MODEL OF ID WELD OF 4-INCH WELDED BELLOWS WITH 15° EDGE TILT DUE TO AN INTERNAL PRESSURE OF 10.0 PSI	123
FIGURE A-12	VARIATION OF MAXIMUM STRESS WITH DISTANCE (s) MEASURED ALONG THE OUTER NORMAL FROM THE NOTCH TIP. CASE 1; 35° TILT ANGLE, OUTER WELD AXIAL LOADING	125
FIGURE A-13	VARIATION OF MAXIMUM STRESS WITH DISTANCE (s) MEASURED ALONG THE OUTER NORMAL FROM THE NOTCH TIP. CASE 1; 15° TILT ANGLE, OUTER WELD AXIAL LOADING	126
FIGURE B-1	INPUT SHEET FOR DATA SETS 13, 14, and 15	138
FIGURE B-2	ACTUAL ENCAPSULATED SHAPE	161
FIGURE B-3	INTERPRETATION OF MEASURED POINTS	161
FIGURE B-4	TRANSFORMED COORDINATES	161
FIGURE B-5	ENLARGED CROSS SECTIONAL VIEW OF A CONVENTIONAL 3.5-INCH WELDED BELLOWS JN-136	171

LIST OF ILLUSTRATIONS (Continued)

	<u>Page</u>
FIGURE B-6 INPUT DATA FOR SAMPLE PROBLEM FOR COMPUTING PROGRAM FIT	173
FIGURE B-7 OUTPUT DATA FROM COMPUTING PROGRAM FIT	178

LIST OF TABLES

	<u>Page</u>
TABLE 1. DIMENSIONS OF ONE CONVOLUTION OF MATHEMATIC MODEL OF A 2-INCH TILT-EDGE WELDED BELLOWS, SPAN = 0.3536 INCH, THICKNESS = 0.005 INCH	12
TABLE 2. DIMENSIONS OF ONE CONVOLUTION OF MATHEMATICAL MODEL OF A 3-INCH TILT-EDGE WELDED BELLOWS, SPAN = 0.5304 INCH, THICKNESS = 0.005 INCH	13
TABLE 3. MAXIMUM INSIDE DIAMETER WELD STRESSES IN A 2-INCH TILT-EDGE WELDED BELLOWS, UNIT AXIAL COMPRESSION PER UNIT BELLOWS LENGTH	15
TABLE 4. MAXIMUM INSIDE DIAMETER WELD STRESSES IN A 2-INCH, TILT-EDGE WELDED BELLOWS, INTERNAL PRESSURE OF 1 PSI	15
TABLE 5. MAXIMUM OUTSIDE DIAMETER WELD STRESSES IN A 2-INCH TILT-EDGE WELDED BELLOWS, UNIT AXIAL COMPRESSION PER UNIT BELLOWS LENGTH	16
TABLE 6. MAXIMUM OUTSIDE DIAMETER WELD STRESS IN A 2-INCH, TILT-EDGE WELDED BELLOWS, INTERNAL PRESSURE OF 1 PSI	16
TABLE 7. MAXIMUM INSIDE DIAMETER WELD STRESSES IN A 3-INCH, TILT-EDGE WELDED BELLOWS, UNIT AXIAL COMPRESSION PER UNIT BELLOWS LENGTH	17
TABLE 8. MAXIMUM INSIDE DIAMETER WELD STRESSES IN A 3-INCH, TILT-EDGE WELDED BELLOWS, INTERNAL PRESSURE OF 1 PSI	17
TABLE 9. MAXIMUM OUTSIDE DIAMETER WELD STRESSES IN A 3-INCH, TILT-EDGE WELDED BELLOWS, UNIT AXIAL COMPRESSION PER UNIT BELLOWS LENGTH	18
TABLE 10. MAXIMUM OUTSIDE DIAMETER WELD STRESSES IN A 3-INCH, TILT-EDGE WELDED BELLOWS, INTERNAL PRESSURE OF 1 PSI	19
TABLE 11. MAXIMUM RELATIVE MERIDIONAL STRESSES FOR 3-INCH, TILT-EDGE WELDED BELLOWS, SPAN = 0.5304 INCH, 45° ID TILT ANGLE AND 50° OD TILT ANGLE	34
TABLE 12. MAXIMUM RELATIVE MERIDIONAL STRESSES FOR 3.5-INCH, TILT-EDGE WELDED BELLOWS, SPAN = 0.378 INCH, SWEEP RADIUS, = 0.07 INCH AND 0.10 INCH	35
TABLE 13. MAXIMUM RELATIVE MERIDIONAL STRESSES IN TILT-EDGE WELDED BELLOWS OF DIFFERENT CONVOLUTION PITCH	38

LIST OF TABLES (Continued)

	<u>Page</u>
TABLE 14. AN OPTIMUM CONVOLUTION SHAPE FOR A 1-INCH, TILT-EDGE WELDED BELLOWS, ID TILT ANGLE = 60°, OD TILT ANGLE = 60°, SPAN = 0.1868 INCH	49
TABLE 15. AN OPTIMUM CONVOLUTION SHAPE FOR A 2-INCH, TILT-EDGE WELDED BELLOWS, ID TILT ANGLE = 50°, OD TILT ANGLE = 60°, SPAN = 0.3476 INCH	50
TABLE 16. AN OPTIMUM CONVOLUTION SHAPE FOR A 3-INCH, TILT-EDGE WELDED BELLOWS, ID TILT ANGLE = 45°, OD TILT ANGLE = 50°, SPAN = 0.5304 INCH	51
TABLE 17. AN OPTIMUM CONVOLUTION SHAPE FOR A 3.5-INCH, TILT-EDGE WELDED BELLOWS, ID TILT ANGLE = 50°, OD TILT ANGLE = 50°, SPAN = 0.378 INCH	56
TABLE 18. AN OPTIMUM CONVOLUTION SHAPE FOR A 3.5-INCH, TILT-EDGE WELDED BELLOWS, ID TILT ANGLE = 45°, OD TILT ANGLE = 50°, SPAN = 0.6188 INCH	57
TABLE 19. MAXIMUM WELD, FITTING, AND OVERALL RELATIVE STRESSES IN OPTIMUM SHAPED TILT-EDGE WELDED BELLOWS	61
TABLE 20. RELATIVE FITTING STRESSES SHOWING THE EFFECT OF END LEAF OD TILT ANGLE VARIATIONS FOR A 3.5-INCH, TILT-EDGE WELDED BELLOWS, ID TILT ANGLE = 45°, OD TILT ANGLE = 50°, SPAN = 0.6188 INCH	63
TABLE 21. RELATIVE FITTING STRESSES SHOWING THE EFFECT OF END LEAF THICKNESS FOR A 3.5-INCH, TILT-EDGE WELDED BELLOWS, ID TILT ANGLE = 45°, OD TILT ANGLE = 50°, SPAN = .6188 INCH	64
TABLE 22. THEORETICAL AND EXPERIMENTAL SPRING RATES FOR INTERIM BELLOWS SPECIMENS	74
TABLE 23. REVISED DIMENSIONS OF OPTIMIZED 3.5-INCH TILT-EDGE BELLOWS	90
TABLE 24. EXPERIMENTAL AND THEORETICAL SPRING RATES FOR FINAL BELLOWS SPECIMENS	92
TABLE 25. COMPARISON OF HYSTERESIS FOR STANDARD BELLOWS AND FINAL BELLOWS	93
TABLE 26. EXCESSIVE VARIATION IN THE FATIGUE LIFE OF STANDARD WELDED BELLOWS	95
TABLE 27. SIMILARITY OF FATIGUE CYCLES FOR OPTIMIZED BELLOWS SPECIMENS	97

LIST OF TABLES (Continued)

	<u>Page</u>
TABLE A-1 STRESS AT OUTER WELD OF 4-INCH BELLOWS WITH 35° EDGE TILT DUE TO AXIAL LOADING -- WITH AND WITHOUT SEPARATION OF MIDSURFACES OF ADJOINING LEAVES	111
TABLE A-2 DESCRIPTION OF CASES TREATED IN STUDY OF STRESSES IN WELD AREA OF BELLOWS WITH APPLIED EDGE LOADINGS	113
TABLE A-3 CALCULATED STRESSES AT NOTCH	127
TABLE A-4 DECREASE IN STRESS AT WELD DUE TO CHANGE IN EDGE TILT ANGLE FROM 15° TO 35°	129
TABLE B-1 COORDINATES FOR SHELL OF FIGURE B-1	160
TABLE B-2. COORDINATE AND THICKNESS MEASUREMENTS FOR 3-1/2-INCH BELLOWS JN136	172

GLOSSARY OF WELDED BELLOWS TERMS

- Bellows Axis** - Centerline of the bellows
- Bending Moment** - Bending couple acting on the bellows at a point. This couple is obtained by integrating through the thickness of the bellows the stresses anti-symmetrically distributed about the bellows midsurface.
- Chill Blocks** - Rings clamped onto a pair of bellows diaphragms adjacent to the point in which the diaphragms are to be welded together. These rings act as heat sinks during the welding operation.
- Chord Angle** - The angle subtended between the cone passing through the ID and OD weld beads of a bellows leaf and the plane passing through the ID weld bead of the leaf normal to the bellows axis.
- Circumferential Direction** - Direction tangent to the circle of intersection between the bellows midsurface and the plane drawn normal to the bellows axis.
- Convolution** - One of a set of identical elements of a bellows. In a welded bellows, one convolution is composed of two leaves.
- Crown** - The point of maximum diameter of a bellows convolution.
- Diaphragm** - One of a pair of stamped annular rings that are to be welded together at the ID to form a bellows convolution.
- Flat** - The straight sections of a welded bellows diaphragm adjacent to the ID or OD weld. These sections are made without curvature so that the chill blocks can make intimate contact with the diaphragms during the welding operation. In conventional welded bellows bellows, the "flats" are truly flat and perpendicular to the bellows axis. In the tilt-edge bellows the "flats" are, in fact, segments of cones.
- ID** - Inside Diameter
- Inner Surface** - Surface of the bellows leaves that would be wetted by a fluid filling the bellows. Because of the way that the shells are defined for computer program NONLIN, this is also the surface in the direction of the "inner normal" for all of the mathematical models used in NONLIN in this research

study.

- Leaf** - One half of a bellows convolution. The terms "leaf" and "diaphragm" are essentially interchangeable. However, "diaphragm" will be used in this report to denote the stamped rings before they are welded together. The term "leaf" will be used to denote the same stamped rings after they have been assembled into a bellows. The terms "upper leaf" and "lower leaf" will be used to denote the upper and lower leaves of a convolution welded at the ID when the tilted edges of the convolution are sloping downward.
- Membrane Force** - The resultant force acting at the point of the bellows in the direction of the midsurface of the bellows. This force is obtained by integrating through the bellows thickness the stresses that are symmetrically distributed about the bellows midsurface.
- Normal Direction** - The direction along the normal drawn to the bellows midsurface at any point.
- OD** - Outside diameter. Bellows will often be identified in terms of the nominal OD in the text. Thus, the term 3-inch bellows will mean a bellows with an OD of approximately 3 inches.
- Outer Surface** - The surface of the bellows leaves on the outside of the bellows. Also, the shell surface in the direction of the outer normal.
- Pitch** - Axial length subtended by one convolution. The pitch may be measured as the distance between the centers of two adjacent crown weld beads.
- Root** - The point on the bellows convolution having minimum distance from the axis.
- Span** - The radial distance subtended by a bellows convolution. $\text{Span} = 0.5 (\text{OD} - \text{ID})$
- Spring Rate** - The ratio between the axial force applied to a bellows and the axial deformation of the bellows.
- Strain Range** - The total difference in the strain imposed at a point of the bellows over a half cycle of a fatigue test. For a deflection fatigue test the strain range is the difference between the strain measured (or calculated) at the point of maximum axial compression and the strain at the point of maximum axial extension.

- Sweep** - A corrugation formed into the bellows diaphragm. It usually consists of a segment of a torus. Bellows may be formed of one or more sweeps and are often characterized in terms of the number of sweeps. Most of the bellows in this study are 3-sweep bellows.
- Sweep Radius** - The toroidal radius of a sweep. (Not the cylindrical radius of the torus segment.)
- Surface Stress** - Stress in the surface fibers of the bellows thickness. The surface stress is obtained by adding together the stresses due to the membrane forces and bending moments.
- Tilt Angle** - The angle between the outer normal for the conical section (flat) at the bellows root or crown and the bellows axis. For zero tilt angle the flat is normal to the bellows axis and thus the normal is directed along the axis.

SECTION I

INTRODUCTION

Under USAF Contract No. 04(611)-10532, an extensive experimental and theoretical study was made of formed and welded bellows and of diaphragms. As described, AFRPL Report TR 69-22,⁽¹⁾ one of the major conclusions of this study was that welded bellows, as they were being made, were unreliable under cyclic load conditions leading to fatigue failure. The scatter in the fatigue life data was so great that no meaningful correlation could be obtained between measured fatigue life and either the theoretically predicted, or experimentally measured maximum strains.

It was apparent that the reason for the erratic fatigue behavior of welded bellows was that the maximum strains occurred at the welds. Thus one of the determining factors in establishing the fatigue life of a welded bellows was the quality of the welding operation. It was known that even the highest quality welds degrade the material in the heat affected zones adjacent to the welds. Further, there is a considerable variability to be expected in the quality of the welds that are made on thin materials even with the best possible welding practices.

As a result of a theoretical study of welded bellows designs carried out under the above mentioned contract⁽¹⁾, a promising idea for changing the shape of the welded bellows cross section was discovered. To describe this shape change, it is first noted that welded bellows are formed with flat sections (called "flats") at the root and crown of each leaf. These flats are intended to mate with relatively heavy rings which act as heat sinks for the bellows when the root and crown welds are made.

In conventional welded bellows, the flats are normal to the bellows axis. As noted above, the maximum strains in such bellows occurred at the welds. By theoretical analysis, it was shown that tilting the bellows flats at an angle to the bellows axis could drastically reduce the stresses at both the root and crown welds.

Although this study was entirely theoretical, it showed that the effects of tilting the convolution edges (which will henceforth be called the tilt-edge effect) gave promise of eliminating many of the disadvantages described above for welded bellows. On the basis of this study, the Air Force Rocket Propulsion Laboratory initiated a new contract with Battelle-Columbus in January, 1968, to conduct theoretical and experimental investigations of the new tilt-edge welded bellows concept.

The initial phase of the research study consisted of a theoretical parameter study to determine by computer analysis the effects of changing tilt angles, span, pitch, and sweep radius, on the performance characteristics of tilt-edge welded bellows. This study demonstrated that tilt angles could be found which minimized the weld stresses for the range of bellows parameters studied. As a consequence of this parameter study, it was determined that the reduction in stresses at the root and crown welds mainly resulted from a reduction of the bending stresses. For conventional bellows the stresses

at the weld were predominantly bending stresses. The optimum tilt angles occurred when the bending stresses at the weld were minimized or eliminated.

The second phase of the research contract involved the design of an optimum configuration for a 3.5-inch tilt-edge bellows. A number of these bellows were fabricated and tested. The results of the tests verified that the tilt-edge design would perform as predicted by the theoretical analysis. In particular, fatigue failure at the welds was suppressed and fatigue lives were dramatically increased.

The present report summarizes the entire research program and gives many results of the theoretical and experimental analyses conducted. As a result of this investigation, it was concluded that the tilt-edge bellows concept does indeed permit design of superior welded bellows.

Two appendices are included in this report. Appendix A describes a detailed investigation of the stresses in the neighborhood of the weld beads. Appendix B gives a description of some new subroutines developed in this program to improve the capability of Program NONLIN.

SECTION II

ANALYSIS OF GEOMETRIC PARAMETER VARIATIONS

Welded bellows have so many design parameters that it would be prohibitively expensive to conduct a complete parametric study. Incomplete but extensive parameter studies of conventional welded bellows have been made previously with somewhat inconclusive results⁽²⁾. Nevertheless, a limited parametric study of tilt-edge bellows was considered necessary in the present study to determine the range of applicability of the tilt-edge bellows concept. Such a parameter study was also necessary to achieve a sufficient understanding of the concept to permit the design of tilt-edge bellows with optimum performance. An initial investigation was directed toward studying the effect of changing tilt angles on the stress distributions near the welds. Subsequent investigations considered the effect of changes in certain bellows dimensions on the stresses at the welds and on the angle of tilt necessary to achieve minimum stresses at the welds.

In this section, a description will be given first of the study of the effects of varying the tilt angles at the root and crowns of 2, 3, and 4-inch bellows, each with three sweeps. Following this, investigations into the effects of changing span, sweep radius and convolution pitch are described. Unless otherwise noted, the thickness was taken to be 0.005 inches in all bellows described in this section.

Nomenclature for Tilt-Edge Welded Bellows

A physical understanding of the various parameters used to describe tilt-edge welded bellows is important in order to appreciate better the effects of these parameters on the stress-deflection behavior of the bellows.

Figure 1 shows the cross section of a single convolution of a typical three-sweep, tilt-edge welded bellows, and the major parameters studied in the present investigation are indicated. The term "three sweep" denotes the number of toroidal sections (three) used in a leaf of the bellows. Conical segments, called "flats", are at the inside and outside diameter welds. These flat surfaces are required so that the chill blocks used in the welding process can make full contact with the bellows leaves and thereby effectively absorb the heat created during welding. During the present study, the sweep radii of the curved sections were normally assumed to be the same for all sweeps in a leaf. Finally, it is noted that the chord angles of the diaphragms are measured in a positive sense from the horizontal in a counterclockwise direction.

Figure 2 shows the cross section of a complete convolution with the dimensional parameters which were used to define the midsurface configurations of the tilt-edge bellows to be discussed in this report. These measurements are consistent with the required input data for Battelle's computer program NONLIN. NONLIN was used to perform the theoretical design studies reported herein. Note that the outer normal points down for the upper leaf and up for the lower leaf. In shell parts 2, 4, and 9 the outer normal points to the sweep center of curvature. For these sweeps the radius is entered in NONLIN as a negative value.

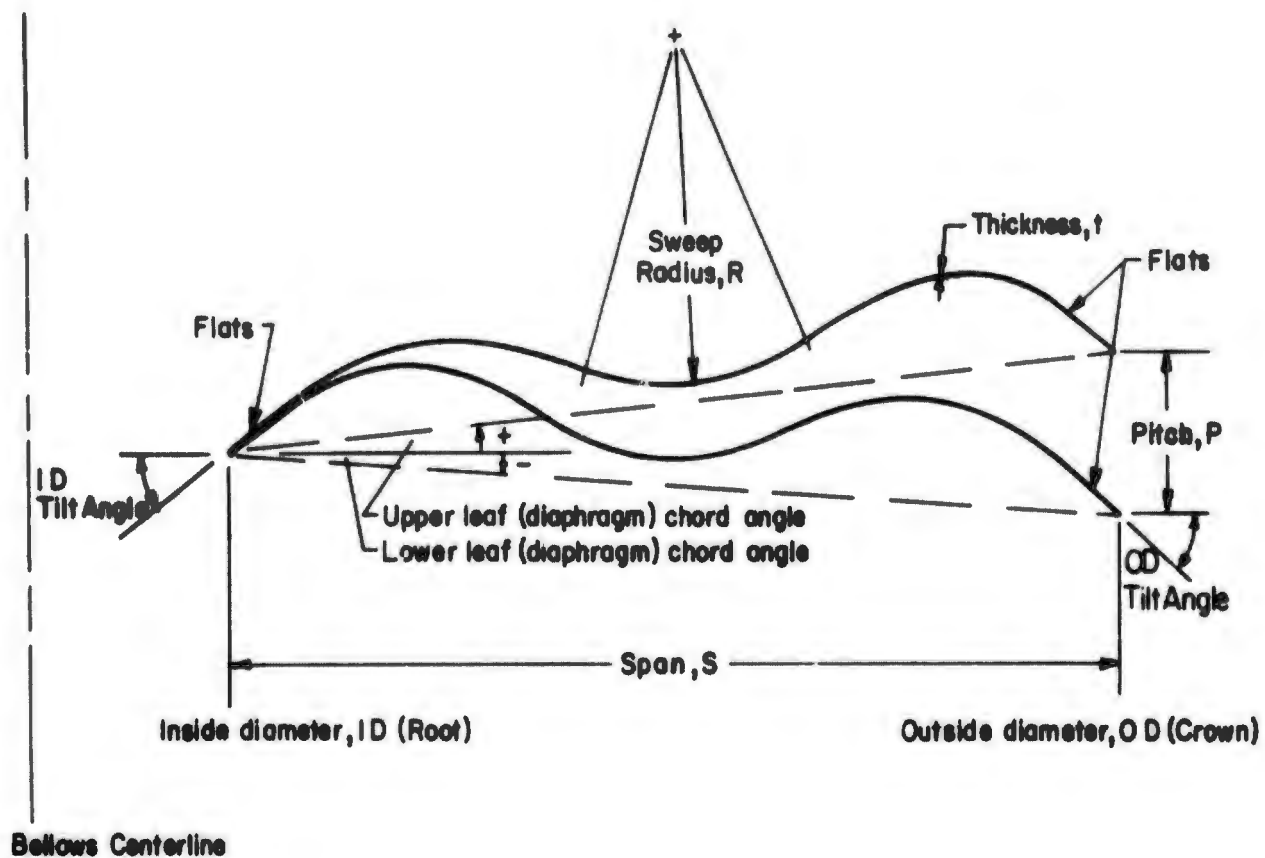


FIGURE 1. CROSS SECTION OF ONE CONVOLUTION OF A TYPICAL TILT-EDGE WELDED BELLOWS

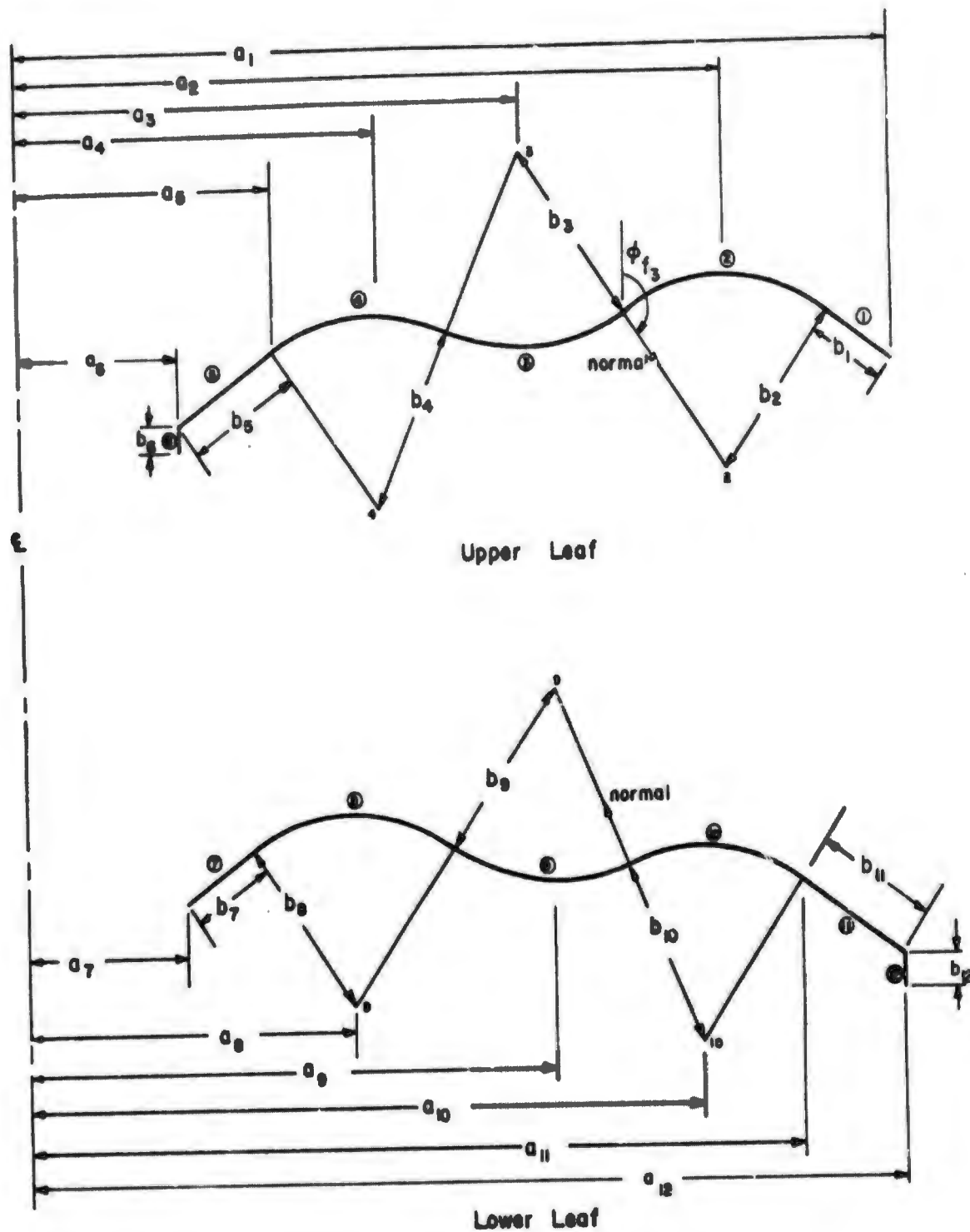


FIGURE 2. CONFIGURATION OF ONE CONVOLUTION OF A TYPICAL TILT-EDGE HELLOS. NUMBERS IN CIRCLES REFER TO THE PART NUMBERS OF THE MATHEMATICAL MODEL

Figure 3 depicts the typical mathematical model used to represent each bellows studied. The model consisted of four leaves (two convolutions) so that the stresses in the second and third leaves would not be affected by the boundary conditions imposed at the OD of the upper and lower leaves. Cylindrical rings were used to represent the weld beads at both the inner and outer leaf junctions. The lengths of the cylindrical sections were taken equal to the vertical distance between the centerlines of the upper and lower leaves at each weld. Normally, each leaf had three sweeps of equal radius plus conical segments at inside and outside ends of each leaf. In all cases, the bellows models were subjected to both an axial deflection loading and an internal pressure loading; calculations were made using linear, elastic, thin shell theory.

Determination of Optimum Tilt Angles for Tilt-Edge Welded Bellows

As stated earlier, Battelle's previous study of welded bellows demonstrated that tilting the flat sections of the edges of a welded bellows would lead to significant reduction in the stress levels near the root and crown diameter welds. Because of the importance of minimizing the weld stresses to achieve an "optimum" bellows design, the present study began with the investigation of the effects of inside and outside diameter tilt angles on the weld stresses in specific welded bellows shapes.

The previous study of the 4-inch, three-sweep bellows showed that the variations in the tilt angle at either the root or the crown had little effect on the stress distributions elsewhere in the bellows if the tilt angle was more than about 30° . Full use was made of this characteristic in a preliminary study of the effects of tilt angle on the weld stresses. In this preliminary study, models were set up as shown in Figures 4 and 5. These models consisted of the conical sections and parts of the torus sections nearest the root and crown welds. Models with tilt angles from 35° to 60° were analyzed for pressure loads and also for axial deflection loads. Membrane forces (N_1, N_2, N_3, N_4) and bending moments (M_1, M_2, M_3, M_4) taken from the analysis of the 4-inch bellows with 35° tilt angles were applied to the edges of the models. The results of this study combined with the previous analysis involving lower tilt angles are summarized in Figures 6 through 9. These figures show the ratio of the surface stresses at the welds to the maximum surface stress in the convolution (surface stress reduction ratio). The existence of tilt angles giving minimum stress conditions is clearly indicated. Although the angles for minimum stresses in the upper and lower leaves for pressure and deflection loads were not all the same, ID and OD tilt angles greater than 45° gave suitably low stresses.

The surface stresses in Figures 6 through 9 are the sum of the bending stresses and the membrane stresses. It is recalled that the membrane stress is constant through the thickness while the bending stress is antisymmetric about the bellows midsurface. An examination of the Figures shows that the large stresses at smaller tilt angles were almost entirely the result of bending stresses since the inner and outer surface stresses are almost equal in magnitude and of opposite sign.

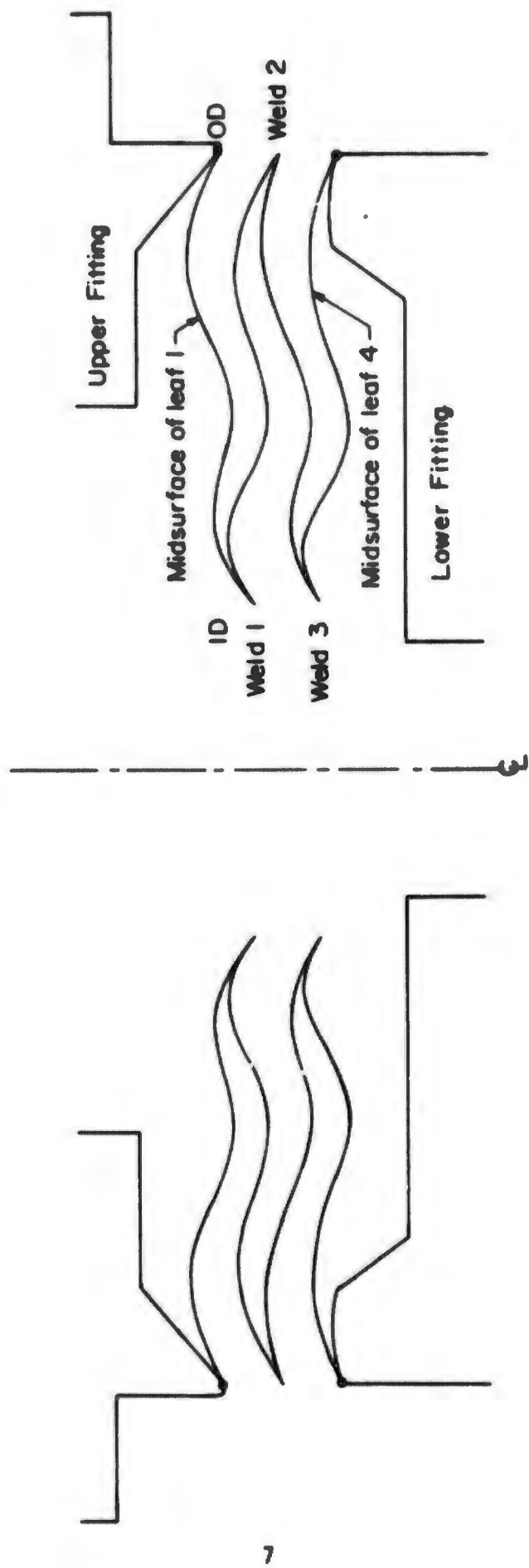


FIGURE 3. TYPICAL MATHEMATICAL MODEL USED IN STUDY OF OPTIMUM TILT-EDGE WELDED BELLOWS

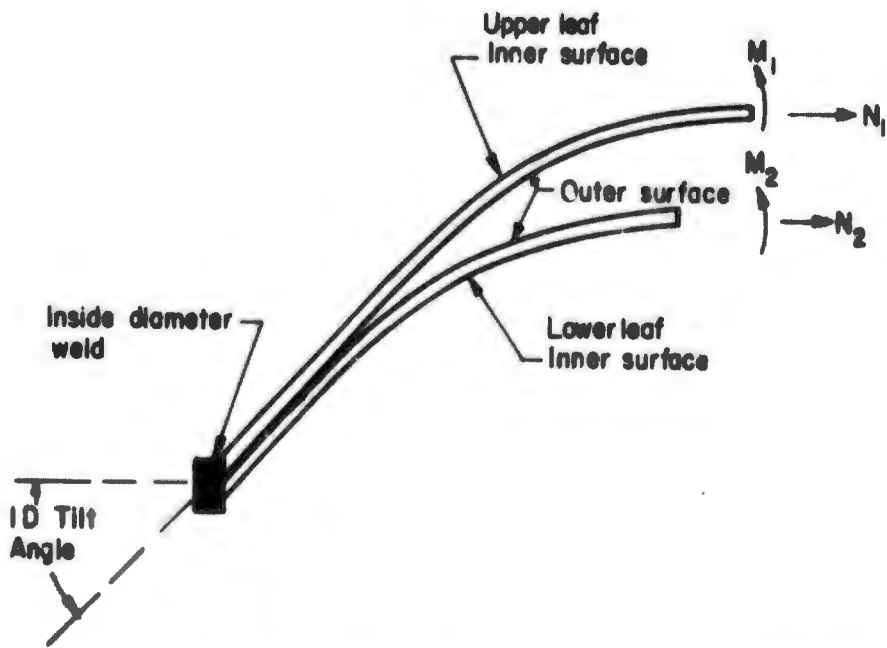


FIGURE 4. MATHEMATICAL MODEL OF INSIDE DIAMETER WELD AREA FOR TILT ANGLE STUDY OF 4-INCH BELLOWS

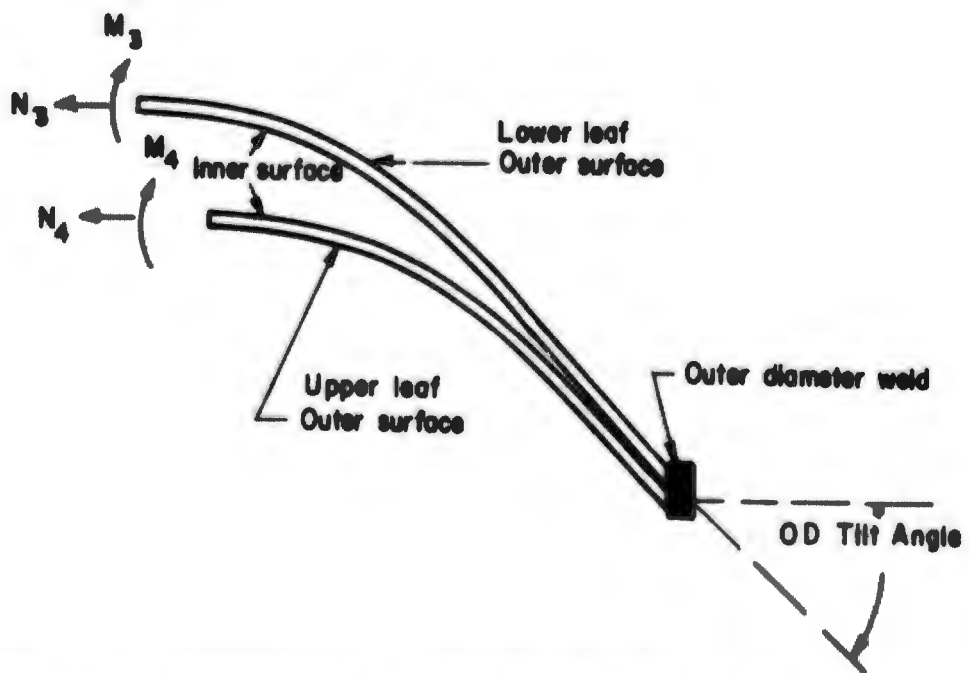


FIGURE 5. MATHEMATICAL MODEL OF OUTSIDE DIAMETER WELD AREA FOR TILT ANGLE STUDY OF 4-INCH BELLOWS

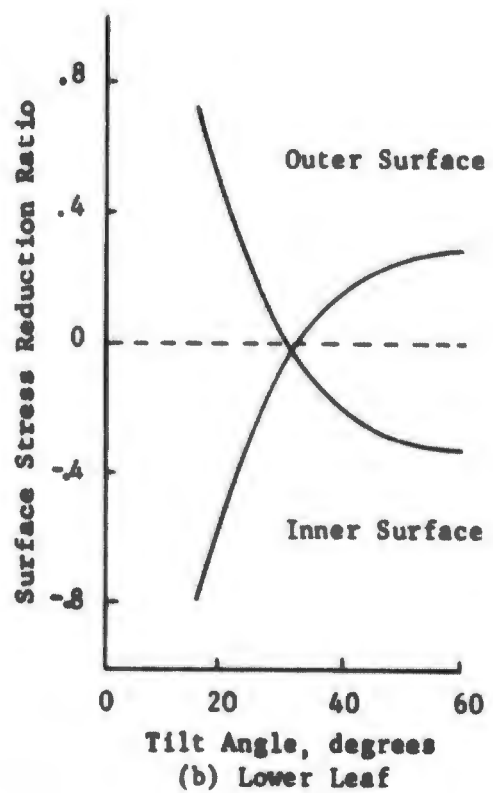
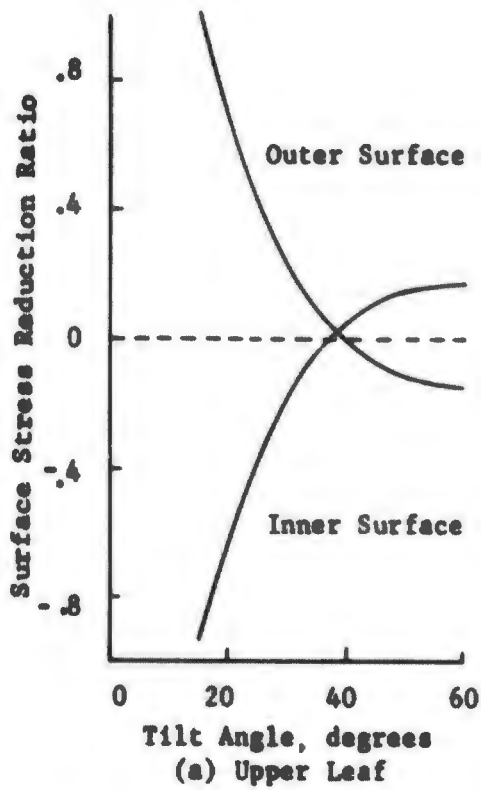


FIGURE 6. INSIDE DIAMETER MERIDIONAL WELD STRESS RATIOS FOR VARIOUS ID TILT ANGLES, 4-INCH WELDED BELLOWS, DEFLECTION LOADING

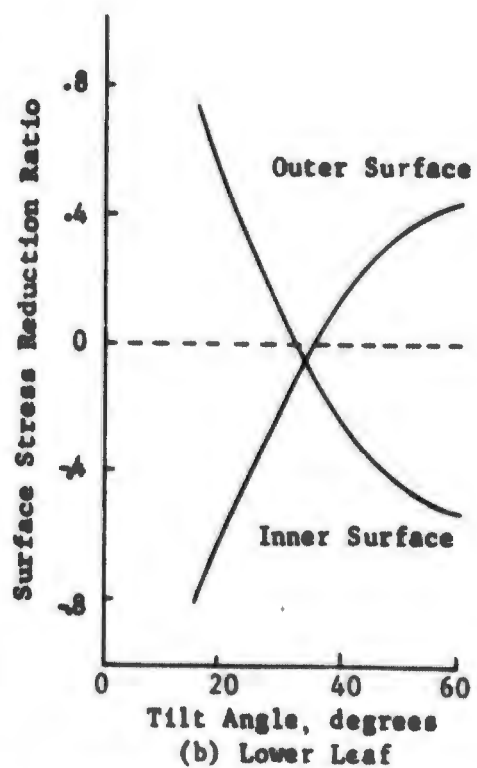
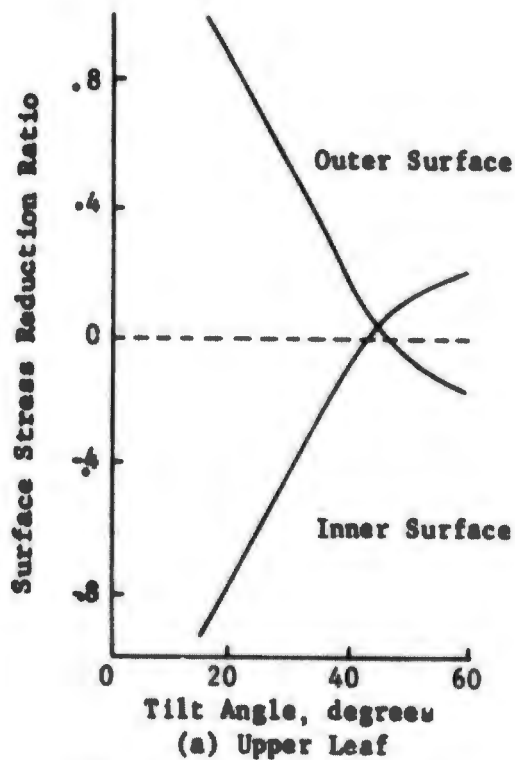


FIGURE 7. INSIDE DIAMETER MERIDIONAL WELD STRESS RATIOS FOR VARIOUS ID TILT ANGLES, 4-INCH WELDED BELLOWS, PRESSURE LOADING

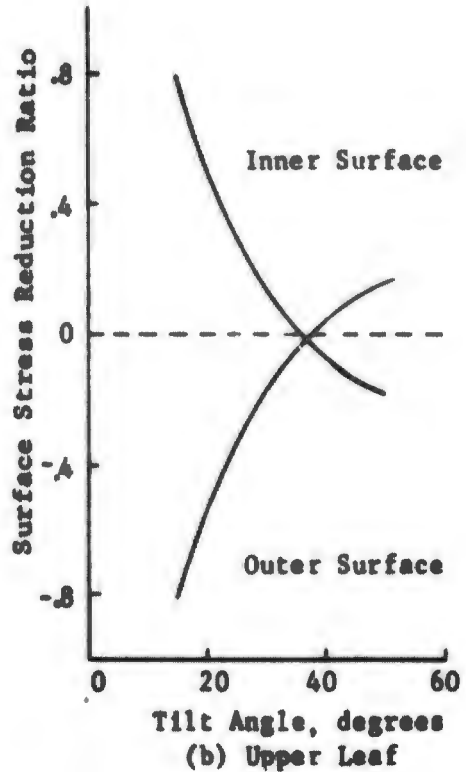
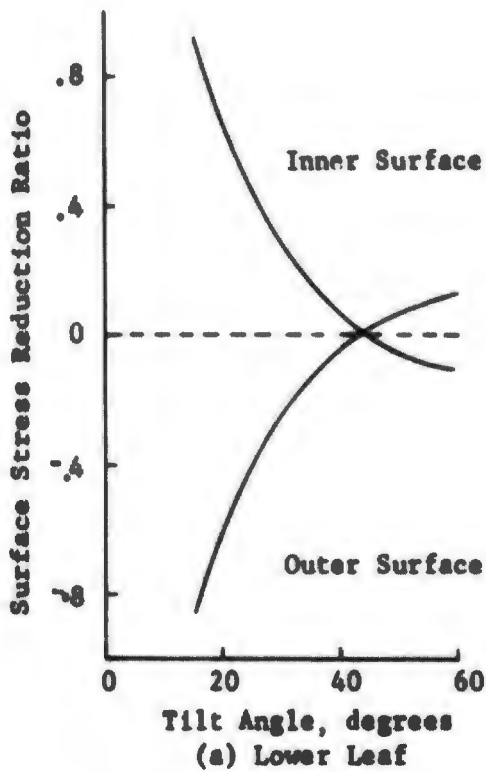


FIGURE 8. OUTSIDE DIAMETER MERIDIONAL WELD STRESS RATIOS FOR VARIOUS OD TILT ANGLES, 4-INCH WELDED BELLOWS, DEFLECTION LOADING

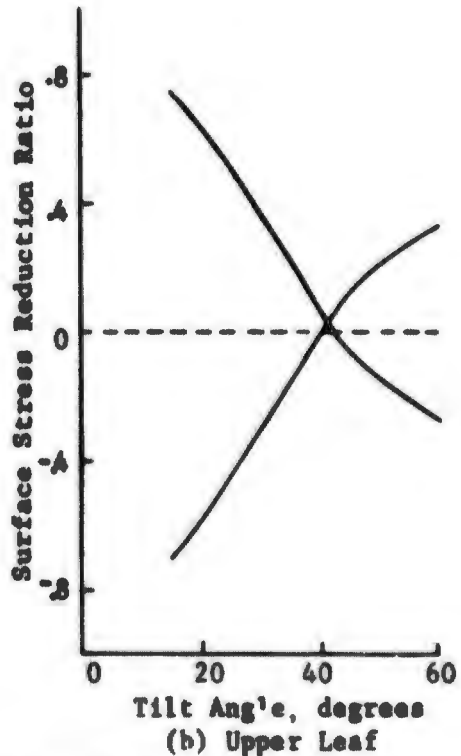
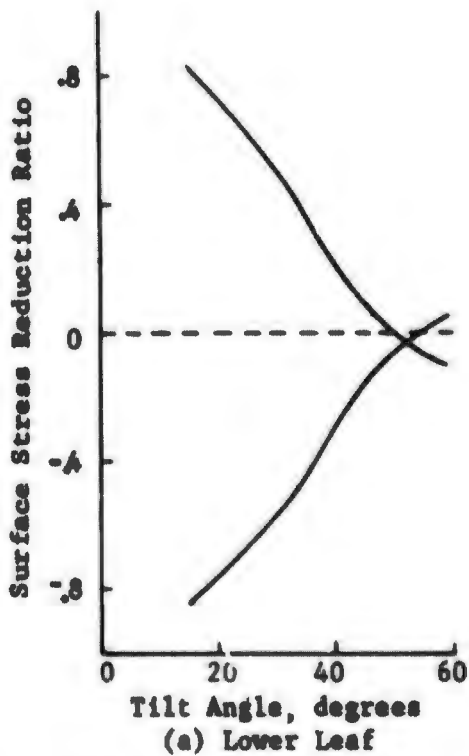


FIGURE 9. OUTSIDE DIAMETER MERIDIONAL WELD STRESS RATIOS FOR VARIOUS OD TILT ANGLES, 4-INCH WELDED BELLOWS, PRESSURE LOADING

The point at which the inner and outer stress curves cross is the point of zero bending stress. It is clear that this is the optimum tilt angle for the particular loading condition. Although the stresses for the conventional bellows with zero tilt angles are not shown, it was determined that stresses for these bellows were predominantly bending stresses. Thus the effect of increasing tilt angles was to reduce the bending stresses at the weld. At the optimum tilt angle the bending stresses were eliminated and the load was transferred from one leaf to the next by membrane action only.

At the higher tilt angles, the crossover in the sign of the surface stresses indicated a reversal in the bending moment. These reversed bending moments tended to bend the leaves toward each other. Since the leaves were already in contact along the flats, this reversed bending was suppressed and the stresses at the welds were thereby considerably reduced. If leaf contact was not accounted for in the theory, the predicted weld stresses were always conservative. Because of this, no attempt was made to account for the effects of the leaf interference at the welds except in the final design.

In further studies of the tilt angle effects, computer analyses were carried out for models of 2-inch and 3-inch bellows with various tilt angles. These studies used models having two complete bellows convolutions as shown in Figure 3. Table 1 lists the dimensions of a 2-inch bellows with 40° ID and 45° OD tilt angles. Table 2 lists the dimension of a corresponding 3-inch bellows with 45° ID and 50° OD tilt angles.* Analyses were made of other bellows identical to these except for the tilt angles and the lengths of the conical sections. Items indicated by asterisks in the tables must be changed to change the tilt angle. In each case the length of the conical section was chosen to give the same OD and ID as the bellows shown in Tables 1 and 2.

*Tables 1 and 2 list bellows dimensions in the format used for input into computer program NONLIN. The columns with heading "Outer Normal" give the angle between the outer normal and the upward bellows axis. These angles are measured at the initial and final ends of the bellows part when going in the direction of integration taken in NONLIN. This direction is from OD to ID on the upper leaf and from ID to OD on the lower leaf. For conical and cylindrical parts, the outer normal has constant direction. Thus, the final angle is not needed. The columns headed "a" and "b" list values of the radial dimensions a drawn in Figure 2 for the shell parts. As indicated earlier, negative values of b_2 , b_4 , and b_6 mean that the outer normal points toward the center of curvature of these toroidal shell sections.

TABLE 1. DIMENSIONS OF ONE CONVOLUTION OF MATHEMATICAL MODEL OF A 2-INCH TILT-EDGE WELDED BELLOWS, SPAN = 0.3536 INCH, THICKNESS = 0.005 INCH

Part No.	Shell Type	Outer Normal, degrees		Radii, inches	
		Initial	Final	a	b
<u>Upper Leaf</u>					
1	Conical	225*	--	1.04480	.02974*
2	Toroidal	225*	145	.96165	-.08785
3	Toroidal	145	205	.86085	.08785
4	Toroidal	205	140*	.78665	-.08785
5	Conical	140*	--	.73020*	.05088*
<u>ID Weld Bead</u>					
6	Cylindrical	90	--	.69120	.00652*
<u>Lower Leaf</u>					
7	Conical	-40*	--	.69120	.03360*
8	Toroidal	-40*	35	.77335	.08785
9	Toroidal	35	-25	.87415	-.08785
10	Toroidal	-25	45*	.94835	.08785
11	Conical	45*	--	1.0147*	.04850*
<u>OD Weld Bead</u>					
12	Cylindrical	90	--	1.04480	0.00707*

* These dimensions vary as the tilt angles at the inside and outside diameters are changed.

TABLE 2. DIMENSIONS OF ONE CONVOLUTION OF MATHEMATICAL MODEL OF A 3-INCH, TILT-EDGE WELDED BELLOWS, SPAN = 0.5304 INCH, THICKNESS = 0.005 INCH

Part No.	Shell Type	Outer Normal, degrees		Radii, inches	
		Initial	Final	a	b
<u>Upper Leaf</u>					
1	Conical	230*	--	1.56720	.03697*
2	Toroidal	230*	145	1.44247	-.13177
3	Toroidal	145	205	1.29127	.13177
4	Toroidal	205	135*	1.7997	-.13177
5	Conical	135*	--	1.08679*	.07070*
<u>ID Weld Bead</u>					
6	Cylindrical	90	--	1.03680	.00707*
<u>Lower Leaf</u>					
7	Conical	-45	--	1.03680	.04252*
8	Toroidal	-45*	35	1.16002	.13177
9	Toroidal	35	-25	1.31122	-.13177
10	Toroidal	-25	50*	1.42252	.13177
11	Conical	50*	--	1.52347*	.06802*
<u>OD Weld Bead</u>					
12	Cylindrical	90	--	1.56720	.00778*

* These dimensions vary as the tilt angles at the inside and outside diameters are changed.

Tables 3 through 6 list calculated meridional and circumferential surface stresses on the upper and lower bellows leaves at the welds for 2-inch bellows with different tilt angles. Tables 7 through 10 list similar stresses for 3-inch bellows. The stresses due to axial loading are given for an assumed unit compression per unit length of bellows (i.e., 1-inch deflection for a 1-inch long bellows). Pressure stresses are given for a 1 psi pressure load. For comparison, the range of maximum bellows stresses for each particular load condition is listed under each table. This maximum stress always occurred on one of the bellows sweeps.

Tables 3 and 5 show a minimum deflection stress at the welds of the 2-inch bellows for ID tilt angles between 45° and 50° and for OD tilt angles between 50° and 55° . In contrast, the pressure stresses tended to decline slightly even at the highest calculated tilt angles.

A study of Tables 7 through 10 indicates that the optimum ID tilt angle was 45° and the optimum OD tilt angle was 50° for the 3-inch bellows. A comparison of the tabulated weld stresses with the maximum bellows stress listed under each table shows that significant reduction of the weld stresses was achieved at each optimized tilt angle for both loading conditions.

From the results of this study, it was determined that optimum tilt angles could be found that gave significant reduction in weld stresses for both pressure loads and axial deflection loads. In fact, the weld stress reductions are of sufficient magnitude that complete prevention of weld failures could be expected in bellows made with the optimum tilt angles.

Effects of Variations in Span

In general, increasing the span of a conventional welded bellows decreases the axial deflection stresses and increases the stresses due to pressure loading. These effects on the stress levels are well known to the manufacturers and designers of such bellows. Such knowledge is often applied whenever a designer wishes to increase the deflection capability of a given bellows for which low design pressures are specified.

To study the effect of changing span for the tilt-edge welded bellows, a 3.5-inch mathematical model with a span of 0.6188 inch was analyzed. The results from this analysis were compared with results obtained for a 3.5-inch bellows with a span length of 0.378 inch. The tilt angles at the ID and OD for both sizes were 45° and 50° , respectively. The upper and lower leaf chord angles were $+5^{\circ}$ and -5° , respectively, for both bellows. The sweep radii and the pitch for the bellows with 0.6188 inch span were slightly larger than for the second bellows. Stresses were compared for both internal pressure and for axial deflection loadings.

Figures 10 through 13 are computer machine plots of the outer surface meridional stresses for the upper and lower leaves of the two bellows models. Because of the somewhat unconventional nature of the plots, they will be explained in some detail here. It is noted that this same format will be used throughout the remainder of this report for plotting the stress distributions.

TABLE 3. MAXIMUM INSIDE DIAMETER WELD STRESSES IN A 2-INCH,
TILT-EDGE WELDED BELLOWS, UNIT AXIAL COMPRESSION PER
UNIT BELLOWS LENGTH

ID Tilt Angle, degrees		Meridional Stress, psi		Circumferential Stress, psi	
		Inner	Outer	Inner	Outer
40	Upper Leaf	51,500	-59,500	20,600	-6,800
40	Lower Leaf	29,700	-21,600	30,800	8,900
45	Upper Leaf	31,000	-38,800	19,200	3,700
45	Lower Leaf	16,800	-8,800	27,600	14,400
50	Upper Leaf	34,200	-42,200	26,200	9,300
50	Lower Leaf	3,800	4,800	38,400	32,500

Maximum bellows stress for all cases was between 156,000 and 175,000 psi.

TABLE 4. MAXIMUM INSIDE DIAMETER WELD STRESSES IN A 2-INCH,
TILT-EDGE WELDED BELLOWS, INTERNAL PRESSURE OF 1 PSI

ID Tilt Angle, degrees		Meridional Stress, psi		Circumferential Stress, psi	
		Inner	Outer	Inner	Outer
40	Upper Leaf	690	-820	440	40
40	Lower Leaf	440	-310	520	230
45	Upper Leaf	440	-570	380	120
45	Lower Leaf	300	-180	450	260
50	Upper Leaf	400	-520	390	150
50	Lower Leaf	120	-4	460	370

Maximum bellows stress for all cases was -1030 psi.

TABLE 5. MAXIMUM OUTSIDE DIAMETER WELD STRESSES IN A 2-INCH, TILT-EDGE WELDED BELLOWS, UNIT AXIAL COMPRESSION PER UNIT BELLOWS LENGTH

OD Tilt Angle, degrees		Meridional Stress, psi		Circumferential Stress, psi	
		Inner	Outer	Inner	Outer
45	Upper Leaf	-25,800	30,700	-19,800	-6,700
45	Lower Leaf	-50,700	45,900	-23,600	8,900
50	Upper Leaf	-16,300	21,200	-19,200	-11,300
50	Lower Leaf	-36,400	31,600	-23,200	400
55	Upper Leaf	-8,200	13,500	-28,600	-26,000
55	Lower Leaf	-40,900	35,900	-30,500	-3,800

Maximum bellows stress for all cases was between 156,000 and 175,000 psi.

TABLE 6. MAXIMUM OUTSIDE DIAMETER WELD STRESS IN A 2-INCH, TILT-EDGE WELDED BELLOWS, INTERNAL PRESSURE OF 1 PSI

OD Tilt Angle, degrees		Meridional Stress, psi		Circumferential Stress, psi	
		Inner	Outer	Inner	Outer
45	Upper Leaf	370	-460	390	180
45	Lower Leaf	700	-620	460	30
50	Upper Leaf	270	-360	360	200
50	Lower Leaf	530	-450	420	100
55	Upper Leaf	150	-230	370	290
55	Lower Leaf	500	-420	420	120

Maximum bellows stress for all cases was -1030 psi.

TABLE 7. MAXIMUM INSIDE DIAMETER WELD STRESSES IN A 3-INCH,
TILT-EDGE WELDED BELLOWS, UNIT AXIAL COMPRESSION PER
UNIT BELLOWS LENGTH

ID	Tilt Angle, degrees		Meridional Stress, psi		Circumferential Stress, psi	
			Inner	Outer	Inner	Outer
35		Upper Leaf	22,600	-28,300	11,600	-200
35		Lower Leaf	7,900	-2,100	15,900	9,300
40		Upper Leaf	10,300	-15,600	10,800	6,200
40		Lower Leaf	-4,600	10,000	14,900	16,100
45		Upper Leaf	1,400	-6,200	10,700	11,300
45		Lower Leaf	-14,000	18,900	14,600	21,700

Maximum bellows stress for all cases was -119,000 psi.

TABLE 8. MAXIMUM INSIDE DIAMETER WELD STRESSES IN A 3-INCH,
TILT-EDGE WELDED BELLOWS, INTERNAL PRESSURE OF 1 PSI

ID	Tilt Angle, degrees		Meridional Stress, psi		Circumferential Stress, psi	
			Inner	Outer	Inner	Outer
35		Upper Leaf	950	1,170	640	80
35		Lower Leaf	490	260	700	390
40		Upper Leaf	570	-780	560	220
40		Lower Leaf	105	110	600	530
45		Upper Leaf	280	-480	500	330
45		Lower Leaf	-190	390	530	650

Maximum bellows stress for all cases was -1790 psi.

TABLE 9. MAXIMUM OUTSIDE DIAMETER WELD STRESSES IN A 3-INCH
TILT-EDGE WELDED BELLOWS, UNIT AXIAL COMPRESSION PER
UNIT BELLOWS LENGTH

OD Tilt Angle, degrees		Meridional Stress, psi		Circumferential Stress, psi	
		Inner	Outer	Inner	Outer
40	Upper Leaf	-22,900	19,400	-13,400	1,400
40	Lower Leaf	-5,800	9,400	-9,800	-7,400
45	Upper Leaf	-14,300	11,000	-13,300	-3,700
45	Lower Leaf	2,900	500	-10,100	-12,800
50	Upper Leaf	-7,300	4,300	-13,300	-8,000
50	Lower Leaf	10,100	-7,000	-10,600	-17,600
60	Upper Leaf	700	-3,200	-15,000	-14,700
60	Lower Leaf	18,900	-16,400	-13,800	-25,800

Maximum bellows stress for all cases was -119,000 psi.

TABLE 10. MAXIMUM OUTSIDE DIAMETER WELD STRESSES IN A 3-INCH,
TILT-EDGE WELDED BELLOWS, INTERNAL PRESSURE OF 1 PSI

ID	Tilt Angle, degrees		<u>Meridional Stress, psi</u>		<u>Circumferential Stress, psi</u>	
			Inner	Outer	Inner	Outer
40	Upper Leaf		950	-800	650	80
40	Lower Leaf		360	-510	500	290
45	Upper Leaf		680	-540	590	190
45	Lower Leaf		100	-240	460	400
50	Upper Leaf		470	-340	560	280
50	Lower Leaf		-110	-210	430	500
60	Upper Leaf		190	-70	550	450
60	Lower Leaf		-410	290	460	690

Maximum bellows stress for all cases was -1790 psi.

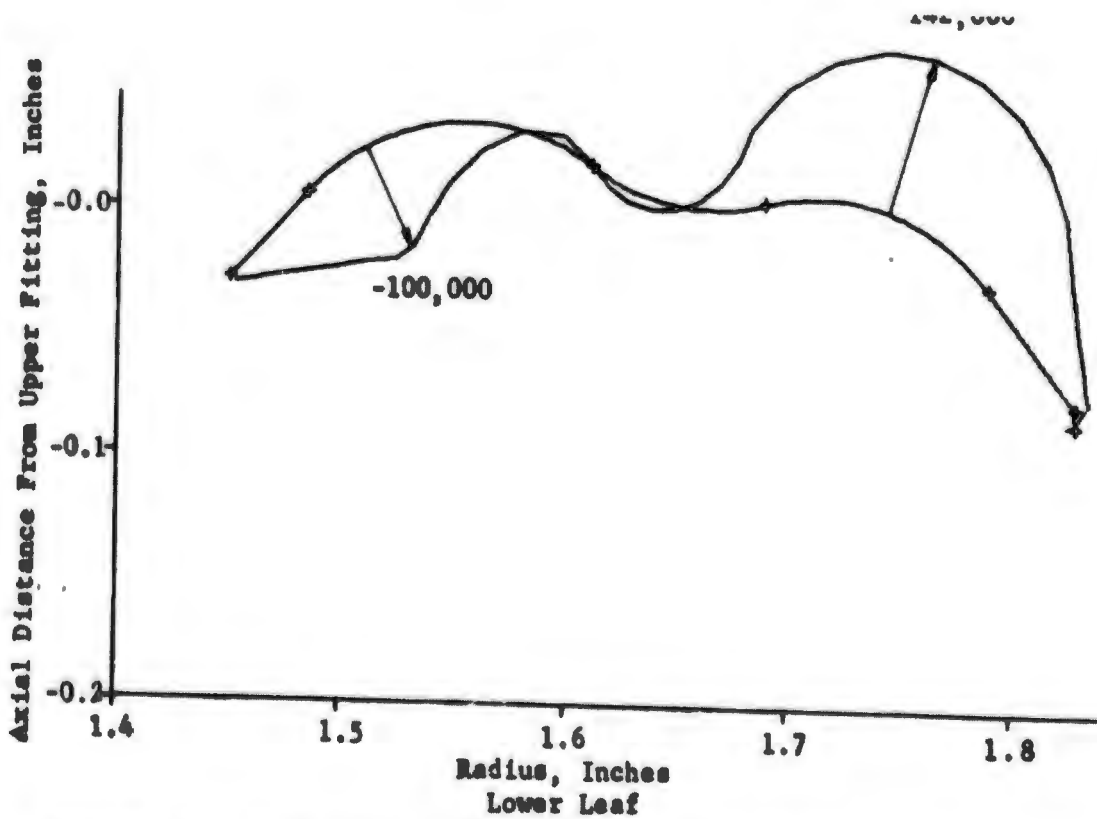
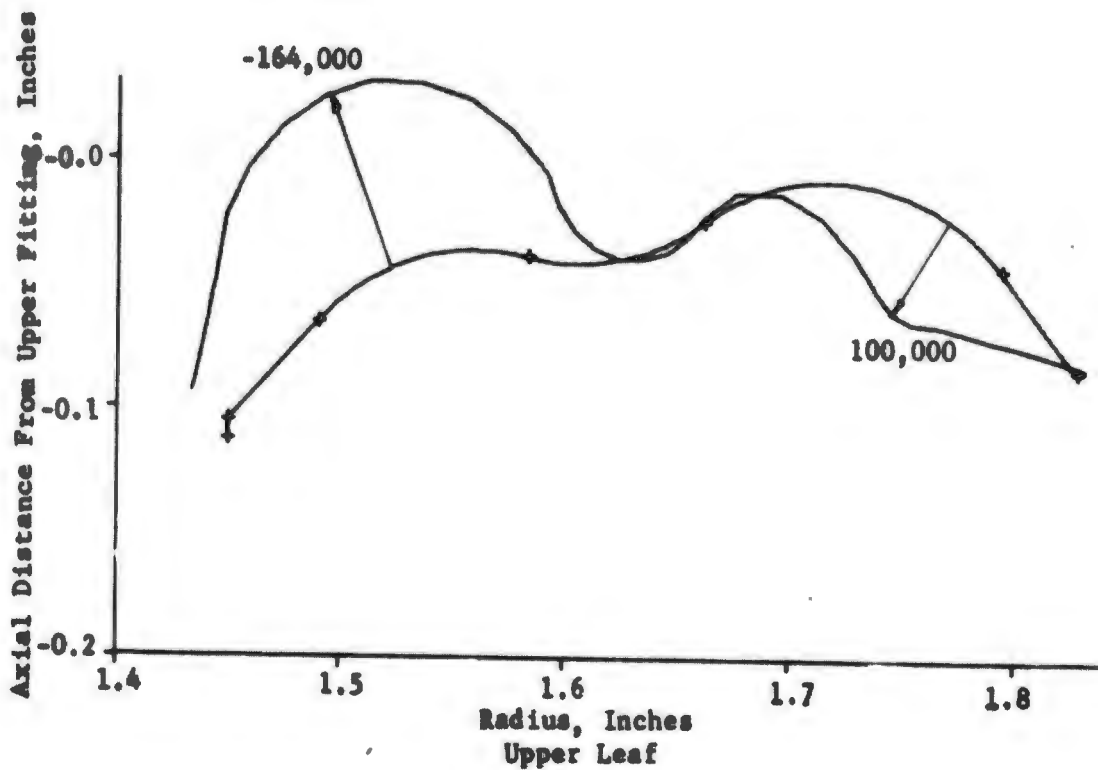


FIGURE 10. OUTER SURFACE MERIDIONAL STRESSES IN AN AXIALLY COMPRESSED 3.5-INCH BELLOWS WITH 45° ID, 50° OD TILT ANGLES, ±5° CHORD ANGLES, 0.10-INCH SWEEP RADII AND 0.378-INCH SPAN (Unit Deflection Per Unit Bellows Length)

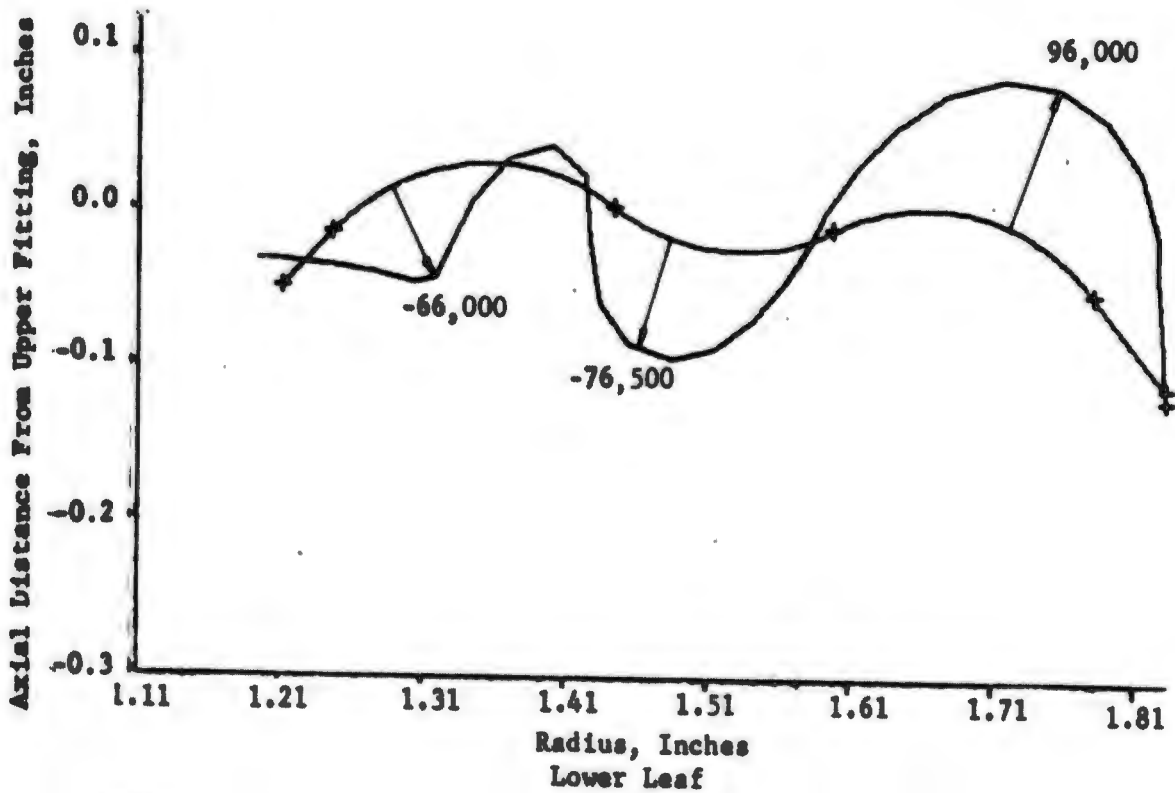
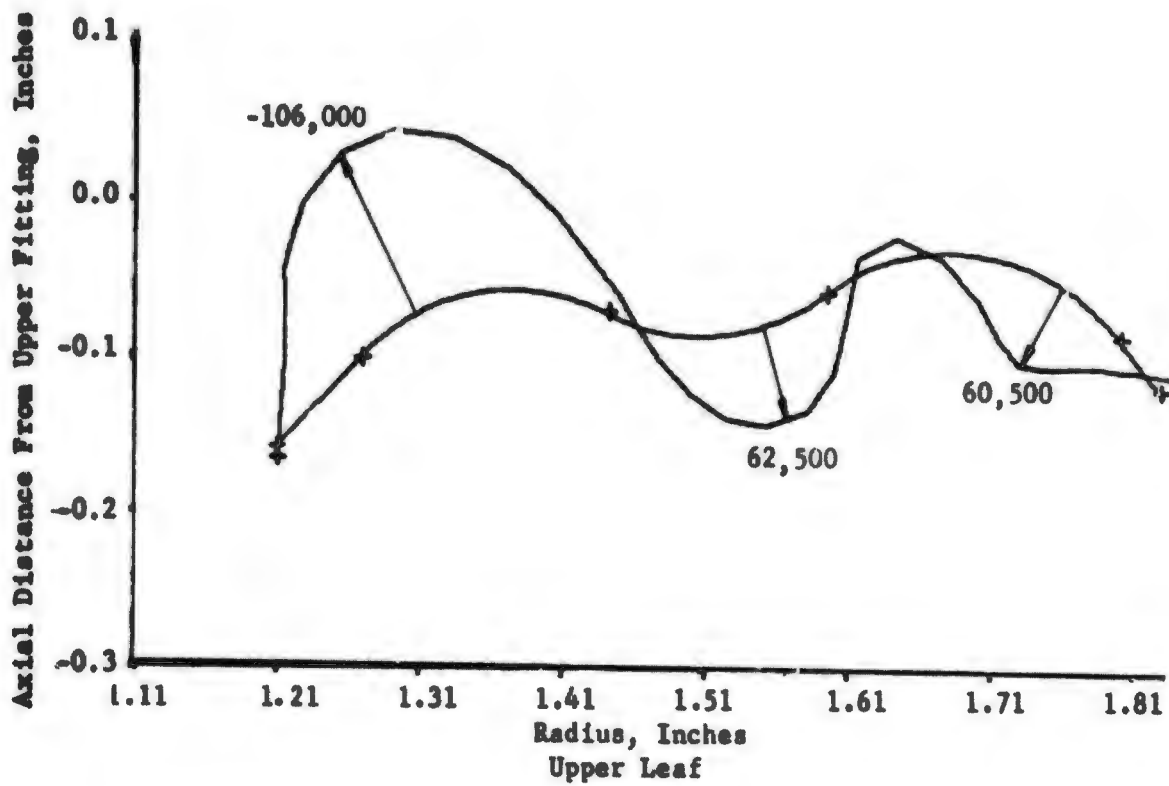


FIGURE 11. OUTER SURFACE MERIDIONAL STRESSES IN AN AXIALLY COMPRESSED 3.5-INCH BELLOWS WITH 45° ID, 50° OD TILT ANGLES, ±5° CHORD ANGLES, 0.15373-INCH SWEEP RADII AND 0.6188-INCH SPAN (Unit Deflection Per Unit Bellows Length)

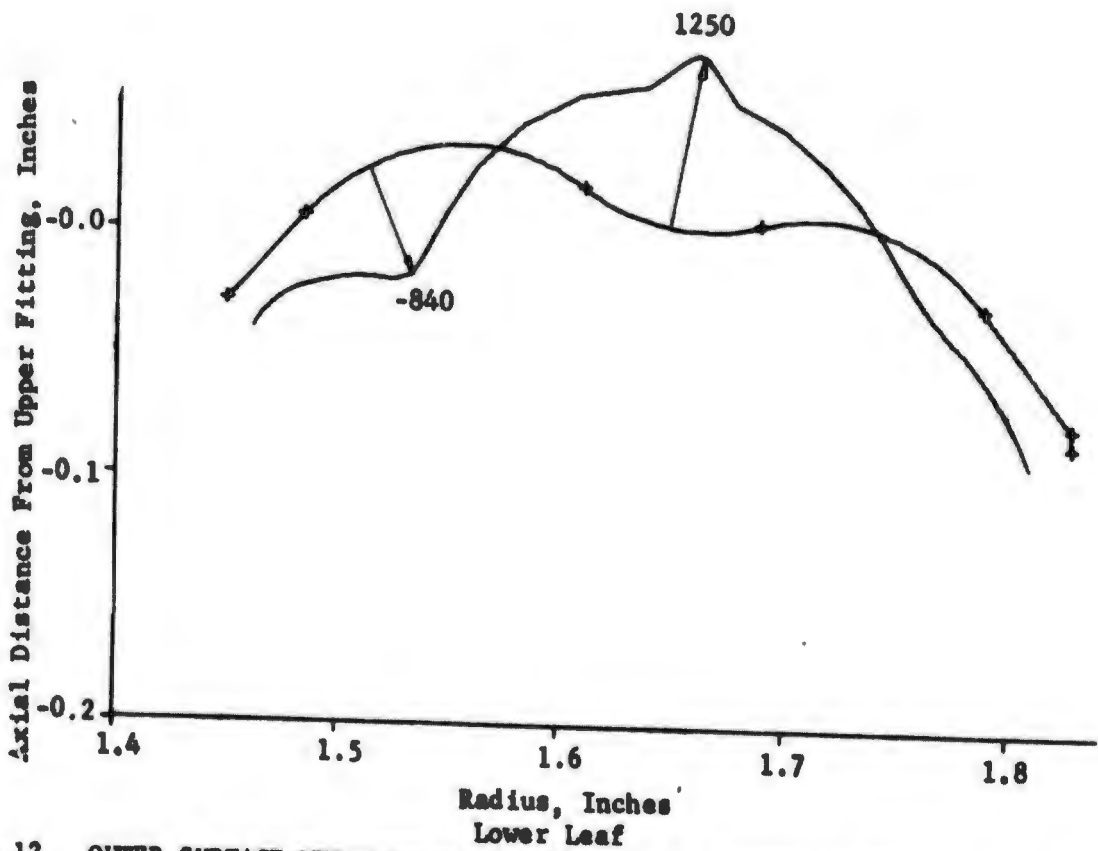
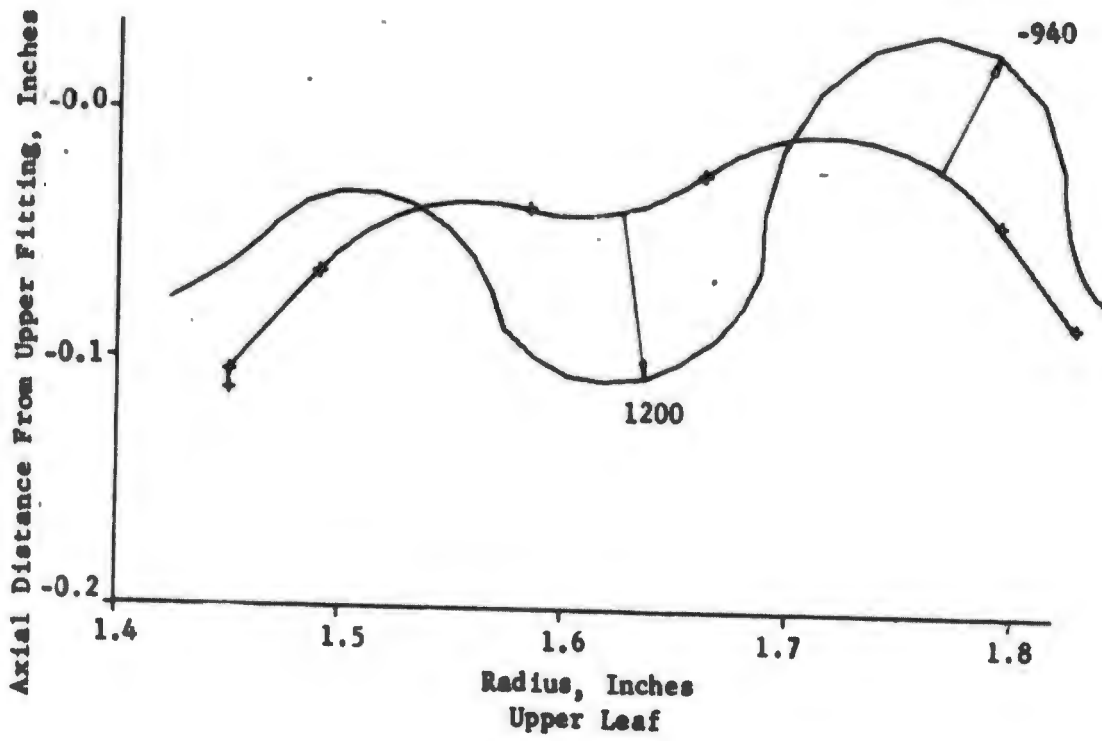


FIGURE 12. OUTER SURFACE MERIDIONAL STRESSES IN AN INTERNALLY PRESSURIZED 3.5-INCH BELLOWS WITH 45° ID, 50° OD TILT ANGLES, ±5° CHORD ANGLES, 0.10-INCH SWEEP RADII AND 0.378-INCH SPAN (Pressure = 1 psi)

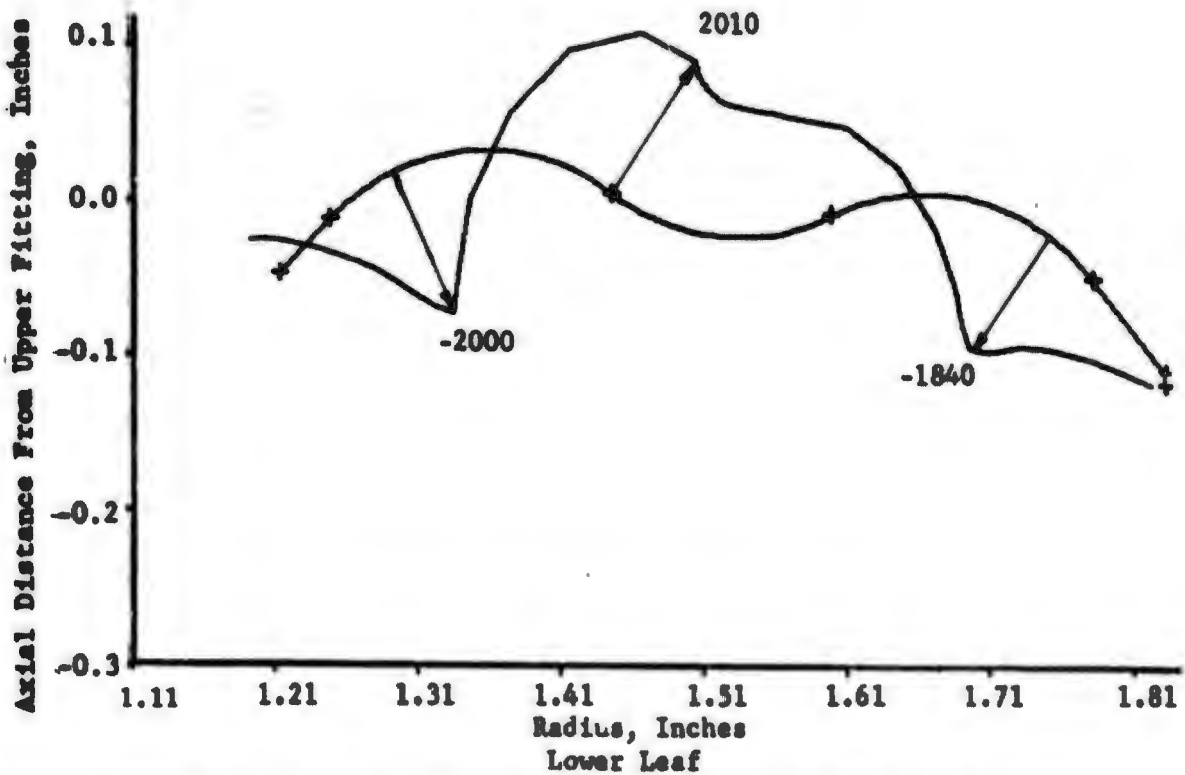
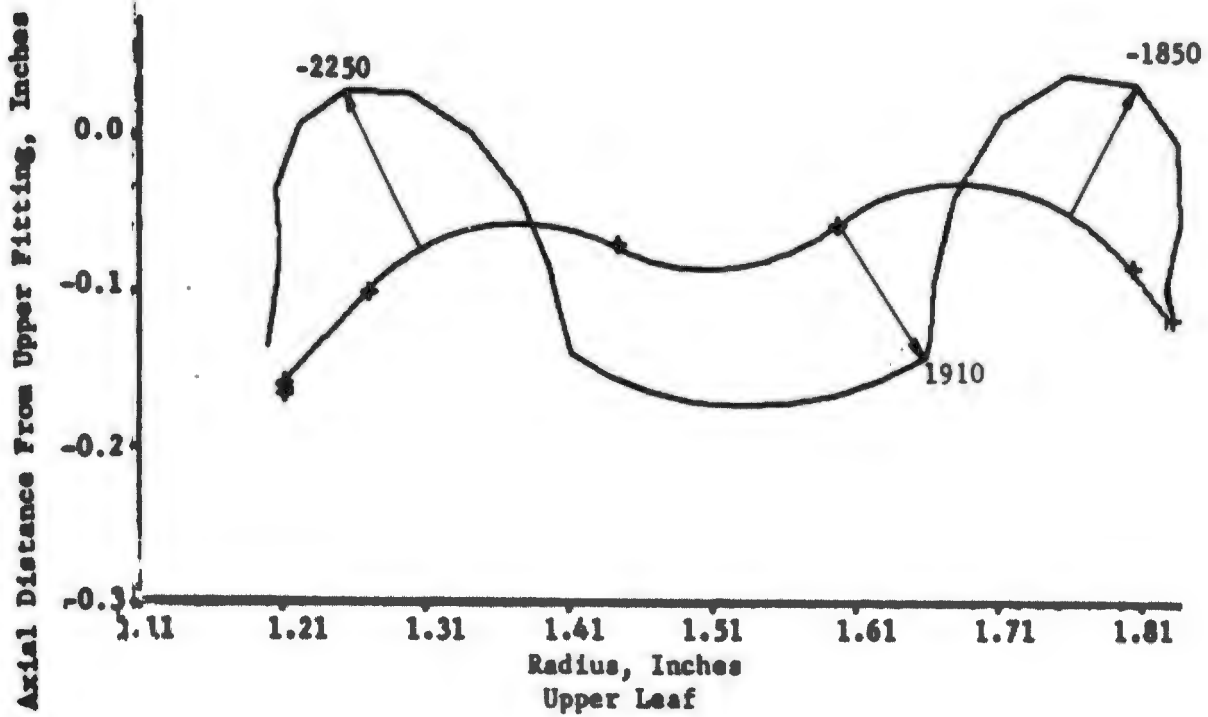


FIGURE 13. OUTER SURFACE MERIDIONAL STRESSES IN AN INTERNALLY PRESSURIZED 3.5-INCH BELLOWS WITH 45° ID, 50° OD TILT ANGLES, ±5° CHORD ANGLES, 0.15373-INCH SWEEP RADII AND 0.6188-INCH SPAN (Pressure = 1 psi)

The figures show stress curves overlaid on curves showing the mid-surface shape of the bellows leaves. Crosses were plotted on the bellows leaf curves to show the points of intersection of adjacent shell parts. These crosses serve to show the number and placement of the shell parts used in the mathematical model. The crosses also are an aid in identifying which of the curves is the bellows leaf.

The curves showing the stresses were plotted in terms of the distance from the shell midsurface. The length along the normal drawn from a point on the bellows midsurface to the stress curve is proportional to the stress at that point of the midsurface. Positive stresses were drawn in the direction of the outer normal. Negative stresses were drawn in the direction of the inner normal. As mentioned previously, the outer normal points downward for the upper leaf and upward for the lower leaf.

The scale used in plotting the stresses was automatically calculated by the computing program so that the length depicting the maximum stress on the curve was less than the local radii of curvature. This permitted the stresses to be plotted as smooth curves. Because of this, the scale factors used to plot the curves turned out to be quite arbitrary. Instead of showing these scale factors, it was decided to show values of stress maxima. These maxima were typed on the figures for each stress curve.

The ordinate in the figures shows the axial distance in inches of the points of the bellows leaves from the upper end fitting of the two convolution mathematical model (Figure 3). As mentioned earlier, the center two leaves shown in Figure 3 were chosen for studying the stresses in typical bellows convolutions. Thus, according to the definition adopted in this report, leaf 3 of the mathematical model was chosen as the upper leaf on which stresses are given. The corresponding lower leaf was chosen as leaf 2 in Figure 3. Because of this choice of leaves, the axial coordinate for the "upper leaf" (leaf 3) in Figures 10 through 13 indicate that it was actually below the "lower leaf" (leaf 2) in the mathematical model.

The stress plots in Figures 10 through 13 show that the bellows with the longer span had lower maximum stresses than the shorter span bellows for the same relative axial compression and higher stresses for the same internal pressures. Thus, changes in span have the same effect on maximum stresses in tilt-edge bellows as in the conventional bellows. This result should help in the design of tilt-edge bellows since bellows designers can use the span to tailor the characteristics of tilt-edge bellows in the way that they have always used the span for design of conventional bellows.

Investigation of Sweep Radius Variation

An investigation of the effects of sweep radius variation was conducted for the 3-inch, and 3.5-inch, three-sweep bellows. For the 3-inch bellows with a 0.5304-inch span, sweep radii of 0.1186-, 0.1318-, and 0.146-inches were assumed. ID and OD tilt angles were 45° and 50° , respectively. For the 3.5-inch bellows with a span of 0.378 inch, sweep radii were 0.07 and 0.10 inches. Two 3.5-inch bellows models were analyzed for each sweep radius. One bellows had equal ID and OD tilt angles of 55° . The second bellows had equal tilt angles of 60° . All bellows had $\pm 5^\circ$ chord angles.

It can be seen from the above dimensions that the 3-inch bellows had sweep radius to span ratios of about 0.22, 0.25, and 0.27 while the sweep radius to span ratios of the 3.5-inch bellows were 0.19 and 0.27. Thus, the relative degrees of flatness of the sweep sections of the two sets of bellows were comparable. (However, the overall curvature of the convolutions for the 3.5-inch bellows was greater than that of the 3-inch bellows because of the larger tilt angles.) Solutions for all geometries were obtained for both axial deflection and pressure loadings.

Figures 14 through 17 show the outer surface, meridional stress distributions in the upper and lower leaves of the 3-inch bellows with sweep radii of 0.1186- and 0.146-inches. Results for the 60° tilt-angle models of the 3.5-inch bellows are presented in Figures 18 through 21. Very similar results were obtained for the 55° tilt-angle models. Note again that the stresses were plotted to different scales automatically chosen by the computer program. Numerical values of stresses at given locations were typed on the figures for reference. Tables 11 and 12 give the values of the maximum relative meridional stresses found at the inner and outer surfaces of the upper and lower leaves for all of the geometries and loadings considered in the study of the sweep radius variation.

Examination of the stress plots presented for the 3-inch bellows indicates that the general shape of the stress variation over the upper and lower leaves remained essentially unchanged. The stress values increased with increase in sweep radius in some locations and decreased with increase in sweep radius in other locations. The main trend occurred in the stress levels in the center sweeps of the upper and lower leaves. As the radii were increased, the stress levels increased for pressure loading and decreased for axial deflection loading. However, the values in Table 11, together with the stress distribution plots, indicate that although the convolution stress levels did not vary with sweep radius in a consistent manner at every point within the convolution, the overall maximum stress in the meridional direction for the axial deflection case remained relatively constant in both magnitude and location even though the sweep radius was increased twenty-two percent. For internal pressure loading, the location of the maximum stress changed, but its absolute magnitude varied less than six percent.

In contrast with the results obtained for the 3-inch, three-sweep bellows, Figures 18 through 21 and Table 12 demonstrate that the maximum stress levels in the sweeps of the 3.5-inch bellows increased with increase in the sweep radius for both axial deflection and pressure loadings. Quantitatively, the forty-three percent increase in sweep radius produced an eleven percent increase in the maximum meridional stress for pressure loading and a twenty percent increase for axial deflection loading.

A comparison of Figures 16 and 17 with Figures 20 and 21 shows much the same change in the pressure stress as the sweep radius was increased and the midsections of the bellows leaves became flatter. The bending stresses in the middle sweeps increased to the point that they became the largest stresses. Thus, for pressure loading the optimum sweep radii lay between 20 and 25 percent of the span for all of the bellows studied.

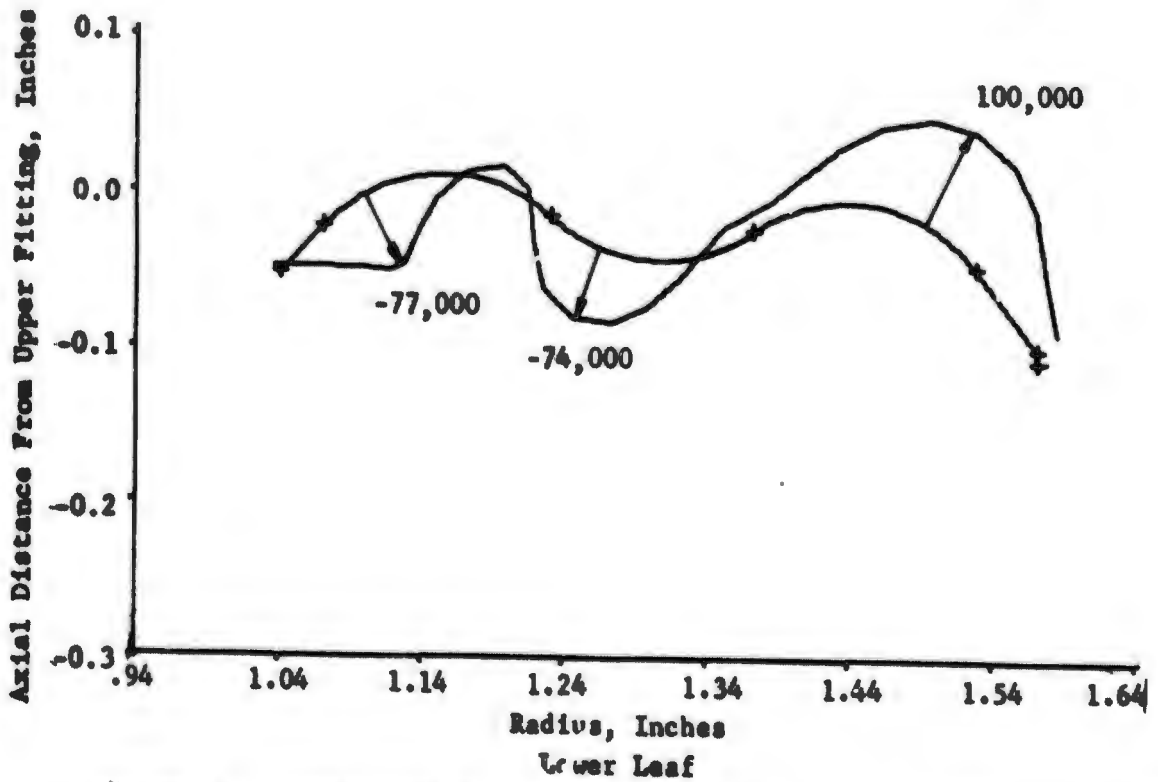
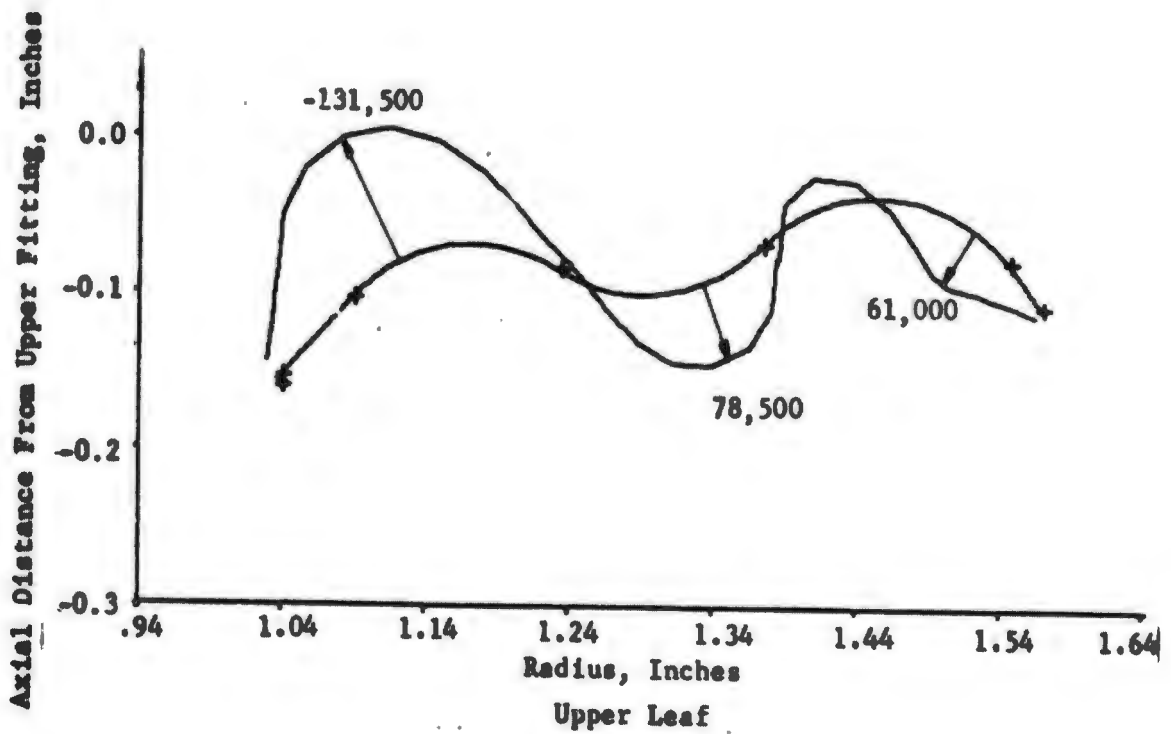


FIGURE 14. OUTER SURFACE MERIDIONAL STRESSES IN AN AXIALLY COMPRESSED 3-INCH BELLOWS WITH 45° ID, 50° OD TILT ANGLES, ±5° CHORD ANGLES, 0.11859 SWEEP RADII, AND 0.5304-INCH SPAN (Unit Deflection Per Unit Bellows Length)

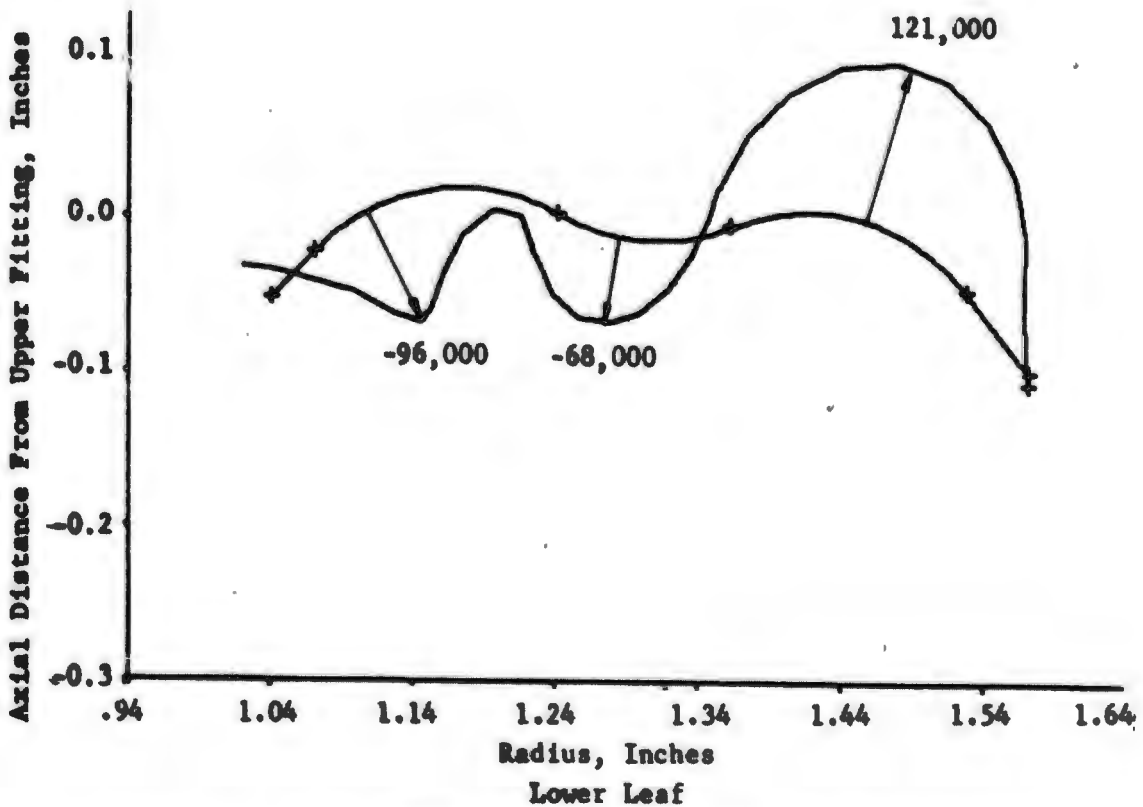
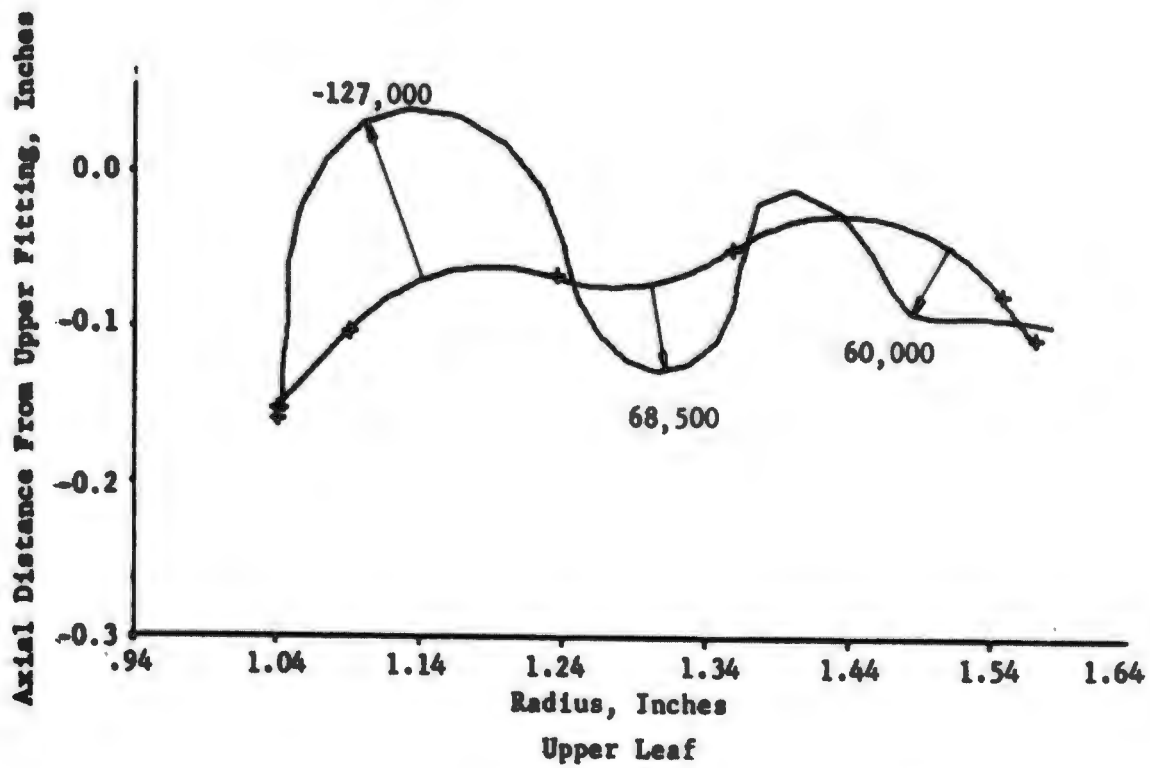


FIGURE 15. OUTER SURFACE MERIDIONAL STRESSES IN AN AXIALLY COMPRESSED 3-INCH BELLOWS WITH 45° ID, 50° OD TILT ANGLES, ±5° CHORD ANGLES 0.14495-INCH SWEEP RADII AND 0.5304-INCH SPAN (Unit Deflection Per Unit Bellows Length)

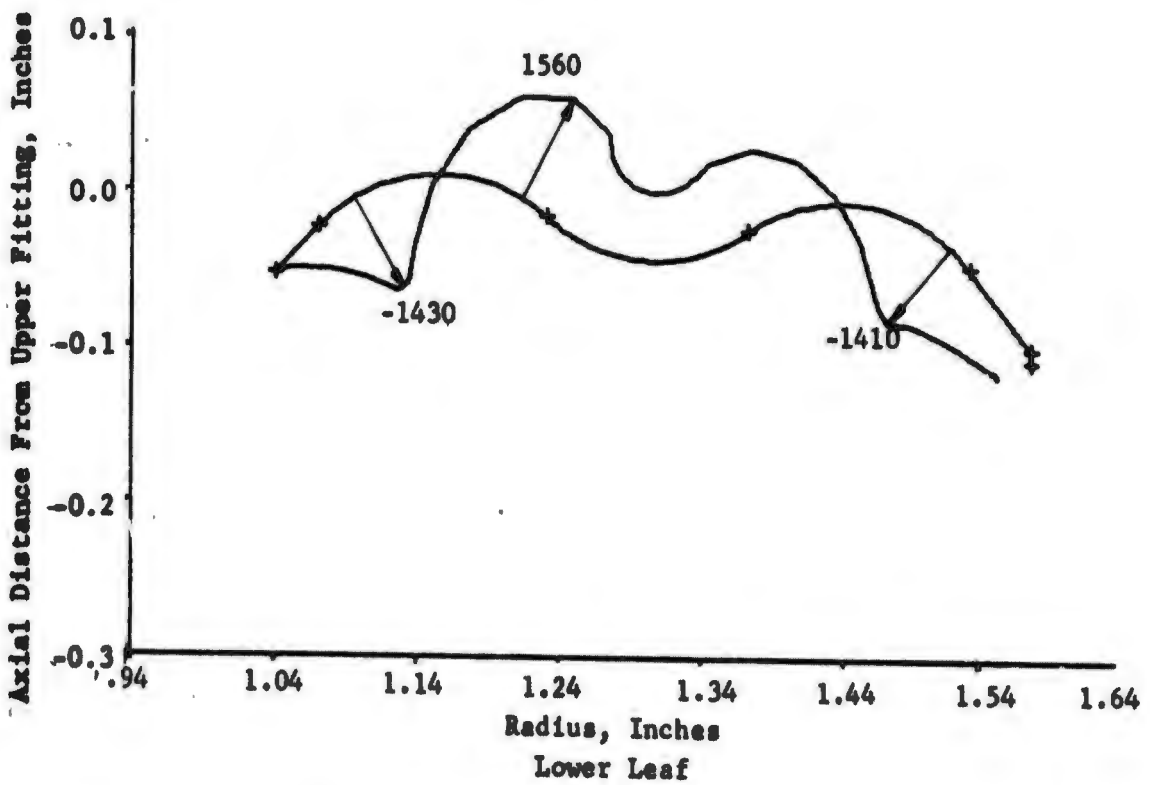
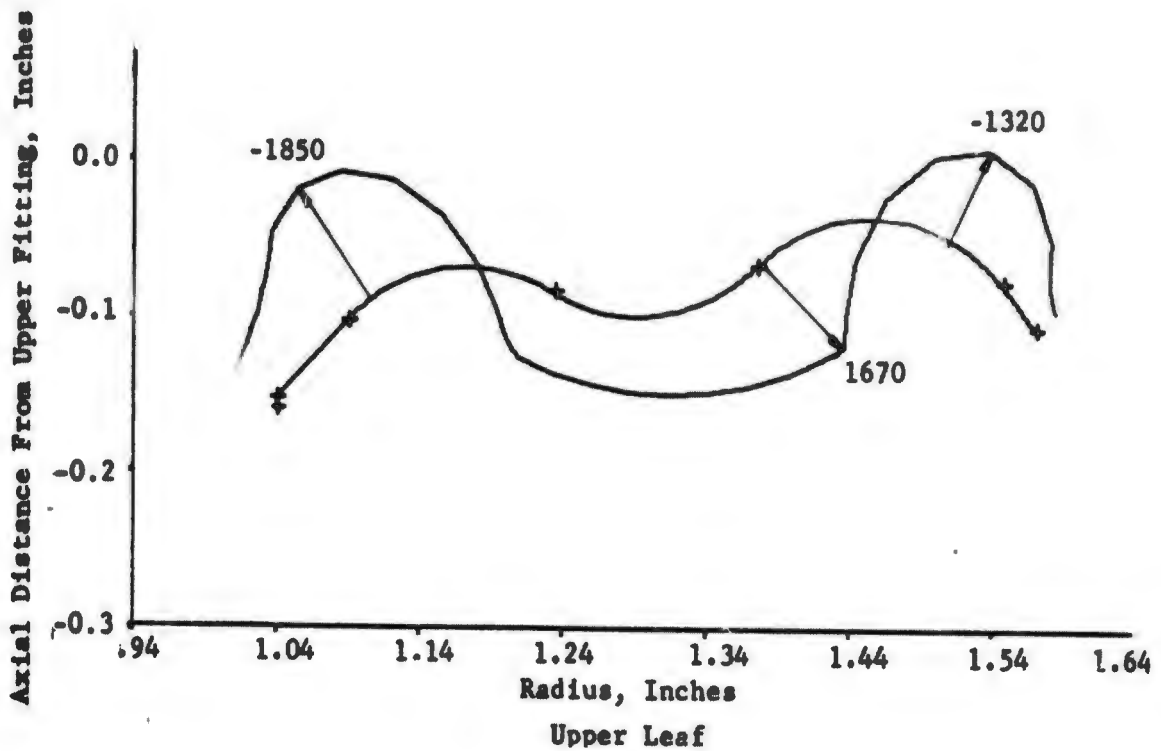


FIGURE 16. OUTER SURFACE MERIDIONAL STRESSES IN AN INTERNALLY PRESSURIZED 3-INCH BELLOWS WITH 45° ID, 50° OD TILT ANGLES, ±5° CHORD ANGLES, 0.11859 SWEEP RADII, AND 0.5304-INCH SPAN (Pressure = 1 psi)

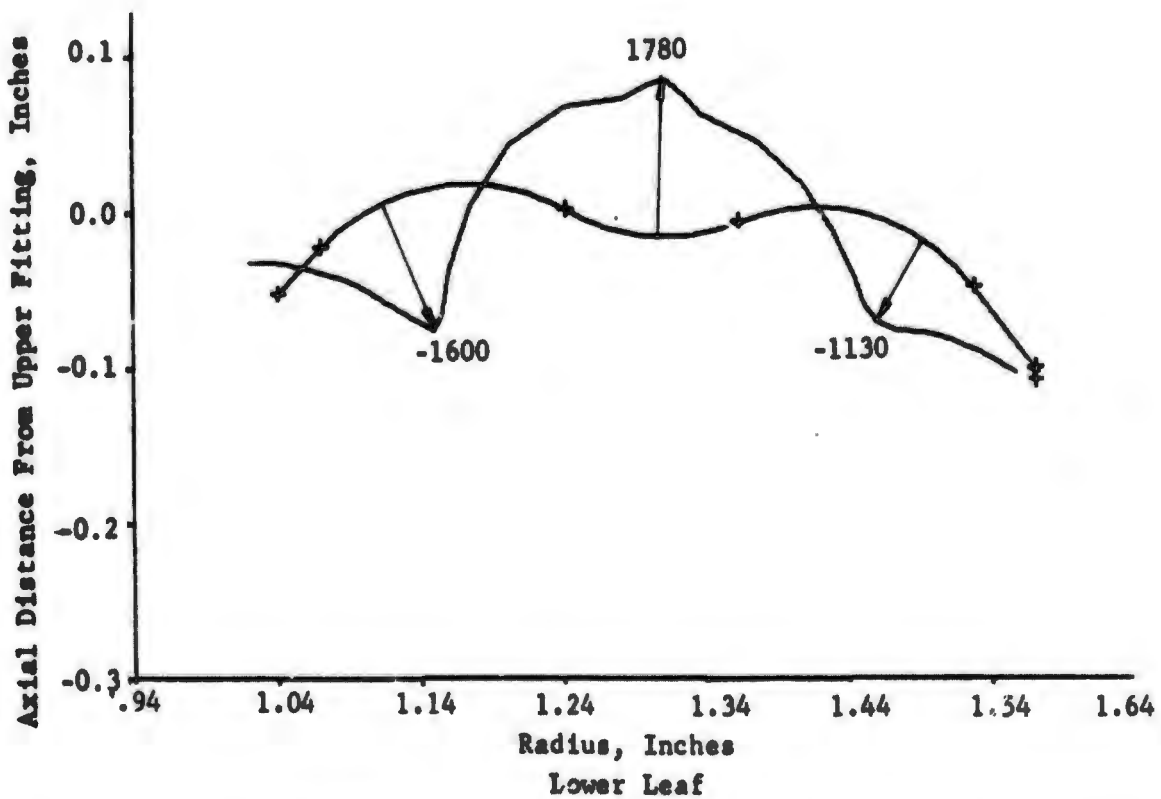
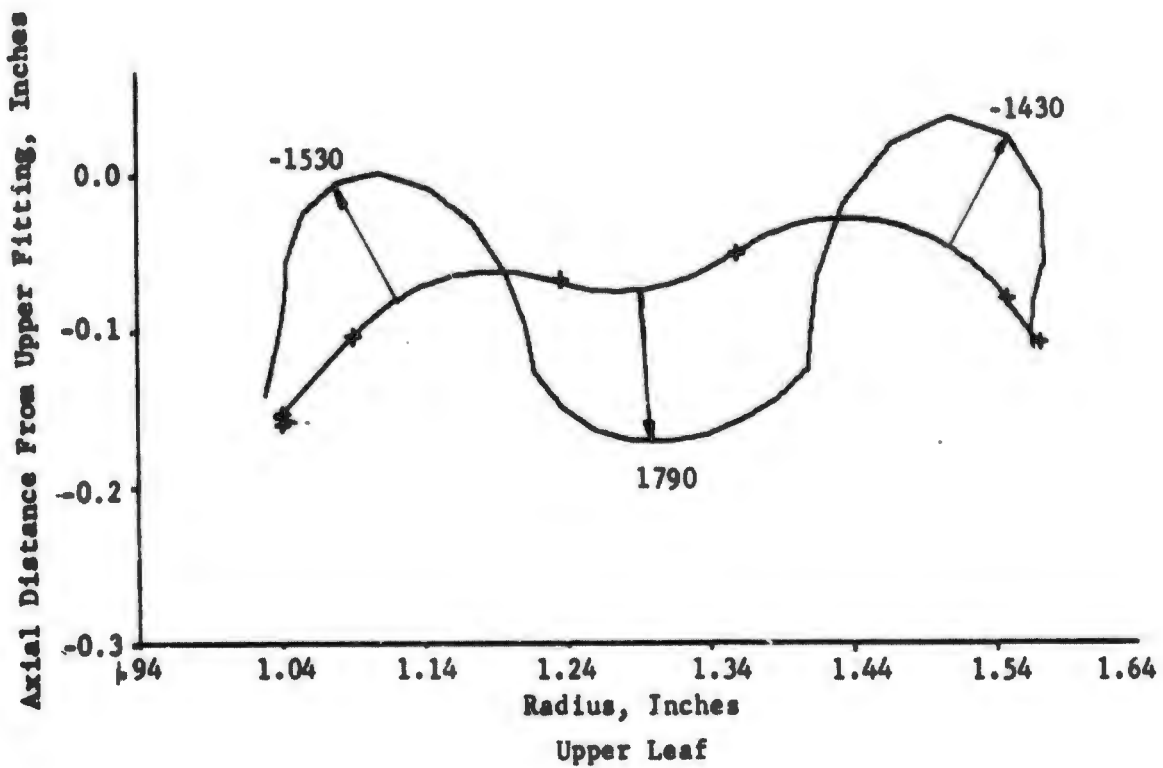


FIGURE 17. OUTER SURFACE MERIDIONAL STRESSES IN AN INTERNALLY PRESSURIZED 3-INCH BELLOWS WITH 45° ID, 50° OD TILT ANGLES, ±5° CHORD ANGLES, 0.14495-INCH SWEEP RADII AND 0.5304-INCH SPAN (Pressure = 1 psi)

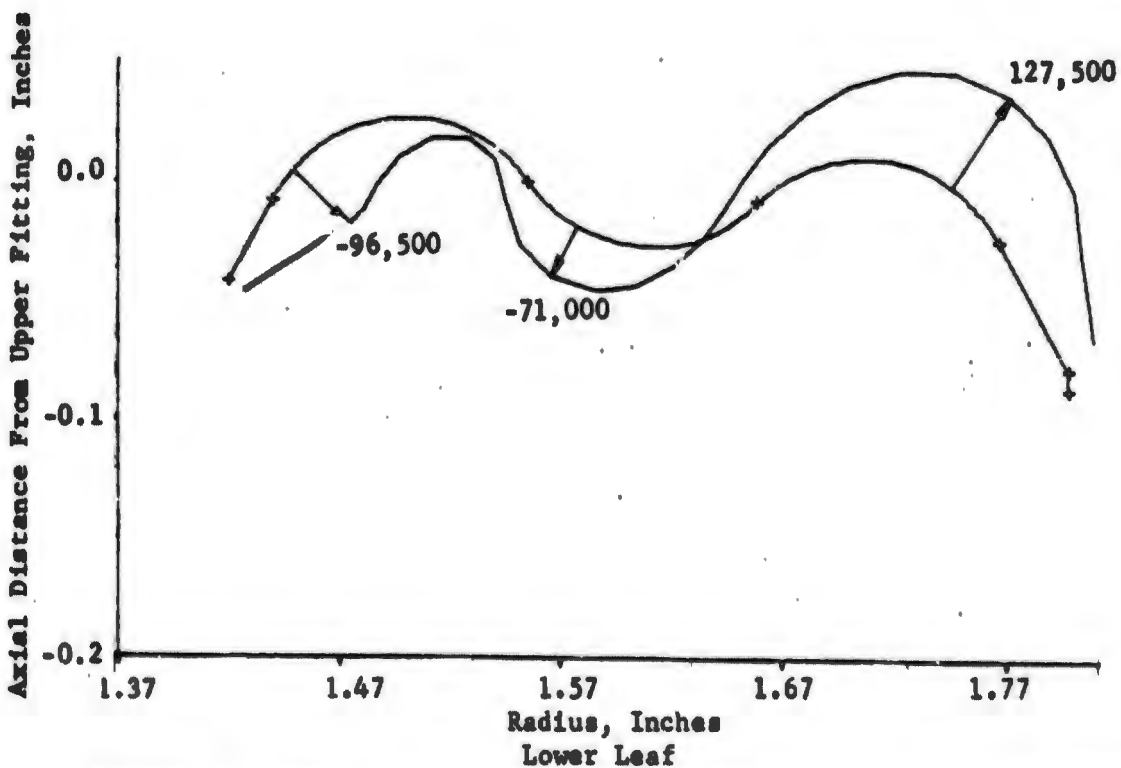
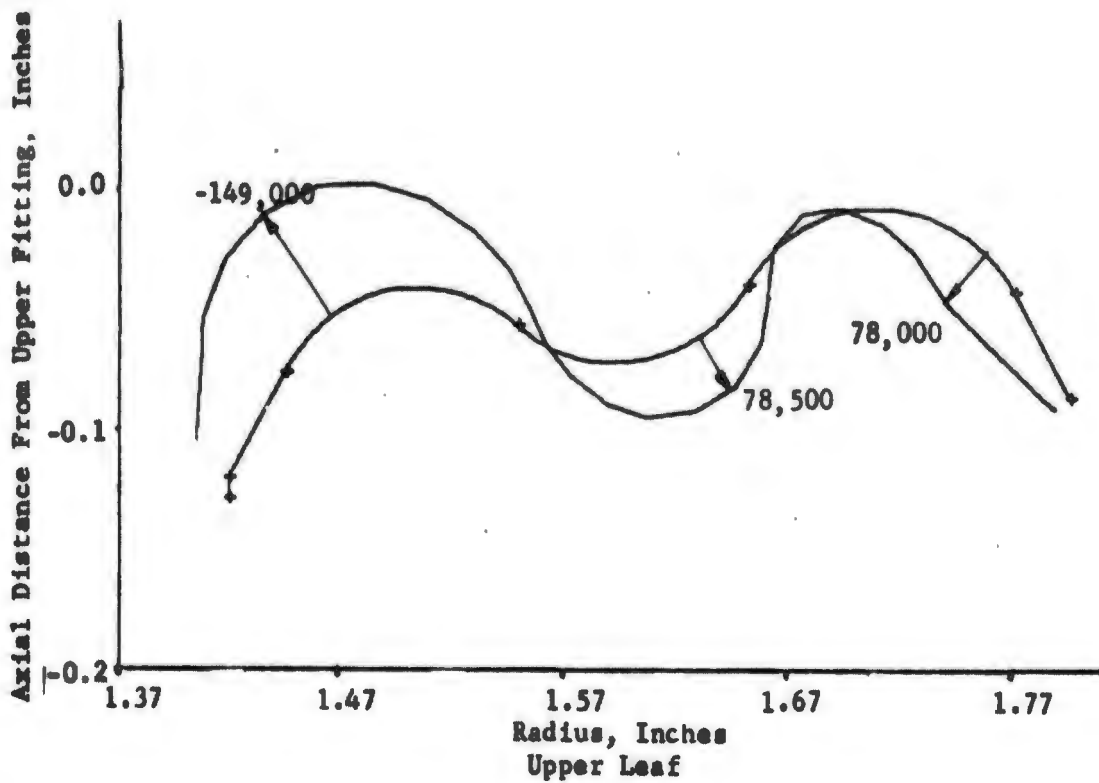


FIGURE 18. OUTER SURFACE MERIDIONAL STRESSES IN AN AXIALLY COMPRESSED 3.5-INCH BELLOWS WITH 60° ID, 60° OD TILT ANGLES, ±5° CHORD ANGLES, 0.07-INCH SWEEP RADII AND 0.378-INCH SPAN (Unit Deflection Per Unit Bellows Length)

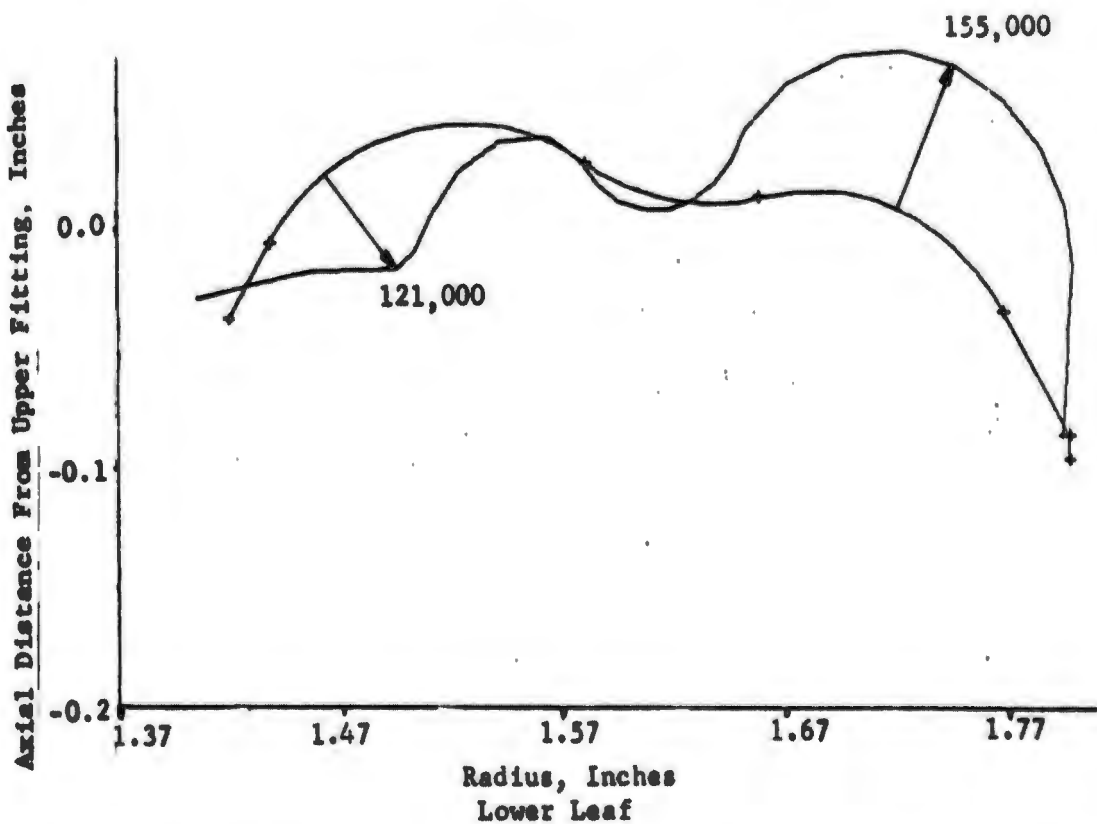
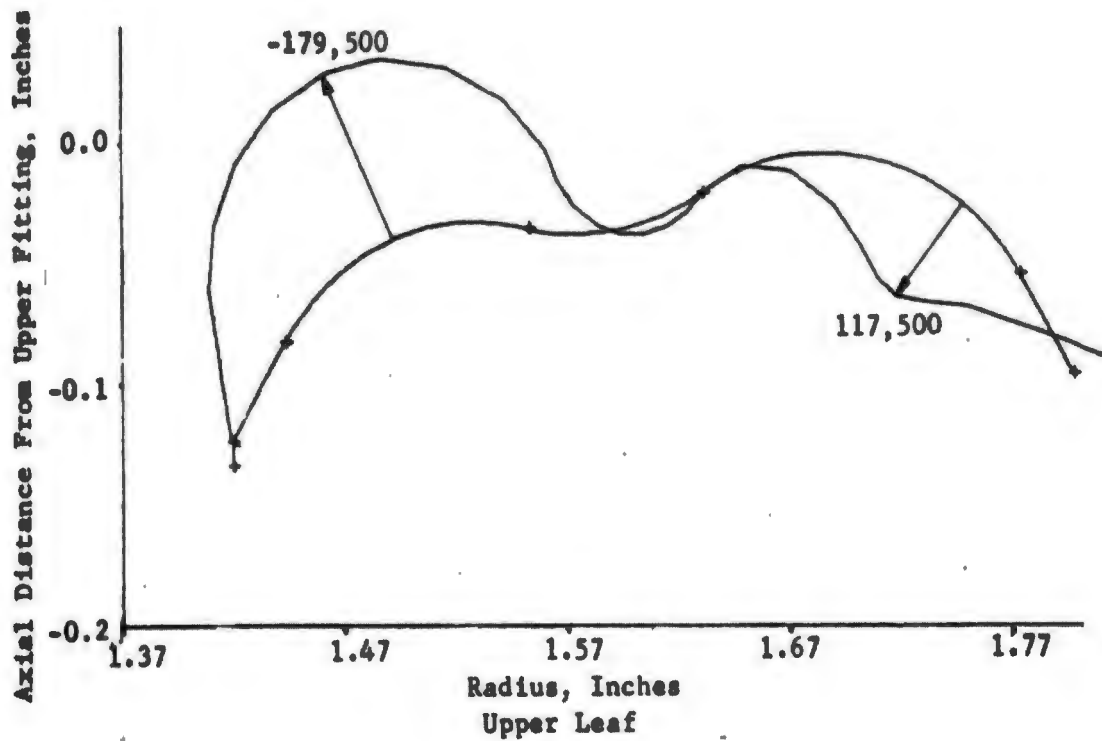


FIGURE 19. OUTER SURFACE MERIDIONAL STRESSES IN AN AXIALLY COMPRESSED 3.5-INCH BELLOWS WITH 60° ID, 60° OD TILT ANGLES, ±5° CHORD ANGLES, 0.10-INCH SWEEP RADII AND 0.378-INCH SPAN (Unit Deflection Per Unit Bellows Length)

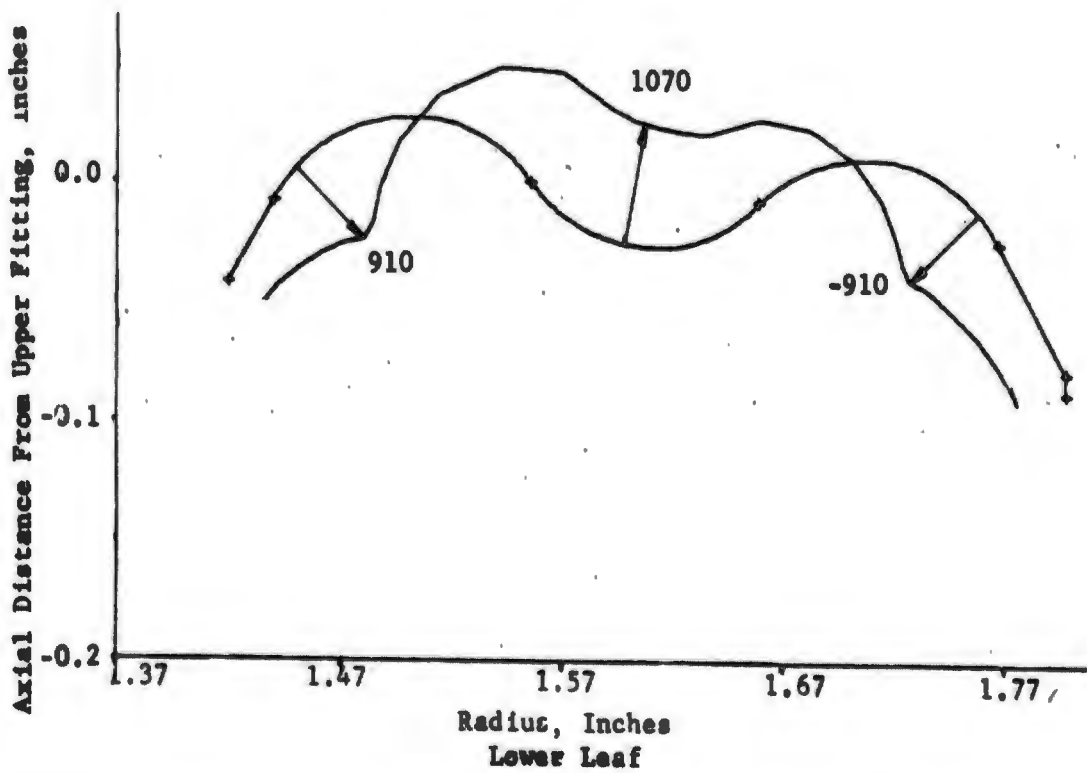
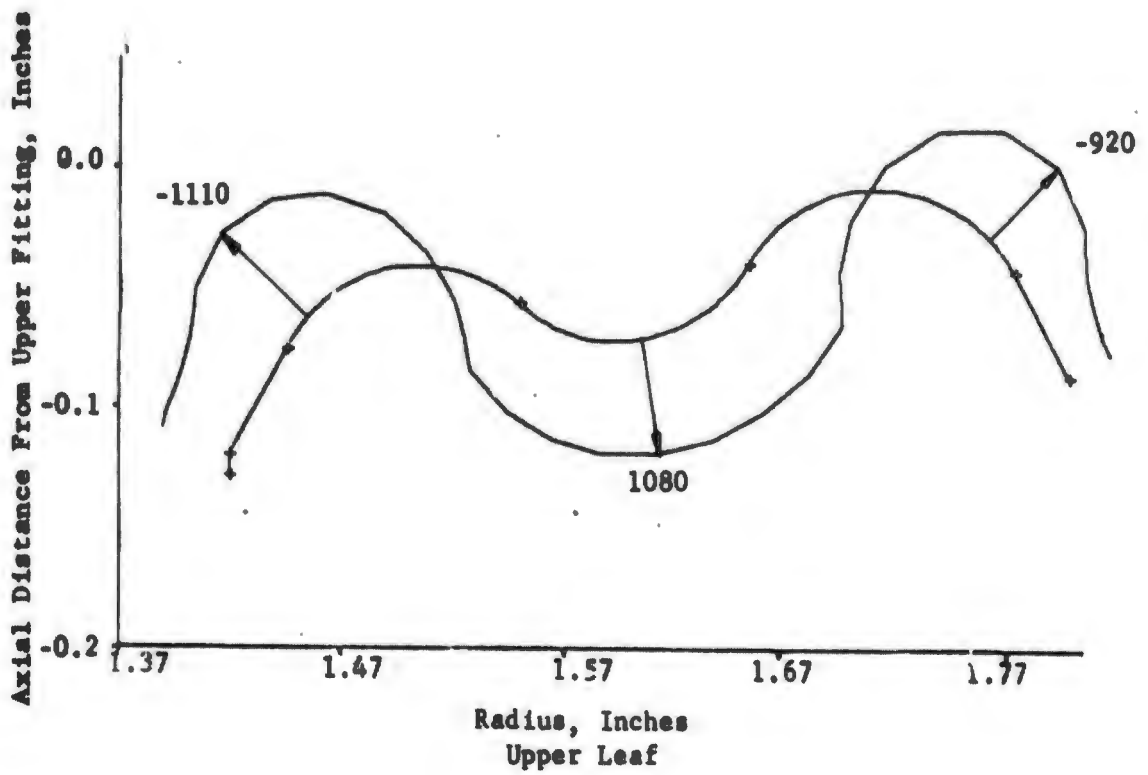


FIGURE 20. OUTER SURFACE MERIDIONAL STRESSES IN AN INTERNALLY PRESSURIZED 3.5-INCH BELLOWS WITH 60° ID, 60° OD TILT ANGLES, 0.07-INCH SWEEP RADII AND 0.378-INCH SPAN (Pressure = 1 psi)

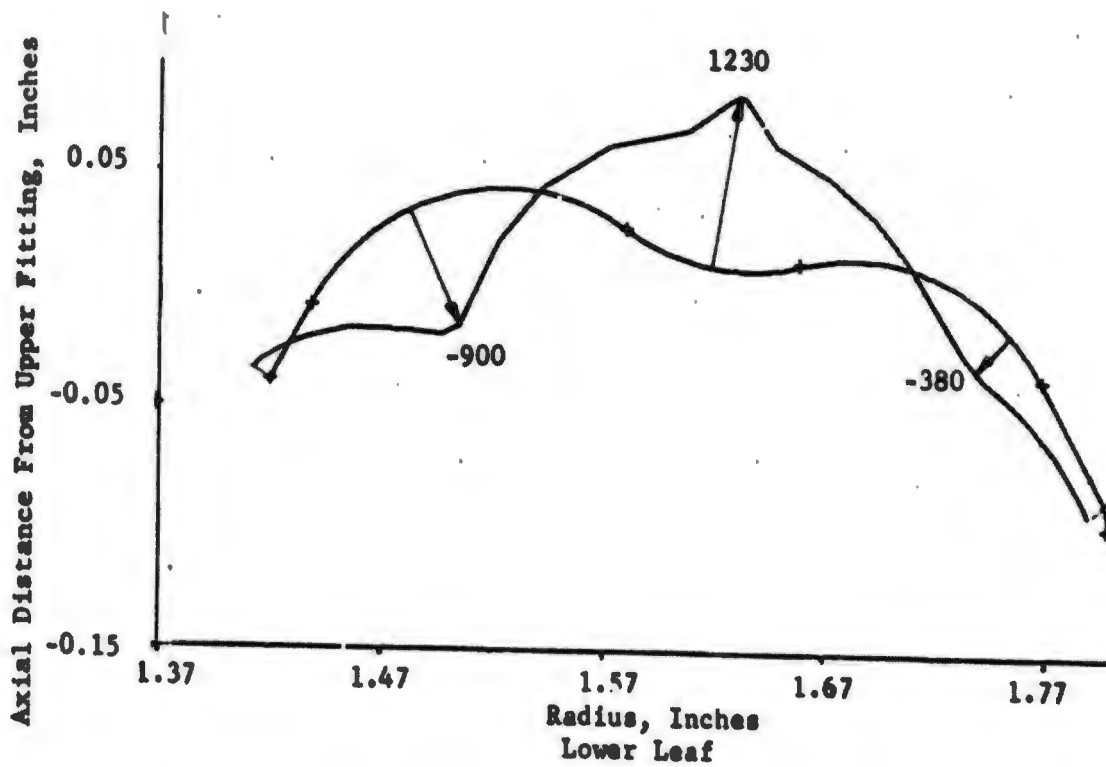
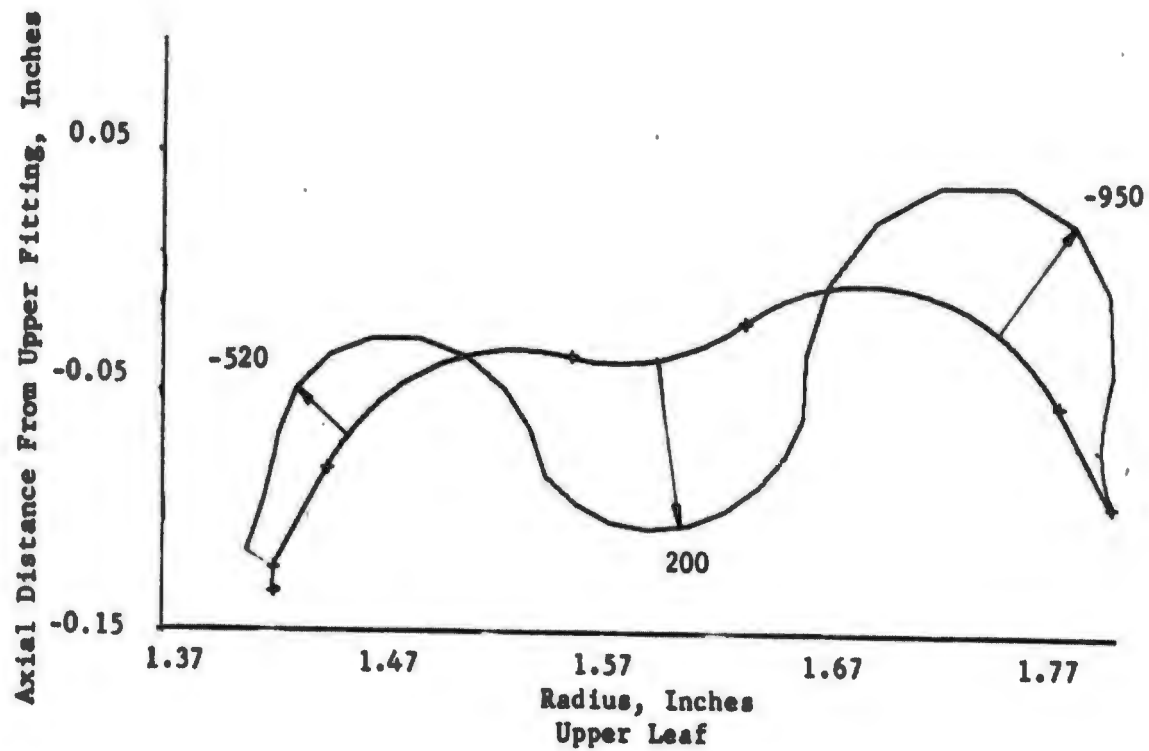


FIGURE 21. OUTER SURFACE MERIDIONAL STRESSES IN AN INTERNALLY PRESSURIZED 3.5-INCH BELLOWS WITH 60° ID, 60° OD TILT ANGLES, ±5° CHORD ANGLES, 0.10-INCH SWEEP RADII AND 0.378-INCH SPAN (Pressure = 1 psi)

TABLE 11. MAXIMUM RELATIVE MERIDIONAL STRESSES FOR
 3-INCH, TILT-EDGE WELDED BELLOWS,
 SPAN = 0.5304 INCH, 45° ID AND 50° OD TILT ANGLE

Location of Stress	Sweep Radius, inches	Inner Surface Stress, psi	Outer Surface Stress, psi
<u>Unit Pressure Loading (a)</u>			
Upper Leaf	0.11859	1,690	-1,850
Lower Leaf	0.11859	1,630	1,560
Upper Leaf	0.13177	1,760	-1,760
Lower Leaf	0.13177	1,600	1,560
Upper Leaf	0.14495	1,780	1,790
Lower Leaf	0.14495	1,800	1,780
<u>Unit Deflection Loading (b)</u>			
Upper Leaf	0.11879	126,000	-131,000
Lower Leaf	0.11879	-104,000	100,000
Upper Leaf	0.13177	120,000	-126,000
Lower Leaf	0.13177	-107,000	103,000
Upper Leaf	0.14495	120,000	-127,000
Lower Leaf	0.14495	-126,000	121,000

- (a) Unit internal pressure load was 1 psi. To get stresses in psi multiply values in table by pressure in psi.
- (b) Unit compression in unit length bellows. To get stresses in psi due to axial deflection, multiply values in table by deflection and divide by free length.

TABLE 12. MAXIMUM MERIDIONAL STRESSES FOR
 3.5-INCH, TILT-EDGE WELDED
 BELLOWS, SPAN = 0.378-INCH
 SWEEP RADIUS, = 0.07 INCH AND 0.10
 INCH

Location of Stress	Sweep Radius, inches	Surface Stresses, psi			
		55° Tilt Angles		60° Tilt Angles	
		Inner	Outer	Inner	Outer
<u>Unit Pressure Loading (a)</u>					
Upper Leaf	0.07	-1,090	1,080	-1,100	1,080
Lower Leaf	0.07	-1,070	1,090	-1,050	1,110
Upper Leaf	0.10	-1,190	1,230	-1,190	1,220
Lower Leaf	0.10	-1,240	1,210	-1,240	1,200
<u>Unit Axial Deflection</u>					
Upper Leaf	0.07	136,000	-140,000	149,000	-154,000
Lower Leaf	0.07	-123,000	120,000	-137,000	133,000
Upper Leaf	0.10	170,000	-180,000	180,000	-189,000
Lower Leaf	0.10	-163,000	155,000	-171,000	163,000

- (a) Unit internal pressure was 1 psi. To get stresses in psi multiply values in table by pressure.
- (b) Unit compression in unit length bellows. To get stresses in psi due to axial deflection, multiply values in table by deflection and divide by free length.

At this optimum point, stresses in the center sweep were equal to the stresses in the inner sweep of the upper leaf. Note that the 3-inch bellows model with a sweep radius of 25 percent of the span was very near the optimum shape. The optimum sweep radius for the 3.5-inch bellows was less than 25 percent of the span. However, it is apparent that the maximum stress for a sweep radius of between 20 and 25 percent of the span was affected very little by the change in sweep radius.

A seemingly contradictory situation existed for the deflection loading of the 3- and 3.5-inch bellows. For the 3-inch bellows, changing the sweep radius did not affect the maximum stresses appreciably, while increasing the sweep radius for the 3.5-inch bellows significantly increased the maximum stresses. A detailed comparison of the stresses in Figures 14 and 15 with Figures 18 and 19 shows the same general trend in the stresses at different points of the bellows as the sweep radius was increased. However, the stresses at the inner sweep of the upper leaf of the 3-inch bellows (which were the largest stresses) decreased with increasing sweep radius. This was the principal difference between the two bellows. The apparent reason for this decrease seemed to be that the middle sweep in the 3-inch bellows participated more in the bending action as the sweep radius was increased. This apparently relieved the bending stresses in the inner sweep slightly. In contrast, the middle sweep was bent less in the case of the 3- and 5-inch bellows as the radius was increased. As seen in Figure 19, the stresses in the middle sweep were almost zero for both upper and lower leaves. This increased the bending deformation required in the inner and outer sweep sections and thus increased their bending stress.

An interesting result of the differences in the stresses in these bellows was that the spring rate for the 3-inch bellows decreased from 52.4 lb/in. for the smallest radius to 46 lb/in. at the largest radius, while the spring rate for the 3.5-inch bellows increased from 91 lb/in. to 109 lb/in. with an increase in radius from 0.07 inch to 0.10 inch.

It would appear from this study that there was a second order interaction between the tilt angles and the effect of changes in sweep radius on the deflection stresses. Although this interaction was not strong, it produced some interesting effects, one of which was that the optimum sweep radius was the same for both pressure and axial deflection loading of the 3-inch bellows with 40° ID and 45° OD tilt angles.

It would seem risky to draw general conclusions on the optimization of tilt-edge bellows with respect to sweep radius on the basis of the results reported above. However, it would appear that a reasonable choice of the sweep radius for a 3-sweep, tilt-edge bellows would be 25 percent of the span. For new designs, analyses can be made with one or two other radii to check whether this would be an optimum sweep radius.

Effects of Variation in Convolution Pitch

In a welded bellows, the pitch of a convolution is an important design parameter for several reasons. First, assuming a conventional welding process, the amount of pitch must be large enough to accommodate chill blocks of sufficient thickness that they can be effectively used to absorb the heat

generated in making the ID and OD weld beads. Second, because the pitch determines the length per convolution of a bellows, its value must be considered when determining the number of convolutions desired or required for a given bellows application. Also, since virtually all welded bellows applications require a certain compression capability for the bellows, the value of the pitch for any given convolution shape should be sufficient to allow the required compression stroke with minimum leaf interference since such interference greatly affects the fatigue life of the bellows.

The effects on both the stress distributions and maximum stress levels due to changes in convolution pitch of a three-sweep tilt-edge bellows were investigated for the 2-inch and 3-inch bellows, all having constant thickness of 0.005 inch. Two sets of tilt angles were used for the 2-inch mathematical model: (a) 45° at the ID with 50° at the OD and (b) 50° at the ID with 55° at the OD. For the 3-inch bellows model, tilt angles were 45° at the ID and 50° at the OD. All other model dimensions were the same as those given in Tables 1 and 2. Analyses were performed for axial deflection as well as internal pressure loadings.

By varying the chord angles of the upper and lower leaves and keeping other major variables virtually constant, two values of pitch were obtained for each of the bellows models studied. Ratios of the pitch to span (P/S) for each of the bellows are shown in Table 13. This table shows the effects of pitch variation on the maximum stress levels in both the upper and lower leaves of a convolution. The numbers in parentheses refer to the location of the stress value in terms of the mathematical model part number shown in Figure 2. The effects of pitch variation on the meridional stress distribution throughout the 2-inch, tilt-edge bellows convolution for both loadings considered can be seen in Figures 22 through 29. These results are typical and so stress distribution plots for the other models studied are not presented.

Relative stresses due to axial deflection are shown in two ways in Table 13. The values of the relative maximum stresses corresponding to unit compressive deflection per unit length of bellows show that, for a fixed deflection per unit length of bellows, an increase in pitch caused a marked increase in the maximum stress values. In other words, the deflection capabilities of the bellows, or their abilities to deflect in proportion to their lengths, changed significantly with change in their pitch. Alternatively, the values of maximum stresses for a deflection of one inch per convolution show that, for a fixed deflection per bellows convolution, an increase in pitch had much less effect on the maximum stress levels. This increase in deflection stress levels with increasing pitch was entirely consistent with results obtained from all other types of bellows. It is interesting to note that although the stress values were increased and the stress distribution in the lower leaf was changed somewhat, the location of the maximum stress for the two bellows sizes investigated was unaltered by changes in convolution pitch. For each of the six models studied, the maximum meridional stress for deflection loading occurred in the upper leaf sweep nearest the inside diameter. Indeed, the maximum deflection stress was found to be on this sweep in nearly all of the geometries studied in this research program.

TABLE 13. MAXIMUM RELATIVE MERIDIONAL STRESSES IN TILT-EDGE WELDED BELLOWS OF DIFFERENT CONVOLUTION PITCH

BelloWS Description	Relative Stress for Unit Deflection per Unit Bellows Length (a)	Relative Stress for Inch of Deflection per Convolution (b)	Relative Stress Due to Internal Pressure (c)
2-inch, 45° ID, 50° OD, P/S = 0.129	Upper Leaf	79,000 (8)	1,760,000 (9)
	Lower Leaf	-97,000 (4)	-2,160,000 (3)
2-inch, 45° ID, 50° OD, P/S = 0.192	Upper Leaf	-132,200 (10)	-1,930,000 (9)
	Lower Leaf	158,200 (4)	-2,310,000 (3)
2-inch, 50° ID, 55° OD, P/S = 0.141	Upper Leaf	85,500 (8)	1,740,000 (9)
	Lower Leaf	-104,900 (4)	-2,140,000 (3)
2-inch, 50° ID, 55° OD, P/S = 0.229	Upper Leaf	-157,000 (10)	-1,900,000 (9)
	Lower Leaf	-190,000 (4)	-2,300,000 (3)
3-inch, 45° ID, 50° OD, P/S = 0.196	Upper Leaf	-106,900 (10)	1,030,000 (8)
	Lower Leaf	-125,900 (4)	-1,210,000 (4)
3-inch, 45° ID, 50° OD, P/S = 0.290	Upper Leaf	-214,500 (10)	-1,400,000 (8)
	Lower Leaf	-231,000 (4)	-1,500,000 (4)

(a) To obtain stresses (in psi) due to deflection, multiply values by deflection and divide by free length of bellows.

(b) To obtain stresses (in psi) due to deflection, multiply values by deflection per convolution in inches.

(c) To obtain stresses (in psi) due to internal pressure, multiply values by pressure in psi.

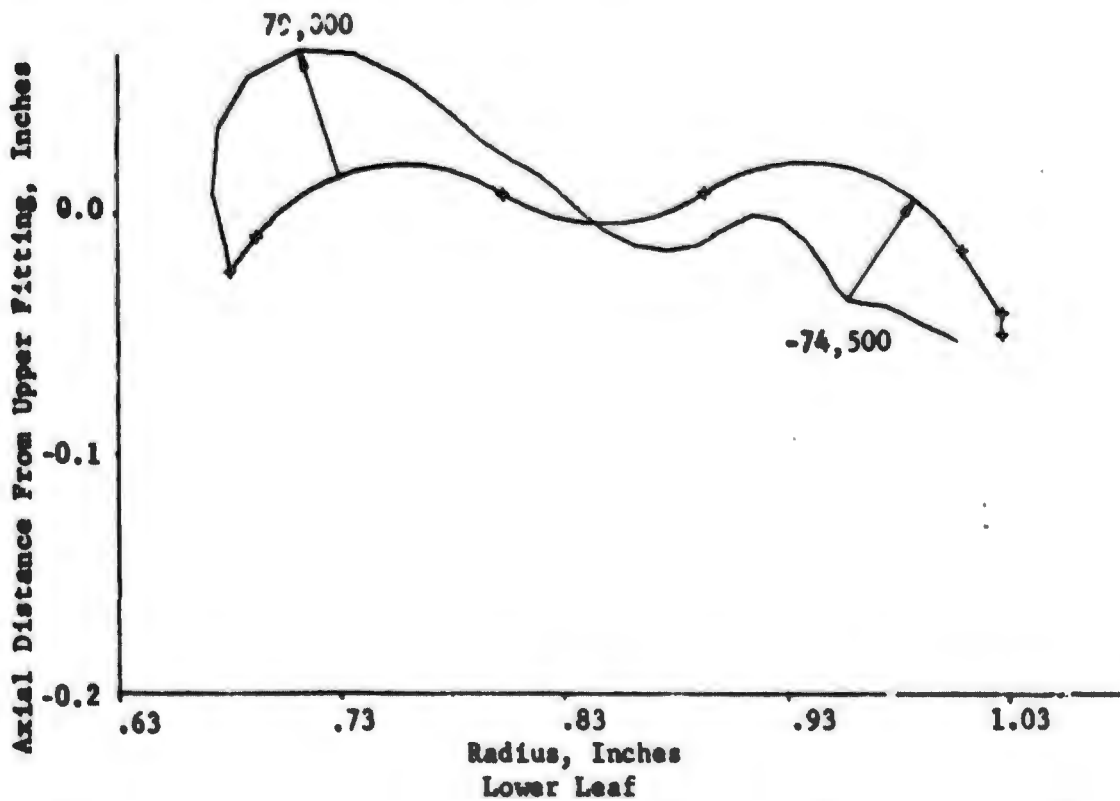
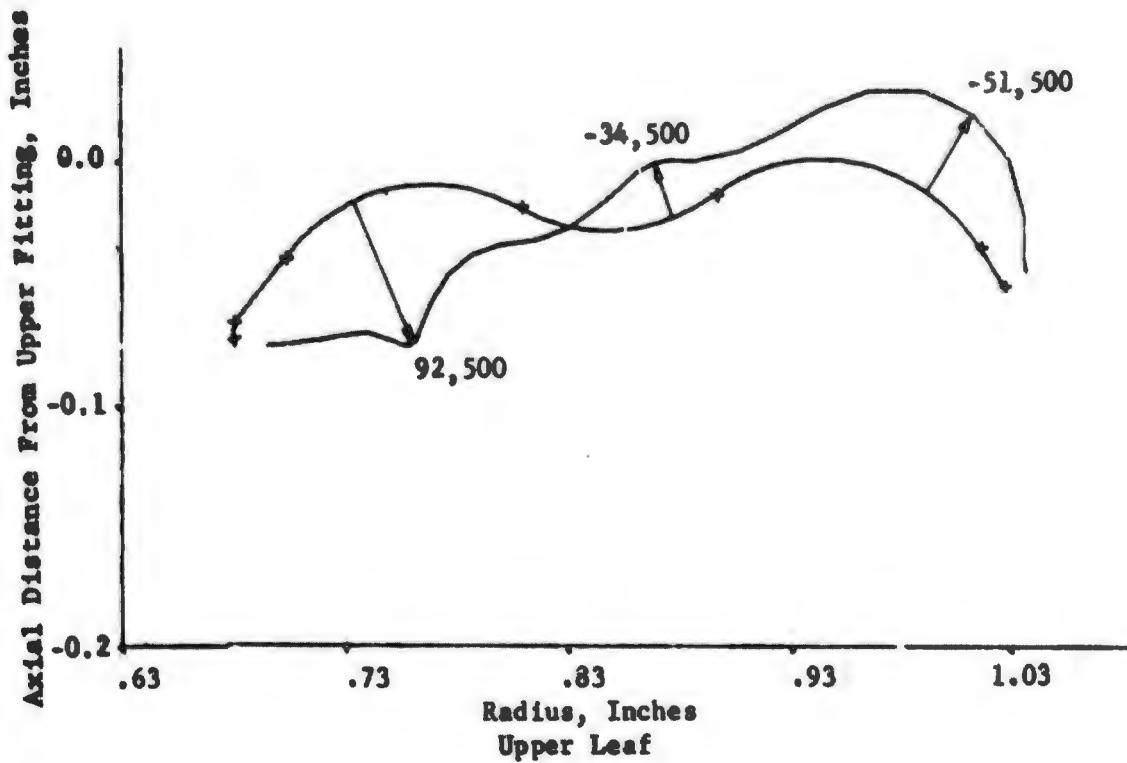


FIGURE 22. INNER SURFACE MERIDIONAL STRESSES IN AN AXIALLY COMPRESSED 2-INCH BELLOWS WITH 50° ID, 55° OD TILT ANGLES, ±2.5° CHORD ANGLES, 0.08635-INCH SWEEP RADII AND 0.3476-INCH SPAN (Unit Deflection per Unit Bellows Length)

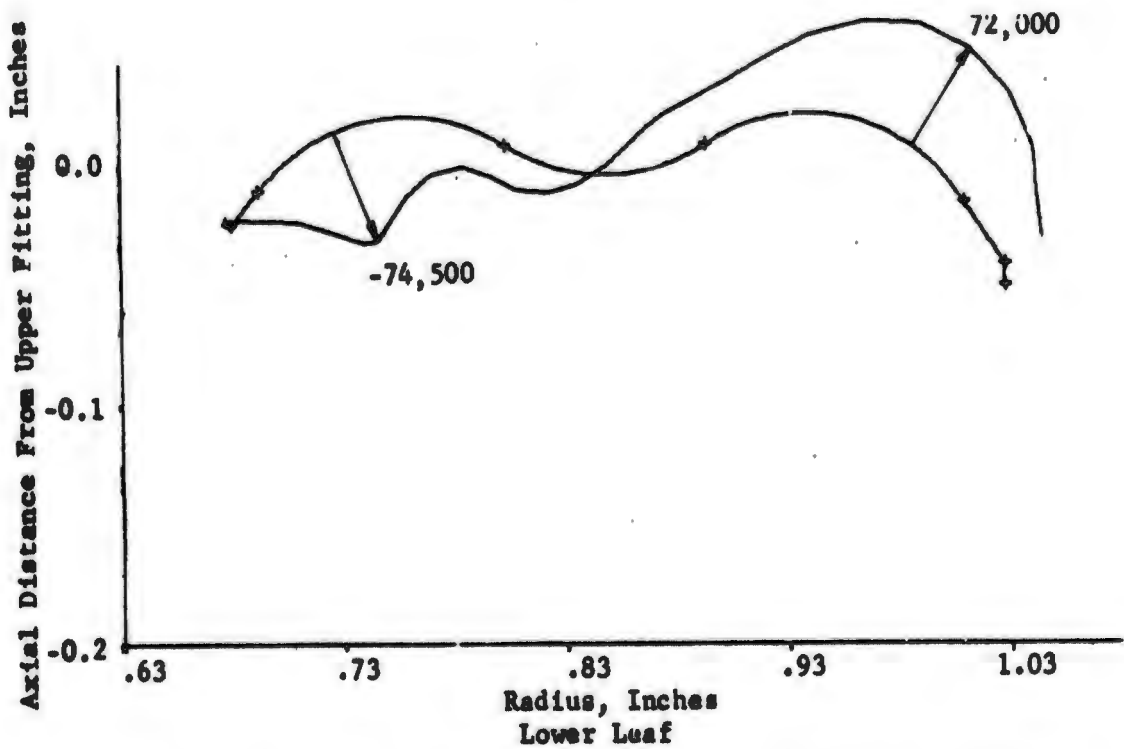
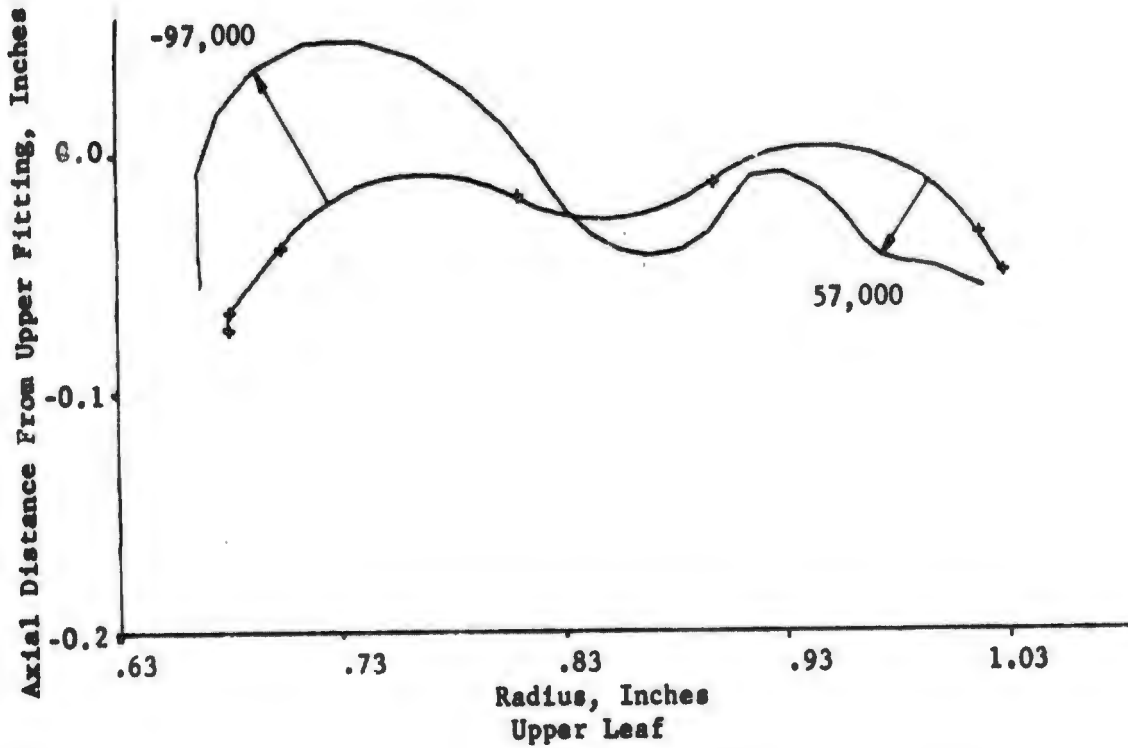


FIGURE 23. OUTER SURFACE MERIDIONAL STRESSES IN AN AXIALLY COMPRESSED 2-INCH BELLOWS WITH 50° ID, 55° OD TILT ANGLES, ±2.5° CHORD ANGLES, 0.08635-INCH SWEEP RADII AND 0.3476-INCH SPAN (Unit Deflection per Unit Bellows Length)

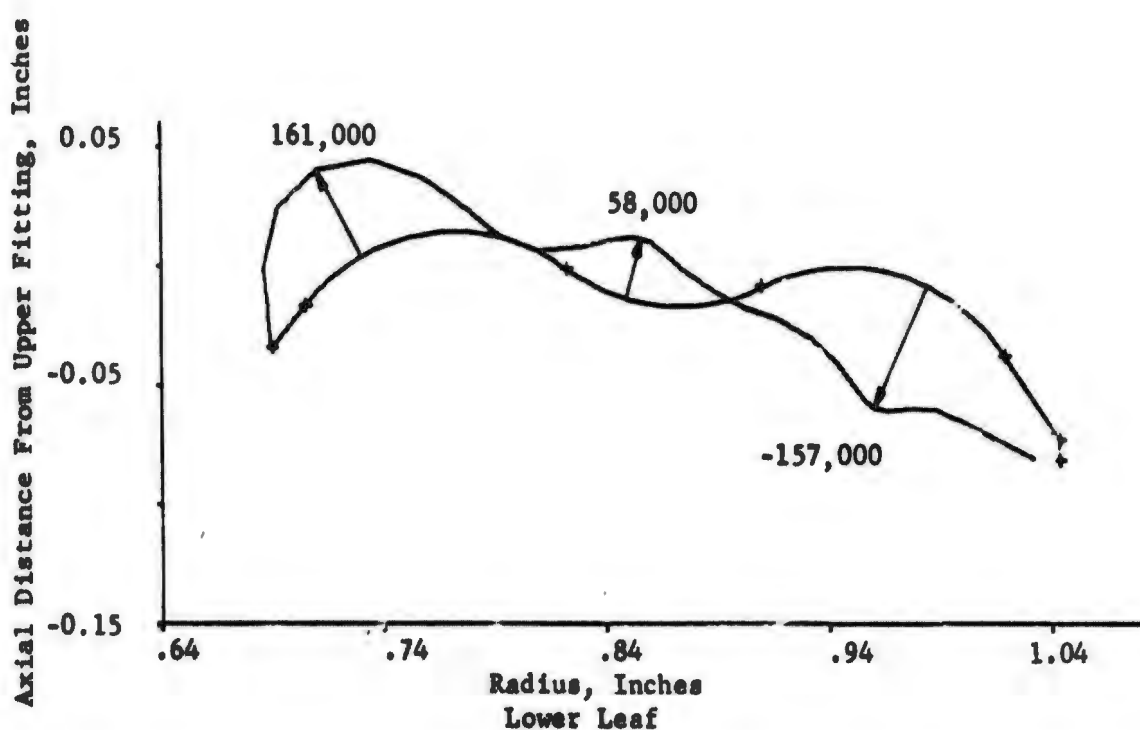
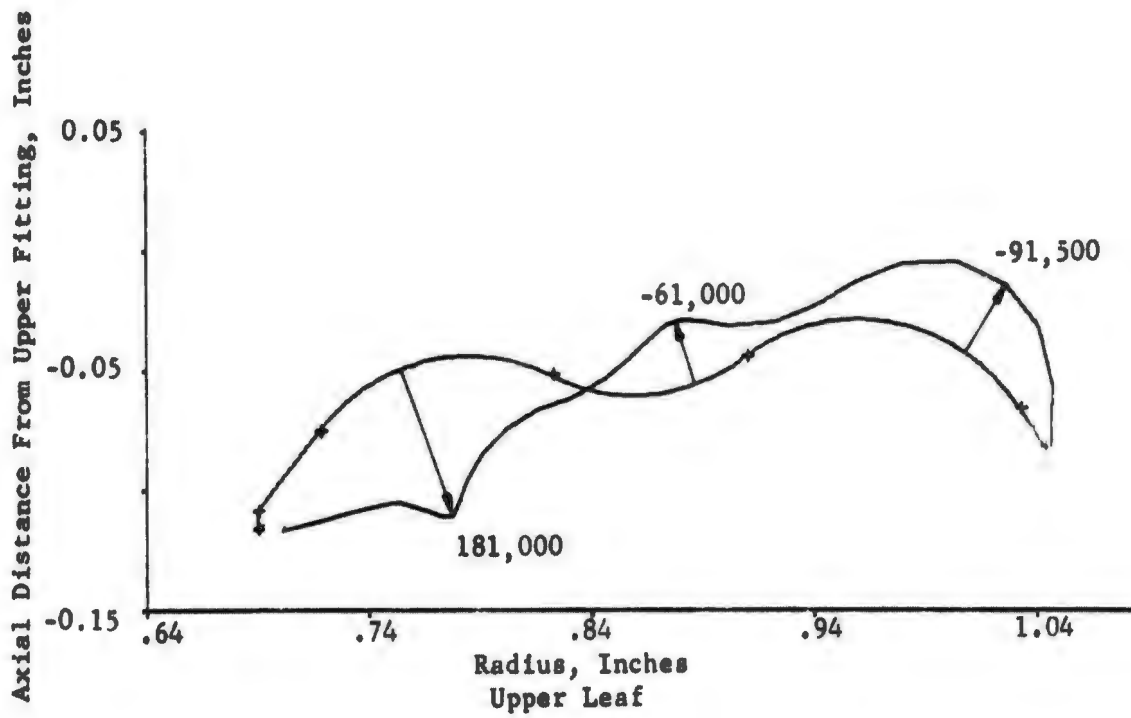


FIGURE 24. INNER SURFACE MERIDIONAL STRESSES IN AN AXIALLY COMPRESSED 2-INCH BELLOWS WITH 50° ID, 55° OD TILT ANGLES, ±5° CHORD ANGLES, 0.08785-INCH SWEEP RADII AND 0.3536-INCH SPAN (Unit Deflection per Unit Bellows Length)

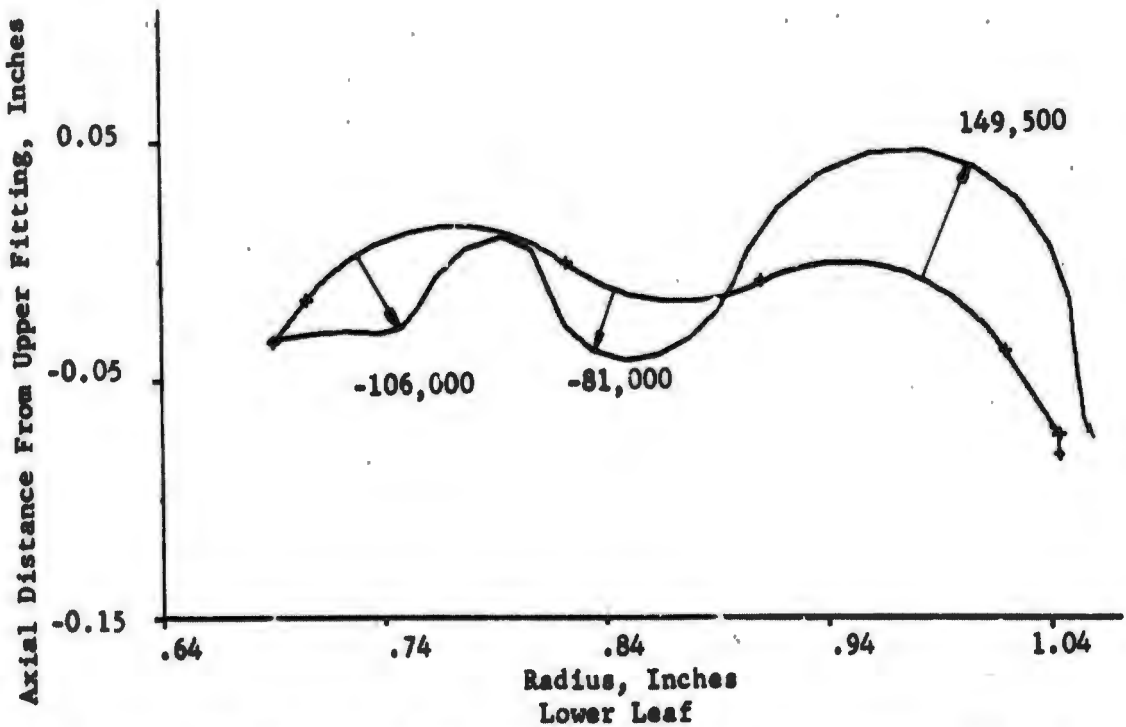
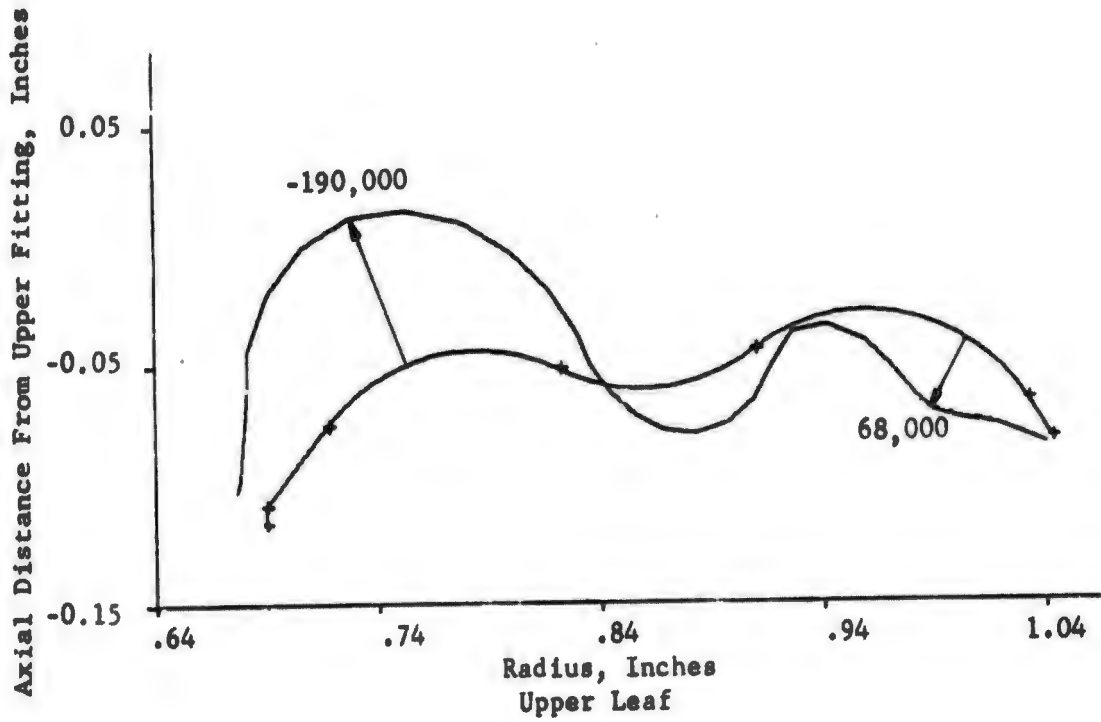


FIGURE 25. OUTER SURFACE MERIDIONAL STRESSES IN AN AXIALLY COMPRESSED 2-INCH BELLOWS WITH 50° ID, 55° OD TILT ANGLES, ±5° CHORD ANGLES, 0.08785-INCH SWEEP RADII AND 0.3536-INCH SPAN (Unit Deflection per Unit Bellows Length)

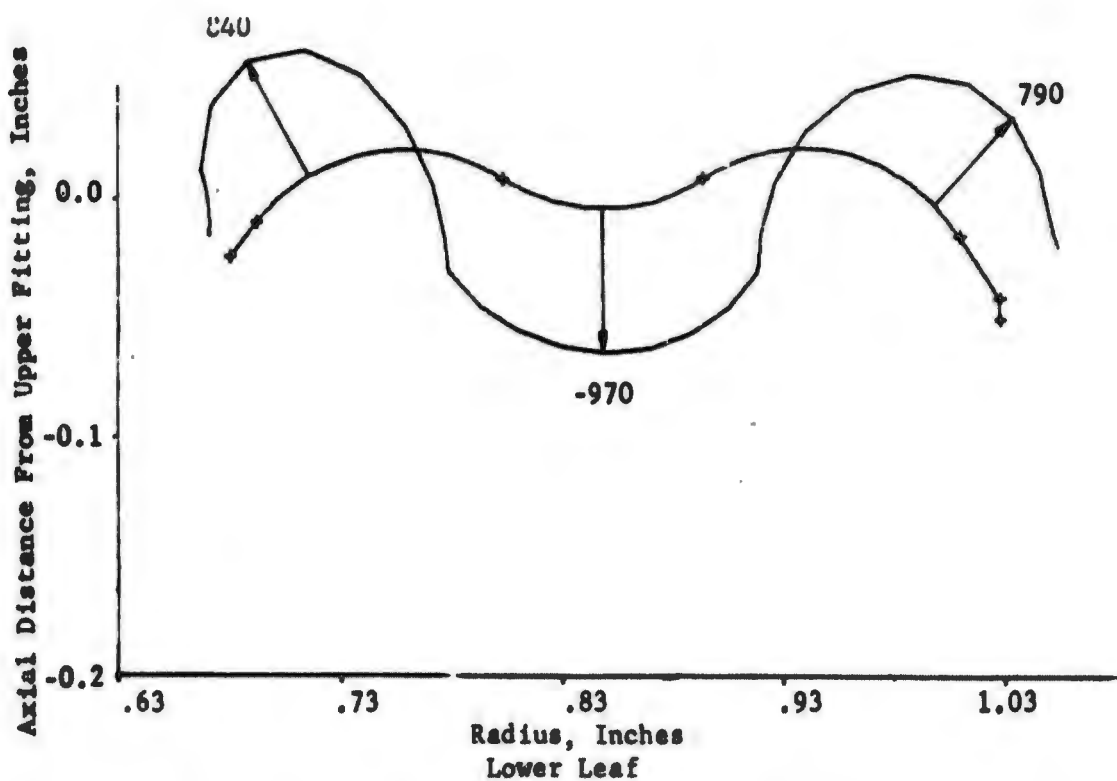
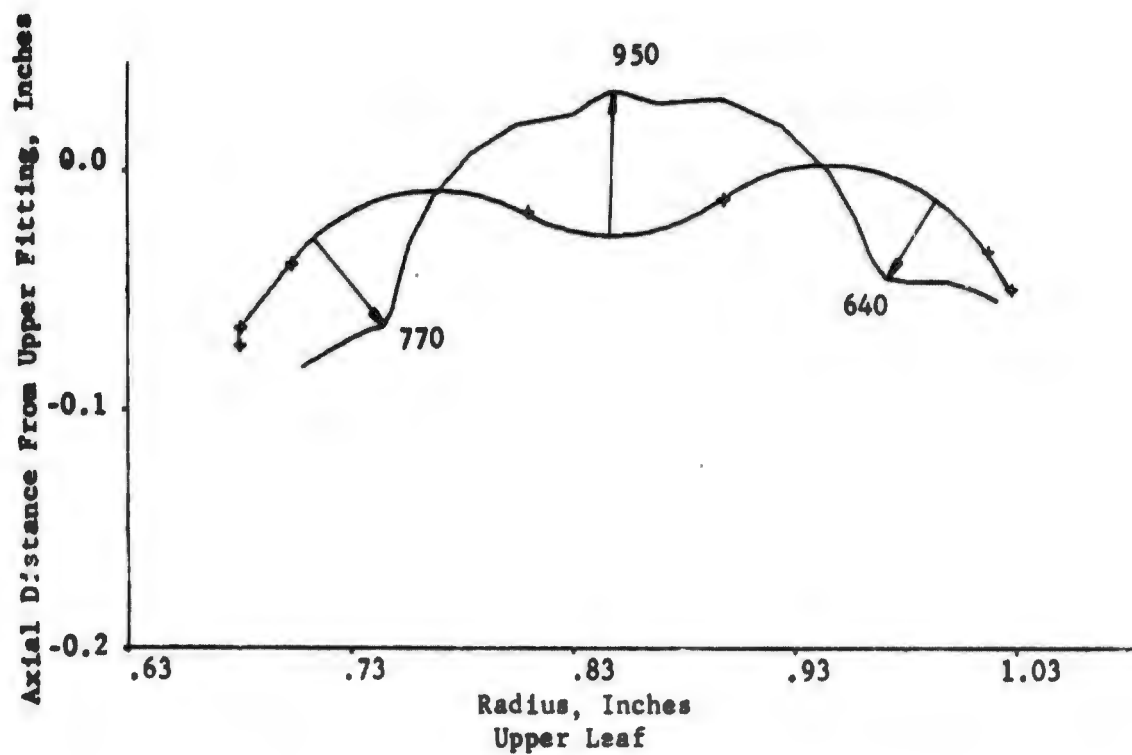


FIGURE 26. INNER SURFACE MERIDIONAL STRESSES IN AN INTERNALLY PRESSURIZED 2-INCH BELLOWS WITH 50° ID, 55° OD TILT ANGLES, ±2.5° CHORD ANGLES, 0.08635-INCH SWEEP RADII AND 0.3476-INCH SPAN (Pressure = 1 psi)

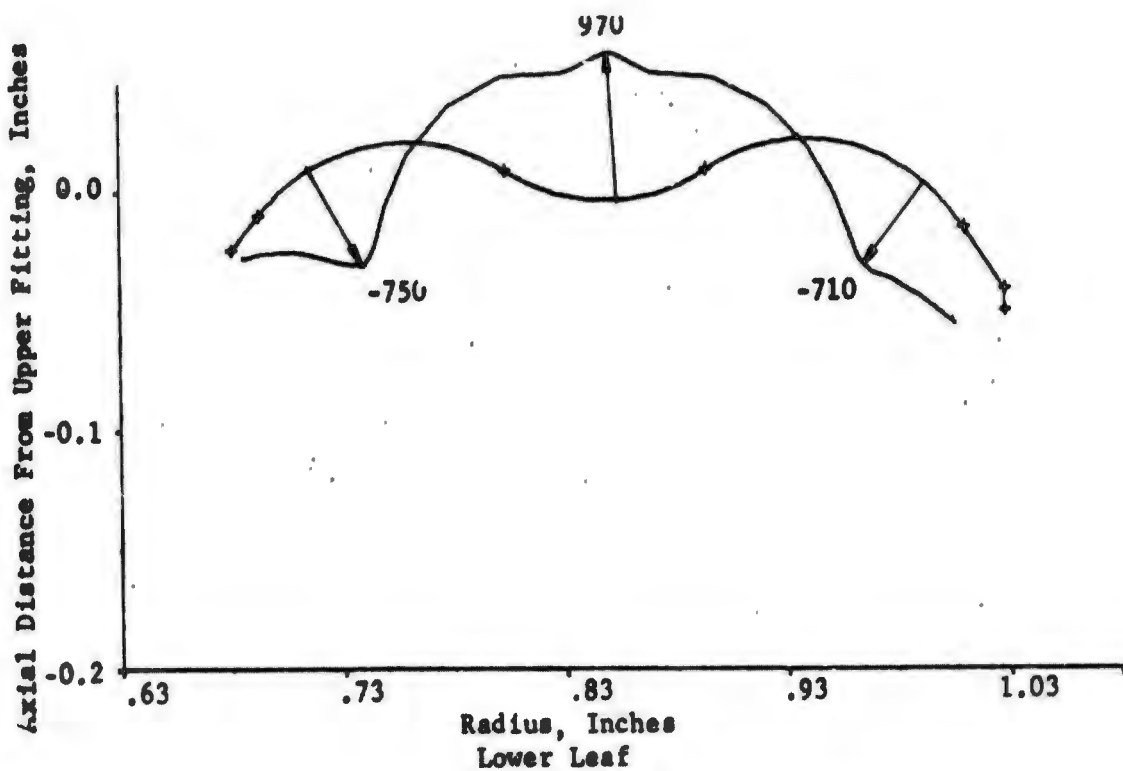
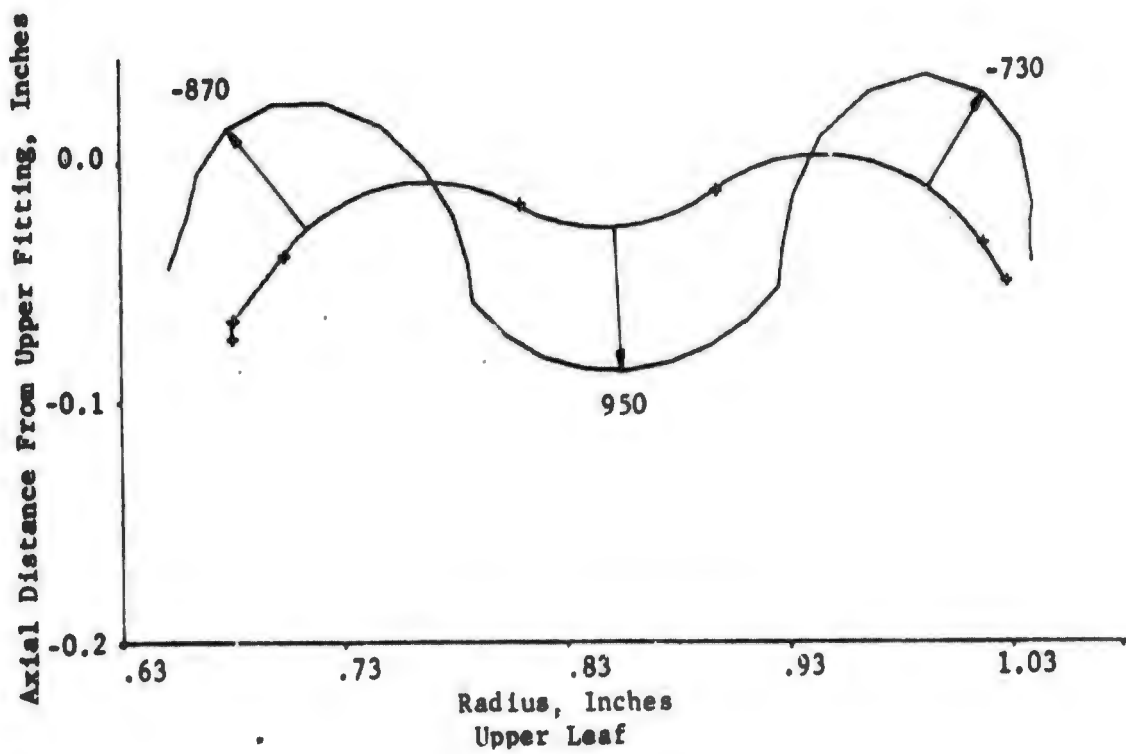


FIGURE 27. OUTER SURFACE MERIDIONAL STRESSES IN AN INTERNALLY PRESSURIZED 2-INCH BELLOWS WITH 50° ID, 55° OD TILT ANGLES, ±2.5° CHORD ANGLES, 0.08635-INCH SWEEP RADII AND 0.3476-INCH SPAN (Pressure = 1 psi)

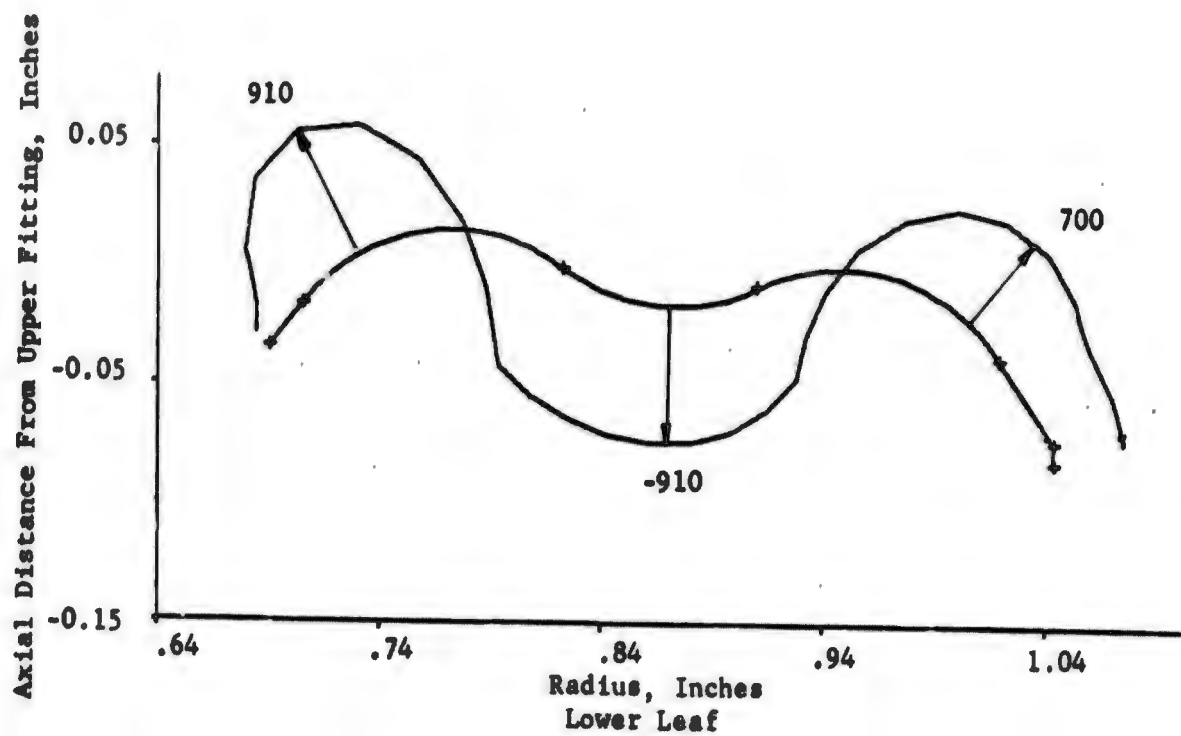
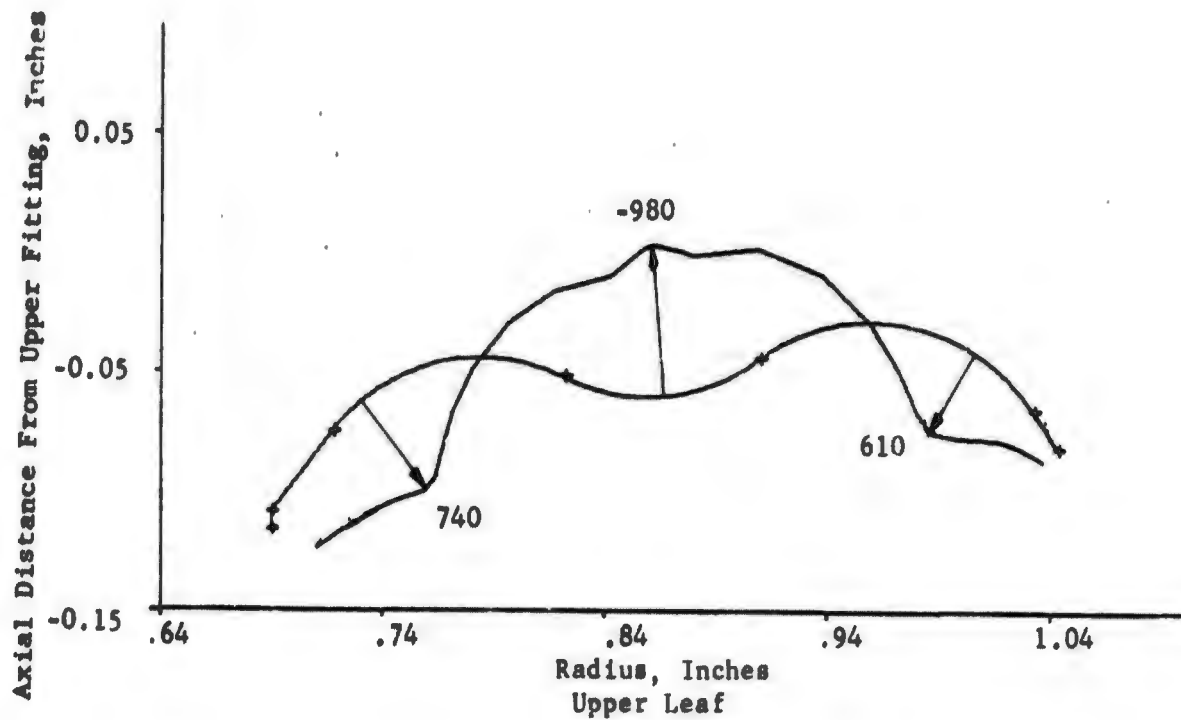


FIGURE 28. INNER SURFACE MERIDIONAL STRESSES IN AN INTERNALLY PRESSURIZED 2-INCH BELLOWS WITH 50° ID, 50° OD TILT ANGLES, ±5° CHORD ANGLES, 0.08785-INCH SWEEP RADII AND 0.3536-INCH SPAN (Pressure = 1 psi)

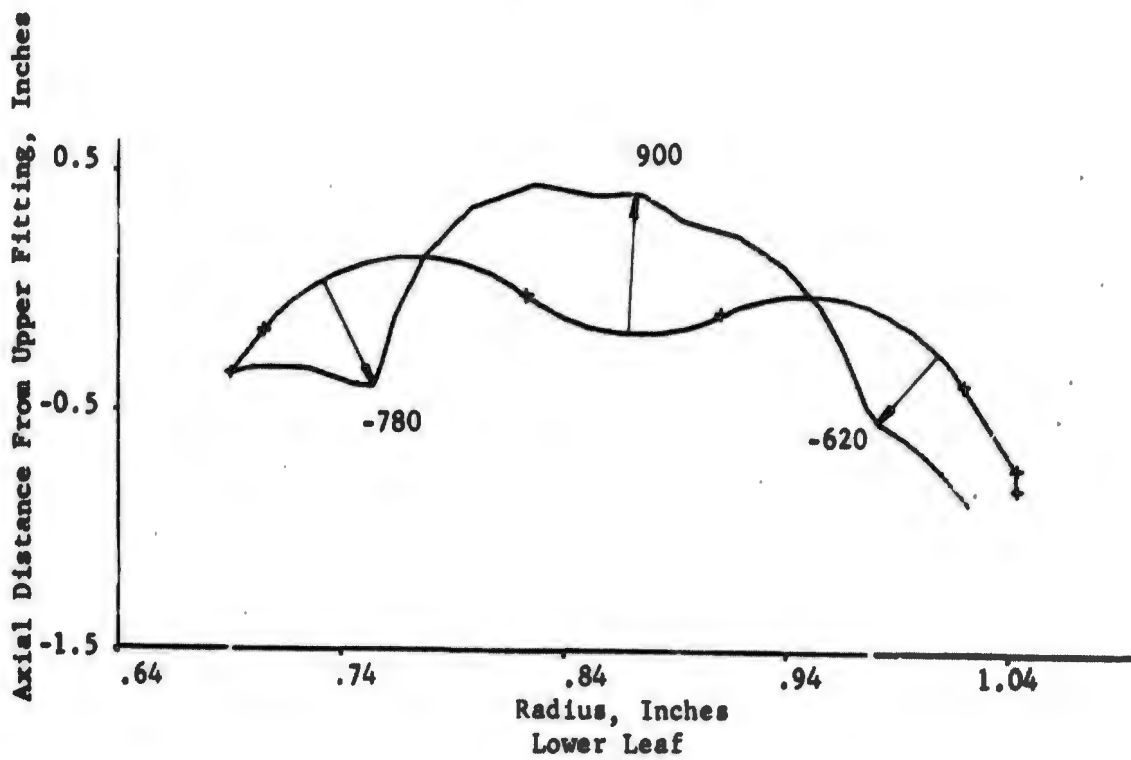
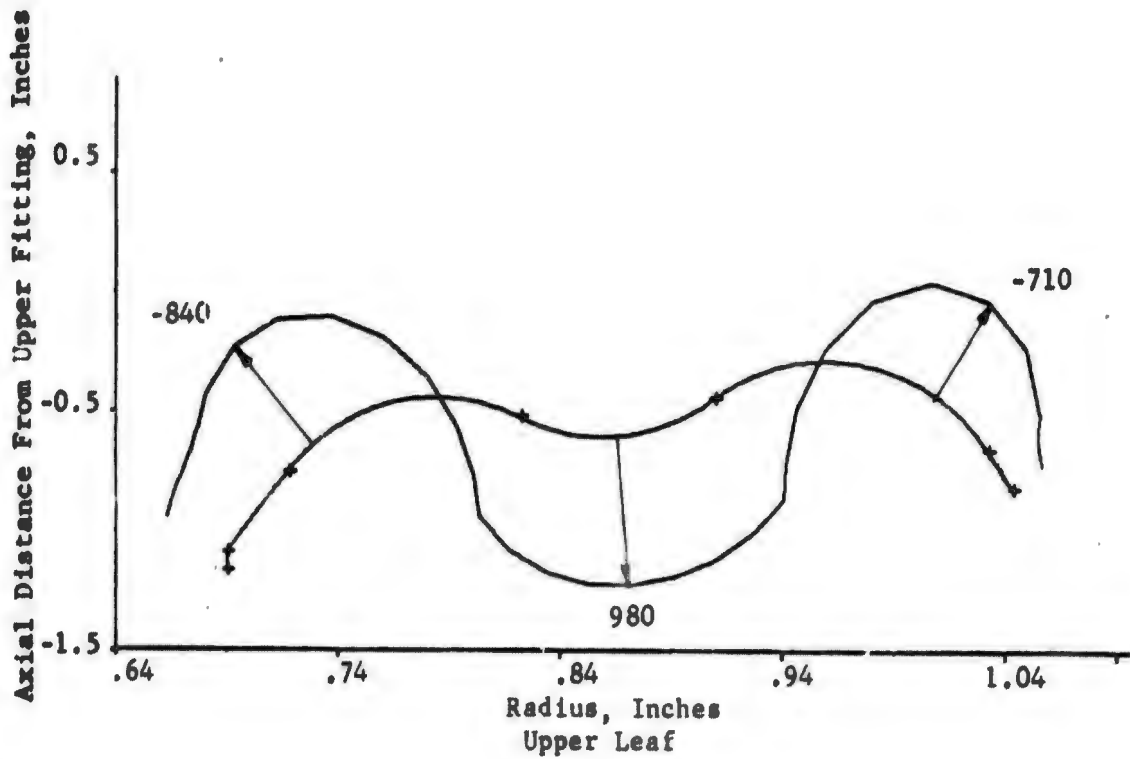


FIGURE 29. OUTER SURFACE MERIDIONAL STRESSES IN AN INTERNALLY PRESSURIZED 2-INCH BELLOWS WITH 50° ID, 55° OD TILT ANGLES, ±5° CHORD ANGLES, 0.08785-INCH SWEEP RADII AND 0.3536-INCH SPAN (Pressure = 1 psi)

In contrast to the rather predictable trend noted for the deflection stresses, the effects of pitch on the pressure stresses was less clear-cut. An examination of the Figures 26 through 29 shows that for the 2-inch bellows, the maximum stress occurred on the middle sweep and switched from the lower leaf to the upper leaf as the pitch was increased. This result was caused by the relative decrease in the arch of the upper leaf and increased arch of the lower leaf as the pitch is increased. It is pointed out in the section on effects of sweep radius that the center sweep exhibited an increased bending stress with decreasing radius under pressure loading.

For the 3-inch bellows, the pressure loading caused maximum stress on the inner sweep nearest the bellows root. At the smaller pitch, the maximum stress was on the upper leaf and increased with increasing pitch. Although an analysis was not made of the 3-inch bellows for pitch to span ratio smaller than 0.2, it is clear that the maximum stress would have occurred on the lower leaf in this case. It appears from a study of the results for pressure loading, that an optimum pitch can be found for pressure stresses at which the maximum stresses in the upper and lower bellows leaves are equal. This seems to occur at pitch to span ratios between 0.15 and 0.02, but depends on the overall arch of the upper and lower leaves. The study of deflection loads also indicated that the pitch should be kept as low as possible. As noted earlier, the restraints imposed by practical considerations such as the welding process and the desirability of operating the bellows in compression would seem to prevent making a bellows with the optimum pitch. Thus, the pitch of tilt-edge welded bellows will be determined by practical considerations in the same way that pitch is determined for conventional welded bellows.

SECTION III

OPTIMIZATION OF BELLOWS CONVOLUTION CROSS-SECTIONS

A major objective of the present study was the determination of optimum convolution shapes in 1-inch, 2-inch, and 3-inch bellows. These shapes were to have minimum stress conditions at the welds and minimum overall stresses both for axial deflection and for internal pressure loads. In addition to minimizing stresses in the bellows convolutions, minimizing stresses in the end bellows leaf where it is welded to some end fitting was also considered. Stress analysis results are presented in this section for certain selected convolution shapes for a 1-, 2-, 3-, and 3.5-inch bellows. Also, a description is given of an investigation that was made into the effects of varying the shape of the bellows end leaves on the stresses near the end fitting welds.

Selection of Optimum Convolution Shapes

As described in the previous sections, the parametric analyses indicated that a sweep radius of between 20 and 25 percent of the span would be near the optimum for a pressure loading and that chord angles between $\pm 2.5^\circ$ and $\pm 5^\circ$ would be desirable for deflection loaded bellows. It was also determined that tilt angles could be found that gave acceptably low stresses in the weld areas for bellows in the 1- to 4-inch range. Convolution shapes were selected within these ranges of parameters for the 1-, 2-, and 3-inch sizes. Tables of the specified dimensions for these bellows are given in Tables 14 through 15 in NONLIN format as in Table 1*. The thickness of the 1-inch bellows was taken as .004 inch because of its smaller size. The outer surface meridional stresses for the 1- and 2-inch bellows are given for internal pressure and axial compression loading in Figures 30 through 33. Similar stress distributions for the 3-inch bellows are given in Figures 10, 11, 14, and 15.

In addition to these bellows, considerable study was given to a 3.5-inch bellows to develop a bellows configuration that could be compared with a conventional welded bellows that had been investigated under the previous research contract. Dimensions of two optimized bellows are given in Tables 17 and 18. Stresses in these two bellows shapes were shown in Figures 12, 13, 16, 17, 19, and 21. The analytical results reported in this section clearly demonstrated that it was possible to design tilt-edge bellows with optimized stress distributions for a range of bellows diameters. The principal interaction noted between tilt angle and bellows size was that the tilt angles must be made steeper for the smaller diameter bellows to achieve satisfactory weld stress reductions. This effect seemed to be more an interrelation between the bellows span and thickness than an effect of the bellows radius. This was demonstrated by the two optimum shapes for the 3.5-inch bellows for which the shorter span had the higher tilt angles.

Alternatively, by invoking geometric similarity, these bellows shapes could be interpreted as 3.5-inch bellows with thicknesses of from

* See footnote to page 11 for a description of the entries in these tables.

TABLE 14. AN OPTIMUM CONVOLUTION SHAPE FOR A 1-INCH TILT-
EDGE WELDED BELLOWS, ID TILT ANGLE = 60°,
OD TILT ANGLE = 60°, SPAN = 0.1868 INCH

Part No.	Shell Type	Outer Normal, degrees		Radii, inches	
		Initial	Final	a	b
1	Conical	240	--	0.52740	0.01708
2	Toroidal	240	145	0.48082	-0.04392
3	Toroidal	145	205	0.43042	0.04392
4	Toroidal	205	120	0.39332	-0.02392
5	Conical	120	--	0.35528	0.02936
6	Cylindrical	90	--	0.34060	0.00800
7	Conical	-60	--	0.34060	0.01606
8	Toroidal	-60	35	0.38667	0.04392
9	Toroidal	35	-25	0.43707	-0.04392
10	Toroidal	-25	60	0.47427	0.04392
11	Conical	60	--	0.51231	0.03018
12	Cylindrical	90	--	0.52740	0.00800

TABLE 15. AN OPTIMUM CONVOLUTION SHAPE FOR A 2-INCH,
TILT-EDGE WELDED BELLOWS, ID TILT ANGLE = 50°,
OD TILT ANGLE = 60°, SPAN = 0.3476 INCH

Part No.	Shell Type	Outer Normal, degrees		Radii, inches	
		Initial	Final	a	b
1	Conical	240.000	--	1.03000	0.01982
2	Toroidal	235.000	145.633	0.94531	-0.08635
3	Toroidal	145.633	207.050	0.84781	0.08635
4	Toroidal	207.050	130.000	0.76879	-0.08635
5	Conical	130.000	--	0.70264	0.03531
6	Cylindrical	90.000	--	0.67944	0.00777
7	Conical	-50.000	--	0.67944	0.01875
8	Toroidal	-50.000	31.000	0.75764	0.08635
9	Toroidal	31.000	-31.650	0.84734	-0.08635
10	Toroidal	-31.650	60.000	0.93796	0.08635
11	Conical	60.000	--	1.01274	0.03452
12	Cylindrical	90.000	--	1.03000	0.01000

TABLE 16. AN OPTIMUM CONVOLUTION SHAPE FOR A 3-INCH
TILT-EDGE WELDED BELLOWS, ID TILT ANGLE = 45°,
OD TILT ANGLE = 50°, SPAN = 0.5304 INCH

Part No.	Shell Type	Outer Normal, degrees		Radii, inches	
		Initial	Final	a	b
1	Conical	230	--	1.56720	0.03697
2	Toroidal	230	145	1.44247	-0.13177
3	Toroidal	145	205	1.29127	0.13177
4	Toroidal	205	135	1.17997	-0.13177
5	Conical	135	--	1.08679	0.07070
6	Cylindrical	90	--	1.03680	0.00707
7	Conical	-45	--	1.03680	0.04252
8	Toroidal	-45	35	1.16002	0.13177
9	Toroidal	35	-25	1.31122	-0.13177
10	Toroidal	-25	50	1.42252	0.13177
11	Conical	50	--	1.52347	0.06802
12	Cylindrical	90	--	1.56720	0.00777

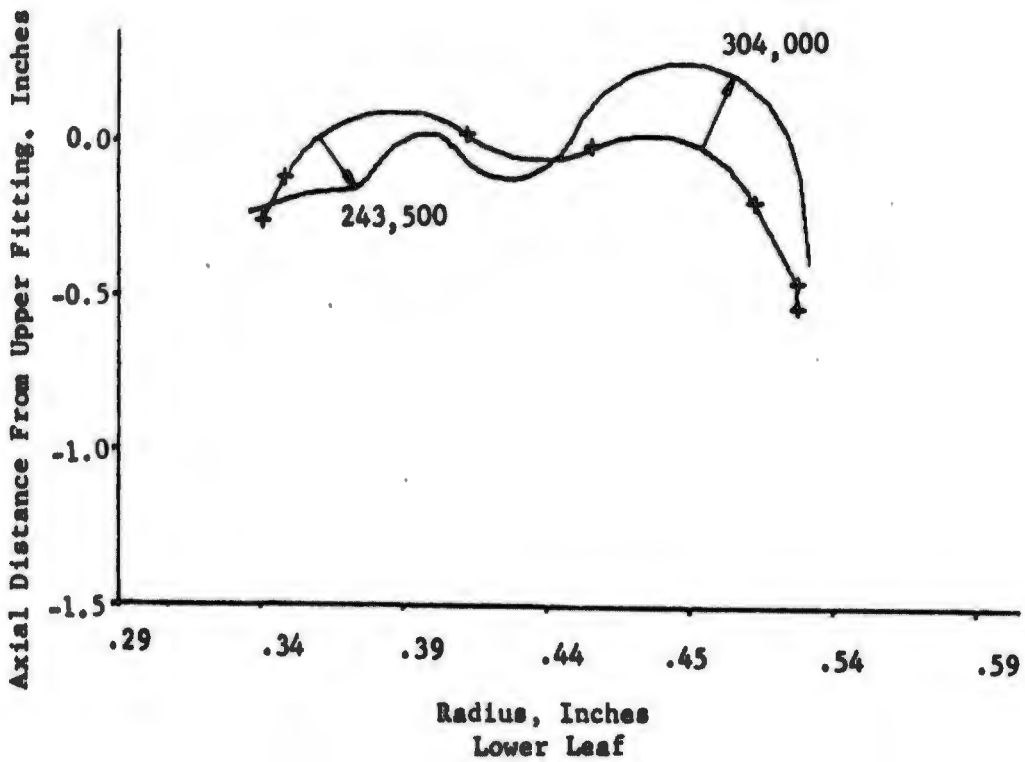
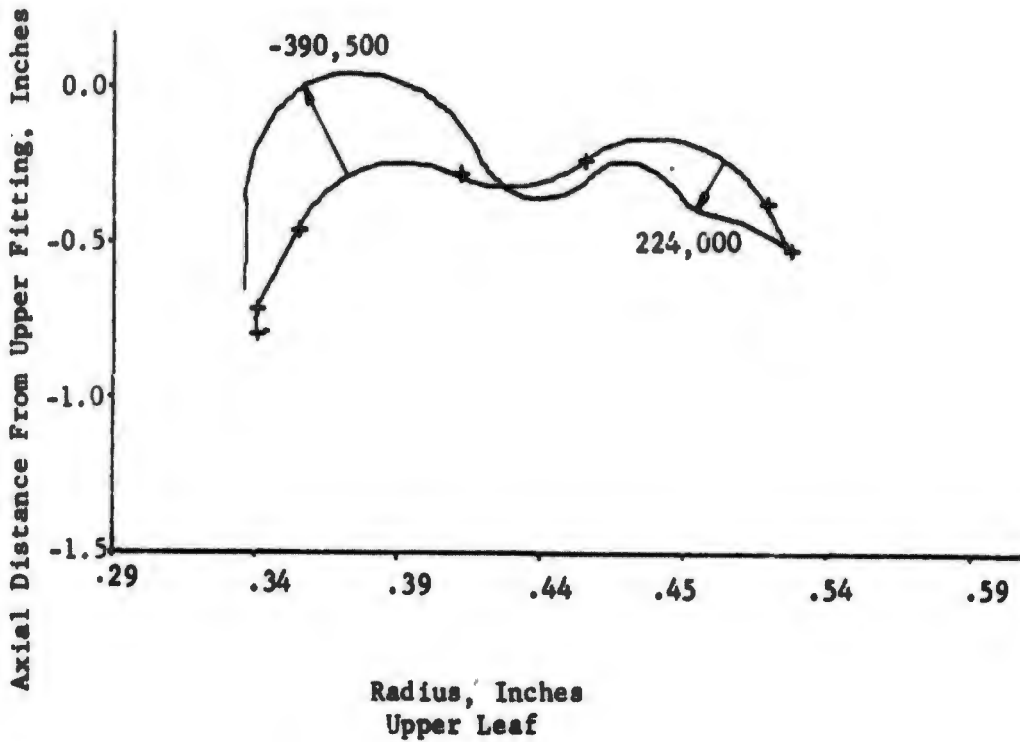


FIGURE 30. OUTER SURFACE MERIDIONAL STRESSES IN AN AXIALLY COMPRESSED 1-INCH BELLOWS WITH 60° ID, 60° OD TILT ANGLES, ±5° CHORD ANGLES, 0.04392-INCH SWEEP RADII, AND 0.1868-INCH SPAN (Unit Deflection Per Unit Bellows Length)

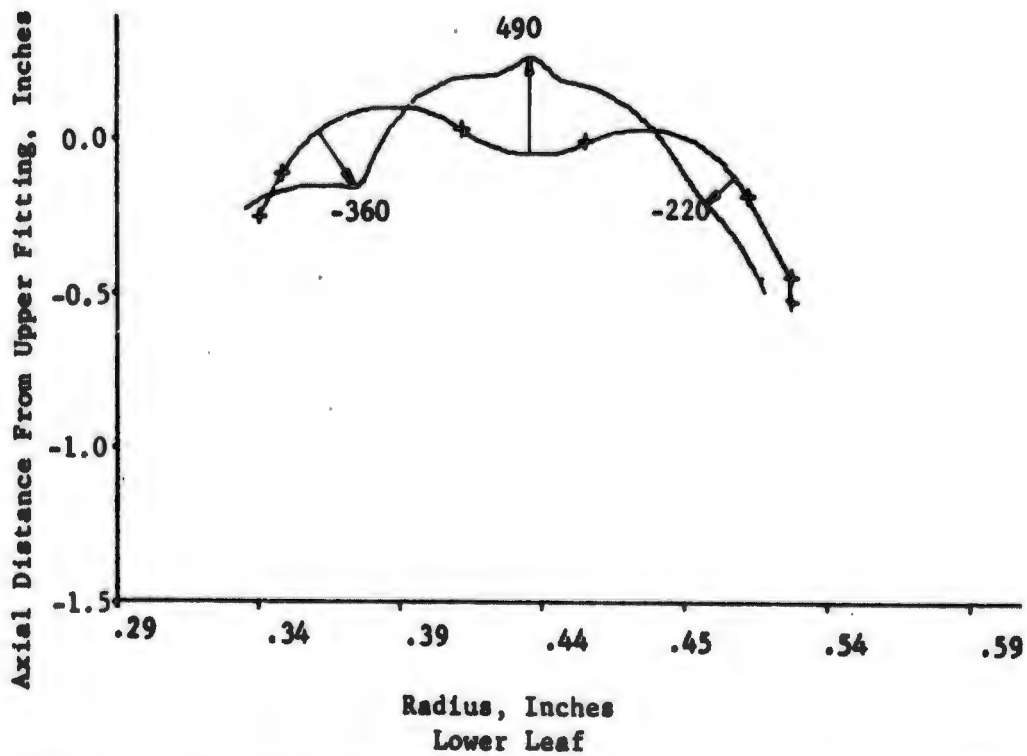
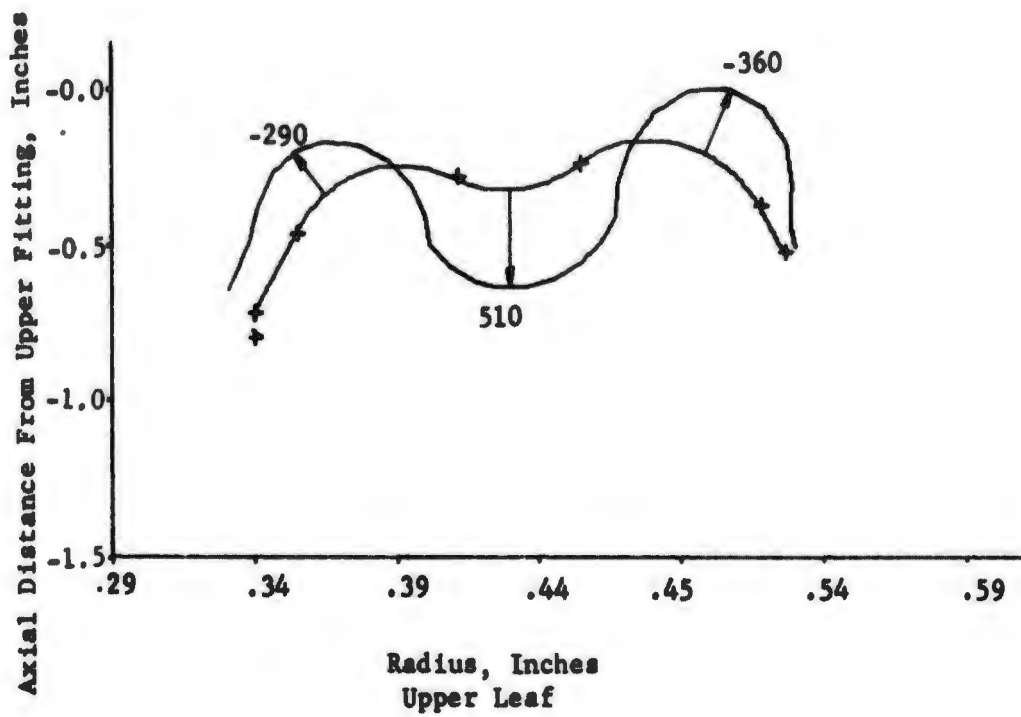


FIGURE 31. OUTER SURFACE MERIDIONAL STRESSES IN AN INTERNALLY PRESSURIZED 1-INCH BELLOWS WITH 60° ID, 60° OD TILT ANGLES, ±5° CHORD ANGLES, 0.04392-INCH SWEEP RADII, AND 0.1868-INCH SPAN (Pressure = 1 psi)

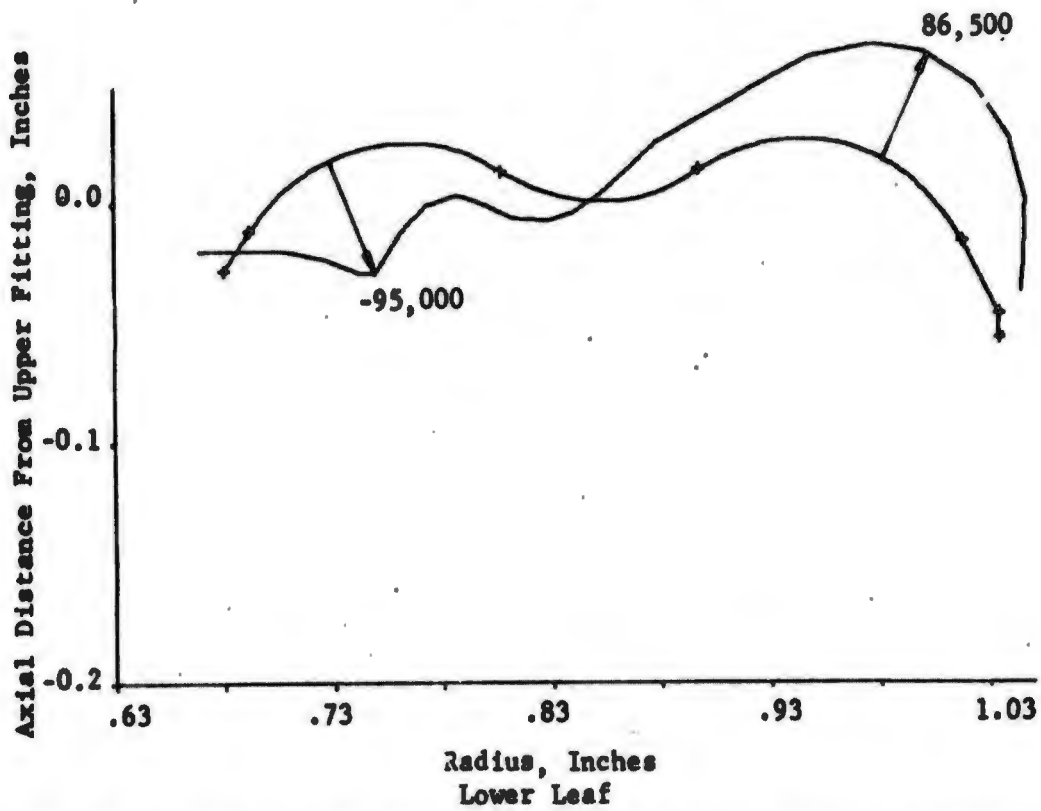
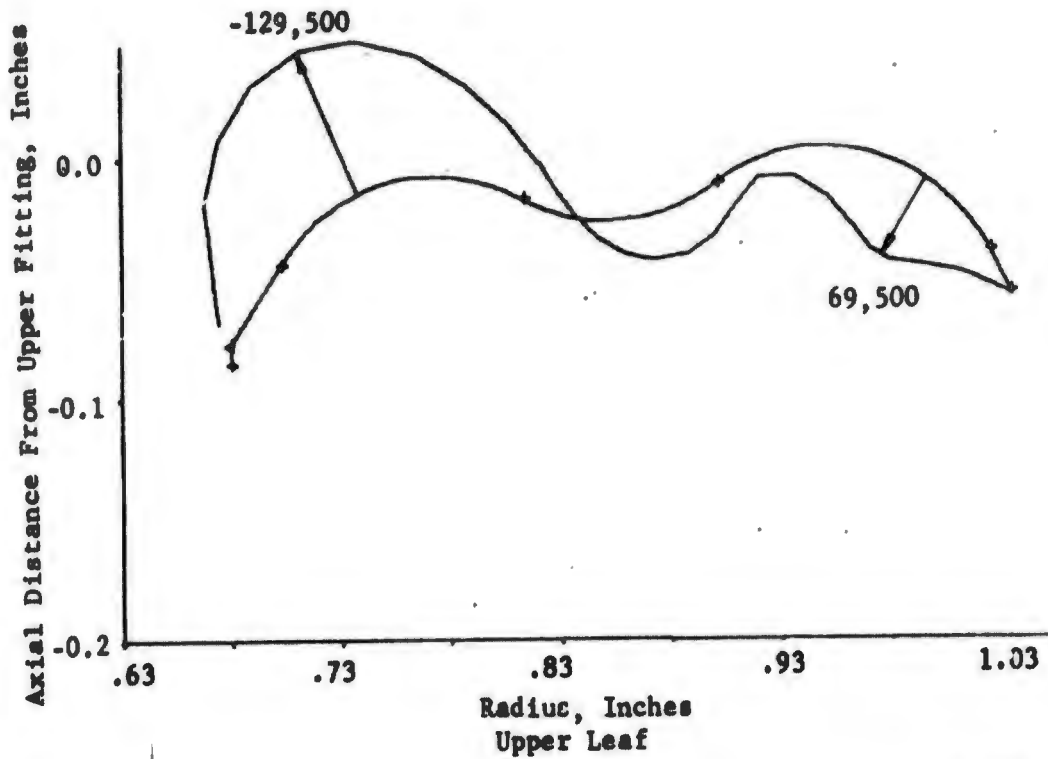


FIGURE 32. OUTER SURFACE MERIDIONAL STRESSES IN AN AXIALLY COMPRESSED 2-INCH BELLOWS WITH 55° ID, 60° OD TILT ANGLES, ±2.5° CHORD ANGLES, 0.08635-INCH SWEEP RADII, AND 0.3546-INCH SPAN (Unit Deflection Per Unit Length Bellows)

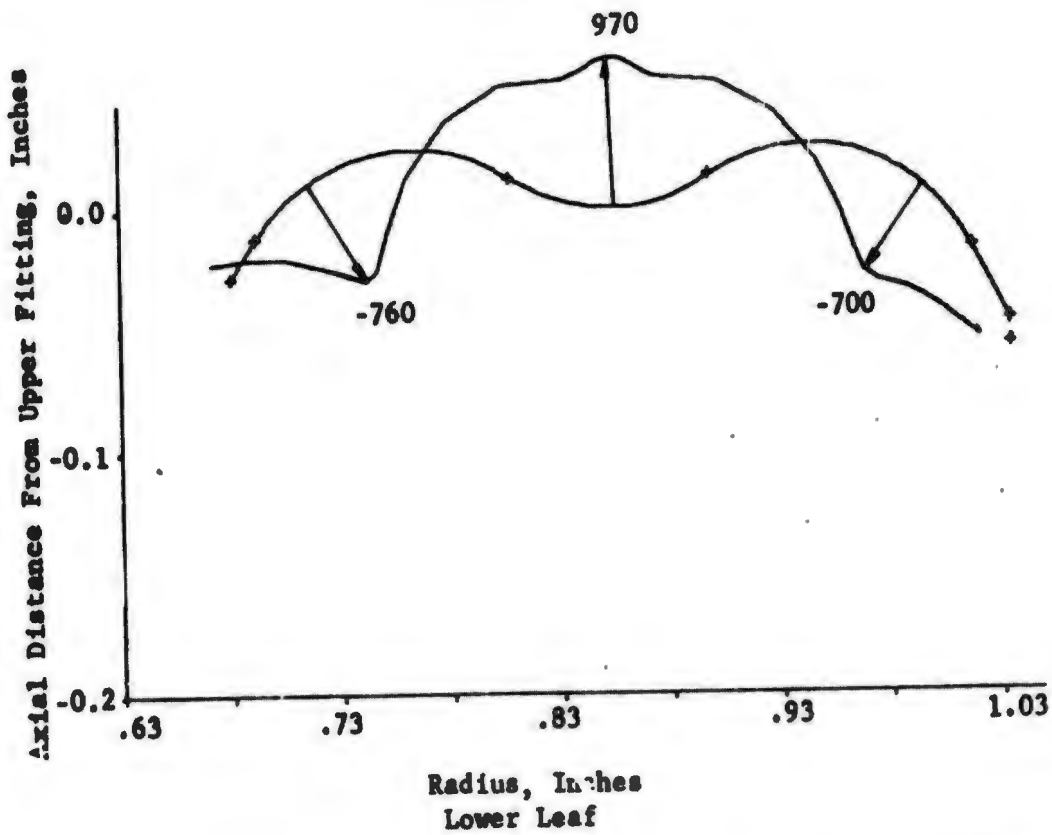
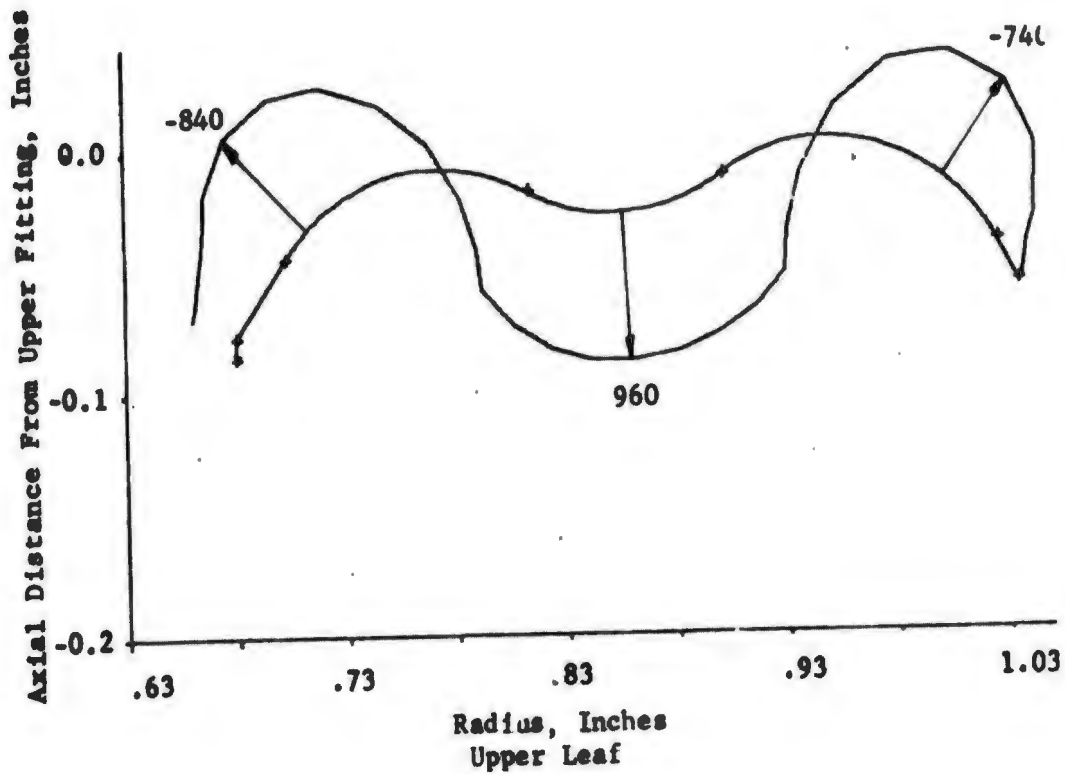


FIGURE 33. OUTER SURFACE MERIDIONAL STRESSES IN AN INTERNALLY PRESSURIZED 2-INCH BELLOWS WITH 55° ID, 60° OD TILT ANGLES, ±2.5° CHORD ANGLES, 0.08635-INCH SWEEP RADII, AND 0.3546-INCH SPAN (Pressure = 1 psi)

TABLE 17. AN OPTIMUM CONVOLUTION SHAPE FOR A 3.5-INCH
TILT-EDGE WELDED BELLOWS, ID TILT ANGLE = 50°,
OD TILT ANGLE = 50°, SPAN = 0.378 INCH

Part No.	Shell Type	Outer Normal, degrees		Radii, inches	
		Initial	Final	a	b
1	Conical	230.000	--	1.79730	0.05288
2	Toroidal	230.000	146.3167	1.68670	-0.10000
3	Toroidal	146.3167	193.2667	1.57522	0.10000
4	Toroidal	193.2667	130.0000	1.52989	-0.10000
5	Conical	130.0000	--	1.45329	0.05287
6	Cylindrical	90.0000	--	1.41930	0.00777
7	Conical	-50.0000	--	1.41930	0.04397
8	Toroidal	-50.0000	33.6000	1.52417	0.10000
9	Toroidal	33.6000	-13.3300	1.63483	-0.10000
10	Toroidal	-13.3300	50.0000	1.68098	0.10000
11	Conical	50.0000	--	1.75758	0.06179
12	Cylindrical	90.0000	--	1.79730	0.00777

TABLE 18. AN OPTIMUM CONVOLUTION SHAPE FOR A 3.5 INCH TILT-
EDGE WELDED BELLOWS, ID TILT ANGLE = 45°, OD
TILT ANGLE = 50°, SPAN = 0.6188 INCH

Part No.	Shell Type	Outer Normal, degrees		Radii, inches	
		Initial	Final	a	b
1	Conical	230	--	1.82840	0.04313
2	Toroidal	230	145	1.68288	-0.15373
3	Toroidal	145	205	1.50648	0.15373
4	Toroidal	205	135	1.37663	-0.15373
5	Conical	135	--	1.26792	0.08248
6	Cylindrical	90	--	1.20960	0.00707
7	Conical	-45	--	1.20960	0.04961
8	Toroidal	-45	35	1.35336	0.15373
9	Toroidal	35	-25	1.52976	-0.15373
10	Toroidal	-25	50	1.65961	0.15373
11	Conical	50	--	1.77738	0.07935
12	Cylindrical	90	--	1.82840	0.00777

0.005-inch for the 3.5-inch size to 0.014-inch for the 1-inch bellows expanded 3.5 times. Note that the 1-, 2-, and 3-inch bellows would have spans of .6538-, .6134-, and .6368-inches, respectively which are all comparable to the longer span 3.5-inch bellows. Using this point of view demonstrated that optimum tilt angles could be found for a bellows of a given size for a range of thicknesses. Clearly, optimum tilt angles increased as the thickness was increased.

Study of End Fitting Stresses

It was mentioned previously that nearly all of the bellows analyses were carried out with two convolution models as shown in Figure 3. The end leaves of this model were fixed at the outside ends to simulate heavy end fittings of the type shown in Figures 34 and 35*. Each analysis was examined for the effects of tilt angle on the end-fitting stresses as well as on the stresses in convolution welds. The general conclusion reached after studying the end-fitting stresses of all of the bellows analyzed was that tilt angles could be found that minimize the stresses at the end-fitting welds for either pressure or axial deflection loads. However, it was difficult to find tilt angles such that the end-fitting stresses for both pressure and axial deflection loads were satisfactorily reduced for the same tilt angle. Usually, the optimum tilt angles reduced stresses at the end-fitting welds, but these were not as low as the stresses at the convolution welds. In addition, the effect of the reversed bending and interleaf contact that reduces the stresses at the convolution welds is not present at the end-fitting.

Table 19 shows a comparison of the stresses at the upper and lower end fitting welds with the maximum bellows stresses and with the stresses at the ID and OD convolution welds. This table shows that at least one of the end fittings has an uncomfortably high stress for axial deflection loads compared to the maximum bellows stress. It is noted that the tilt angle at the upper end weld is usually lower than the optimum angle while the tilt angle at the lower end-fitting weld is usually higher than the optimum. It can be seen from Figure 3 that increasing the tilt angle at the upper end-fitting or decreasing the tilt angle at the lower end-fitting would lead to the possibility that the OD weld of the adjacent convolutions would interfere with the end fittings if the bellows were compressed.

Because of the design difficulties just described, an investigation was carried out to determine whether some simple geometric perturbation of the end leaf geometry could be found that would reduce the end fitting stresses to a level consistent with the stresses at the convolution welds. The two-convolution model of Figure 3 was used in the study to insure that the end-fitting stresses would represent the stresses in an actual bellows

* End fittings of this type have been used in all of the bellows assemblies tested in this and the previous bellows study. Behavior of these assemblies may be considered representative of the behavior of welded bellows in valve applications.

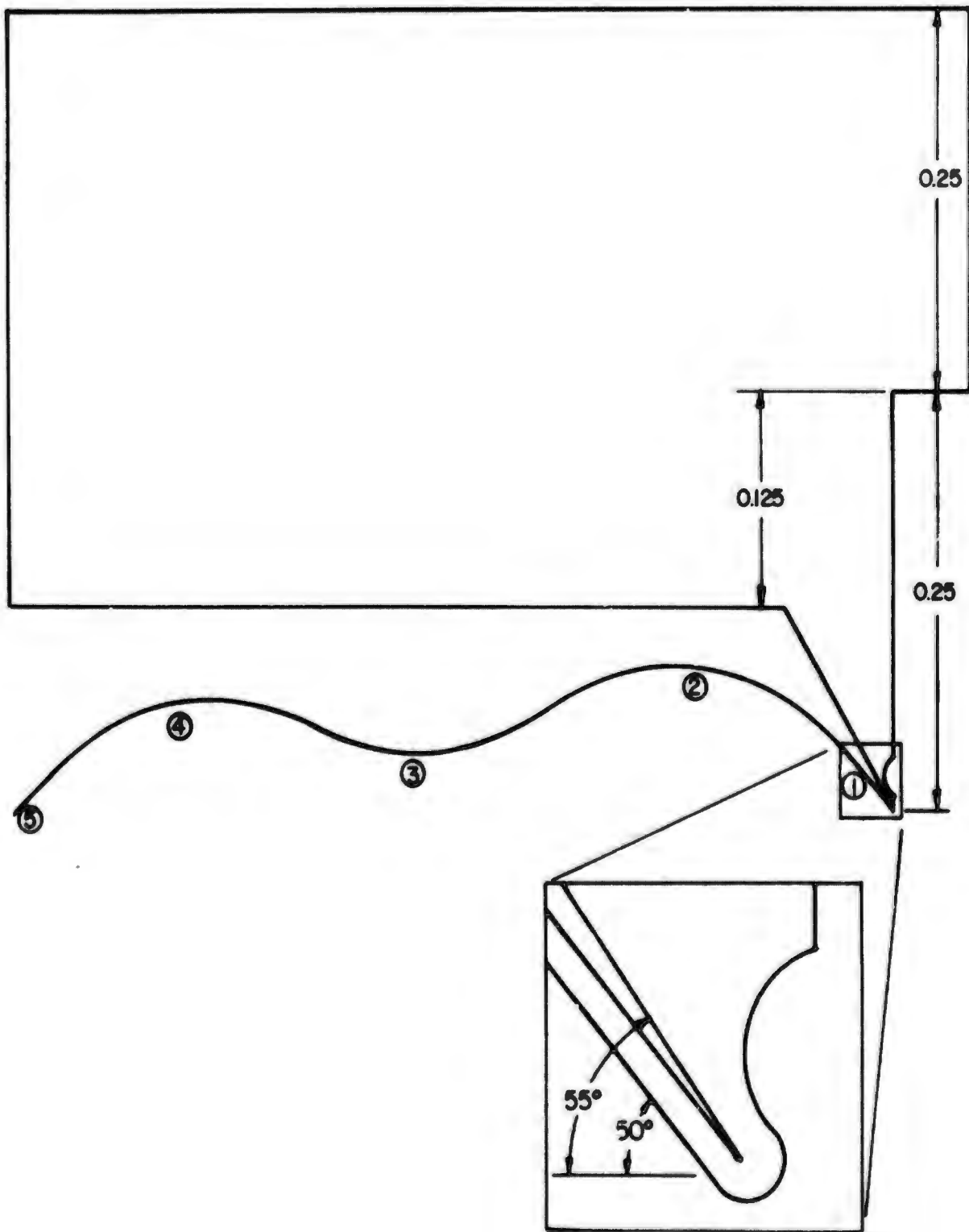


FIGURE 34. A TYPICAL UPPER END FITTING FOR A 3.5-INCH TILT-EDGE WELDED BELLOWS

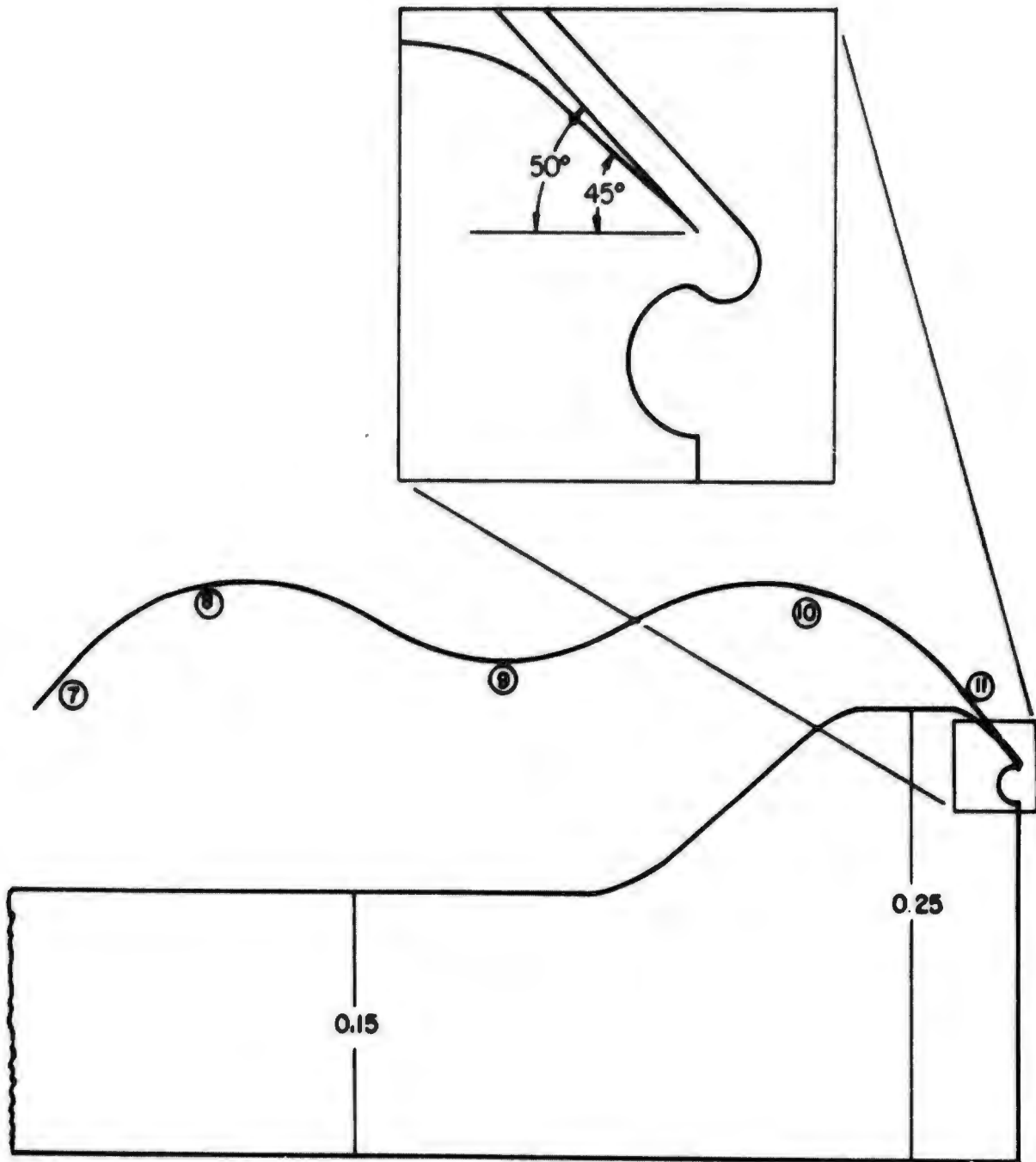


FIGURE 35. A TYPICAL LOWER END FITTING FOR A 3.5-INCH TILT-EDGE WELDED BELLOWS

TABLE 19. MAXIMUM WELD, FITTING, AND OVERALL RELATIVE STRESSES
IN OPTIMUM SHAPED TILT-EDGE WELDED BELLOW*

Bellows OD inches	Load Type	Maximum ID Weld Stress, psi	Maximum OD Weld Stress, psi	Maximum Fitting Stresses Lower psi	Maximum Fitting Stresses Upper psi	Overall Maximum Stress psi
1	Axial Compression	54,000	-61,000	-127,000	106,000	-318,000
1	Internal Pressure	-190	-210	50	-100	-520
2	Axial Compression	-27,000	-19,700	-13,500	24,500	100,700
2	Internal Pressure	-600	340	140	-180	-980
3	Axial Compression	18,044	-8,969	-37,427	32,380	-119,120
3	Internal Pressure	-530	530	1,770	-370	-1,790
3.5 **	Axial Compression	-26,800	-16,250	-77,300	67,200	-147,000
3.5 ***	Internal Pressure	-520	520	380	-270	-1,250
3.5 ***	Axial Compression	22,300	13,850	-37,500	17,030	-105,000
3.5 ***	Internal Pressure	600	430	310	-200	-2,250

* To get stress (in psi) for axial deflection, multiply values by deflection and divide by free length of bellows. To get stress (in psi) for pressure loading, multiply values by pressure in psi.

** 0.378 inch span.

*** 0.6188 inch span.

assembly. The study was confined to the basic 3.5-inch bellows model with dimensions given in Tables 17 and 18. Variables considered in the study were the OD tilt angles of the end leaves, the lengths of the conical segments of the end leaves, the thicknesses of the end leaves and the addition of shape-stiffened segments such as conical or toroidal sections.

In spite of the possibility of the interference at the end fitting welds mentioned above, a study of tilt angles was conducted to verify the existence of optimum end fitting tilt angles. Such optimum tilt angles were found for the models studied. These tilt angles were not only different from the optimum angles required for the convolution welds but also were different for the upper fitting than for the lower fitting. The stresses at the upper and lower fittings for the optimum 3.5-inch bellows (span = 0.6188 inch) are given in Table 20 for three different sets of tilt angles. Minimum stress conditions at the upper fitting occurred for a 55° - OD tilt angle. However, at the lower fitting, an OD tilt angle of 45° minimized the pressure loading stresses, and a 35° tilt angle yielded the lowest deflection stresses although the optimum OD tilt angle for the middle leaves was 50°. As noted, this solution was not satisfactory because of the possibility of leaf interference at the end fittings under compression loading.

The effect on the end-fitting stresses of varying the length of the conical end segments at the end-fitting welds was investigated for the 3.5-inch bellows (span = 0.378 inch). It was found to be almost insignificant for the convolution shape studied. For the internal pressure loading, little change occurred in the stresses whether the end segments were lengthened or shortened. For the axial deflection case, halving the end segment length increased the fitting stresses less than 10 percent, while increasing the segment length by 50 percent decreased the stresses only about 10 percent. Therefore, varying the end-segment lengths appeared to be both an inefficient (for axial deflection) and an ineffective (for pressure loading) means of reducing the stress levels at the end-fitting welds.

Additional segments, both conical and toroidal, were added to the bottom end leaf of the 3.5-inch bellows (span = 0.378 inch) to determine if such end-fitting attachments would reduce the stress levels there. When added, both segment shapes reduced the axial deflection end-fitting stresses significantly, with the toroidal section being more effective than the conical section. However, the stress levels for the pressure loading case were then found to be excessive. No satisfactory compromise between the pressure loading case and axial deflection case was achieved for the shape-stiffened end segments studied. Thus, use of such additional segments was not considered promising as an effective means of optimizing the end-fitting stresses in a tilt-edge welded bellows.

Table 21 shows the effect on the end-fitting stresses of increasing the thickness of the end leaf attached at the lower fitting for the optimum 0.6188-inch span, 3.5-inch bellows shape. Results were obtained for the three thicknesses for leaf 4 (0.005 inch, 0.007 inch, and 0.009 inch). Leaves 1 through 3 had a constant thickness of 0.005 inch. This method of minimizing the fitting stresses was the most generally effective method studied. Table 21 clearly shows that increasing the end leaf thickness gave an adequate reduction in the end-fitting stresses for both the axial deflection and

TABLE 20. RELATIVE FITTING STRESSES SHOWING THE EFFECT OF
 END LEAF OD TILT ANGLE VARIATIONS FOR A 3.5-
 INCH, TILT-EDGE WELDED BELLOW, ID TILT ANGLE =
 45°, OD TILT ANGLE = 50°, SPAN = 0.6188 INCH

Location of Stresses	Axial Deflection Stresses, psi (a)				Internal Pressure Stresses, psi (b)			
	Meridional Inner	Meridional Outer	Circumferential Inner	Circumferential Outer	Meridional Inner	Meridional Outer	Circumferential Inner	Circumferential Outer
Upper Fitting, Tilt Angle = 50°	-14,550	17,030	-4,370	5,120	24	-197	7	-59
Lower Fitting, Tilt Angle = 50°	34,600	-37,600	10,400	-11,250	-149	305	-45	91
Upper Fitting, Tilt Angle = 55°	-6,930	9,320	-2,080	2,800	-256	89	-77	27
Lower Fitting, Tilt Angle = 45°	30,900	-34,200	9,270	-10,300	69	98	21	29
Upper Fitting, Tilt Angle = 55°	-6,930	9,320	-2,080	2,800	-256	90	-77	27
Lower Fitting, Tilt Angle = 35°	18,800	-23,050	5,630	-6,920	660	-469	198	-141

(a) Unit axial deflection in a unit bellows length.

(b) For internal pressure of 1 psi

TABLE 21. RELATIVE FITTING STRESSES SHOWING THE EFFECT OF
 END LEAF THICKNESS FOR A 3.5 INCH, TILT-EDGE
 WELDED BELLOWS, ID TILT ANGLE = 45°, OD TILT
 ANGLE = 50°, SPAN = 0.6188 INCH

Location of Stresses	Axial Deflection Stresses, psi (a)				Internal Pressure Stresses, psi (b)			
	Meridional		Circumferential		Meridional		Circumferential	
	Inner	Outer	Inner	Outer	Inner	Outer	Inner	Outer
Upper Fitting	-14,550	17,030	-4,370	5,120	24	-197	7	-59
Lower Fitting	34,600	-37,600	10,400	-11,250	-149	305	-45	91
Upper Fitting	-16,450	-19,250	-4,930	5,770	32	-206	9	-62
Lower Fitting	24,200	-26,800	7,250	-8,030	96	14	29	4
Upper Fitting	-17,400	20,300	-5,210	6,100	34	-208	10	-63
Lower Fitting	16,850	-19,100	5,050	-5,740	174	-92	52	-28

(a) Unit axial deflection in a unit bellows length.

(b) For internal pressure of 1 psi

internal pressure loadings. Thus, optimum (minimum) end-fitting stresses were obtained for the 3.5-inch bellows. It should be mentioned that the effect of the increased bellows stiffness, due to the presence of a thicker end leaf, led to increases in the stresses in leaves 2 and 3 for an axial deflection loading. The stress level increases were not severe, particularly when compared with the sizeable reductions achieved in the end-fitting stresses. In an actual welded bellows assembly, the number of convolutions will be large enough that the effect of increasing the thickness of the two end leaves should be very small. The results of this section show that if the end-fitting stresses were too high for a particular welded bellows design, the most reliable remedy would be to increase the thickness of the end leaves. Although this would require the use of blanks of different thickness, it has the advantage to the manufacturer that different dies are not needed to form the end leaves. Assuming that the bellows manufacturer would accept the inconvenience of providing for increased thickness end leaves, it would appear that the end-fitting stresses can be reduced to acceptable levels for tilt-edge bellows by use of such end leaves.

SECTION IV

ANALYSIS, FABRICATION AND EVALUATION OF TILT- EDGE BELLOWS DESIGNS

One of the objectives of the research study was to design, fabricate, and test a tilt-edge bellows with dimensions comparable to one of the conventional bellows tested in the previous bellows study. It was decided that the 3.5-inch OD, 347 stainless steel bellows described in Appendix H of Technical Report No. AFRPL-TR-68-22 would be used for comparison. A design study was therefore carried out to develop an optimized tilt-edge bellows with a 3.5-inch OD.

Because of the novelty of the tilt-edge bellows concept, it was decided to carry out a preliminary investigation of the fabricability of tilt-edge bellows to uncover any fabrication problems at an early stage of the contract. Such problems could then be remedied before the final bellows design was made. Further, the 4-inch OD tilt-edge bellows described in Appendix C of AFRPL Technical Report No. TR-68-22 (1) had sufficiently low weld stresses under axial loading that it could be expected to demonstrate fatigue failure in the convolutions rather than at the welds. Accordingly, it was decided to fabricate and test this bellows configuration, which will be called the interim bellows. The following section describes the investigation of the fabricability of tilt-edge bellows and then the fabrication and testing of the interim bellows. Following this, the design, fabrication, and testing of the optimized tilt-edge bellows will be described.

Fabrication and Evaluation of an Interim Tilt-Edge Bellows Design

As explained previously, the decision was made to fabricate and test an interim tilt-edge bellows configuration prior to the fabrication and evaluation of an optimized design. This interim test step was expected to provide a better understanding of the fabrication requirements and performance characteristics of tilt-edge bellows, thus increasing the probabilities of success with an optimized configuration.

Preliminary Fabrication Investigation

The major fabrication differences between a tilt-edge bellows and a standard welded bellows appeared to be associated with the flat portions near the inner and outer weld beads. In most standard welded bellows these portions of the convolutions are essentially perpendicular to the bellows centerline. Present welding procedures incorporate equipment based on this configuration.

In the tilt-edge bellows, the flat portions near the weld beads were to be tilted at some angle to the bellows centerline. Preliminary tests were conducted at Battelle to determine whether the tilting of the edges presents any problems in the use of standard welding equipment and procedures.

The tungsten inert-gas (TIG) welding process was selected as being representative of the procedures used by welded bellows manufacturers. A

tracked, motorized carrier was used to support a welding fixture and to drive it under a small TIG torch at controlled speeds. The welding fixture consisted of copper-infiltrated, tungsten carbide jaws capable of holding rectangular strips of metal approximately 3 inches by 3/8 inch.

Type 347 and Type 321 stainless steels were selected as being typical of the bellows materials used for rocket propulsion systems. A thickness of 0.005 inch was also selected as being typical. Pairs of metal strips were positioned in the weld fixture with the 3-inch dimension horizontal and with a measured amount of material protruding above the clamp face. The welding torch was placed directly above the strips at measured angles to simulate angular relationships between the eventual production bellows and the production welding torch.

Approximately 100 edge-burndown welding runs were made, varying the following welding parameters:

Travel speed: 5.5 to 18 in. per minute
Welding Current: 1.4 to 2.6 amp
Stickout Distance: 0.090 to 0.265 in.
Electrode-to-Work Distance: 0.008 to 0.015 in.
Gas Flow Rate: 8 to 20 cu ft per hr
Torch Inclination: 0 to 55° from vertical

Based on this work it was concluded that the tilt-edge bellows should present no unusual problems in the achievement of uniform weld beads using standard TIG welding procedures and equipment.

Bellows Manufacturer Selection

The interest of bellows manufacturers in participating in an experimental development effort can vary considerably depending on personnel, work load, and corporate policy. Six of the major manufacturers of welded bellows were selected in the first month of the program. Requests for quotations for price and delivery were sent for the following items:

- (1) Six 4-inch welded bellows, with end fitting attached, having a convolution configuration like that determined during the previous bellows program [Contract No. 04(611)-10532].
- (2) Fifty each of the blanked and formed male and female diaphragms of the configuration that would be used in making these bellows.
- (3) A lot of from 12 to 24 welded bellows, approximately 4 inches OD, having an unspecified tilt-edge configuration to be determined during the present program, with end fittings attached.
- (4) Two-hundred-fifty each of the male and female blanked and formed diaphragms of the design to be specified in Item (3).

The material was to be either Type 321 or Type 347 stainless steel, at the supplier's option. It will be noted that the request was intended to

select a manufacturer for both the interim bellows [Items (1) and (2)] and the optimized bellows [Items (3) and (4)].

Four quotations were received. The lowest quotation was received from the Sealol Corporation in Providence, Rhode Island. They also promised satisfactory delivery time. Sealol's bid was approximately 40 percent lower in cost than the next lowest bidder. Because Sealol was known to be a leading manufacturer of welded bellows and had submitted a very attractive quotation, Sealol was selected to manufacture the interim bellows. The performance on this requirement was expected to be a check on whether Sealol should subsequently be selected to make the optimized bellows.

Interim Bellows Fabrication

The fabrication of 6 interim bellows and the associated extra diaphragms was completed by Sealol without incident. When tests with these bellows (see below) showed interference between the end diaphragms and the end fittings (through design oversight), seven additional interim bellows were ordered. The extra diaphragms obtained with the original six bellows were used for the additional bellows. New end fittings with additional clearance were machined.

Figures 36 through 40 show the tooling fabricated by Sealol to achieve clamping and cooling of the diaphragms during welding of the interim bellows. The setups for making an inner convolution weld and an outer convolution weld are shown in Figures 36 and 37, respectively. Figure 38 shows a partial disassembly of the inner-convolution-weld tooling, while Figures 39 and 40 show a partial and a complete disassembly of the outer-convolution-weld tooling.

Interim Bellows Inspection

The inspection planned for the interim bellows was related to determining whether the bellows were as uniformly made as standard welded bellows. For this purpose, the weld beads were inspected for uniformity of size and color. The major dimensions were measured to determine dimensional uniformity. The visible parts of the diaphragms were also inspected for dents and scratches and other signs of handling damage. The same inspection procedures were applied to both sets of interim bellows.

According to the visual inspection, the bellows were comparable in quality to state-of-the-art welded bellows. Measurement of major dimensions such as free length, pitch length, and convolution inner and outer diameters also showed uniformity comparable to that achieved for standard welded bellows. The subsequent inspection of cross sections of failed bellows showed good weld bead and convolution uniformity.

Based on the inspection of the 13 interim bellows, it was concluded that tilt-edge bellows could be fabricated satisfactorily by present manufacturing techniques.

Interim Bellows Tests

Two types of experimental information were selected as being important for the interim bellows: (1) spring rate and (2) fatigue characteristics.

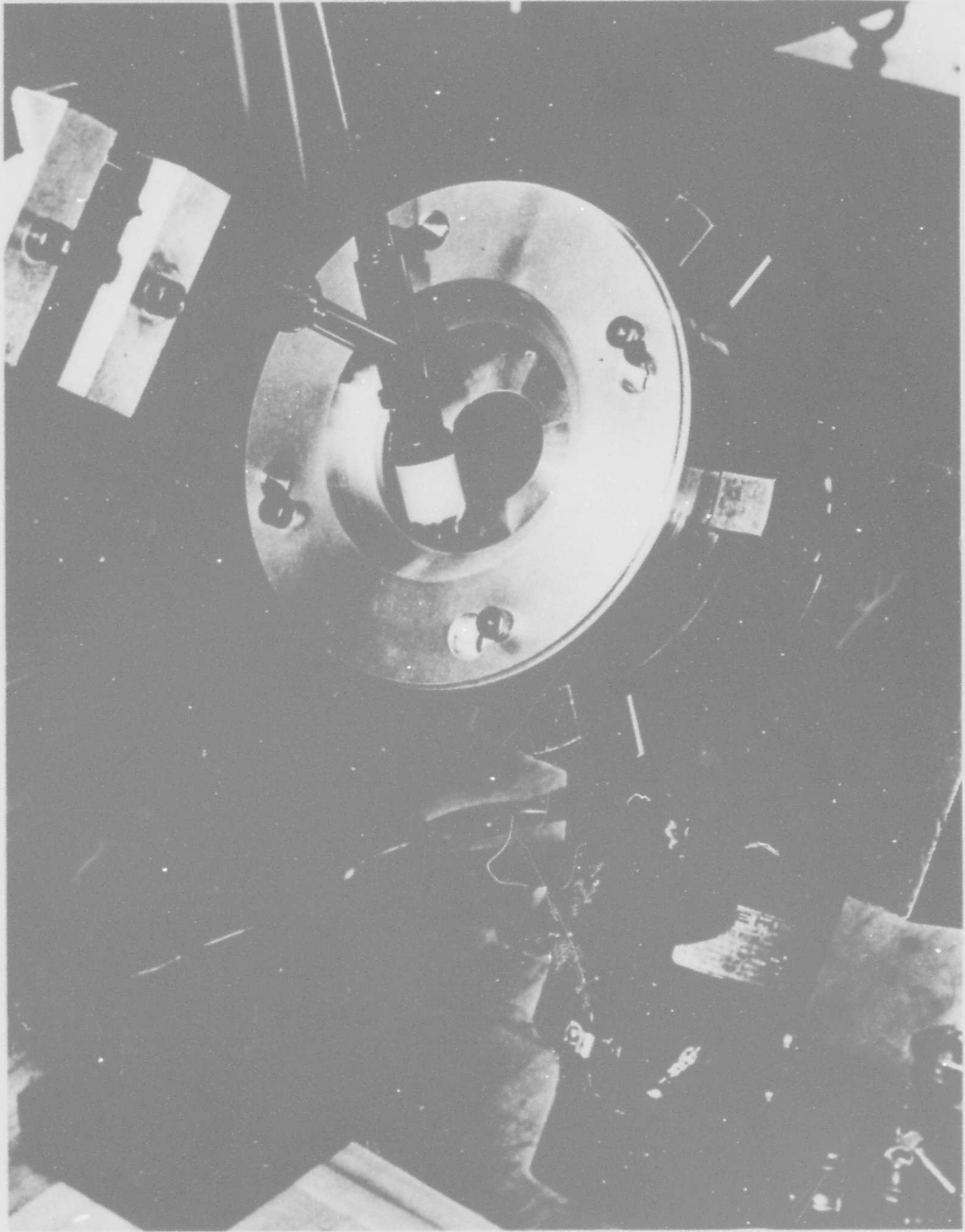


FIGURE 36. SETUP FOR MAKING AN INNER CONVOLUTION WELD

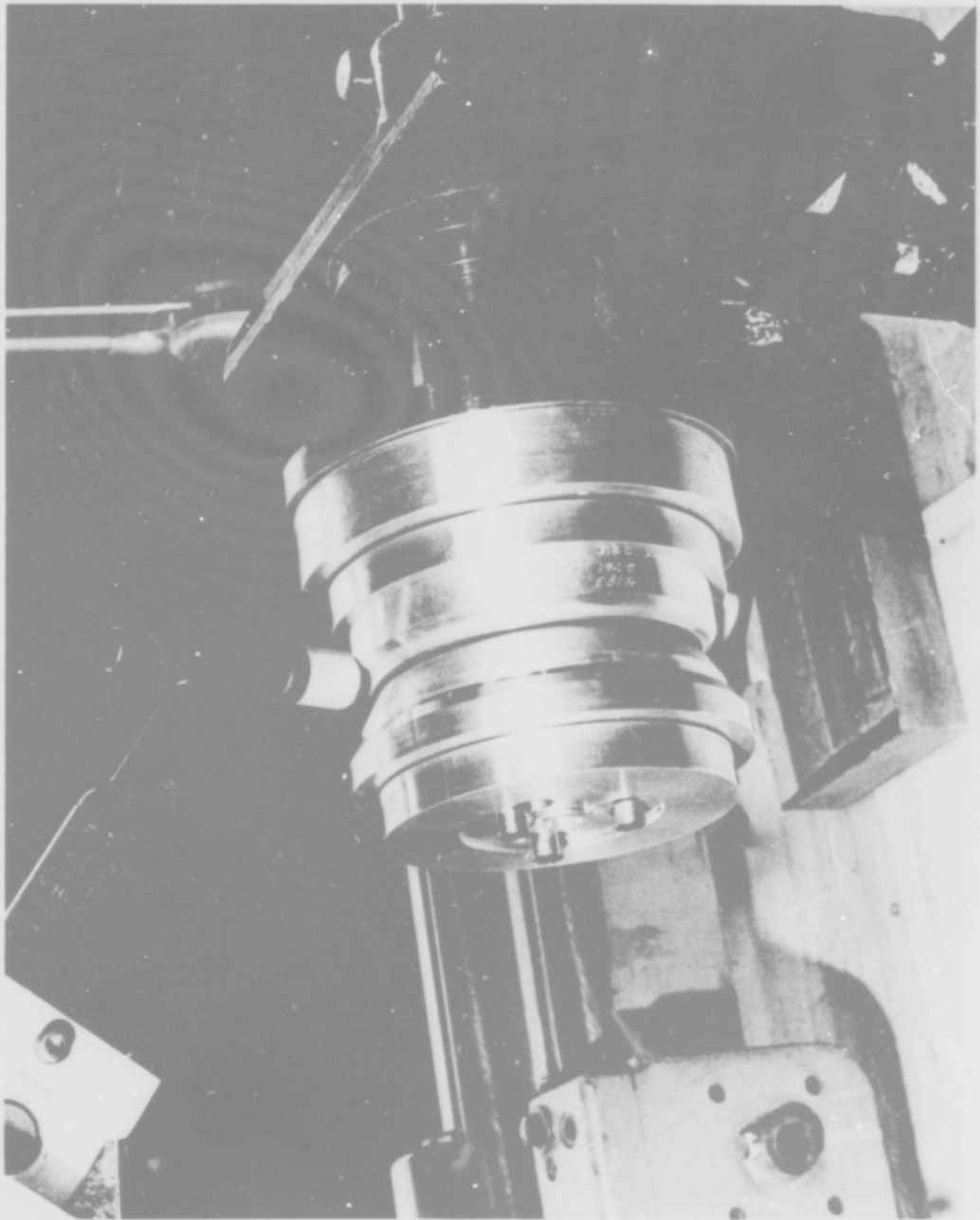


FIGURE 37. SETUP FOR MAKING AN OUTER CONVOLUTION WELD

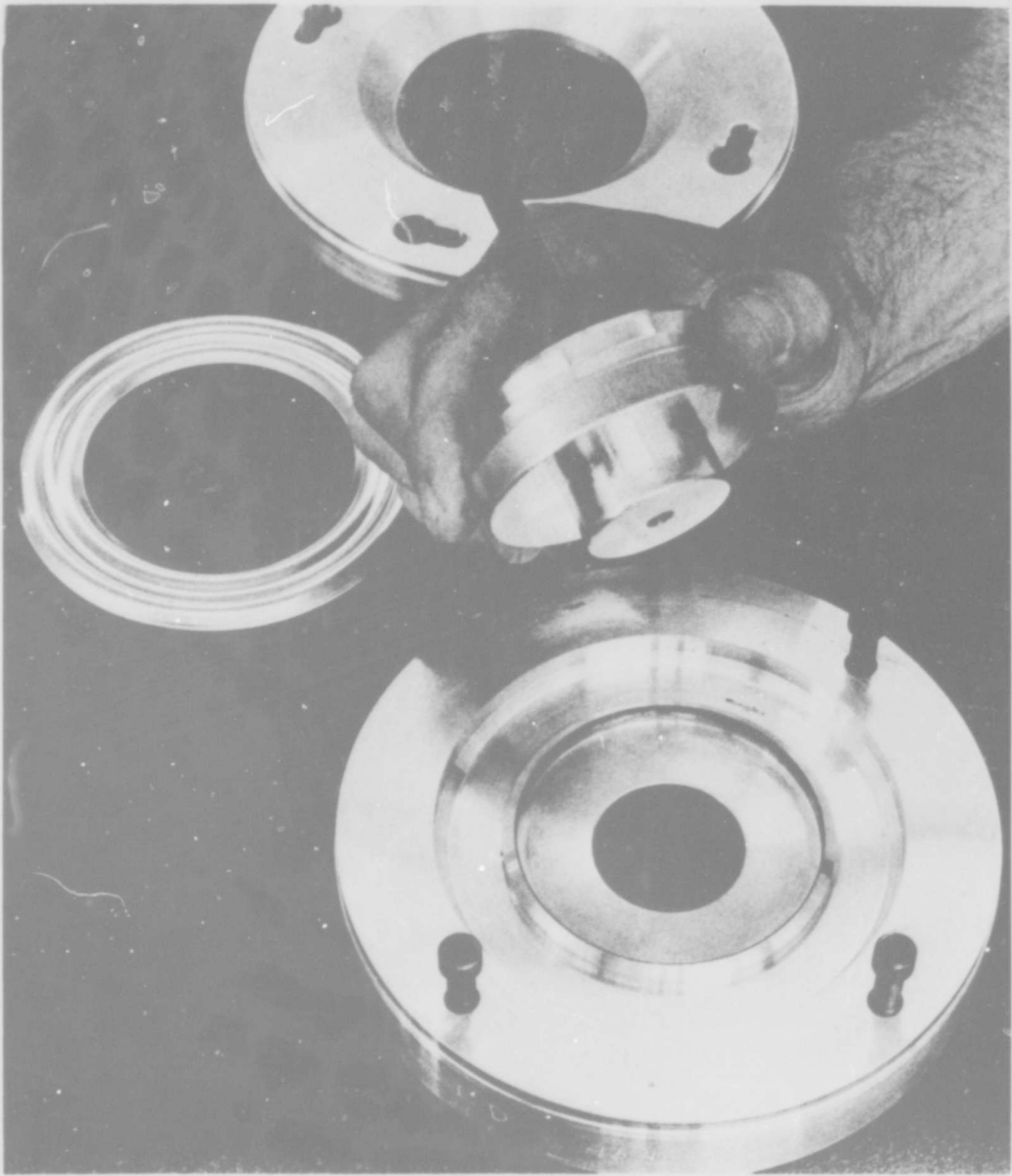


FIGURE 38. PARTIAL DISASSEMBLY OF THE INNER-CONVOLUTION-WELD TOOLING

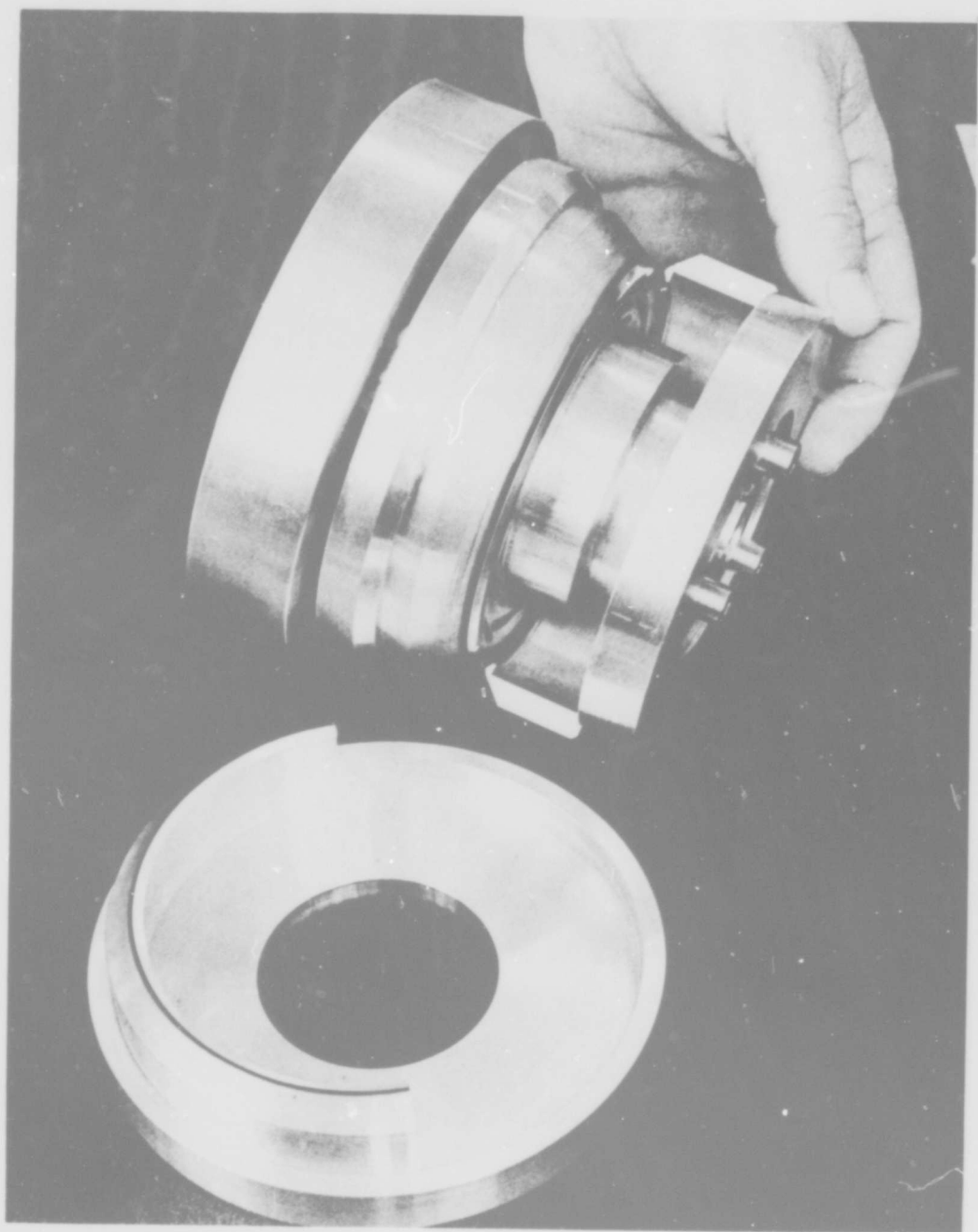


FIGURE 39. PARTIAL DISASSEMBLY OF THE OUTER-CONVOLUTION-WELD TOOLING

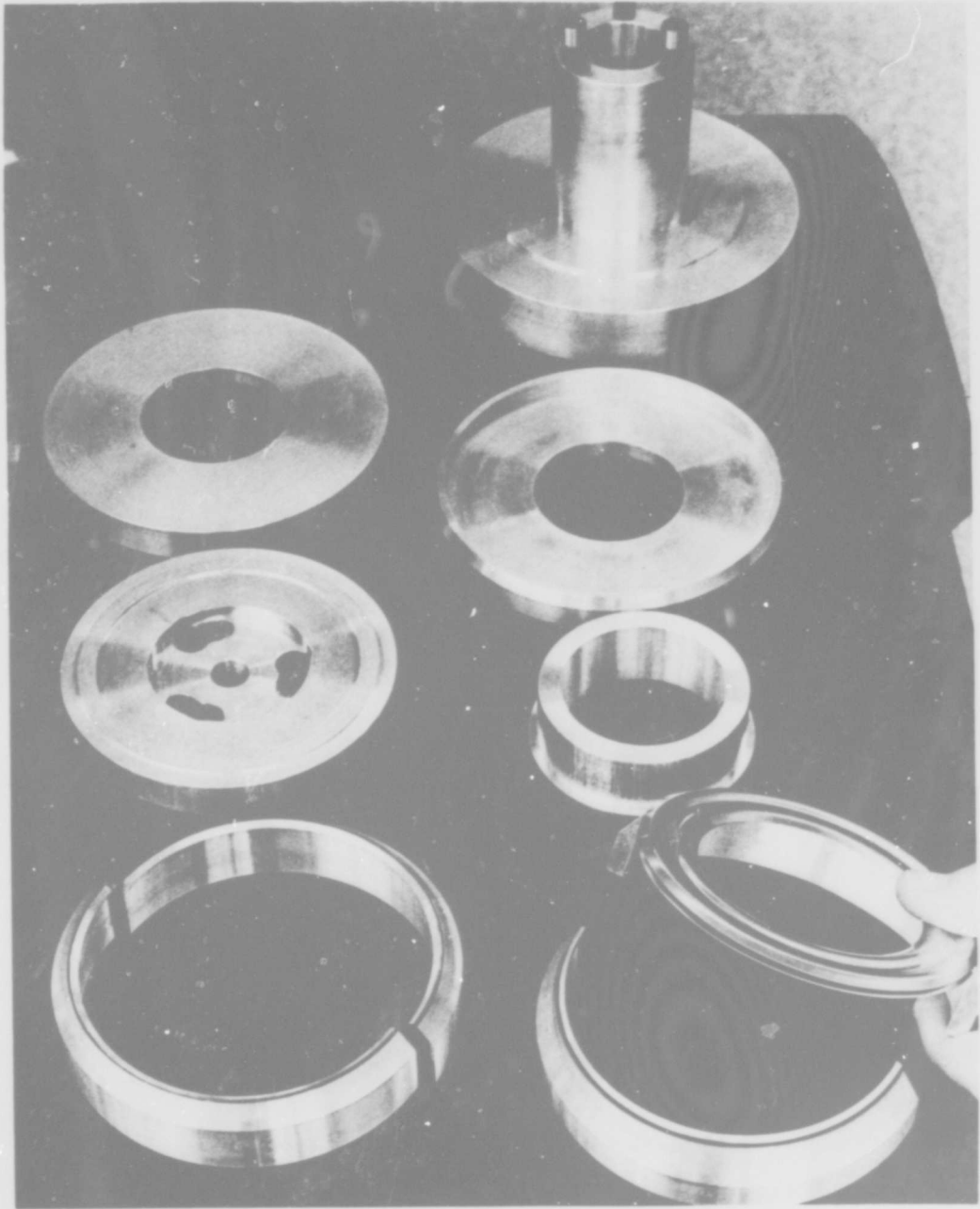


FIGURE 40. COMPLETE DISASSEMBLY OF THE OUTER-CONVOLUTION-WELD TOOLING

Spring Rate. Although calculations during the previous bellows program had shown that the spring rates of tilt-edge bellows could be made comparable to the spring rates of standard welded bellows, it was known that the tilted edges provided some stiffening to the diaphragms. Because spring rate is one of the principal design characteristics of welded bellows, it was important to show that the actual spring rates of a tilt-edge welded bellows could be approximated by the theoretical calculations.

Table 22 shows the spring rates measured for the 13 interim bellows with 1/2 inch compression and 1/2 inch extension. Also shown is the theoretical spring rate as determined by a linear calculation. The theoretical value compared very closely with the experimental extension values, as was the case with the standard bellows that were analyzed and tested during the previous program. Table 22 shows a lower compression spring rate than the extension spring rate. This same difference in compression and extension spring rates were also observed for the standard bellows tested in the previous program (page 22, Reference 1). This difference in spring rates was not investigated further for the interim bellows, since the primary interest was in the fatigue behavior of these bellows.

TABLE 22. THEORETICAL AND EXPERIMENTAL SPRING RATES FOR INTERIM BELLOWS SPECIMENS

Bellows No.	Spring Rate, lb/in.	
	1/2-Inch Compression	1/2-Inch Extension
KT-1	32.6	40.0
KT-2	31.7	39.8
KT-3	31.7	52.1
KT-4	31.8	39.2
KT-5	31.8	39.1
KT-6	32.2	39.7
KT-7	30.9	40.0
KT-8	30.1	40.6
KT-9	30.4	39.6
KT-10	30.6	40.1
KT-11	30.5	40.1
KT-12	31.1	39.1
KT-13	30.3	40.2
Theoretical Spring Rate (Linear)	40.8	40.8

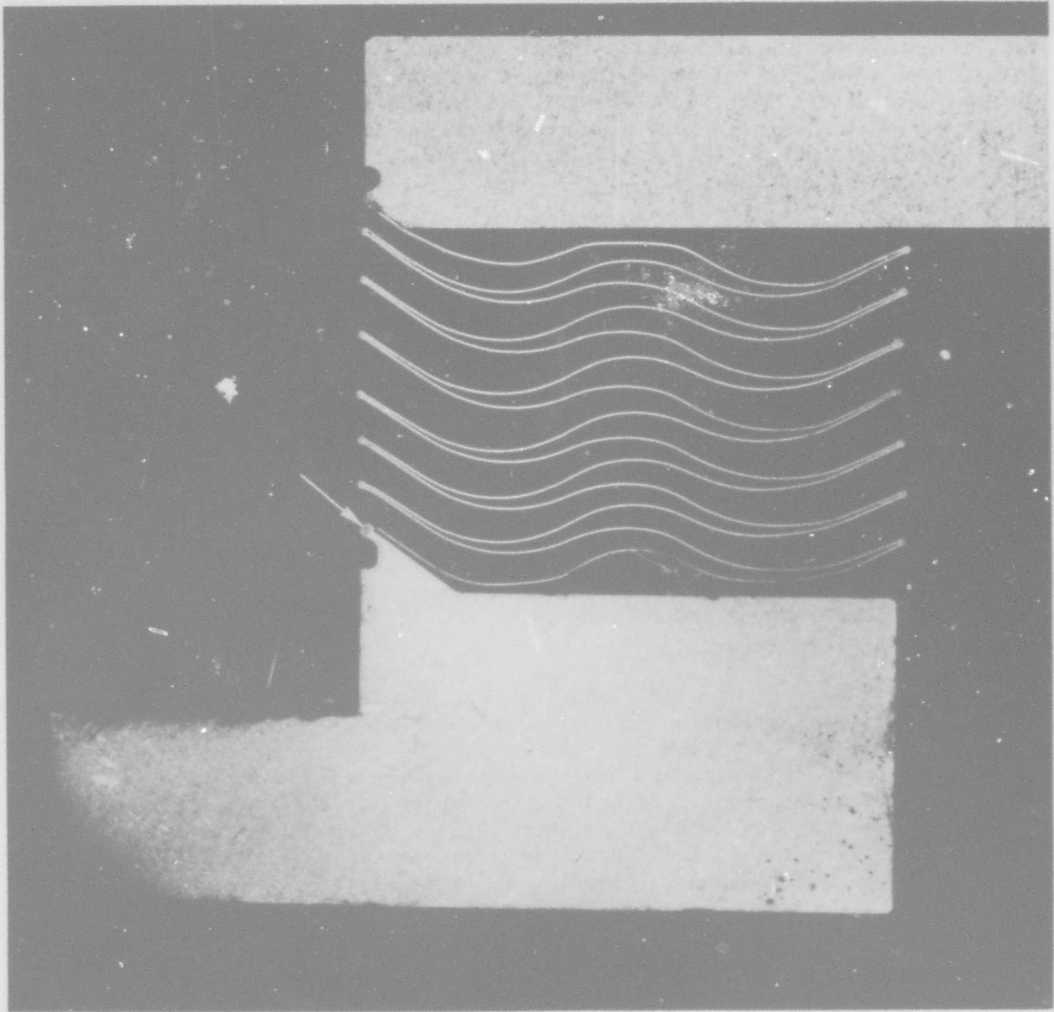
Fatigue Characteristics. A major purpose of the tilt-edge configuration was to prevent fatigue failure in the inner and outer weld beads. Because this had never been achieved intentionally in a design, the location of the fatigue failures was of prime importance. By achieving failure in the parent metal of the diaphragm, it was expected that the fatigue values of the bellows would be more predictable and uniform than for standard welded bellows, where failure occurs in the weld beads. Thus, the ability to estimate fatigue life from a strain calculation at the point of failure and the spread of the fatigue values were also important for the interim bellows. The fatigue machine developed during the previous program was used for these tests. The cycle rate was 80 cpm. Fatigue failure was indicated by the detection of small amounts of gas leakage.

The results with the first 6 interim bellows were erratic. The first two bellows failed at an end fitting because of interference (through design oversight) between the end convolutions and the end fittings (see Figure 41). The next three bellows were tested with increased amounts of extension instead of compression, to avoid end-fitting interference. Although failure occurred in the diaphragms in the area of maximum stress (see Figures 42 and 43), the fatigue values did not correlate well with the theoretical estimate nor with each other. Further, the sixth bellows failed at an end fitting. It was concluded that the tests had little value and that additional specimens were needed. Seven more bellows were ordered identical to the first six but with modified end fittings to avoid interference.

The results with the second batch of interim bellows were very promising. Six of the seven bellows developed fatigue cracks in the parent metal of the diaphragms in the area of highest stress. The seventh bellows failed prematurely at an end fitting. The end-fitting failure appeared to be caused by a poor weld.

A linear calculation of the maximum strain range (total strain for the entire bellows deflection at the location of maximum strain) for the interim bellows with 1/2-inch compression and 1/2-inch extension gave a value of 3700 microinches/inch. This strain occurred near the intersection of the inner flat (conical section) and the first torodial section. Using Figure L-6 from the final report on the previous program (Figure L-6 is duplicated in Figure 44), two fatigue life ranges were estimated. If the bellows performed like formed bellows, the fatigue values would range from about 30,000 cycles to about 400,000 cycles. If the bellows performed like metal coupons (as hoped) the fatigue values would range from about 250,000 cycles to about 1,000,000 cycles.

As noted above, one bellows failed prematurely (at 6114 cycles) because of a poor weld. The other six bellows gave the following fatigue values: 112,115 cycles, 292,900 cycles, 356,142 cycles, 389,465 cycles, 511,952 cycles, and 904,207 cycles.

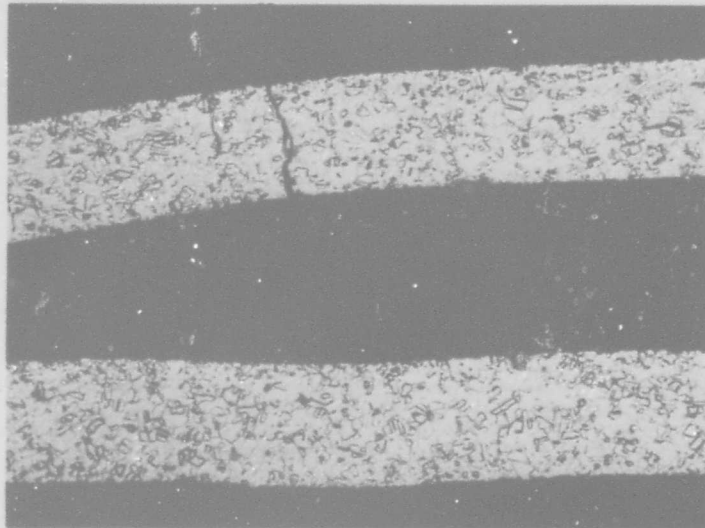


5X

Aqua Regia

3D537

FIGURE 41. CROSS SECTION OF FIRST INTERIM BELLOWS (KT-4) SHOWING
END-FITTING FAILURE AND END-FITTING INTERFERENCE

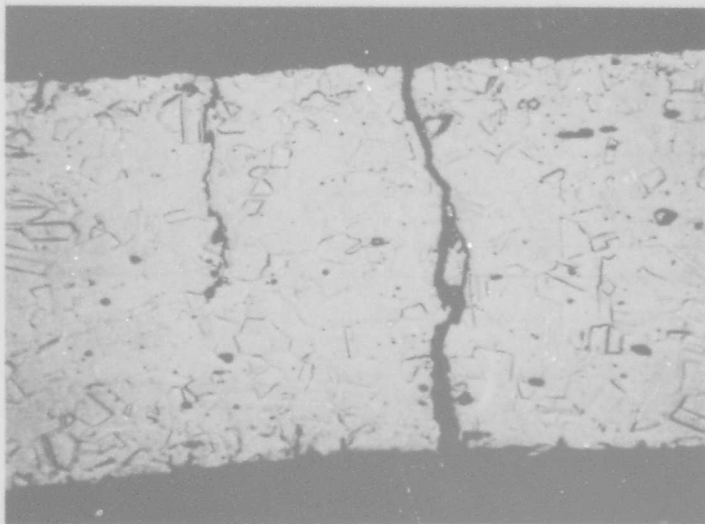


150X

Glyceregia

3D723

FIGURE 42. CROSS SECTION OF FATIGUE FRACTURE IN INNER TOROIDAL SEGMENT OF FOURTH CONVOLUTION OF INTERIM BELLOWS KT-1



500X

Glyceregia

3D725

FIGURE 43. FATIGUE FRACTURE IN FIGURE 42 AT HIGHER MAGNIFICATION

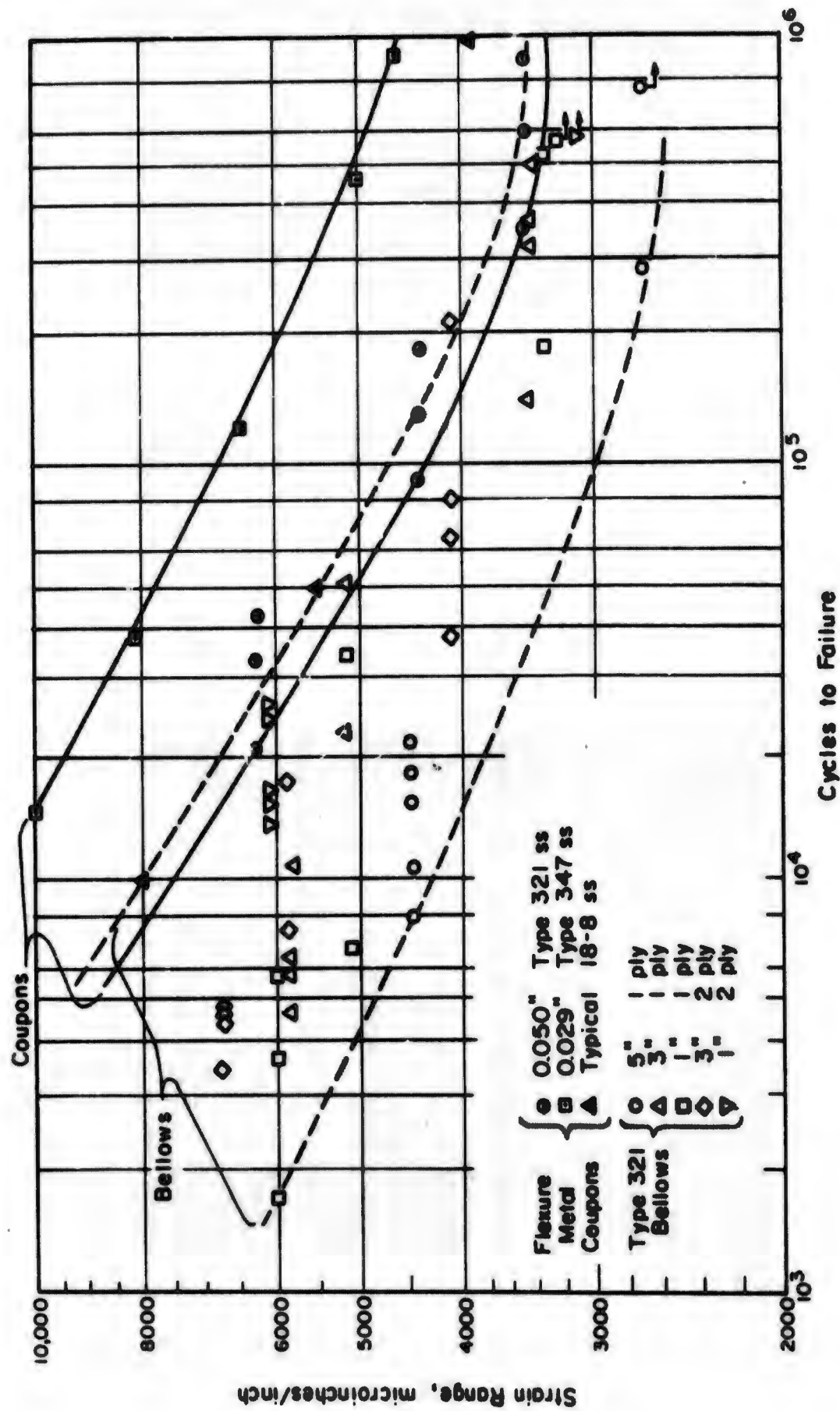


FIGURE 44 FATIGUE RESULTS OF STAINLESS STEEL FORMED BELLOWS AND STAINLESS STEEL COUPONS

Interim Bellows Conclusions

From the tests of the interim bellows, the following conclusions were made:

- (1) The theoretical stress analysis procedure appeared to be even more applicable to the tilt-edge bellows configuration than it was to standard welded bellows.
- (2) The average fatigue life of tilt-edge bellows could be estimated using data from bending-fatigue tests of sheet metal coupons made of the same material if some allowance was made for manufacturing variability in making the bellows.
- (3) The fatigue life spread would be somewhat greater for the bellows than for the coupons, but much less than for standard welded bellows.
- (4) In addition to minimizing stresses at the convolution welds, the stresses at the end fitting of the optimized bellows should be made as low as possible to minimize the possibility of early fatigue failure caused by unsound end-fitting welds.

Design, Fabrication, and Evaluation of an Optimum Bellows Configuration in Comparison With a Conventional Welded Bellows

As mentioned above, the conventional bellows selected for comparison was a 3.5-inch OD stainless steel bellows. This bellows had a thickness of about 0.005 inch and a span of 0.378 inch. The average spring rate for this bellows was 57 lb/in. Details of the stress analysis and testing of this bellows were reported in Appendix H and Appendix N of Technical Report No. AFRPL-TR-68-22.

The general objective in comparing a tilt-edge bellows to a conventional welded bellows was to demonstrate that a tilt-edge bellows could be used to replace the conventional bellows and would significantly outperform it. To achieve this objective, the tilt-edge welded bellows design parameters (i.e., number of convolutions, outside diameter, inside diameter, height, and spring rate) should be comparable to the standard welded bellows.

Two tilt-edge bellows configurations were developed for comparison with the standard bellows. In the first, all the major dimensions of the tilt-edge bellows were the same as for the standard bellows. One difference was that the tilt-edge bellows had three sweeps instead of the four sweeps used in the standard bellows. An odd number of sweeps was chosen to give the tilt-edge bellows convolution symmetry. The shape for this bellows was given in Table 17.

An analysis of this first tilt-edge configuration showed that the maximum stresses occurred well away from the weld areas, as desired. This

is shown in Figures 19 and 21. However, the tilt-edge bellows had a slightly higher calculated spring rate than the standard bellows. The maximum calculated pressure stress was about half that of the standard bellows, while the maximum calculated deflection stress was about the same as that of the standard bellows. This meant that the tilt-edge configuration was optimized with regard to pressure capability rather than deflection capability.

In a discussion with the Air Force Technical Monitor, it was agreed that most bellows applications of interest to the Rocket Propulsion Laboratory require increased deflection capability rather than increased pressure capability. It was decided that the span length could be increased by making the bellows ID smaller (from 2.838 inches to 2.328 inches) without detracting from the usefulness of the bellows. This bellows would have comparable pressure stresses, but lower deflection stresses than the standard bellows. Accordingly, a purchase request was made for a tilt-edge bellows having a 0.62-inch span. The dimensions of this bellows were essentially the same as those given in Table 18 except that the pitch was reduced to about 50 mil to correspond with the pitch of the conventional bellows. A purchase request was sent to Sealol Manufacturing Company for fabrication of these bellows.

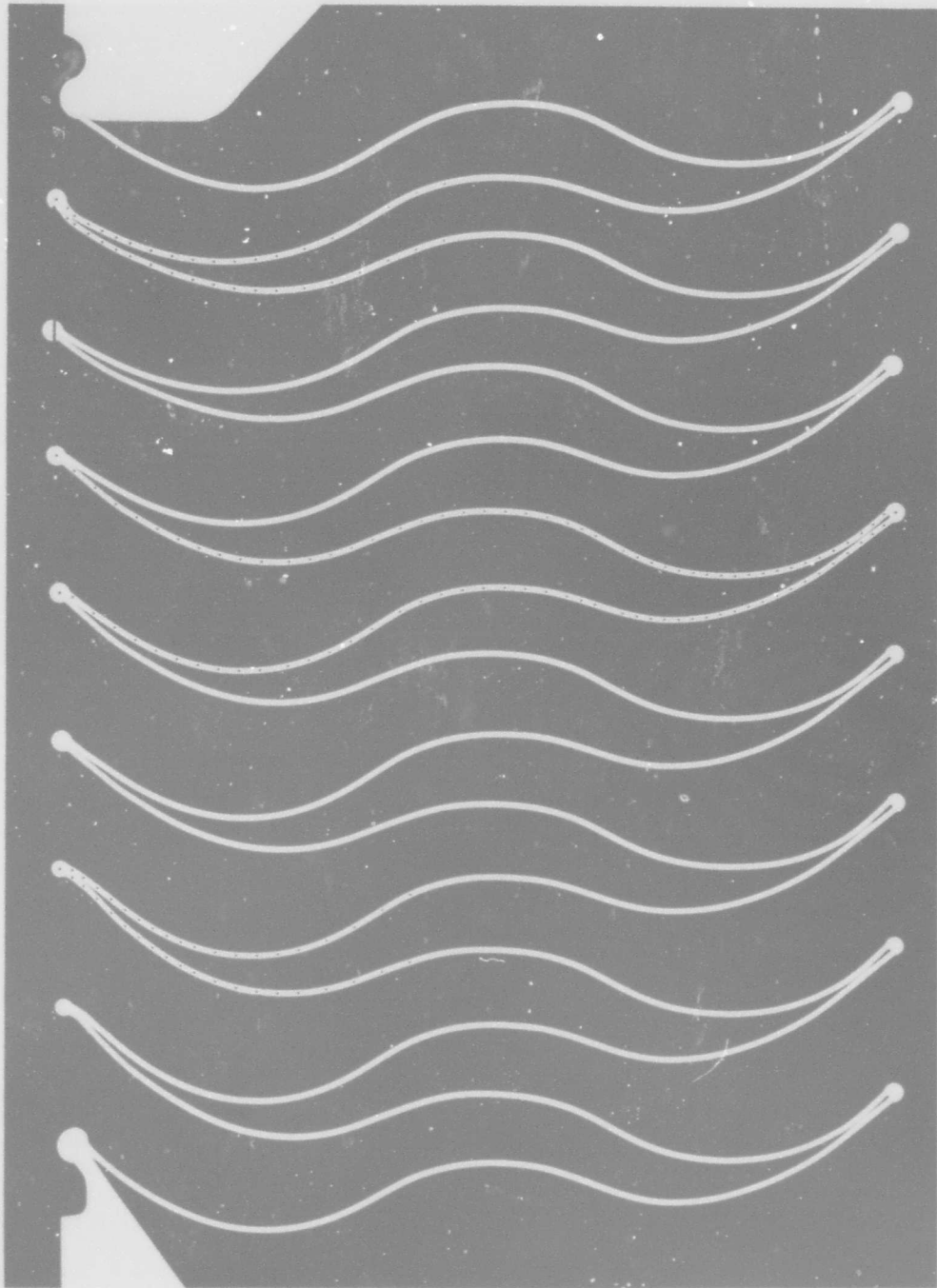
During the final stages of fabrication, Sealol notified Battelle-Columbus that the diaphragms for the optimized bellows were not as close to the required dimensions as expected. This was caused by improper specification of the tilt angles by Sealol when the die drawings were made from the configuration drawings submitted by Battelle. Because most of the bellows cores (the convolution assemblies) had been completed, it was mutually agreed that a completed specimen would be sent to Battelle-Columbus, and that a stress analysis would be made to determine whether the bellows were sufficiently close to the desired configuration to be acceptable.

The sample bellows specimen was encapsulated in plastic at Battelle-Columbus, cross sectioned, and polished. Hardness indentations were made along the centerlines of the leaves of a typical convolution (see Figure 45). Measurements were made of the locations of these centerline points.

A two-convolution analysis model was then prepared. Some of the significant parameter deviations noted in the cross section were:

- (1) The tilt angle at the ID was 38° as compared to a specified angle of 45°
- (2) The tilt at the OD was 37° as compared to a specified angle of 50°
- (3) The pitch of the bellows specimen was about twice the specified pitch
- (4) The radii for the toroidal shells were significantly different than specified.

The results of the stress analysis (for axial deflection and pressure loading) for the specimen were compared to the corresponding results



7D083

FIGURE 45. CROSS SECTION OF UNSATISFACTORILY FABRICATED BELLOWS SPECIMEN

obtained for the optimized shape. Figures 46 and 47 are typical stress plots for the optimized shape; Figures 48 and 49 are the corresponding plots for the specimen. Although the maximum stresses and their locations for the specimen were comparable to the optimized shape, the weld area stresses, without exception, were considerably higher for the specimen than for the optimized shape. Also, the end fitting design was no longer optimum.

Examination of the bellows cross section also showed that some of the convolutions had been crimped next to the outer diameter welds. This can be seen in Figure 45 for the convolutions adjacent to the end fittings. The decision was made that the bellows could not be used to evaluate the design.

Satisfactory Bellows Fabrication

Sealol agreed to remake the optimized bellows without additional charge. To facilitate the welding operation it was mutually agreed that the pitch be increased. This provided a better fit between the outer weld clamping fixture and the diaphragms with a two-part clamping insert. If the original pitch had been maintained, a three-part clamping insert would have been required. A slight increase in the flat portions near the inner and outer welds was also incorporated in the redesigned bellows to permit better fit with the clamping fixtures.

These changes in design were readily accomplished, using the computer analysis program to verify the acceptability of the revised dimensions. The revised design was sent to Sealol three days after the request for modification. The dimensions of this design are listed in Table 23.

When a sample specimen of the modified design was received at Battelle-Columbus, it too was encapsulated, cross sectioned, and measured. Figure 50 shows the bellows cross section. Figure 51 shows the typical convolution that was selected for measurement.

The measurements of the cross-sectioned bellows showed that the convolutions were very close to the dimensions given by the drawings for the theoretical bellows. A mathematical model was constructed from these measurements and analyzed with Program NONLIN. The thickness of the bellows leaves was measured at intervals along the leaves and this thickness variation was incorporated in the mathematical model. (Thickness variation of from 0.00450 to 0.00509 inch was recorded.) The outer surface meridional stresses for pressure and deflection loading are shown in Figures 52 and 53, respectively. These figures show satisfactorily low weld stresses. The predicted upper and lower end-fitting stresses were -460 and +310 psi, respectively, for a 1-psi pressure, and 3,400 and 26,400 psi for a unit deflection. These stresses were slightly higher than the convolution weld stresses. However, it was believed that these stresses were sufficiently lower than the maximum stresses in the parent metal of the convolutions that failure would not be expected at the end-fitting welds.

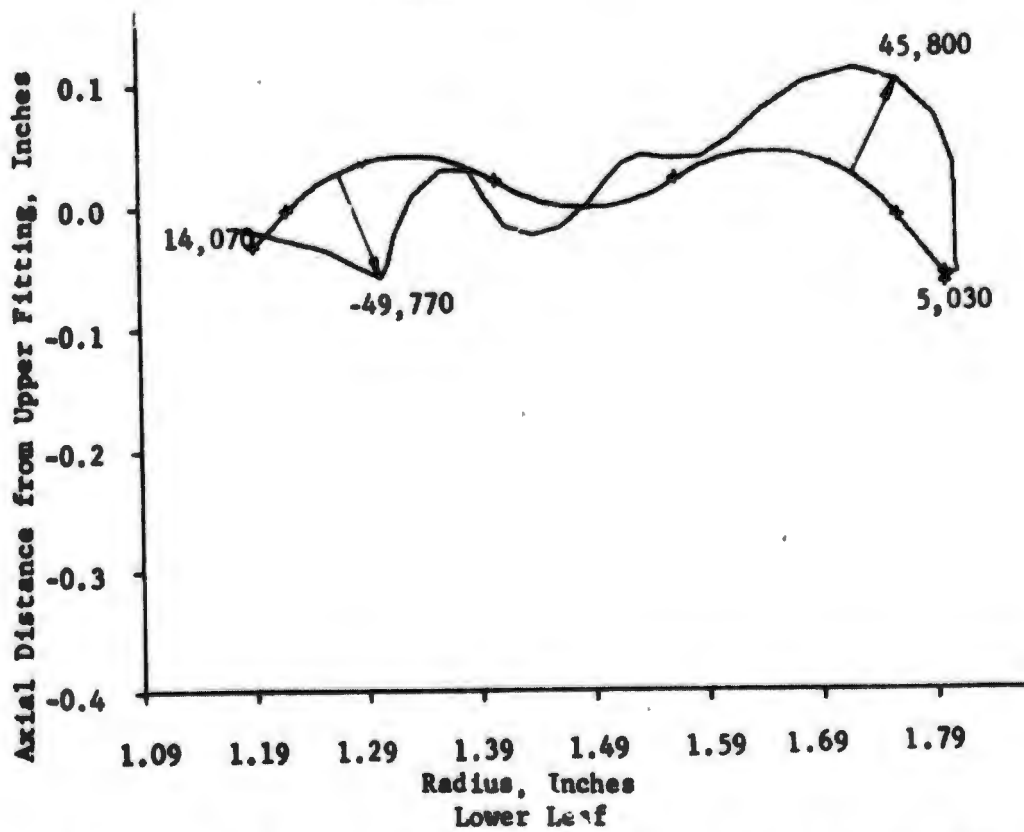
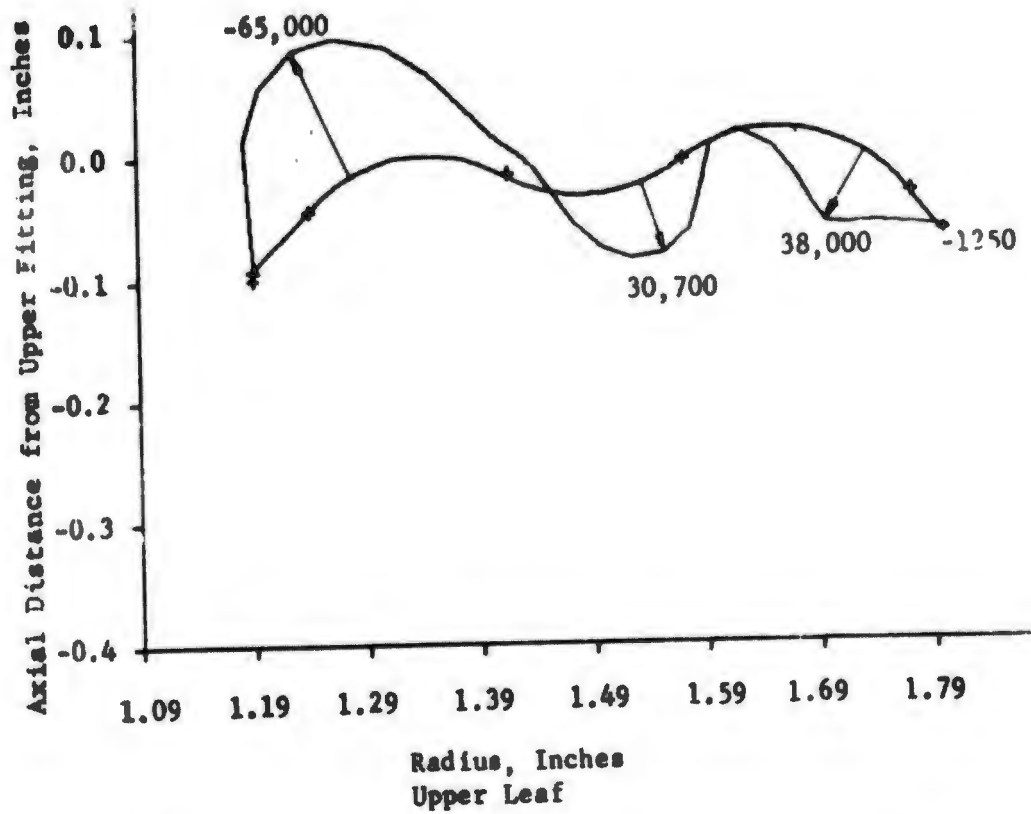


FIGURE 46. OUTER SURFACE MERIDIONAL STRESSES IN THE 3.5-INCH WELDED BELLOWS AS DESIGNED (Unit Axial Compression Per Unit Bellows Length).

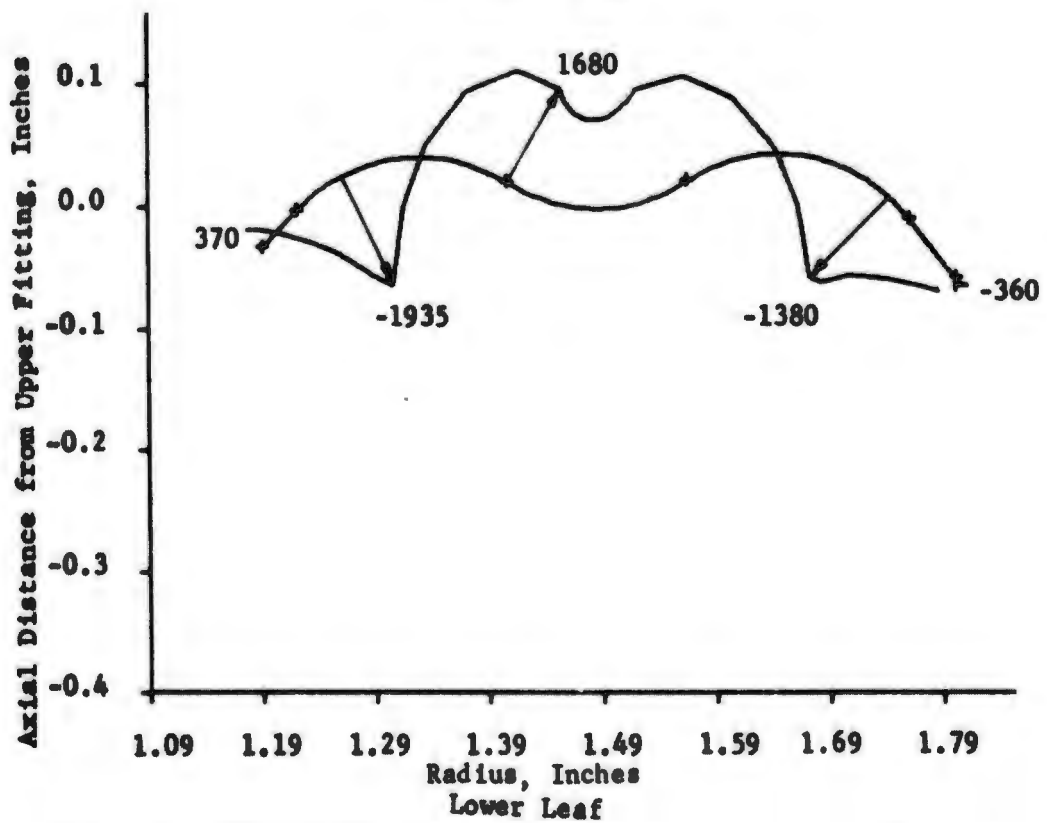
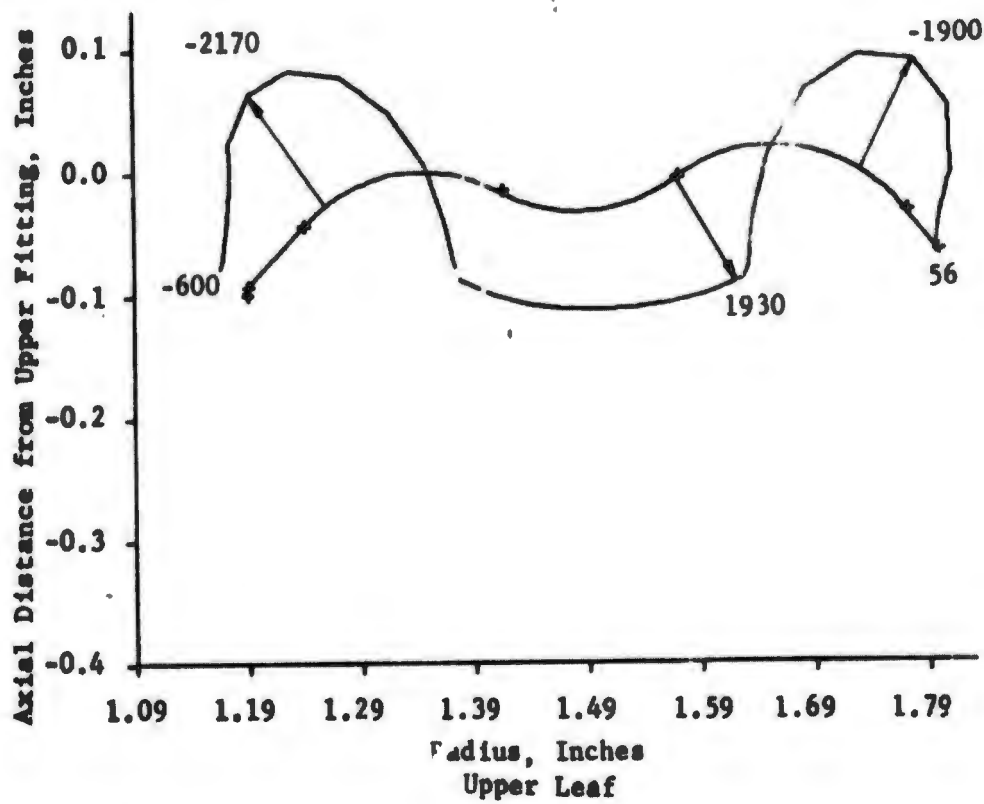


FIGURE 47. OUTER SURFACE MERIDIONAL STRESSES IN A 3.5-INCH WELDED BELLOWS AS DESIGNED (Internal Pressure = 1 psi).

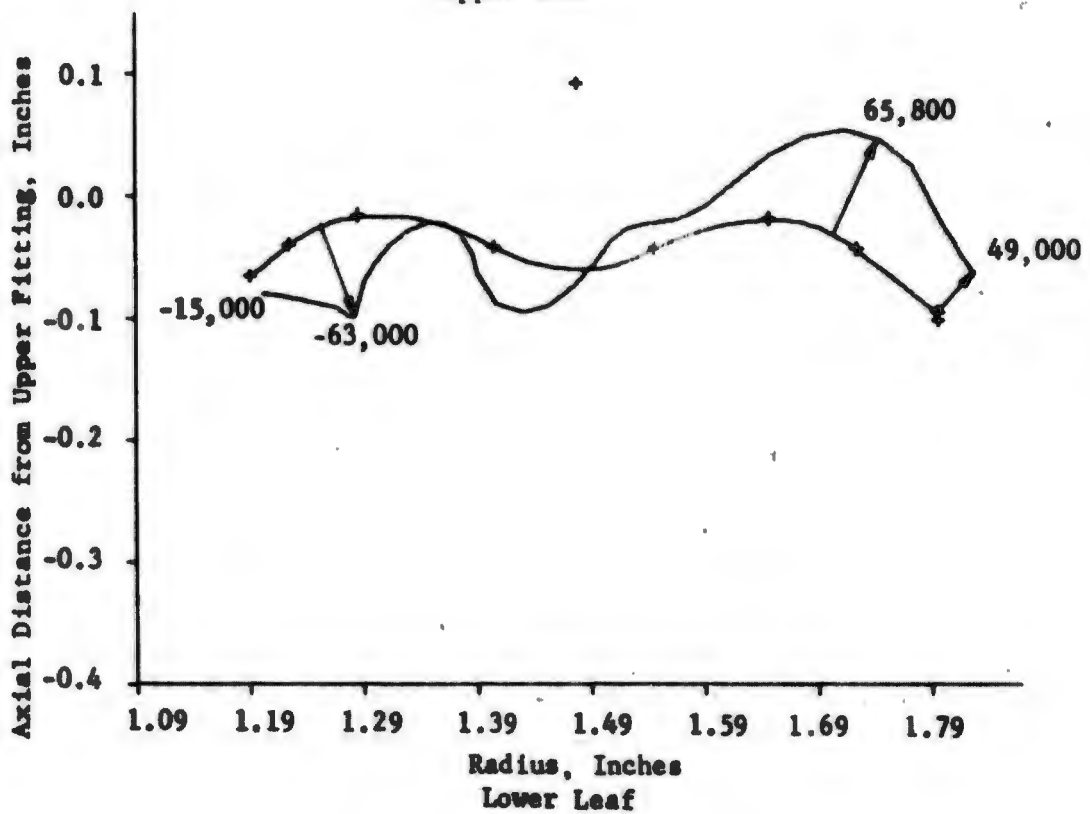
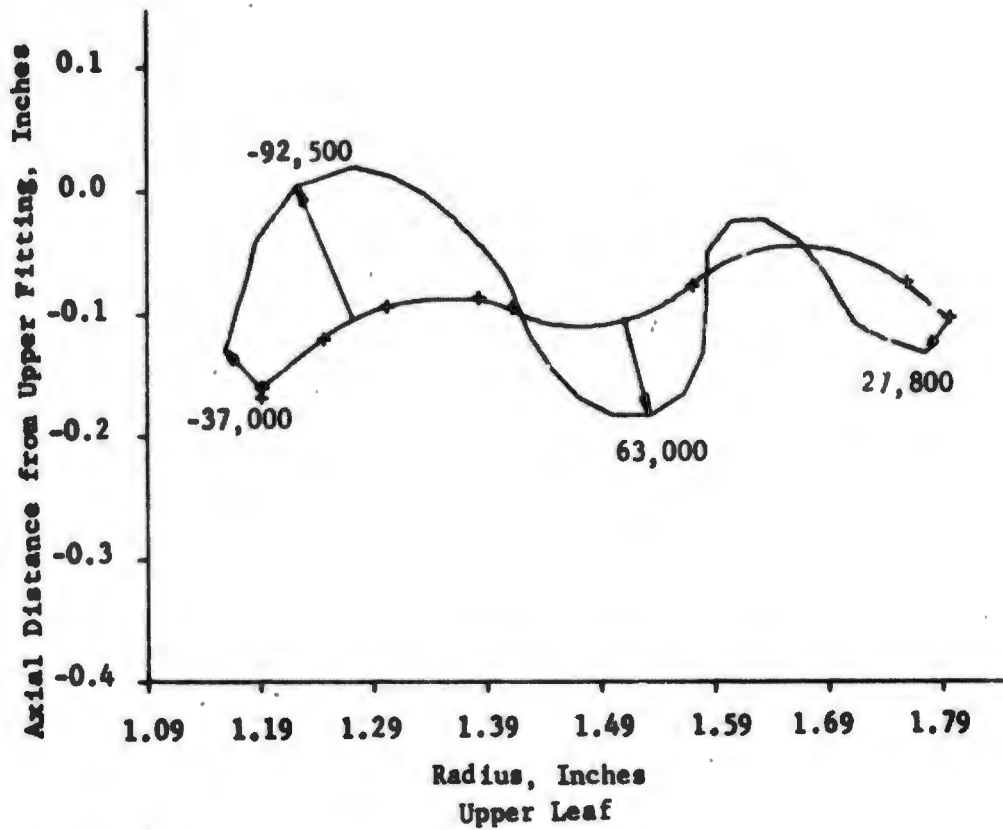


FIGURE 48. OUTER SURFACE MERIDIONAL STRESSES IN THE 3.5-INCH WELDED BELLOWS AS FABRICATED (Unit Axial Compression Per Unit Bellows Length).

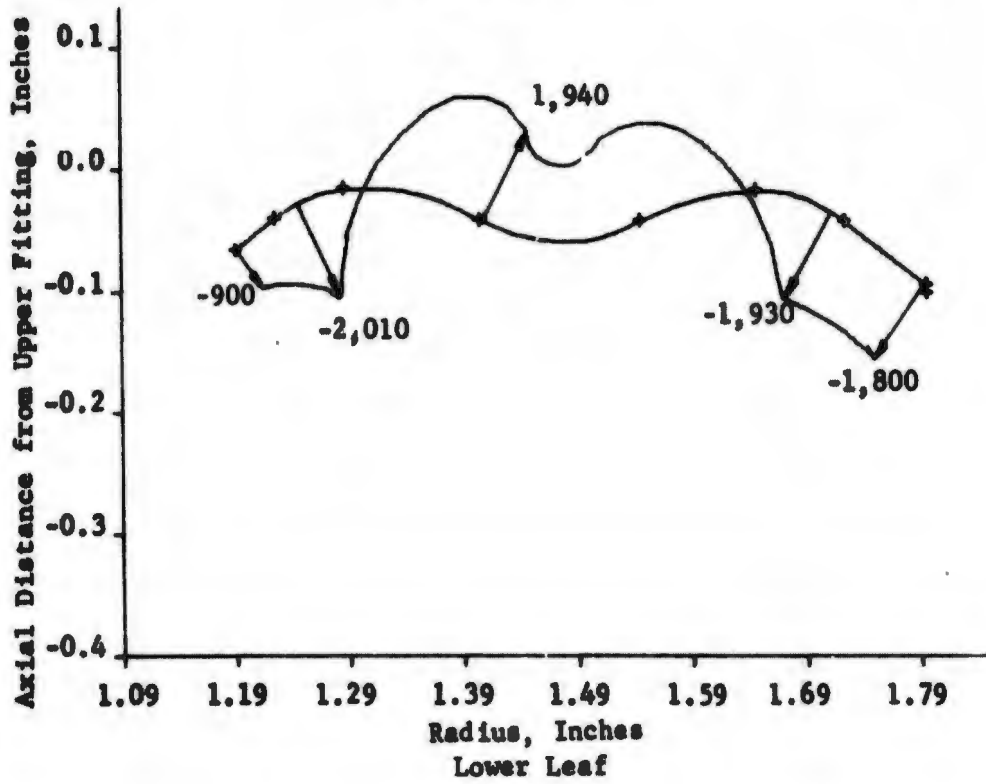
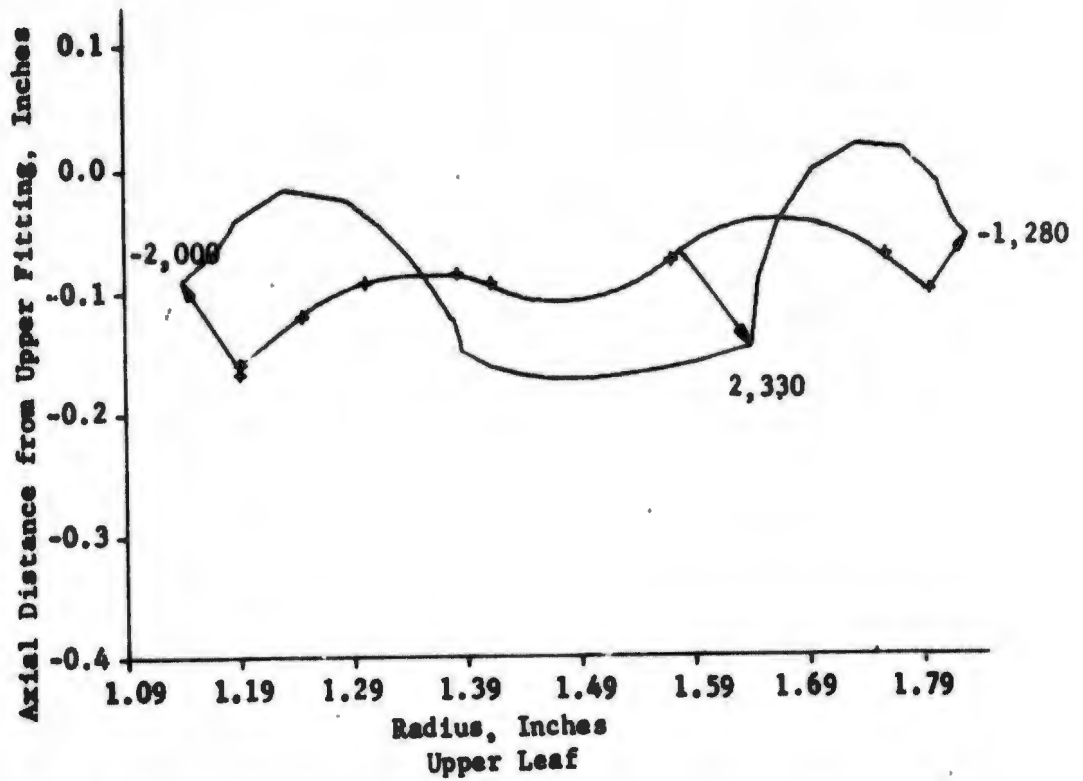


FIGURE 49. OUTER SURFACE MERIDIONAL STRESSES IN THE 3.5-INCH WELDED BELLOWS AS FABRICATED (Internal Pressure = 1 psi).

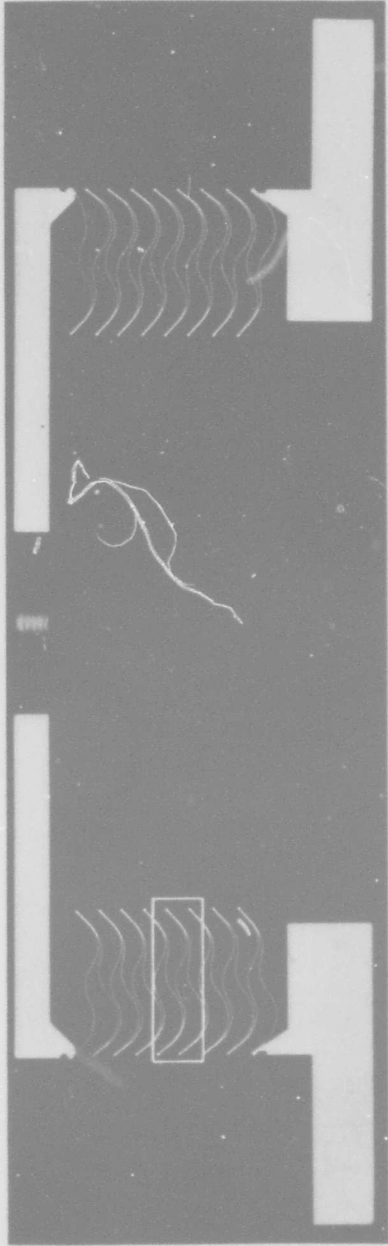


FIGURE 50. CROSS SECTION OF MODIFIED OPTIMIZED BELLOWS SPECIMEN

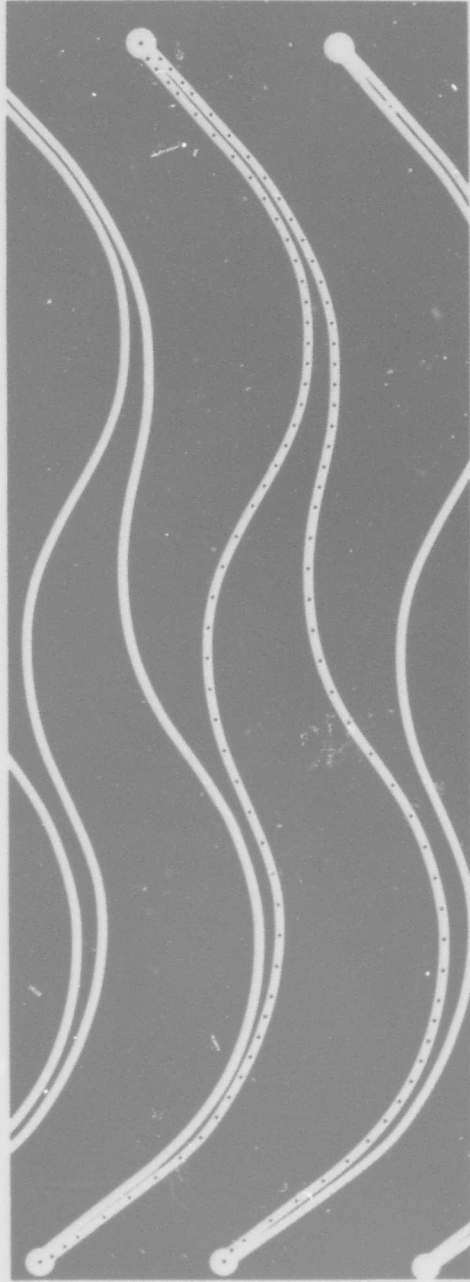


FIGURE 51. CONVOLUTION OF MODIFIED OPTIMIZED BELLOWS SPECIMEN SELECTED FOR MEASUREMENT

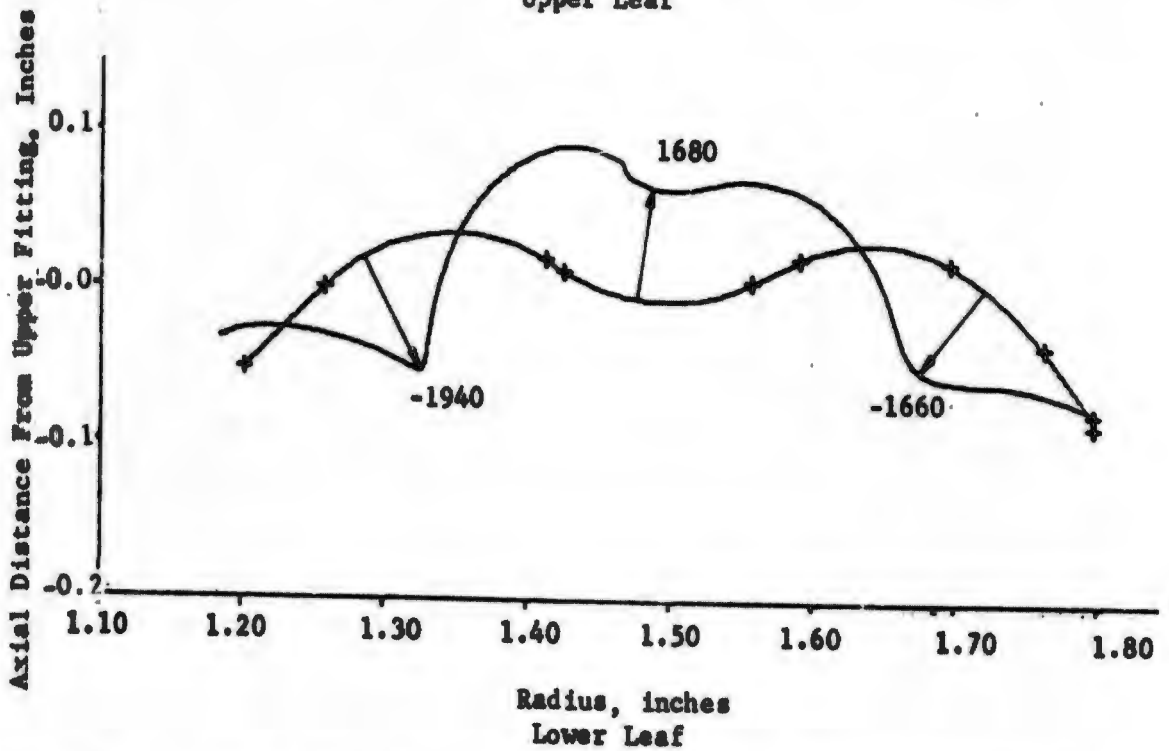
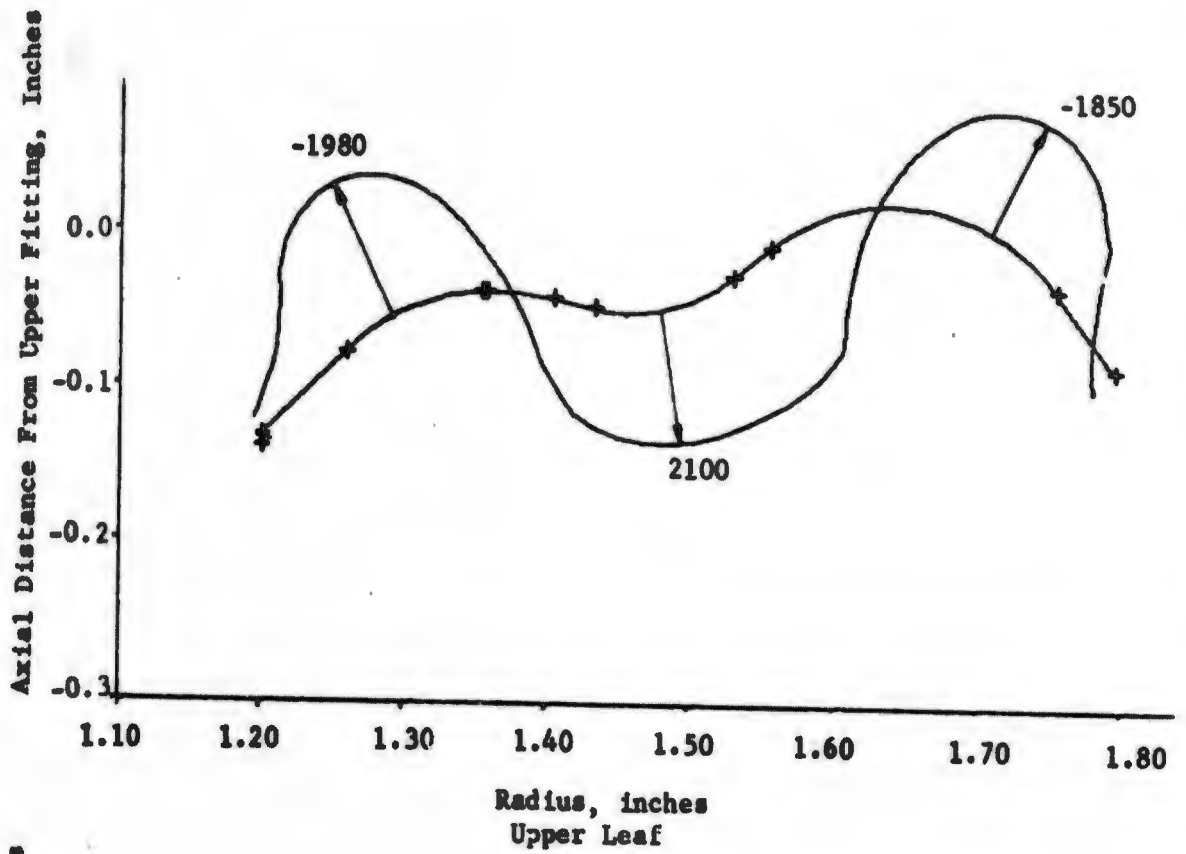


FIGURE 52. OUTER SURFACE MERIDIONAL STRESSES FOR INTERNAL PRESSURE IN AN EXACT MATHEMATICAL MODEL OF FABRICATED 3.5-INCH BELLOWS WITH 43° ID, 51.5° OD TILT ANGLES, 0.086-INCH PITCH AND 0.5950-INCH SPAN, (Pressure = 1 psi)

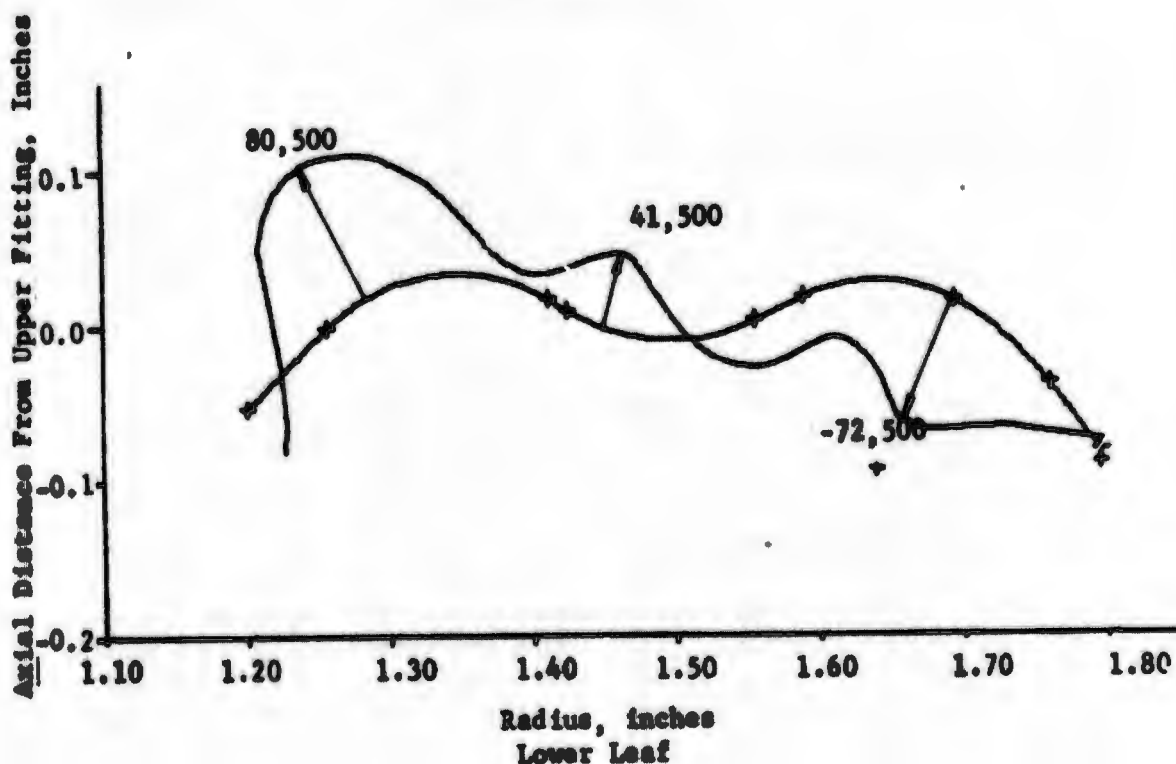
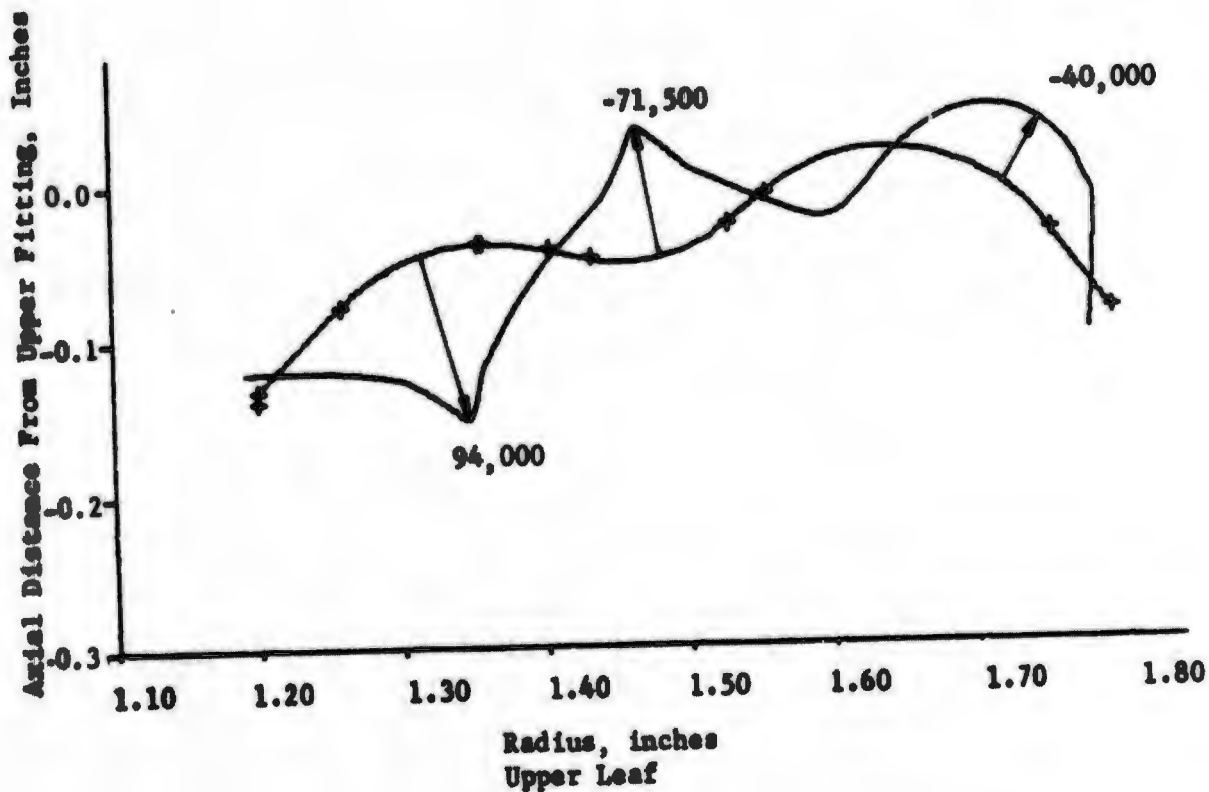


FIGURE 53. OUTER SURFACE MERIDIONAL STRESSES FOR AXIAL TENSION OF AN EXACT MATHEMATICAL MODEL OF FABRICATED 3.5-INCH BELLOWS WITH 43° ID, 51.5° OD TILT ANGLES, 0.086-INCH PITCH AND 0.5950-INCH SPAN, (Unit Deflection Per Unit Bellows Length)

TABLE 23. REVISED DIMENSIONS OF OPTIMIZED
3.5-INCH TILT-EDGE BELLOWS

Part No.	Shell Type	Outer Normal, degrees		Radii, inches	
		Initial	Final	a	b
Upper Leaf					
1	Conical	230.000	---	1.7973	0.06000
2	Toroidal	230.000	138.150	1.64297	-0.15112
3	Toroidal	138.150	195.821	1.44132	0.15112
4	Toroidal	195.821	135.000	1.35892	-0.15112
5	Conical	135.000	---	1.25206	0.09000
Lower Leaf					
7	Conical	-45.000	---	1.18902	0.08500
8	Toroidal	-45.000	30.600	1.3428	0.13250
9	Toroidal	30.600	-31.850	1.48661	-0.15000
10	Toroidal	-31.850	50.000	1.63621	0.13350
11	Conical	50.000	---	1.7385	0.09150

Optimized Bellows Inspection

The optimized bellows were given essentially the same inspection as the interim bellows. A variety of small blemishes were noted on several of the bellows, but these were judged to be typical of the state of the art in welded-bellows manufacture.

One exception was an end-fitting weld on one bellows. The weld had poor uniformity and a skipped region at one spot. This is shown in Figure 54. This bellows was returned for rewelding of the end fitting and subsequent inspection showed that the new weld was satisfactory.

Optimized Bellows Evaluation

Selected tests were conducted with the optimized bellows specimens to compare the optimized bellows with the selected standard welded bellows. The tests, which are described below, were selected as being most important for the application of tilt-edge welded bellows in typical rocket propulsion systems.

Primary tests included tests for leakage and measurements of spring rate, hysteresis, and fatigue life. In addition a test was made to determine the internal pressure that causes snap buckling of the bellows leaves.

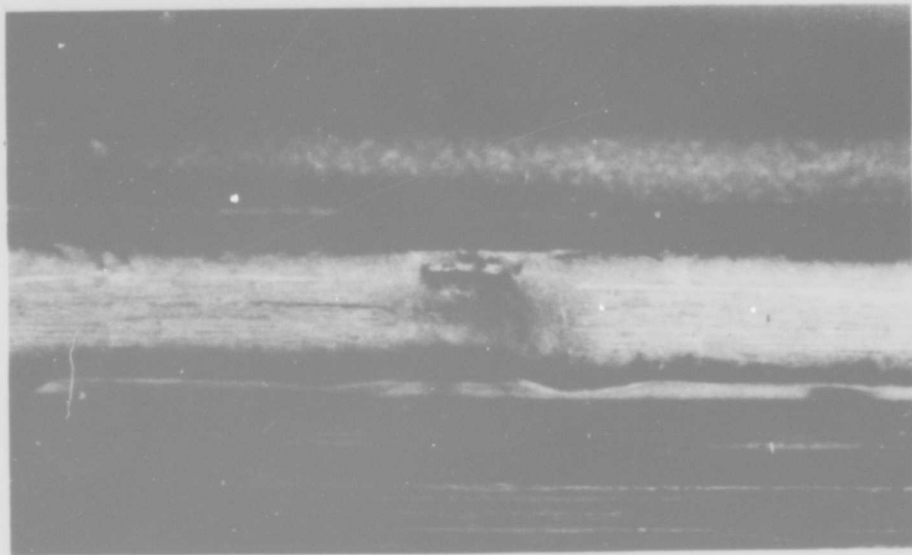


FIGURE 54. POOR END-FITTING WELD OF BELLOWS THAT WAS RETURNED FOR REWELDING

Leakage Analysis. Although inspection of the optimized bellows specimens showed a fabrication quality comparable to standard welded bellows, it was necessary to demonstrate that very low leakage assemblies had been produced. No leakage was measured with a helium mass spectrometer for any of the bellows specimens. These results were the same as those obtained with the standard bellows specimens and showed that any leaks in the bellows were less than 1×10^{-9} atm cc/sec of helium.

Spring Rate Analysis. As described previously for the interim bellows, it was important to compare the measured spring rates of the bellows specimens with the calculated spring rate. It was also important to compare the spring rates of the optimized configuration with the spring rates of the standard welded bellows measured during the previous program.

Table 24 shows the calculated (46 lb/in.) and measured spring rates for the optimized bellows specimens. It was concluded that the values were comparable in spread with those obtained during the previous program for standard welded bellows.

TABLE 24. EXPERIMENTAL AND THEORETICAL SPRING RATES FOR FINAL BELLOWS SPECIMENS

Bellows	Measured Compression Spring Rate (3/8-Inch Deflection), lb/in.	Measured Tension Spring Rate (3/8-Inch Deflection), lb/in.
KT-16	45.0	44.2
KT-17	43.9	45.2
KT-18	48.9	44.1
KT-19	44.1	45.3
KT-20	44.8	43.8
KT-21	44.2	44.8
KT-22	42.0	43.6
KT-23	39.5	42.7
KT-24	40.4	44.5
KT-25	42.9	45.7
KT-26	47.5	44.4
KT-27	47.6	45.3
KT-28	46.9	44.0
KT-29	43.6	43.8
KT-30	39.2	44.0
KT-31	45.2	44.3
KT-32	41.0	44.8
KT-33	41.4	45.0
KT-34	45.3	45.0
KT-35	40.6	42.7
KT-36	42.8	43.6
Theoretical Spring Rate (linear)	46.0	46.0

The calculated spring rate for the 3.5-inch standard welded bellows that the optimized configuration was to be compared with was 57 lb/in. This demonstrated that adequate flexibility can be achieved in a tilt-edge design despite the stiffening contributions of the conical diaphragm segments near the inner and outer weld beads.

Hysteresis Analysis. Hysteresis is the difference between the deflections of a bellows or diaphragm at a given load for increasing or decreasing loads. Table 25 shows the hysteresis for the optimized bellows specimens at 0 load after three compression cycles and after three tension cycles. Also shown are values for the "standard" 3.5-inch stainless steel bellows. The different deflections that were used corresponded to the full compression capability of each type of bellows. It can be seen that the amount of hysteresis in the tilt-edge bellows was significantly greater than in the standard bellows even when the difference in deflection is considered. Thus, the tilt-edge bellows configuration did not seem to be preferred over the standard bellows for those applications requiring low hysteresis.

TABLE 25. COMPARISON OF HYSTERESIS FOR STANDARD BELLOWS AND FINAL BELLOWS

Hysteresis in Standard Bellows for 0.240-Inch Deflection			Hysteresis in Final Bellows for 0.375-Inch Deflection		
Bellows No.	Compression Set, inch	Tension Set, inch	Bellows No.	Compression Set, inch	Tension Set, inch
JD-131	0.003	0.020	KT-16	0.007	0.044
JD-132	0.005	0.023	KT-17	0.009	0.044
JD-133	0.006	0.022	KT-18	0.010	0.040
JD-135	0.005	0.025	KT-19	0.008	0.043
JD-137	0.004	0.019	KT-20	0.016	0.037
JD-138	0.004	0.022	KT-21	0.014	0.037
JD-139	0.004	0.023	KT-22	0.011	0.049
JD-140	0.004	0.025	KT-23	0.011	0.052
JD-141	0.003	0.027	KT-24	0.010	0.046
JD-142	0.005	0.026	KT-25	0.011	0.035
			KT-26	0.012	0.039
			KT-27	0.010	0.039
			KT-28	0.012	0.040
			KT-29	0.008	0.049
			KT-30	0.009	0.045
			KT-31	0.023	0.035
			KT-32	0.008	0.048
			KT-33	0.008	0.047
			KT-34	0.010	0.044
			KT-35	0.023	0.076
			KT-36	0.020	0.058

(a) After 3 loadings each in compression and then in tension.

Buckling Pressure Analysis. The design of any bellows, whether welded or formed, requires a compromise between deflection capability and pressure capability. As the bellows is made more flexible to achieve greater deflection capability, its pressure capability decreases. As the bellows is made more pressure resistant, it becomes stiffer. As described earlier, it was decided that the bellows should be designed to give optimum deflection capability with pressure stresses comparable to the standard welded bellows. Although the fatigue behavior of the bellows under axial deflection was of primary interest in the program, it was also important to determine the pressure carrying capability of the optimized bellows.

Tests with the standard 3.5-inch welded bellows had shown a practical pressure limitation of about 40 psi. At an internal pressure of this magnitude, the diaphragms were sufficiently distorted that the fatigue life had been reduced to about 5000 cycles for a deflection of 0.480 inch. In contrast, the fatigue life of the same standard bellows with an internal pressure of 10 psi and a total deflection of 0.480 inch was about 150,000 cycles.

Although pressure reduced the fatigue life of the optimized configuration (see below), it was found that the tilt-edge design had a different pressure limitation from the standard bellows. This was oil-canning of a diaphragm; i.e., with a sufficiently high pressure, one of the bellows diaphragms would reverse. Although the bellows did not leak with this occurrence, its performance characteristics were altered sufficiently that it no longer functioned in an acceptable manner. For the optimized design it was found that the buckling (oil-canning) pressure with internal pressure was about 60 psi while the buckling pressure with external pressure was about 30 psi. Because of this buckling phenomena, it is believed that a bellows subjected to pressure or pressure surges up to 30 psi should be designed with decreased span to make it more resistant to pressure effects.

Fatigue Analysis. As with the interim bellows described earlier, three fatigue characteristics were of particular interest for the optimized bellows specimens (1) the location of the fatigue cracks, (2) the range of the fatigue life values for a given test condition and (3) the comparison of the fatigue lives with values estimated from calculated strains. It was shown in the previous study⁽¹⁾ that the fatigue failure of conventional welded bellows always occurred at the convolution welds. Because of the variable properties of the welds, large scatter was observed in the fatigue lives of the various conventional bellows tested. From the analytical results described earlier and from the results of the tests of the interim bellows, it was expected that fatigue failure at the welds could be prevented in the optimized tilt-edge bellows. It was believed that prevention of weld failures would not only improve welded-bellows fatigue life but also improve the reliability of the bellows.

It was believed that fatigue tests with the optimized bellows specimens would show that the design goals had been met:

- (1) If the fatigue failure occurred in the parent metal of the convolution rather than in the weld beads

- (2) If the range of fatigue failures for given test conditions was narrower than for standard welded bellows
- (3) If the fatigue lives of the optimized tilt-edge bellows were greater for a given stroke than for the standard welded bellows selected for comparison.

It was also hoped that, with fatigue failure occurring in the parent metal of the bellows, the fatigue life of the tilt-edge bellows could be estimated using calculated maximum strains and coupon fatigue data from the literature.

Of the 14 bellows that failed in fatigue, 13 developed fatigue cracks in the parent metal of the diaphragms near the point of calculated maximum stress. One bellows failed prematurely at an end fitting when the diaphragm welded to the end fitting buckled. The cause of the buckling could not be determined, although the diaphragm may have been deformed during the welding operation. Because of the otherwise consistent failure in the parent metal, it was judged that the prevention of weld-bead fatigue failures had been amply demonstrated.

Table 26 duplicates Table N-8 which was included in Appendix N of Technical Report No. AFRPL-TR-68-22 to show the excessive variation in the fatigue life of standard welded bellows that were encountered during the previous program. It is important to note that bellows having early failures were not found to be poorly made either by the manufacturers nor during careful inspection at Battelle. In addition, cross sections of the bellows showed generally good welding practices.

TABLE 26. EXCESSIVE VARIATION IN THE FATIGUE LIFE OF STANDARD WELDED BELLOWS

Bellows	OD, inch	Bellows Material	Internal Pressure, psi	Stroke, inch	% Stroke in Tension	Fatigue Life, hr.
JD141	3-1/2	347 S.S.	20	0.240	0	453
JD135	3-1/2	347 S.S.	20	0.240	0	NF 1,747,069
JD132	3-1/2	347 S.S.	20	0.240	50	73,322
JD131	3-1/2	347 S.S.	20	0.240	50	NF 768,870
JD166	3	AM350	40	0.240	50	37,145
JD164	3	AM350	40	0.240	50	NF 1,000,000

Table 27 shows 9 different test conditions for the optimized tilt-edge bellows, each involving two or more test specimens. It has been shown that the fatigue failures of identical metal coupons can vary as much as 3 to 1 or more for identical test conditions. Only one bellows test condition produced a spread significantly greater than 3 to 1 (80,709 cycles vs. 10,935 cycles) and the early failure was caused by diaphragm buckling rather than fatigue cracking. These data, combined with the interim bellows data presented earlier, are believed to demonstrate clearly that the fatigue failure range for tilt-edge bellows is comparable to that obtained from coupon specimens. This spread is not only much better than that obtained with conventional welded bellows, but is better than that obtained with formed bellows, as shown in Figure 44.

Another aspect of the fatigue analysis of the optimum bellows specimens was a comparison of the deflection capability of the optimized bellows with the deflection capability of the standard welded bellows tested during the previous program. Figure 55 shows the comparison results. The largest deflection tested for the standard bellows was 0.240-inch compression and 0.240-inch extension. Four internal pressures were used, 4 psi, 10 psi, 20 psi, and 40 psi. Fatigue failure occurred in 158,115 and 158,570 cycles at 4 psi, 195,600 cycles at 10 psi, 11,382 cycles at 20 psi, and 4,219 cycles at 40 psi. Spring rate measurements showed that as the internal pressure of the standard bellows was increased above 15 psi, the spring rate of the bellows increased. This was thought to be caused by pressure-induced interference of the diaphragms. This, in turn, was believed to be the cause of the reduced fatigue life of the standard bellows at 20 and 40 psi.

For the optimized bellows, it can be seen that the fatigue life was far superior for a 0.240-inch compression and 0.240-inch extension. During the program it was not determined how many cycles could be obtained at internal pressures of 20 psi and below. Even with a 50 percent increase in stroke, the lives of the optimum bellows specimens were substantially greater than that of the standard welded bellows. Thus, in accordance with the design objective, the optimized tilt-edge bellows was shown to have substantially better deflection capabilities than the standard bellows selected for comparison.

The ability to estimate the fatigue life of an optimized bellows specimen was found to be good at low pressure. However, an increase in internal pressure caused a reduction in fatigue life and this effect was not predicted by a linear analysis. The analysis of this condition is summarized briefly.

A linear calculation for the optimized bellows configuration showed a strain range of 3200μ in/in for 3/8-inch compression and 3/8-inch tension. From Figure 44, a fatigue life of from 1 to 2 million cycles was estimated for this test condition. As shown in Table 27, specimens KT-17, KT-25, and KT-28 gave 938,573 cycles, 2,066,147 cycles, and 2,433,778 cycles, respectively with an internal pressure of 2 psi. This was believed to be good correlation.

However, an increase in internal pressure to 10 psi decreased the fatigue life of KT-16 and KT-19 to 251,808 cycles and 382,710 cycles, respectively. An increase in internal pressure to 40 psi decreased the

TABLE 27. SIMILARITY OF FATIGUE CYCLES FOR OPTIMIZED BELLOW SPECIMENS

Bellows No.	Total Stroke, in.	% Stroke in Tension	Internal Pressure, psi	Calculated Max. Strain Range, μ -in./in.	Cycles to Failure	Estimated Fatigue Life Range at Zero Pressure, hr.	
						Lower	Upper
KT-17	0.750	50	2	3200	938, 573	8x10 ⁴	1x10 ⁸
KT-25	0.750	50	2	3200	2,066, 147	8x10 ⁴	1x10 ⁸
KT-28	0.750	50	2	3200	2,433, 778	8x10 ⁴	1x10 ⁸
KT-22	1.000	62	2	4266	51, 375	2x10 ⁴	2x10 ⁵
KT-27	1.000	62	2	4266	42, 600	2x10 ⁴	2x10 ⁵
KT-16	0.750	50	10	3200	251, 808	8x10 ⁴	1x10 ⁸
KT-19	0.750	50	10	3200	382, 710	8x10 ⁴	1x10 ⁸
KT-20	0.750	66	10	3200	272, 252	8x10 ⁴	1x10 ⁸
KT-21	0.750	66	10	3200	81, 873	8x10 ⁴	1x10 ⁸
KT-23	0.750	50	40	3200	47, 500	8x10 ⁴	1x10 ⁸
KT-24	0.750	50	40	3200	58, 191	8x10 ⁴	1x10 ⁸
KT-29	0.480	50	4	2050	2,962, 300 NF	1x10 ⁷	1x10 ¹⁰
KT-30	0.480	50	4	2050	2,962, 300 NF	1x10 ⁷	1x10 ¹⁰
KT-31	0.480	50	20	2050	2,046, 222 NF	1x10 ⁷	1x10 ¹⁰
KT-32	0.480	50	20	2050	2,046, 222 NF	1x10 ⁷	1x10 ¹⁰
KT-33	0.480	50	40	2050	1,418, 086	1x10 ⁷	1x10 ¹⁰
KT-34	0.480	50	40	2050	2,345, 678 NF	1x10 ⁷	1x10 ¹⁰
KT-35	0.620	50	40	2650	10, 935 (Buckling Failure)	1x10 ⁶	1x10 ⁹
KT-36	0.620	50	40	2650	80, 709	1x10 ⁶	1x10 ⁹

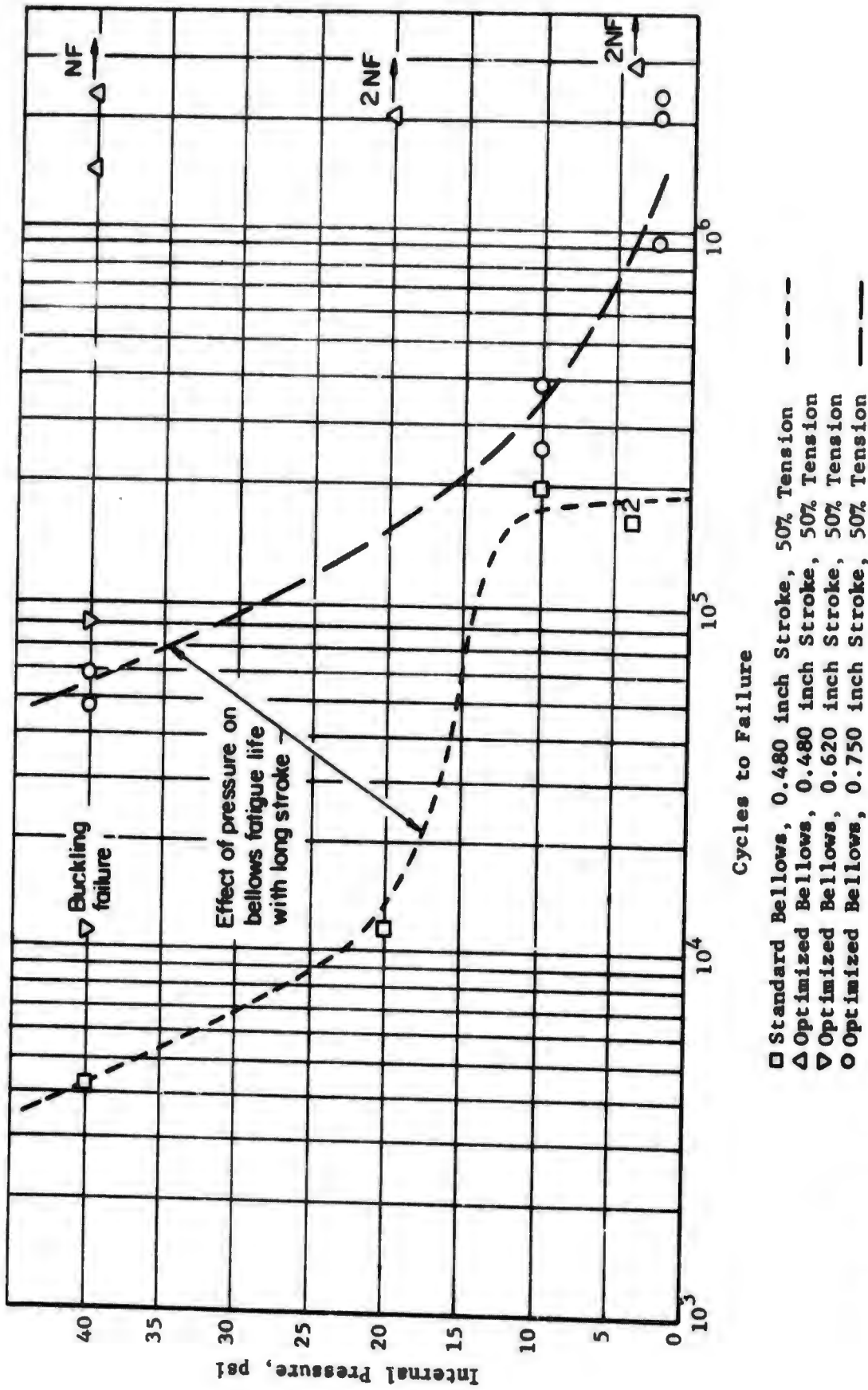


FIGURE 55. FATIGUE FAILURE COMPARISON OF OPTIMIZED TILT-EDGE BELLOWS WITH STANDARD BELLOWS

lives of KT-27 and KT-24 to 47,500 cycles and 58,191 cycles, respectively. An examination of a strain-gaged bellows subjected to 3/8-in compression and 3/8-inch extension with different amounts of internal pressure showed that the pressure was causing some parts of the diaphragms to press together or lock up. This reduced the effective length of the diaphragms and increased the strain in the diaphragms for given amounts of deflection of the bellows. Although it was believed that the computer analysis program could be modified to analyze this geometrically nonlinear condition, it was not possible to accomplish this in the current program.

SECTION V

CONCLUSIONS

As a result of the research study, it was concluded that tilt-edge bellows can be designed to give significantly better performance than conventional welded bellows. However, certain problems were identified with regard to the nonlinear effects of pressure on tilt-edge bellows. These problems should be studied further in order to develop a complete understanding of the behavior of tilt-edge bellows. Such an understanding will be required before tilt-edge bellows are generally used in place of conventional welded bellows.

The conclusions reached as a result of the theoretical design study and as a result of the fabrication and testing program are summarized in the following sections.

Theoretical Design Study

The theoretical design study was concerned with the effects of variations in tilt angle, span, sweep radius, and convolution pitch. The conclusions reached in studying these parameter effects are as follows:

Tilt Angle. It was found that properly selected tilt angles reduced the stresses at the root and crown welds to very nearly zero values under either pressure loading or axial deflection loading for all bellows sizes studied (1- to 3.5-inch OD). The optimum tilt angle for pressure loads was always higher than the optimum tilt angle for deflection loads. However, in all cases, tilt angles could be found (usually between the two optimum angles) that gave satisfactorily low stresses at the root and crown welds for either deflection or pressure loading.

Span. The effects of changes in the span were essentially the same for tilt-edge bellows as for conventional bellows. Increasing span lowered the maximum deflection stress almost in proportion to the change in span.

Convolution Pitch. Changing convolution pitch had little effect on the stresses due to pressure. The stresses due to axial deflection increased with pitch for an assumed unit deflection per unit length bellows. However, when an axial load of a 1-inch deflection per bellows convolution was considered, the maximum bellows stresses were relatively independent of pitch. This behavior was also similar to the behavior of conventional welded bellows.

Sweep Radius. The effects of sweep radius variations on the maximum stresses in tilt-edge bellows were found to be less pronounced than the effect of the above parameters. However, it was found that optimum sweep radii did exist that minimized the maximum convolution stresses. In the bellows considered, this sweep radius was approximately 25 percent of the bellows span.

End Fitting Stresses. End-fitting stresses were found to be satisfactorily low for many of the optimized convolution shapes with the end leaves identical to the optimum convolution leaf shapes. In those designs exhibiting unsatisfactorily high end-fitting stresses, it was found that the only reliable method of reducing these end-fitting stresses was to increase the thickness of the bellows end leaf that was welded to the fitting with high stresses.

As an overall result of the analytical design phase of the research study, it was found that theoretically optimized tilt-edge bellows designs could be found with very low stresses at the weld beads and at the end fittings.

Fabrication

Two different tilt-edge bellows models were fabricated. Based on this experience, the following conclusions were reached.

Formability of Bellows Diaphragms. It is possible to form the bellows diaphragms to precisely the shape required provided that appropriate allowance is made for spring back. Because of the greater overall curvature of the tilt-edge bellows diaphragms with respect to the standard welded bellows diaphragms, the spring back is greater. However, with a minimum amount of experience, this increased spring back can be anticipated in making the forming dies.

Weldability. The execution of the ID weld to join the upper and lower bellows diaphragms into a full convolution offers little difficulty. However, difficulties can be encountered in making the OD weld to join adjacent convolutions. The difficulties are primarily associated with fitting chill rings between the bellows leaves. It was found that the difficulty of using properly fitting chill rings increased as the OD tilt angle was increased and the convolution pitch was decreased. For very large tilt angles and small pitch it could become necessary to make the OD weld without using chill rings.

Experimental Program

The experimental program verified that the tilt-edge design did indeed have sufficiently low weld stresses to prevent fatigue failure in the welds. However, it was concluded that some problems still existed requiring further study. The following conclusions were reached as a result of the experimental program.

Spring Rate and Hysteresis. The spring rate of tilt-edge bellows can be calculated using NONLIN at least as accurately as for formed bellows. A tilt-edge bellows has about 10 percent to 20 percent higher spring rate than a conventional welded bellows with the same pitch, span, and thickness. However, this spring rate can easily be adjusted by changing the span.

When tested at their maximum stroke, the tilt-edge bellows exhibited more hysteresis than the standard bellows. However, since the maximum stroke given the tilt-edge bellows was much larger than the stroke given the standard bellows, it was concluded that both bellows exhibited sufficiently low hysteresis to meet Air Force standards.

Fatigue Life Under Cyclic Axial Loads. It was found that when cycled at moderate deflection ranges and at low pressures, the fatigue life of a tilt-edge bellows could be reliably estimated using the strain range calculated from the theoretical analysis and the appropriate coupon fatigue data. Further, it was found that the spread in fatigue life for sets of tilt-edge bellows tested at the same maximum strain range was almost as small as for coupon data. This low scatter was observed for a wide range of pressures and strain ranges and indicated that reproducible fatigue lives could be expected in tilt-edge bellows.

However, the experimental program showed that pressure had a significant effect on the performance of tilt-edge bellows. This pressure effect was manifested in two ways: (1) by a gradual reduction of the fatigue life under axial loading as the pressure was increased and (2) by snap-through buckling of an upper leaf at high internal pressure. Similar snap-through buckling of the lower leaf was observed for external pressure.

It was concluded that the first effect of pressure in reducing the fatigue life was similar to that observed in standard welded bellows. This effect was believed to be a combination of leaf interference caused by the pressure and the displacement of the mean stress point of the load cycle by the pressure stress.

The snap through buckling (oil canning) of the bellows leaves at higher pressures was not observed for standard bellows. However, it is a common phenomena with single-sweep bellows. It was concluded that the oil-canning was a result of the overall arch in the tilt-edge leaves that make them behave like a single sweep bellows with similarly arched leaves. The standard multi-sweep bellows leaves tended to be fairly flat and apparently deformed in response to the pressure from either side without buckling. It was concluded that the leaf buckling poses a definite limitation on the pressure capacity of a tilt-edge bellows.

SECTION VI

RECOMMENDATIONS

1. It is recommended that tooling arrangements and welding procedures be developed that would simplify the OD welding of bellows with relatively large tilt angles or with small values of pitch. This would be of considerable benefit for manufacturers who have not yet developed such techniques.
2. It is recommended that a theoretical and experimental investigation be carried out to develop procedures for predicting the effects of pressure on tilt-edge bellows. This investigation would involve extending NONLIN to account for leaf interaction and to predict the snap through buckling pressures. Further testing would also be needed, particularly to test for buckling loads. It is believed that such a research program would lead to the development of methods for predicting the performance of tilt-edge bellows under pressure with nearly the same reliability as was found for performance at low pressures.

APPENDIX A

ANALYSIS OF WELD AREA OF BELLOWS

APPENDIX A

ANALYSIS OF WELD AREA OF BELLOWS

An analysis of a welded bellows as a thin shell of revolution does not give a complete picture of the stresses in the area of the weld bead. A detailed analysis requires that this area be treated as an axisymmetric solid, in order that the local stress distributions can be calculated about the notch at which failures normally occur. This appendix describes such an analysis in which a single weld bead and short segments of the adjoining leaves were separated (for purposes of analysis) from the remainder of the bellows for detailed study. This removed portion was then analyzed with Battelle's computer program, AXISOL. AXISOL is applicable to such an axisymmetric solid of rather irregular cross section. Several representative cases were considered in this way: inner and outer welds, both small and large edge tilts, and both axial and pressure loading. The calculated stresses agreed with those of the thin shell analysis, except in the immediate area of the weld bead. In this area the effect of the notch on the level and distribution of stresses was determined.

The Finite Element Computer Program AXISOL

Battelle's computer program, AXISOL, was used to calculate the detailed stress distribution in the weld area. This computer program is well suited for this application, since it is capable of analyzing the stresses in axisymmetric bodies of general cross section. Only a brief description of the program will be given here, since it is rather widely used in the aerospace industry and is well documented (3).

The stresses in an elastic solid (such as that represented by the weld area of a bellows) can be described by the equations of the linear theory of elasticity. However, the geometry and loadings are far too complex in this case to allow an exact analytical solution of the problem. One must then consider numerical methods to obtain an approximate solution. One possible approach is to approximate the governing differential equations, as is done in the method of finite differences. In contrast, the approach on which the computing program AXISOL is based does not utilize the governing differential equations. It approximates the solid with an appropriate structural model and then calculates the exact response of this model. This approach is described as the finite element method.

In the program AXISOL, the solid is modeled as an assembly of ring elements which can be of either quadrilateral or triangular cross section. It is assumed that the stresses and strains within each element are constant, but that they change from one element to the next. Thus, in areas where the stresses change rapidly, closely spaced elements are required for accurate results. The elements are interconnected at their mutual corners, which are designated nodal points. Equilibrium equations in terms of the unknown nodal point displacements and the known elemental stiffnesses are formulated. The solution of these equations describes the deformation of the finite element approximation of the continuous solid. There is no restriction in

AXISOL on the shape of the solid provided that it is a body of revolution. However, the number of elements required to accurately model the solid is restricted by the computer storage capacity. Over 2000 elements are permitted, which is far more than the approximately 300 elements needed in this study to describe the bellows weld area. The stresses in the solid may be calculated for either arbitrarily prescribed boundary deformations or boundary stresses, as well as thermal loadings. Computation times of between 1 and 2 minutes on Battelle's CDC-6400 digital computer were experienced in the weld area analysis.

Procedure of Analysis

For study of the bellows weld area it was assumed that the results of the thin shell analyses were accurate, except very near the welds. Thus, only a very limited portion of the bellows near a weld had to be considered in each finite element calculation. This portion consisted of the weld and short lengths of the two adjoining shell leaves, which were considered to be cut from the bellows a few shell thicknesses from the weld. On these imaginary cuts the action of the remainder of the bellows on the weld area was represented as external loads. The appropriate force and moment values were obtained from a separate shell calculation.

The basic finite element pattern that was used for all the calculations is shown in Figure A-1. This figure was produced by the computer plotting facility on the basis of input data describing the finite element model. The conception and specification of the precise number and arrangement of the elements is a key step in each problem and rests largely on the judgment of the analyst. With a well-constructed pattern one can obtain accurate stress results with a reasonable number of elements and thereby minimize the effort required to prepare the input data and the machine computation time. In the modeling of the bellows weld area, a minimum of six elements through the leaf thickness was believed necessary to represent the bending stress variation between the inner and outer surfaces. Elements of excessively elongated cross section were avoided in this area. Increasingly smaller elements were taken near the tip of the notch to represent the stress peak there. In contrast, relatively large elements were used in the outer portion of the weld. A total of 288 elements were utilized for the analysis. Figure A-1 represents but one of four weld geometries considered. It is a model of an outer weld with an edge tilt of 35 degrees. Since considerable time and effort were required to produce this mesh, this basic configuration was used as data to produce the meshes for the other three cases. A simple computer program was written to transform the coordinate data by applying appropriate rigid body translations and rotations while maintaining the element pattern. In this way, the mesh could be positioned to represent either an inner or outer weld with the required tilt angle.

The notches in actual welded bellows show considerable geometrical variation as can be seen in cross-sectioned bellows. The particular notch configuration that was assumed for this study was believed to be reasonably representative. For analysis purposes the notch tip was taken as perfectly sharp with no radius. A realistic value for this radius would have been

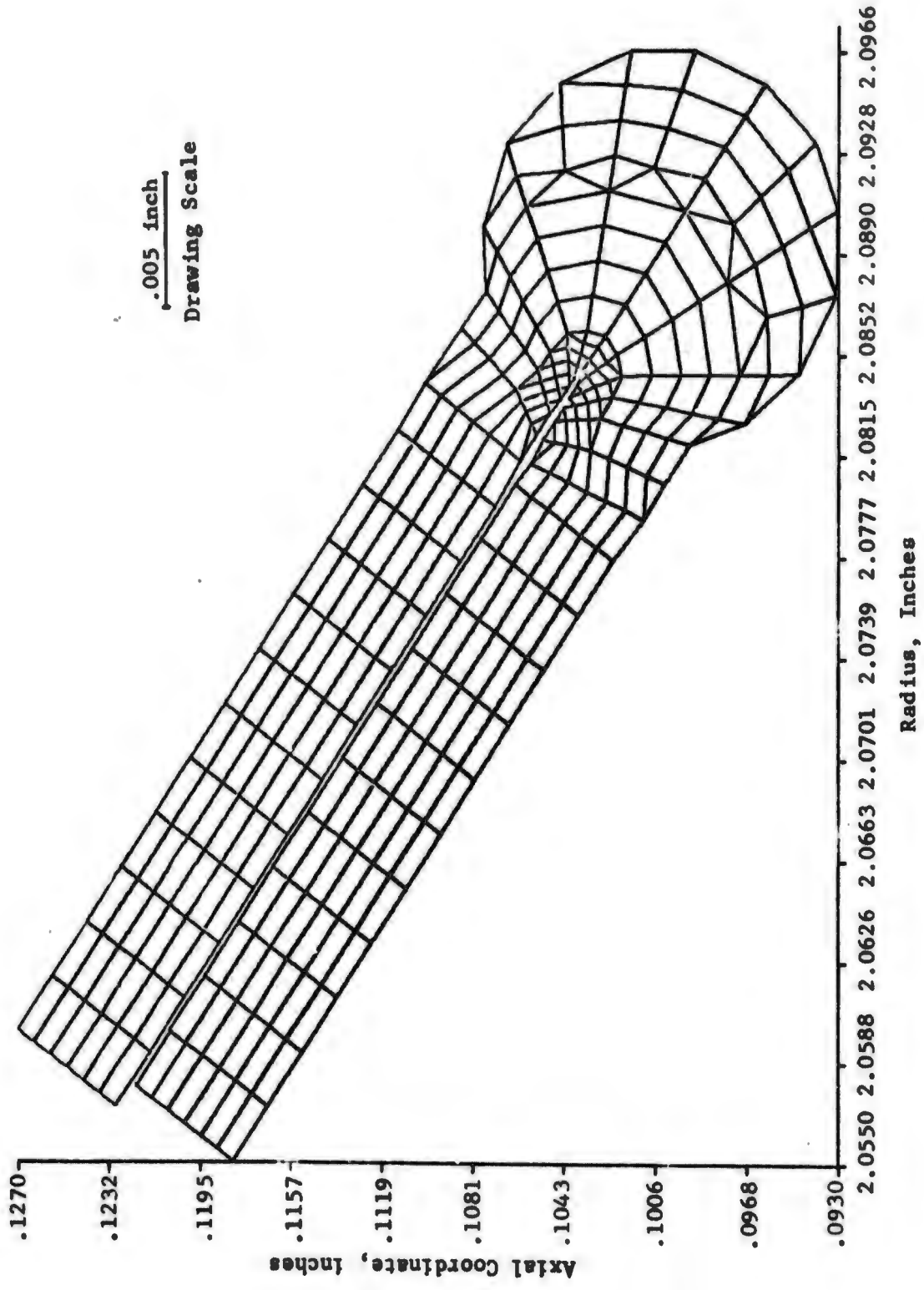


FIGURE A-1. MESH CONFIGURATION FOR MATHEMATICAL MODEL OF OD WELD OF 4-INCH WELDED BELLOWS WITH 35° EDGE TILT

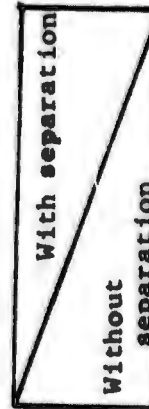
smaller than could have been conveniently represented with the finite element mesh. No attempt was therefore made in this study to model a rounded notch tip. Another factor of potential importance was the distance that the notch extended into the weld material. The effect of variation of this distance on the stress distribution in the weld could have been explored by changing the finite element model of the notch area. However, this was beyond the scope of the study.

Precise application of the force and moment loads to the edges of the leaf segments as equivalent sets of nodal point forces was an important step in the analysis. To ensure accuracy and to eliminate hand calculations, a Fortran IV subroutine was written for AXISOL to allow the resultant moment and the normal and shear force resultants obtained by the thin shell calculation to be specified directly as input data for AXISOL. Particular care was taken to calculate a nodal point load pattern that had the precise force and moment resultants. The exact distribution was believed to be of lesser importance. Such a procedure was considered important, since it was anticipated that the calculated stresses (in particular, the hoop stress component) would be quite sensitive to even small variations in the net applied loads.

In thin-shell analysis of welded bellows it had not been the practice to include separation of the midsurfaces of the two leaves joined at the weld. These were taken to be coincident, with the midsurface separation corresponding to the leaf thickness being ignored. In the detailed analysis of the weld area as a solid of revolution, this separation was, of course, included. During the study it became apparent that this separation had a local effect near the weld. It was concluded that this effect must be included in the shell calculation in order to obtain a consistent set of edge loadings for the finite element analyses. This local effect could be explained by the fact that the membrane forces in the two adjacent leaves (which are nearly equal and opposite in direction) had their lines of action separated by a distance of about one shell thickness. This produced a couple of the same order of magnitude as the shell bending moments. This had a local effect on the shell equilibrium. Thus, to determine the correct shell resultants for application as external loads in the finite element analysis, the weld beads were represented in the shell calculations as short segments of cylindrical shells. Numerical values of stresses, calculated with and without separation provided in this manner, are tabulated in Table A-1. At the weld there were fairly large differences in the stresses calculated with the thin shell program. A few shell thicknesses away these differences were significantly smaller. The results of the finite element calculation showed a more dramatic effect, however. In one case the edge loads were based on shell calculations with no midsurface separation. In the other case, separation was included. It is seen that the calculated meridional stresses (SPHI) for both cases were similar, but that the circumferential stresses differed by an order of magnitude. When separation of the leaves at the weld is included, the shell and finite element calculations gave consistent results for the circumferential stresses.

TABLE A-1. STRESS AT OUTER WELD OF 4-INCH BELLOWES WITH 35° EDGE TILT DUE TO AXIAL LOADING -- WITH AND WITHOUT SEPARATION OF MIDSURFACES OF ADJOINING LEAVES

	Upper Leaf						Lower Leaf						
	At Cut		At Weld		At Cut		At Weld		At Cut		At Weld		
	SPHI	STHETA	SPHI	STHETA	SPHI	STHETA	SPHI	STHETA	SPHI	STHETA	SPHI	STHETA	
Shell Calculation	Membrane	-1,156	1,257	-1,151	-3,349	1,196	2,484	1,161	-4,269	1,194	1,194	-1,079	68
	Bending	-1,213	1,665	-1,194	-1,794	1,190	4,161	2,050	4,607	4,694	4,694	1,019	
Finite Element Calculation	Membrane	23,757	7,439	10,264	3,612	17,297	4,607	20,581	5,592	1,190	2,418		
	Bending	19,560	6,100	4,694	1,797	20,581	5,592	17,200	18	1,190	27,450	3,900	
	Membrane	-1,150	1,692			1,190	2,418						
	Bending	-1,180	37,700			1,190	27,450						
		20,500	6,500			15,000	3,900						
		16,800	9,950			17,200	18						



SPHI = Meridional stress
STHETA = Circumferential stress

Description of Cases Considered

Calculations were performed for a total of eight cases to explore the importance of weld position (inner or outer weld), edge tilt angle, and type of loading (axial load or internal pressure). All the cases considered were for a nominal bellows with an outside diameter of 4.0 inches and a leaf thickness of 0.005 inch. The basic bellows configurations were the same as the 35° tilt-edge bellows that was described in Appendix D of the final report AFRPL-TR-68-22. A list of the cases is given in Table A-2. Included are the values of the loadings that were applied along the edges where the weld areas were assumed (for purposes of analysis) to have been cut from the remainder of the bellows. These loadings were obtained from thin-shell analysis as explained previously. Each of the cases represented a separate finite element calculation.

Two tilt angles were selected: 15° and 35°. With the 15° tilt angle, the bellows leaves were subjected to considerable bending in the weld area, as is characteristic for small edge tilts. The 35° tilt angle was intended to represent a more favorable edge tilt. For this angle, little bending was observed and the applied axial load was carried mainly as membrane and shearing forces in the weld area.

For the cases of axial loading, the stresses were calculated for an imposed axial deflection of 0.09838 inch per convolution. The pressure loadings corresponded to an internal pressure of 10.0 psi. Pressure and axial loadings were treated separately. Thus, the effects of combined loadings were not considered.

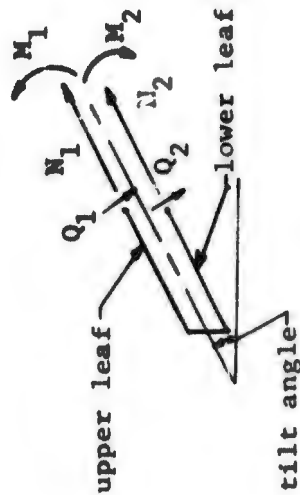
Results and Discussion

The results of the stress calculations are shown in Figures A-2 through A-11 in the form of stress contours. Contours of principal (or maximum) stress are shown for all cases, while contours of circumferential (or hoop) stress (which are of less interest) are shown for only two cases. The principal stress contours are based only on the two principal stress components acting in the r-z plane. The third principal stress is the circumferential stress. In the finite element solutions the stress states in the bellows leaves (away from the weld bead) correspond to the meridional membrane and bending stresses of the shell calculations. However, about the notch the stress pattern becomes more complex and the stresses increase rapidly. In this area, there are two nonzero components of principal stress. This complicated the plotting of the stress contours. A convention was thus adopted to indicate, at a given point, that component that was largest in absolute value. No such difficulty was encountered in plotting the principal stresses in the bellows leaves where the characteristic thin shell stress distribution existed. Here the stress normal to the shell surface is always one of the two principal stresses and was nominally zero. The principal stress of interest was composed of the meridional membrane and bending stresses.

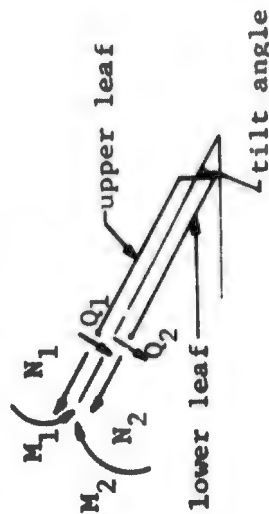
The character of the stress in the weld area is apparent from the contours of Figures A-2 through A-11. In all cases there was a concentration of stress at the tip of the notch, while the outer portions of the weld bead

TABLE A-2 DESCRIPTION OF CASES TREATED IN STUDY OF STRESSES IN WELD
AREA OF BELLOWS WITH APPLIED EDGE LOADINGS

Configuration				Prescribed Edge Loads							
Case	Inner or Outer Weld	Tilt Angle	Type of Loading	N_1 lb/in.	M_1 in.-lb/in.	Q_1 lb/in.	N_2 lb/in.	M_2 in.-lb/in.	Q_2 in.-lb/in.		
1	outer	35°	axial	-5.77897	.098978	-1.49099	5.9765	.073735	1.6265		
2	outer	15°	axial	-5.61011	.19635	.268798	4.2286	.16456	-.63306		
3	inner	35°	axial	-8.24315	-.093082	2.0467	8.8936	-.068648	-2.5124		
4	inner	15°	axial	-9.67209	-.21614	.035447	8.0923	-.16301	.383622		
5	outer	35°	pressure	5.22403	-.052849	.13205	-5.8155	-.036324	-.56815		
6	outer	15°	pressure	6.2029	-.14796	-1.2834	-6.3734	-.11951	1.2350		
7	inner	35°	pressure	7.254	-.052163	.51718	8.2343	-.033546	-1.2623		
8	inner	15°	pressure	9.8931	-.166965	-1.12896	10.4271	-.11920	.95444		



Notation - Inner Weld



Notation - Outer Weld

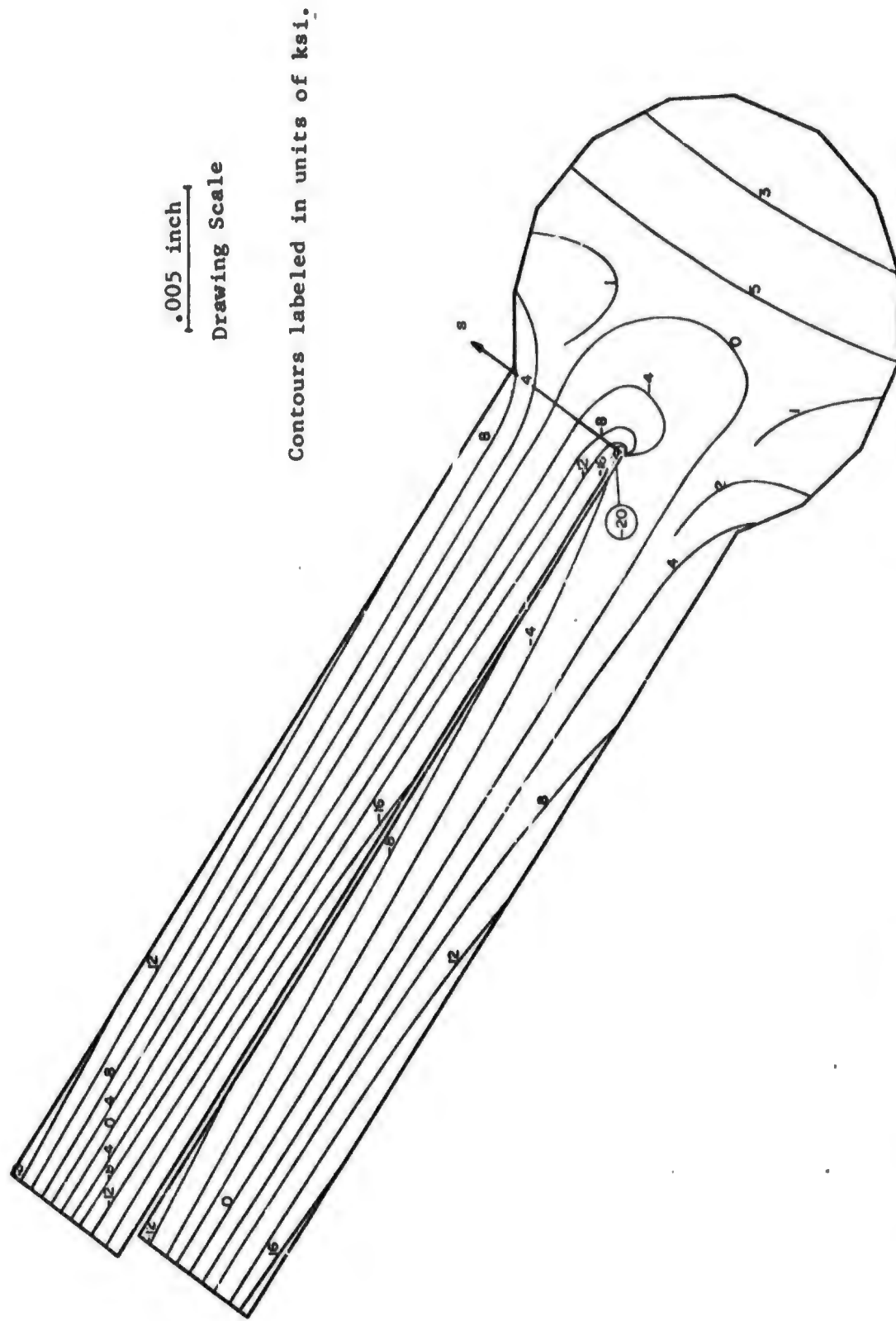


FIGURE A-2. CONTOURS OF PRINCIPAL STRESS IN MATHEMATICAL MODEL OF OD WELD OF 4-INCH WELDED BELLOWS WITH 35° EDGE TILT DUE TO AN AXIAL DEFLECTION OF $\delta = 0.09838$ INCH PER CONVOLUTION

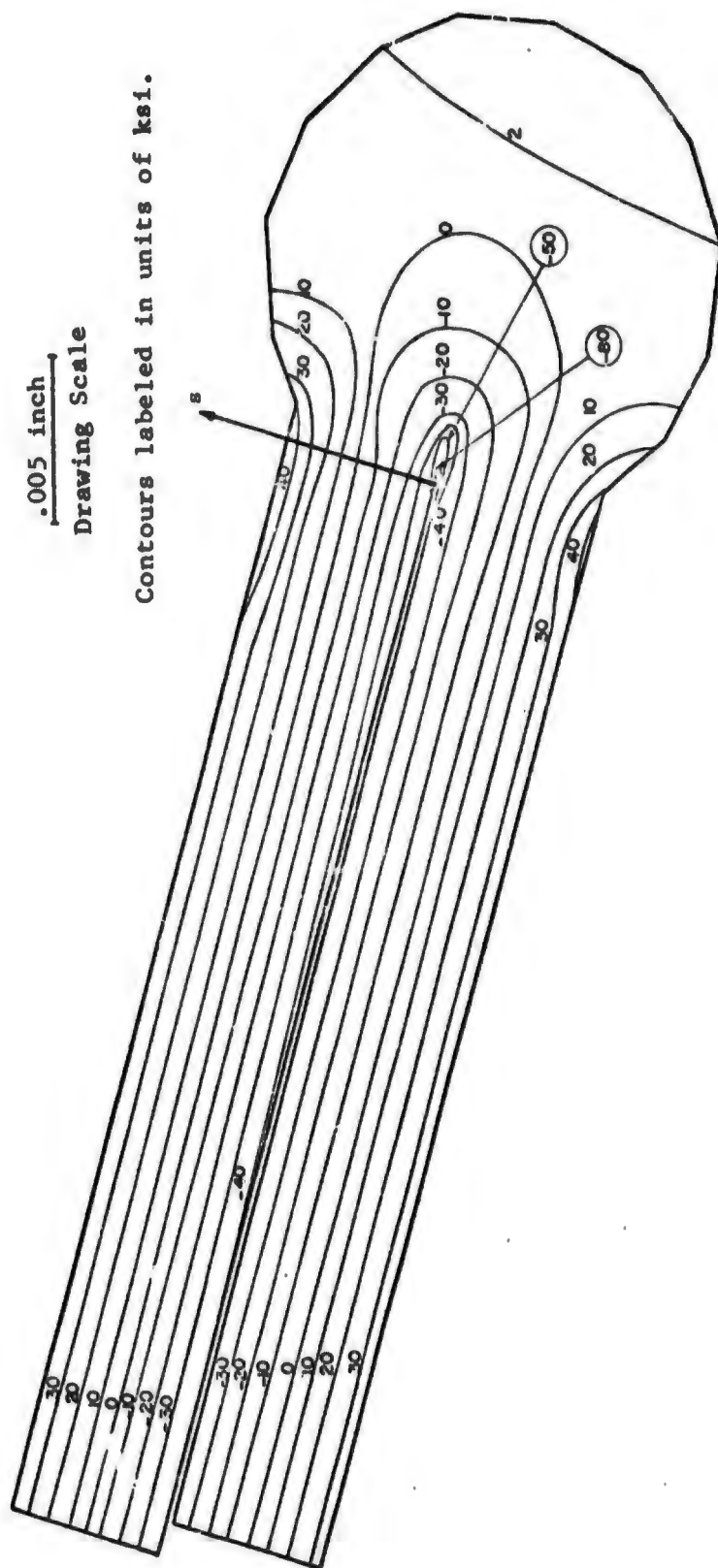


FIGURE A-3. CONTOURS OF PRINCIPAL STRESS IN MATHEMATICAL MODEL OF OD WELD OF 4-INCH WELDED BELLOWS WITH 15° EDGE TILT DUE TO AN AXIAL DEFLECTION OF $\delta = 0.09838$ INCH PER CONVOLUTION

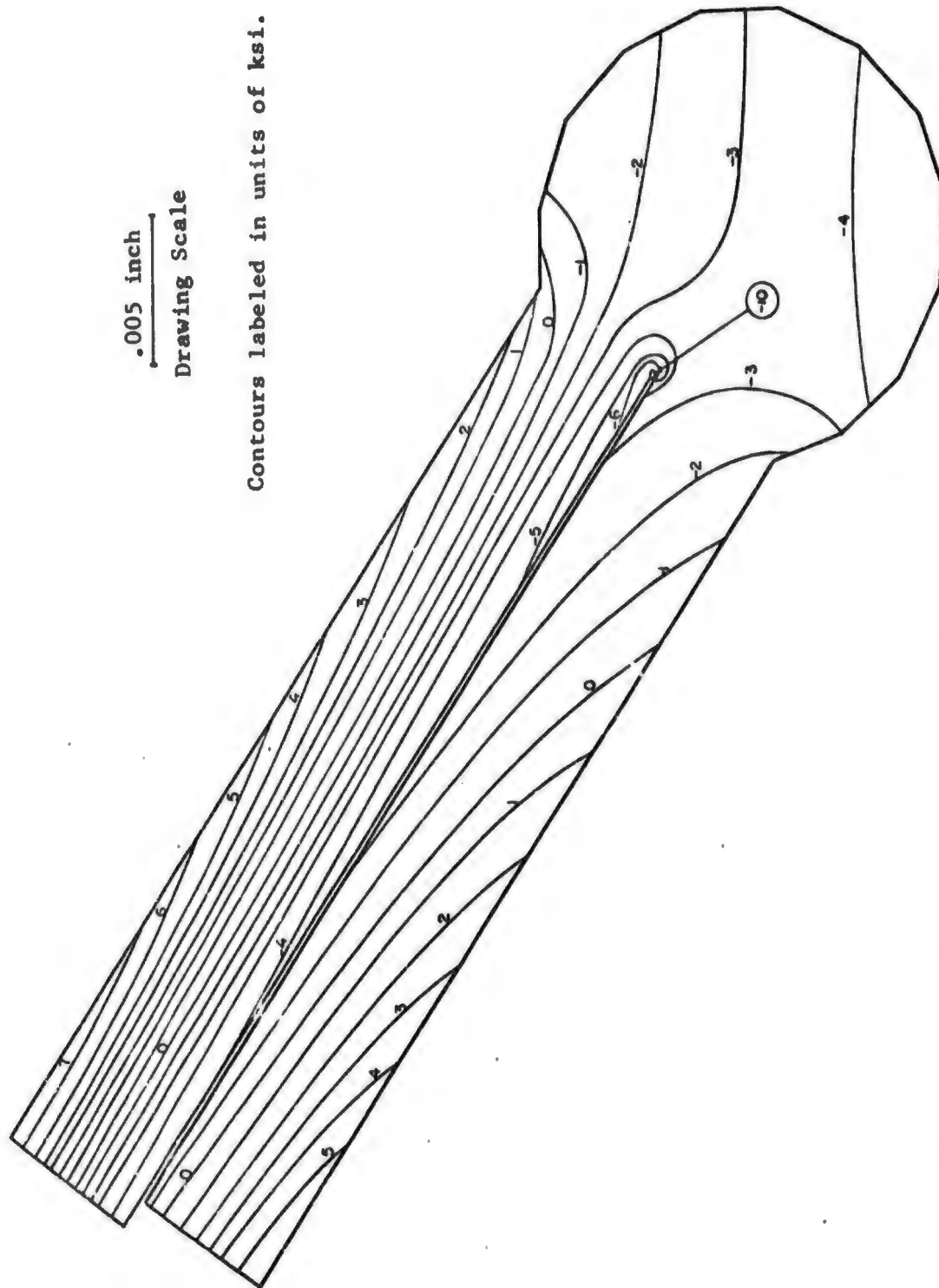


FIGURE A-4. CONTOURS OF HOOP STRESS IN MATHEMATICAL MODEL OF OD WELD OF 4-INCH WELDED BELLOWS WITH 35° EDGE TILT DUE TO AN AXIAL DEFLECTION OF $\delta = 0.09838$ INCH PER CONVOLUTION

.005 inch

Drawing Scale

Contours labeled in units of ksi.

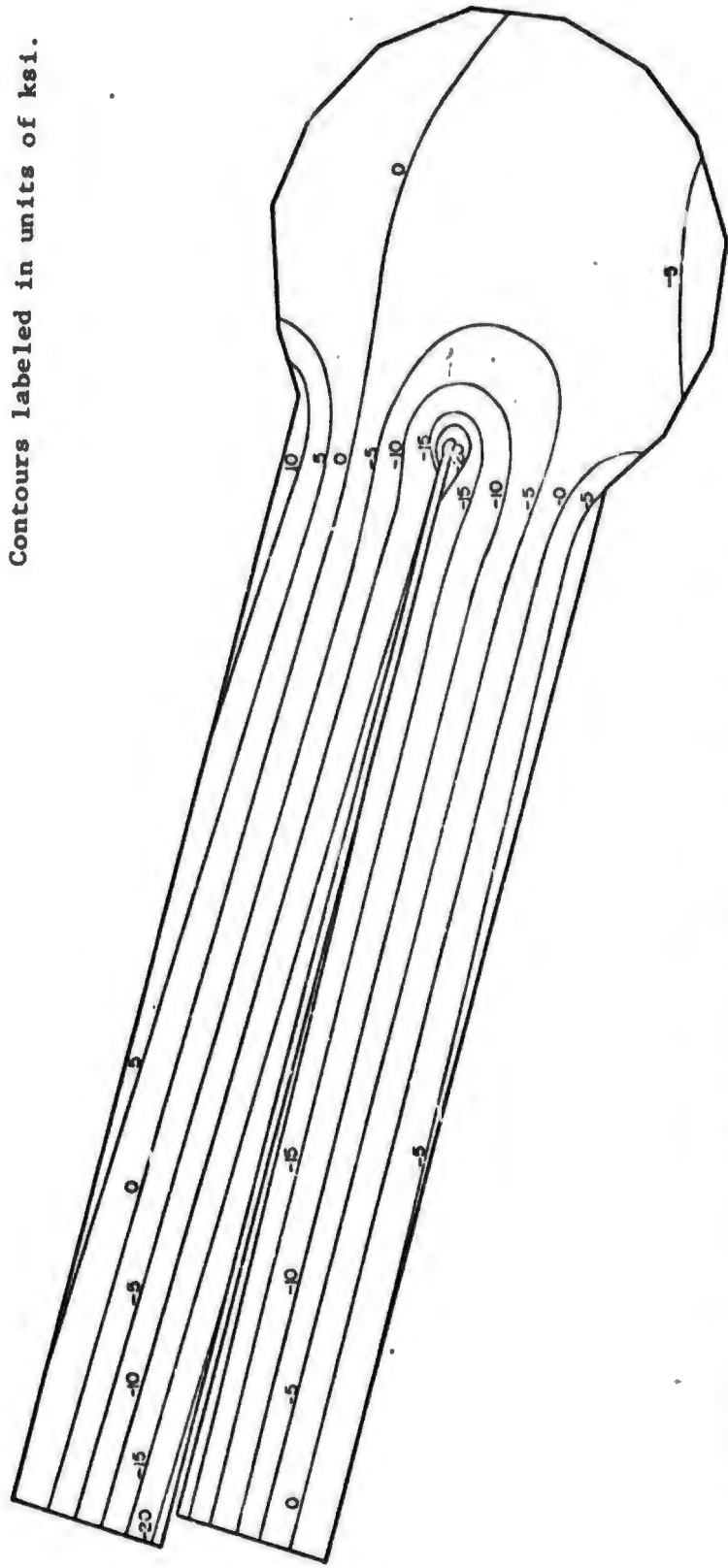


FIGURE A-5. CONTOURS OF HOOP STRESS IN MATHEMATICAL MODEL OF OD WELD OF 4-INCH WELDED BELLOWS WITH 15° EDGE TILT DUE TO AN AXIAL DEFLECTION OF $\delta = 0.09838$ INCH PER CONVOLUTION

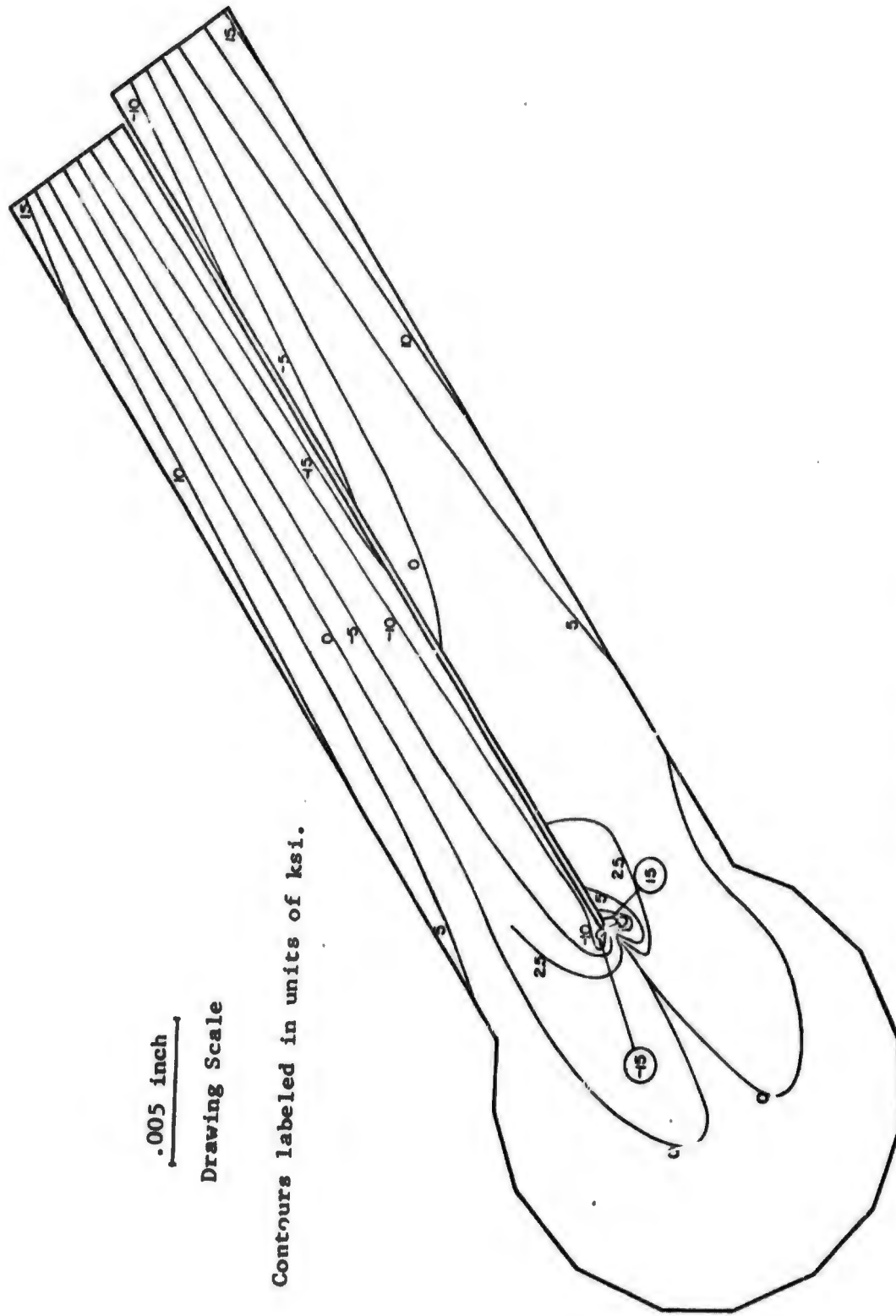


FIGURE A-6. CONTOURS OF PRINCIPAL STRESS IN MATHEMATICAL MODEL OF ID WELD OF 4-INCH WELDED BELLOWS WITH 35° EDGE TILT DUE TO AN AXIAL DEFLECTION OF $\delta = 0.09838$ INCH PER CONVOLUTION

.005 inch
Drawing Scale

Contours labeled in units of ksi.

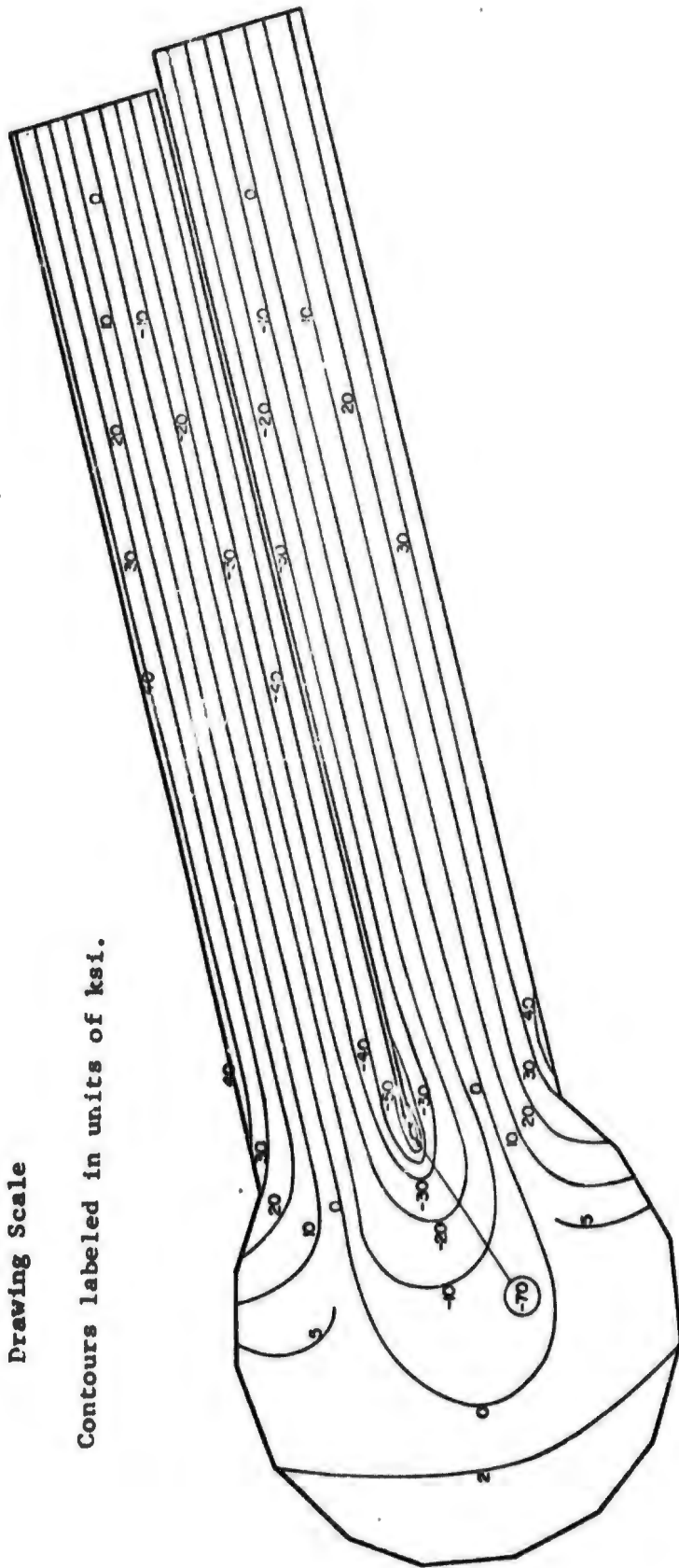


FIGURE A-7. CONTOURS OF PRINCIPAL STRESS IN MATHEMATICAL MODEL OF ID WELD OF 4-INCH WELDED BELLOWS WITH 15° EDGE TILT DUE TO AN AXIAL DEFLECTION OF $\delta = 0.09838$ INCH PER CONVOLUTION

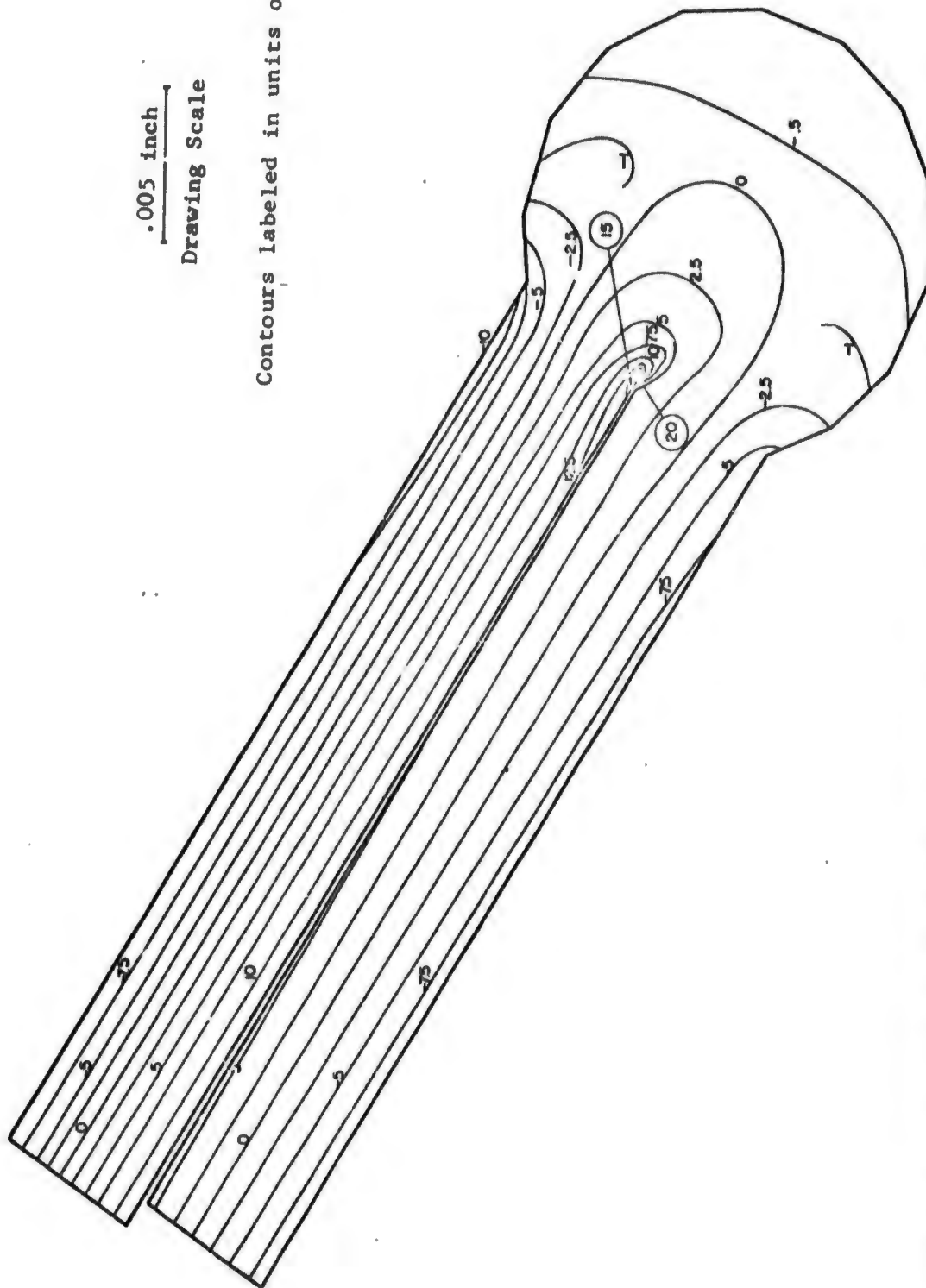


FIGURE A-8. CONTOURS OF PRINCIPAL STRESS IN MATHEMATICAL MODEL OF OD WELD OF 4-INCH WELDED BELLOWS WITH 35° EDGE TILT DUE TO AN INTERNAL PRESSURE OF 10.0 PSI

.005 inch

Drawing Scale

Contours labeled in units of ksi.

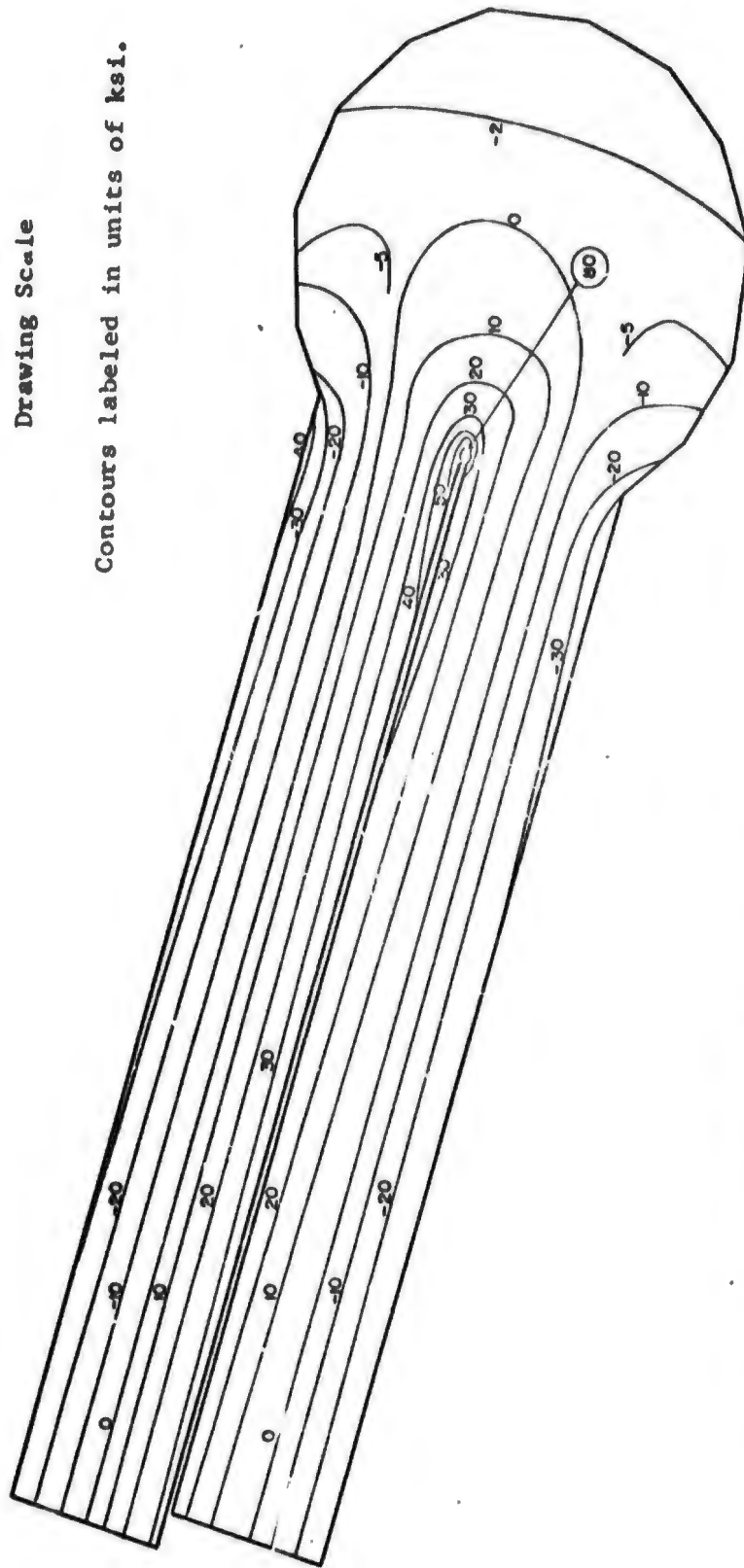
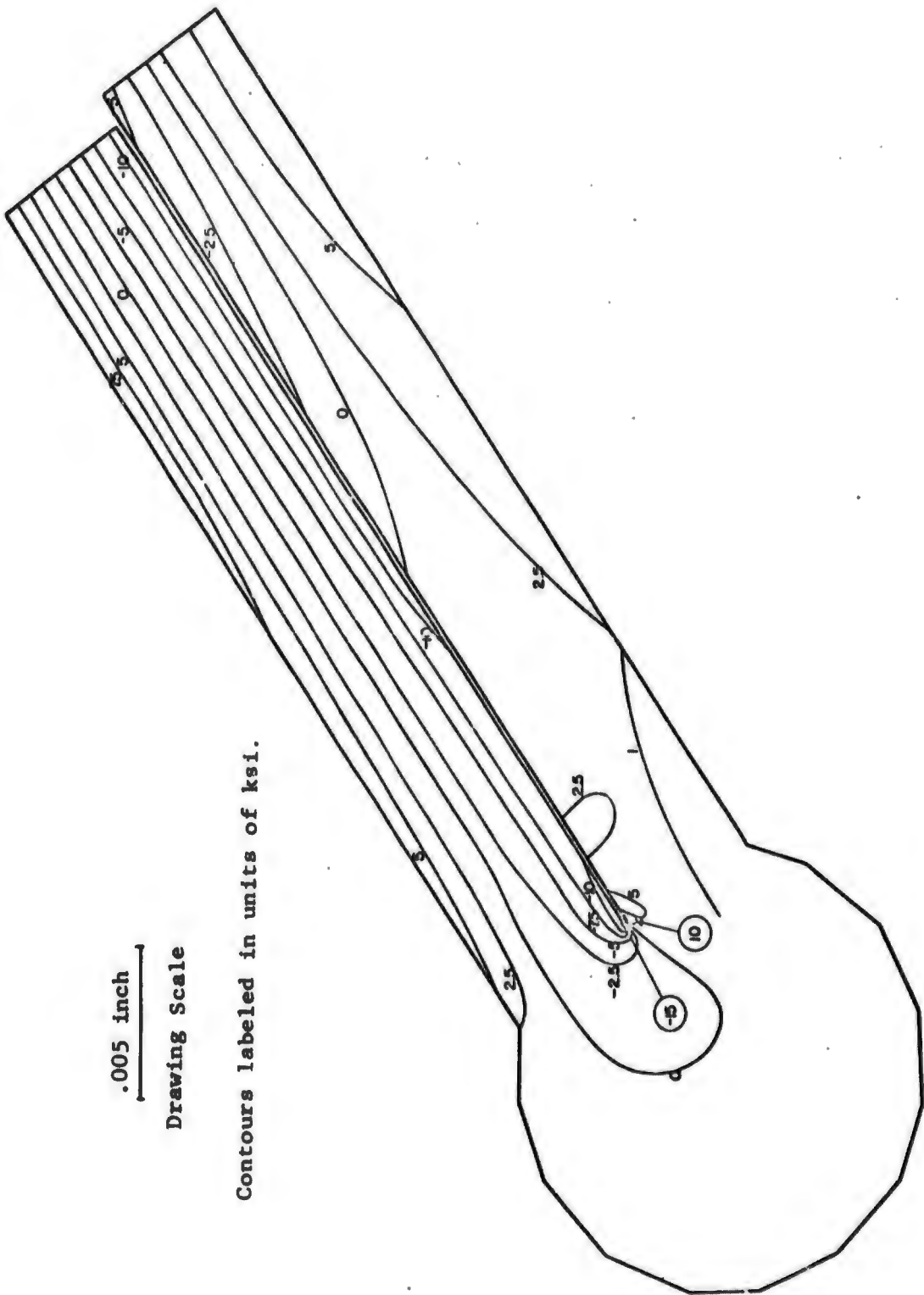


FIGURE A-9. CONTOURS OF PRINCIPAL STRESS IN MATHEMATICAL MODEL OF OD WELD OF 4-INCH WELDED BELLOWS WITH 15° EDGE TILT DUE TO AN INTERNAL PRESSURE OF 10.0 PSI



.005 inch
 Drawing Scale

Contours labeled in units of ksi.

FIGURE A-10. CONTOURS OF PRINCIPAL STRESS IN MATHEMATICAL MODEL OF ID WELD OF 4-INCH WELDED BELLOWS WITH 35° EDGE TILT DUE TO AN INTERNAL PRESSURE OF 10.0 PSI

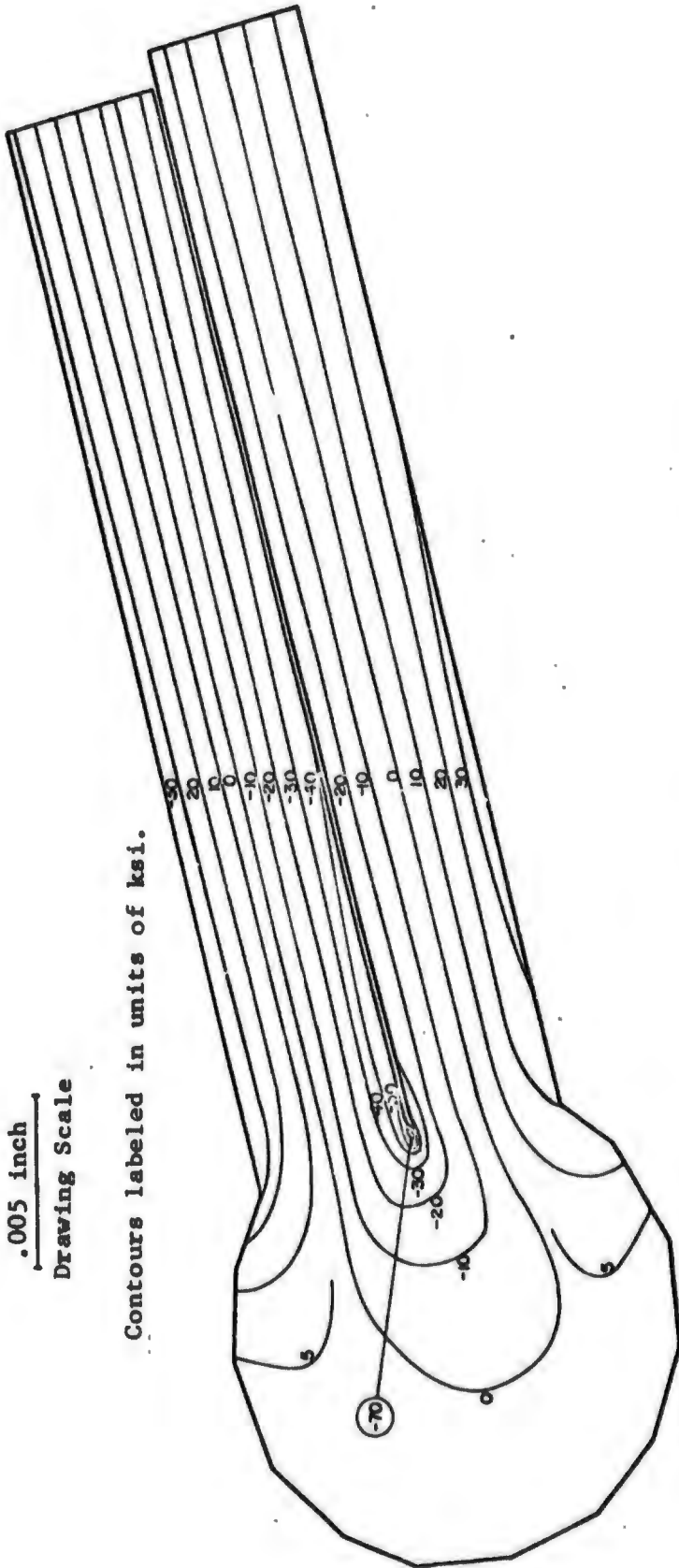


FIGURE A-11. CONTOURS OF PRINCIPAL STRESS IN MATHEMATICAL MODEL OF ID WELD OF 4-INCH WELDED BELLOWS WITH 15° EDGE TILT DUE TO AN INTERNAL PRESSURE OF 10.0 PSI

were only slightly stressed. The peak stress values that were calculated near the notch tip require special interpretation. The finite element results represented an approximation of the stress peak (infinite stress for a perfectly sharp notch) that an exact, analytical solution for the elastic stress field would show. If the mesh of finite elements were made much finer near the notch, the calculated stresses would more closely approximate such a closed-form solution. However, continued refinement of the element representation would be of little practical value, since in an actual bellows a small zone of plastic deformation will relieve these high stresses at the notch tip. For this reason, no effort was made in this study to increase the number of elements over that shown in Figure A-1. Thus, in viewing the plotted stress contours in the notch area, one should not attach much importance to the exact numerical values shown at the tip. For plotting purposes the numerical value of the innermost contour was based on the value for the element at the tip with the highest calculated stress.

Figures A-12 and A-13 show more clearly the rise in stress near the notch. The curves show the variations in principal stress for Cases 1 and 2 along the direction of the line labeled "s" in Figures A-2 and A-3. This line is approximately in the direction of the maximum stress gradient for both cases. This line cuts normal to the surface of the upper leaf at the notch tip. The linear variation of the stress, as predicted by the shell calculation, is shown for comparison purposes. As indicated, the stresses calculated by the finite element method were in reasonable agreement with the shell results, at distances greater than .0005 inch from the notch tip. For distances less than .0005 inch, the results diverged rapidly. The curve passed through the finite element data points appears to rise asymptotically. In this zone, the elastic stresses would be very high and plastic deformation is indicated. The results suggest that the plastic zone was relatively small, on the order of one-tenth the shell thickness.

The rising nature of the curves in Figures A-12 and A-13 also suggested that larger stress could be calculated if one had added additional elements nearer the notch tip. However, the element representation used in this analysis appeared to have been sufficient to detect the stress peak. Thus, the stresses calculated for the elements adjacent to the notch tip should give some indication of the elastic stress level at the distance from the notch tip corresponding to the centers of these elements. Also, since identical element patterns were used for all eight cases, element-by-element comparison between the cases should provide a basis for determination of the effect of the notch on the relative stress levels corresponding to different tilt angles and loadings. Table A-3 gives the values of the stresses at the notch from both the shell and finite element calculations. Results for both the upper and lower leaves are shown for each of the eight cases. A stress intensification due to the notch was calculated for each case. This was defined as the ratio of the maximum stress as calculated by the shell analysis to the maximum stress as calculated by the finite element analysis. Values ranging from 1.3 to 1.9 were obtained. These values are of qualitative value since much larger values could have been obtained had more elements been taken near the notch tip. Referring to Figure A-1, the tabulated stresses correspond to the two elements closest to the notch, whose centers are about .00015 inch from the tip.

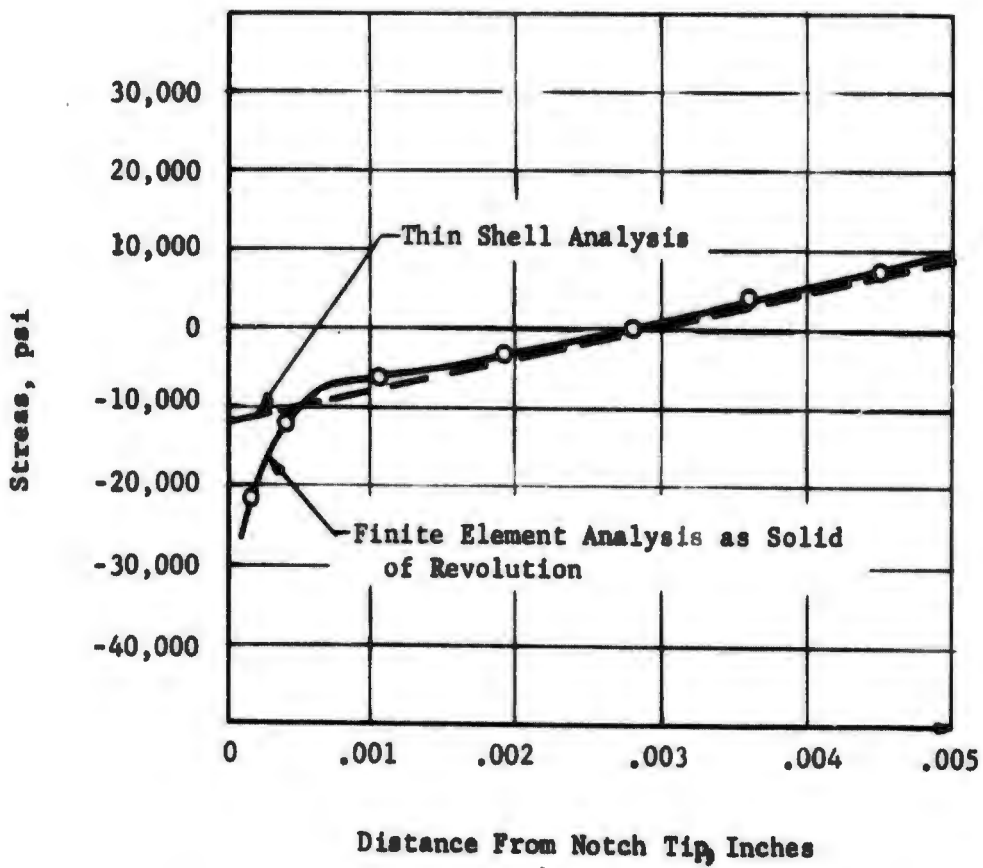


FIGURE A-12. VARIATION OF MAXIMUM STRESS WITH DISTANCE (s) MEASURED ALONG THE OUTER NORMAL FROM THE NOTCH TIP (Fig. 3); CASE 1; 35° TILT ANGLE, OUTER WELD, AXIAL LOADING

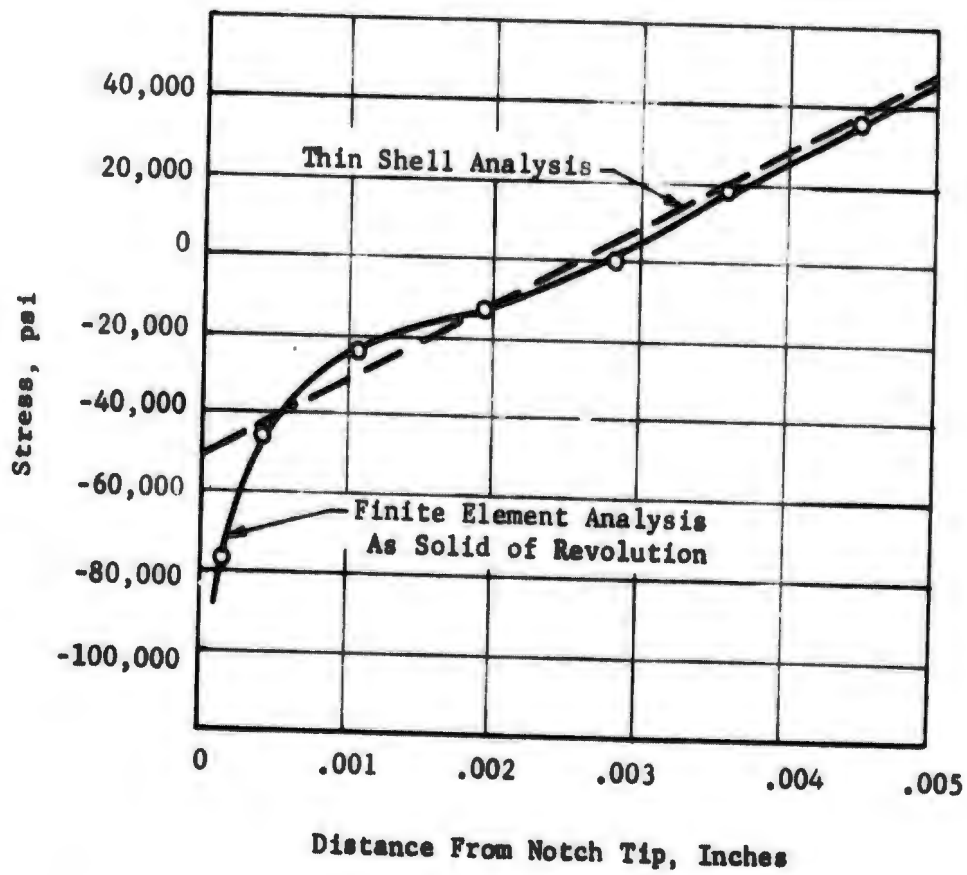


FIGURE A-13. VARIATION OF MAXIMUM STRESS WITH DISTANCE (s) MEASURED ALONG THE OUTER NORMAL FROM THE NOTCH TIP (Fig. 3); CASE 1; 15° TILT ANGLE, OUTER WELD, AXIAL LOADING

TABLE A-3. CALCULATED STRESSES AT NOTCH

Case	Inner or Outer Weld	Tilt Angle	Type of Loading	Maximum Stress Shell Analysis psi	Maximum Stress Finite Element Analysis psi	Stress Intensification*
1	Outer	35°	Axial	Upper Leaf	-11,415	1.9
				Lower Leaf	-889	
2	Outer	15°	Axial	Upper Leaf	-50,610	1.6
				Lower Leaf	-49,958	
3	Inner	35°	Axial	Upper Leaf	-6,229	1.5
				Lower Leaf	9,361	
4	Inner	15°	Axial	Upper Leaf	-55,210	1.4
				Lower Leaf	-40,696	
5	Outer	35°	Pressure	Upper Leaf	13,362	1.8
				Lower Leaf	4,681	
6	Outer	15°	Pressure	Upper Leaf	49,578	1.6
				Lower Leaf	40,136	
7	Inner	35°	Pressure	Upper Leaf	-10,394	1.4
				Lower Leaf	2,461	
8	Inner	15°	Pressure	Upper Leaf	-54,701	1.3
				Lower Leaf	-38,609	

* Stress Intensification = $\left(\frac{\text{maximum stress from finite element analysis}}{\text{maximum stress from shell analysis}} \right)$

The thin shell analysis of the welded bellows indicated that large reductions in stress at the welds could be achieved by tilting the edges of the bellows. However, the shell calculations did not include any stress-intensification effects of the notch. It was not known how such effects might interact with the effect of tilting the bellows edge. The more detailed, finite element analyses of the weld area provide valuable support to previous conclusions that were based on the shell calculations. Table A-4 shows the effect of changing the edge tilt from 15 to 35 degrees. Ratios of the maximum stress at the weld for 35 degrees tilt to the maximum stress for 15 degrees tilt are given. The ratios were calculated from the stress values given in Table A-3. Remarkable agreement was found between the ratios calculated based in one case on the results of shell analysis and in the other case on the results of the finite element analysis. Considering the conventions used to calculate these ratios, no significance should be attached to the fact that slightly smaller reductions in stress due to increasing the edge tilt were predicted in each case by the finite element calculation.

Conclusions

The results of the weld area analysis can be summarized with the following conclusions:

- (1) Except for an intense stress peak at the tip of the notch, the stresses in the weld bead material were low compared to the stresses in the adjacent leaves.
- (2) The peak stresses at the notch were much greater than the nominal stresses predicted by thin shell calculations. However these peak stresses were very localized and decayed to the shell stress distribution within a distance of about one tenth of a leaf thickness from the notch tip.
- (3) Optimization of the edge tilt angle on the basis of the nominal stresses calculated with thin shell theory was valid, since variation of the edge tilt angle had a comparable effect on both nominal and peak stress in the weld area.
- (4) In the analysis of welded bellows with thin shell theory, separation of the midsurfaces of the joined bellows leaves should be included in the shell model. The representation of the weld bead as a short, cylindrical, shell part had a significant local effect on the calculated shell stresses. It yielded nominal stress values that are consistent with the more exact analysis of the weld area as a solid of revolution.

TABLE A-4. DECREASE IN STRESS AT WELD DUE TO CHANGE IN EDGE TILT ANGLE
FROM 15° TO 35°

Cases	Stress Reduction	
	Shell Analysis	Finite Element Analysis
Outer Weld, Axial Load Case No. 1 vs. Case No. 2	.23	.27
Inner Weld, Axial Load Case No. 3 vs. Case No. 4	.17	.18
Outer Weld, Pressure Case No. 5 vs. Case No. 6	.27	.30
Inner Weld, Pressure Case No. 7 vs. Case No. 8	.19	.20

$$\text{Stress Reduction} = \left(\frac{\text{maximum stress } 35^\circ \text{ tilt}}{\text{maximum stress } 15^\circ \text{ tilt}} \right)$$

APPENDIX B

ADDITIONAL SUBROUTINES TO AID IN
THE INVESTIGATION OF WELDED BELLOWS

APPENDIX B

ADDITIONAL SUBROUTINES TO AID IN THE INVESTIGATION OF WELDED BELLOWS

During the course of the investigation of improved welded bellows configurations, two major subroutines to aid in the analyses have been developed, namely subroutines FIT and PLT. The subroutine FIT uses the x-y coordinates of the bellows to be analyzed and automatically prepares the shell-parameter input data as required by program NONLIN. PLT was developed so that plots of preselected variables (deflections, stresses, etc.) could be made and superimposed on the shape of the bellows model being analyzed.

These additional subroutines required that certain changes be made in the original versions of NONLIN, INPUT, and PRINT. They were described in Appendix B of the "Final Report on the development of Analytical Techniques for Bellows and Diaphragm Design", Technical Report No. AFRPL-TR-68-22⁽¹⁾. Also, several, smaller subroutines were developed for use with the program FIT. This appendix describes the changes required in the original program versions reported previously and the new subroutines developed for use with FIT. It presents the FORTRAN listings of all the new programs developed, along with detailed instructions on their proper usage.

Description of Subroutine PLT

This portion of the appendix describes the new subroutine called "PLT" which has been incorporated into the computer program NONLIN. NONLIN has been presented in Appendix B of the "Final Report on the Development of Analytical Techniques for Bellows and Diaphragm Design", Technical Report No. AFRPL-TR-68-22.

PLT is written in FORTRAN IV and is operational on the CDC 6400 at Battelle-Columbus. It makes use of CALCOMP 565 plotter and various plotting subroutines developed at Battelle. These routines are QIKPLT, QLINE, PLOT, SYMBOL, and ENCODE. These routines are on the System Library tape at Battelle-Columbus. The purpose of PLT is:

(1) To define the Input Mathematical Model in an x-y coordinate system, to select a proper scale such that the model fits in an 8-1/2 by 11-inch plotting area, and then to draw the shape of the model. It also identifies the first and last points on each shell part by point (+) plots on the model already drawn.

(2) To superimpose on the shape of the model the value of a preselected variable (deflection, stress, etc.) so that the model cross section corresponds to zero "variable" level. The variable is plotted along the normal to the shell and on a suitable scale automatically determined by PLT.

The incorporation of PLT in NONLIN involved an extension of "Input Data Preparation" (Appendix B, Paragraph B-II-d of Technical Report No. AFRPL-TR-68-22). The program now includes 15 data sets. A previously coded variable in Data Set 5 was activated; this variable initiates the call to PLT and also specifies the number of variables to be plotted. Revised Data Set 5 and Data Sets 13, 14, and 15 are described below.

In order to make PLT operational, a minimum number of changes were made in NONLIN, PRINT, and INPUT. These changes consist of only activating those portions on NONLIN, PRINT, and INPUT which had previously been coded for use in a plot subroutine. The particular changes in portions of the program NONLIN and the subroutines INPUT and PRINT required for the incorporation of PLT are presented at the end of this section together with a complete FORTRAN listing of the new subroutine PLT.

It should be mentioned that since it has been found that toroidal, conical, and cylindrical parts are sufficient to represent even the most irregular bellows, the present plot routine PLT does not accept a model with either ellipsoidal, paraboloidal, or spheroidal shell parts. Also, for welded bellows analysis, PLT has the capability of plotting up to two convolutions or four leaves of the mathematical model. Each leaf cross section, together with the desired superimposed curve of stress or deformation variable, is plotted automatically on a separate sheet.

New Data Sets Required for Use with PLT

Data Set 5

```
READ (5,561)  IBRM, ITER, NDUMMY, PLOT, INTPRN, INTVAL, LEVEL 1, LEVEL 2,  
              ERP, CONVER, NUMHAR, (NF0URA (1), I = 1, 8)
```

```
561 FORMAT (8I5, 2E10.3, 10I2)
```

IBRM = number of parts in composite shell

ITER = number of iterations at a load level for nonlinear calculations
ITER = 0 for linear analysis

NDUMMY = not presently used

PLOT = number of variables to be plotted; maximum number that can be specified is 10. If PLOT is other than 0, then Data Sets 13, 14, and 15 are to be read in.

Use PLOT = 0 for no plot.

INTPRN = 0 indicates that intermediate results from the nonlinear analysis, i.e., values of parameters and slopes will not be printed out.
Use 1 to obtain values.

INTVAL = 0 indicates that the intermediate results from the initial value integrations will not be printed out. Use 1 to obtain values.

- LEVEL 1 = number of increments into which the loading is divided for nonlinear analysis.
- LEVEL 2 = not presently used.
- ERP = accuracy for integration subroutine. If left blank, it is internally set to $1.0 \text{ E} - 05$.
- CØNVER = convergence criteria for use in nonlinear analysis.
- NUMHAR = number of FØURIER harmonics in the analysis. For a nonlinear analysis, NUMHAR = 1. For a linear analysis, NUMHAR must not be greater than 8. If the shell is axisymmetrically loaded, NUMHAR = 1. For a nonsymmetrically loaded shell which has the same boundary conditions for all harmonics, NUMHAR can have any value up to 8.
- NFØURA (I) = FOURIER harmonic value.
For an axisymmetric deformation NFØURA (1) = 0.

Data Set 13

READ (5,525) (IPL~~OT~~ (I), I = 1, PL~~OT~~)
READ (5,526) (J~~OB~~PLT (I), I = 1, PL~~OT~~)

525 F~~OR~~MAT (10I5)

526 F~~OR~~MAT (10A8)

IPL~~OT~~ (I) is the code number for the variable to be plotted against the geometry of the shell parts. See left-hand side of the table given after J~~OB~~PL~~OT~~ (I)

J~~OB~~PL~~OT~~ (I) is the variable name. See right-hand side of the table below.

<u>Code Number</u>	<u>Variable Name</u>
1	W
2	Q PHI
3	U PHI
4	N PHI
5	BETA PHI
6	M PHI
7	N THETA
8	M THETA
9	EPS THET
10	EPS PHI
11	SIG NPHI
12	SIG MPHI
13	SIG PHII
14	SIG PHI 0
15	SIG NTHI
16	SIG MTHI
17	SIG THTI
18	SIG THT 0
19	TAU PHI

Data Set 14

READ (5,2001) (YTITL~~E~~ (I,J), I=1, 8), J = 1, PL~~OT~~1)

2001 F~~OR~~MAT (8A10)

YTITL~~E~~ is full title of the variable. For each plot a separate card is needed. Each title takes 42 columns. An * is required in column's 1 and 42. (PL~~OT~~1) is the name for PL~~OT~~ local to the subroutine PLT.)

Data Set 15

READ (5, 2002) NLS

2002 FORMAT (I5)

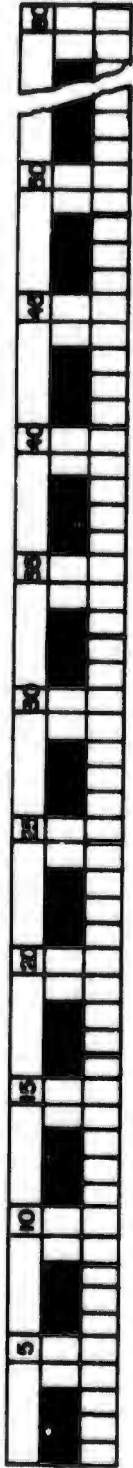
READ (5,2003) (INLS (I), I = 1, NLS)

2003 FORMAT (4I5)

NLS is the number of leaves in the mathematical model. NLS can be either 1, 2, 3, or 4.

INLS (I) is the last part number (IBRM) of each leaf.

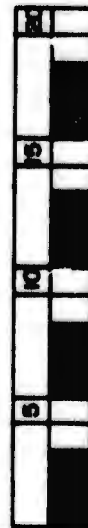
Data sheets showing the proper format for Data Sets 13, 14, and 15, described above are shown in Figure B-1.



DATA SET 13 (PLOT CODE AND VARIABLE NAME)



DATA SET 14 (TITLE OF PLOT)



DATA SET 15 (NO. OF LEAVES AND LAST PART NO.)

FIGURE B-1. INPUT SHEET FOR DATA SETS 13, 14, and 15

Required Changes in NONLIN, INPUT, and PRINT

The following FORTRAN IV listings indicate the changes made in NONLIN, INPUT, and PRINT which were required for the incorporation of the new subroutine PLT. Only those parts of the listings which differ from the original versions given in Battelle's earlier report on analytical techniques for bellows and diaphragm design are presented. The particular changes are clearly marked.

CHANGES IN NONLIN

```

PROGRAM NONL,IM,INPUT,OUTPUT,PLOT,TAPE3=INPUT,TAPE6=OUTPUT,PUNCH,TA
1
DIMENSION
    IA(8)      * SI(60)      * IPAR(60)
    IB(8)      * S1(60)      * INT(60)
    GA(8)      * PRNT(8)     * ISS(60)
    GB(8)      * ERR(8)      * PSR(60)
    Y(8)       * DM(8,61)    * EYM(60)
    DY(8)      * TL(8,8)     * A(8,9)
    TR(8,8)    * TL(8,R)     * JOEPLT(10)
    TR1(8,8)   * TRY(8,61)   * TR2(8,8)
    SOUT(275)  * D(9,9,60)  * P(5,275)
    SLOPE(8,275) * TRI(8,8) * E(9,60)
    V3(R)      * VM17(68)   * YAM172)
    DYAM(72)   * AM(21)     * YAM18)
    WACK(60)   * YSAVE(R)   * DTERM(10)
    IPLOT(10)  * XPLT(350)  * YPLOT(350,10)
    STROUT(350) * SIGMPH(350) * SIGMTH(350)
    SIGMT(350) * SIGTMT(350) * SIGTMR(350)
    TAUPH(350) * VARTK(60) * POINT(60)
    OMSAVE(6,61)
DIMENSION
XPLI(350),YPLI(350,10)
COMMON / BLOCKA / NU, PI, HLU, NYYPE, INDEX, IGR, PN, NPOINT,
1
COMMON / BLOCKB / M, R1, R2, R3, SIN, COS
COMMON / BLOCKC / DM, GA, GB, MF, MFP, MPL, MM, MN, TRY
COMMON / BLOCKD / TL, TR, TLI, TRI, ALFL, ALFR
COMMON / BLOCKE / MFF, SMX1, SZERO, GO, ERP, ISS, E,
COMMON / BLOCKF / MAX, IMPRM, INTVAL, MPP
COMMON / BLOCKG / MPARTS, PM11, V3, KIND, NT, MT, SPRINT, VN, EYM,
1
COMMON / BLOCKH / NDE
COMMON / BLOCKI / DELA, POEL, ABC, EAM
COMMON / BLOCKJ / PIN, PMIN, MO, IO, EMIN, EMAR
COMMON / BLOCKK / YAM, DYAM
COMMON / BLOCKL / YSAVE
COMMON / BLOCKM / BETERM
COMMON / BLOCKN / PLOT, PLTIME, SPLOT, PLOTPI, IPLOT, YMOD, KST,
COMMON / BLOCKO / TIME, VARTK, NVARTK
COMMON / BLOCKP / JOEPLT, ALAL, ALAR, JA, IB, NOPUNC, IMPUM,
COMMON / BLOCKQ / CONVER, SI, SA, INT, IPAR, PSR, ITER, MTRY,
COMMON / BLOCKR / MERROR, IRRM, TRYIM, IRRMAX
COMMON / BLOCKS / LEVEL1, LEVEL2
COMMON / BLOCKT / IEX(8), DUM(4)
COMMON / PLATRC / XPLI,YPLI,MC
COMMON
EQUIVALENCE (Y(1), PRNT(1)), (Y(11), YAM(2)), (DY(1), DYAM(2)),
1
EQUIVALENCE (S, YAM(1)), (VARTK(1)), POINT(1))
    (SLOPE(1), XPLT(1))
    (D(476), XPLT(1))
    (D(826), STROUT(1))
    (D(1176), SIGMTH(1))
    (D(1126), SIGMPH(1))
    (D(1876), SIGMT(1))
    (D(2226), SIGMTR(1))

```



```

415 WRITE (6,402)
ALFL = ALXLRMPD
ALFR = ALXLRMPD
CALL SCND
DO 258 I = 1, 8
DO 259 J = 1, 8
TL(I,J) = 0.0
TR(I,J) = 0.0
CONTINUE
DO 26 J=1,NDE
DO 26 I=1,NDE
K=IA(I)
L=IB(I)
DM(I,J)=TL(K,J)
20 A (I,J)=TR(L,J)
DO 23 I=1,NDE
DO 23 J=1,NDE
TL(I,J)=DM(I,J)
23 TR(I,J)=A (I,J)
DO 21 I=1,NDE
DO 21 J=1,NDE
TL(I,J)=TR(I,J)
21 TR(I,J)=TL(I,J)
CALL INVERT (TL,NDE,0,DET,ISCAL)
CALL INVERT (TR,NDE,0,DET,ISCAL)
IF (INTVAL,00, 0) GO TO 410
WRITE(6,22) (TL(I,J), J = 1, 0), (TR(I,J), J = 1, 0),
1
WRITE (6,24) (TL(I,J), J = 1, 0), (TR(I,J), J = 1, 0),
1
WRITE(6,22) (I = 1, NDE)
1
NFP = MPARTS * I
DO 859 I = 1, IORN
BACK(I) = 1.0
CONTINUE
DO 770 IOR = 1, IORN
ISM = ISS(IOR)
GO TO (770, 770, 770, 770, 770, 770, 770, 770), ISM
IF (SI(IOR) .GT. SI(IOR)) GO TO 7710
BACK(IOR) = -1.0
SI(IOR) = 100.0 - SI(IOR)
SI(IOR) = 100.0 - SI(IOR)
7710 SI(IOR) = SI(IOR)*RPO
SI(IOR) = SI(IOR)*RPO
CONTINUE
IF (ISS(IORN) .EQ. 1) GO TO 855
IORMAX = IORN
GO TO 856
855 IORMAX = IORN - 1
856 DO 1100 J = 1, NFP
DO 1100 I = 1, 8
TRY(I,J) = 0.0
CONTINUE
DO 1103 L = 1, IORNMAX
DO 1103 I = 1, 8
DM(I,L) = 0.0

```

```

1103 CONTINUE
NN = 1
MYPE = 1
CALL CALCUL
CALL PRINT
MSE=2
CALL PLI
WRITE(6,993) DETERM(1)
IF(ITER.EQ. 0) GO TO 999
WRITE(6,991) PH, GA(1), GA(2), GB(4), GB(5)
FACTOR = 1.0/FLOAT(LEVEL)
DO 420 I = 1, NPP
DO 420 J = 1, 6
TRY(I,L) = BM(I,L)*FACTOR
420 CONTINUE
NN = 0
MFAIL = 0
MTYPE = 2
NMMAX = LEVEL
PMMAX = VN(S,1)
DEMAX1 = GA(1)
DEMAX2 = GA(2)
DEMAX3 = GB(4)
DEMAX4 = GB(5)
GA(1) = 0.0
GA(2) = 0.0
GB(4) = 0.0
GB(5) = 0.0
PMSINCR = PMMAX/FLOAT(NMMAX)
DEINC1 = DEMAX1/FLOAT(NMMAX)
DEINC2 = DEMAX2/FLOAT(NMMAX)
DEINC3 = DEMAX3/FLOAT(NMMAX)
DEINC4 = DEMAX4/FLOAT(NMMAX)
TEMP = 0.0
DO 105 L = 1, NPP
DO 105 I = 1, 6
DMSAVE(I,L) = 0.0
105 CONTINUE
DO 400 NNN = 1, NMMAX
TEMP = TEMP + PMSINCR
DO 397 L = 1, 1000
VN(S,L) = TEMP
397 CONTINUE
GA(1) = GA(1) + DEINC1
GA(2) = GA(2) + DEINC2
GB(4) = GB(4) + DEINC3
GB(5) = GB(5) + DEINC4
ITERCT = 0
810 NN = NN + 1
CALL CALCUL
COMMENT CHECK CONVERGENCE
ITERCT = ITERCT + 1
MAXIX = MPARTS - 1
DO 811 L = 2, MAXIX

```

```

DO 011 I = 1, 6
IF (TRY(I,L) .EQ. 0.0) GO TO 011
IF (DM(I,L) .EQ. 0.0) GO TO 011
IF (ABS(DM(I,L) - TRY(I,L))/DM(I,L)) .GT. CONVER) GO TO 050
011 CONTINUE
DO 110 L = 1, NFP
DO 110 I = 1, 6
TRY(I,L) = 2.0*DM(I,L) - DMSAVE(I,L)
110 CONTINUE
DO 112 L = 1, NFP
DO 112 I = 1, 6
DMSAVE(I,L) = DM(I,L)
112 CONTINUE
GO TO 015
050 IF (ITERCT .EQ. ITER) GO TO 0115
DO 100 L = 1, NPARTS
DO 100 I = 1, 6
TRY(I,L) = DM(I,L)
100 CONTINUE
GO TO 010
0115 NFAIL = 1
015 CALL PRINT
MCC=2
CALL PLI
WRITE(6,901) FM, GA(1), GA(2), GB(4), GB(5)
IF (NFAIL .EQ. 0) GO TO 3951
WRITE(6,902) ITER
GO TO 394
3951 WRITE(6,689) ITERCT
ITERCT = 0
396 WRITE(6,690)
DO 425 I = 1, NN
WRITE(6,691) I, DETERM(I)
425 CONTINUE
IF (NFAIL .EQ. 1) GO TO 999
NN = 0
400 CONTINUE
GO TO 999
403 FORMAT (1M022X, 20MT MATRIX AT LEFT END,44X, 21MT MATRIX AT RIGHT)
22 ] END)
24 FORMAT(1M0)
693 FORMAT(1M0, 50NDETERMINANT OF FLEXIBILITY MATRIX FOR LINEAR ANALYS
115 WAS E15.0)
601 FORMAT(1M0, 32NLOADINGS FOR THIS ANALYSIS WERE /
5 6M FM = E14.7 /
5 9M GA(1) = E14.7 /
5 9M GA(2) = E14.7 /
5 9M GB(4) = E14.7 /
5 9M GB(5) = E14.7 /
692 FORMAT(1M0, 20MCONVERGENCE NOT OBTAINED IN I1, 11M ITERATIONS)
689 FORMAT(1M0, 34MCONVERGENCE OBTAINED ON ITERATION I1)
690 5 WERE )
691 FORMAT(1M, 10MITERATION I1, 3X, E15.0)
END

```

CHANGES IN INPUT:

```

SUBROUTINE INPUT
DIMENSION
  TITLE(20)
  TITLE2(20)
  NAME1(6)
  NAME2(6)
  TDIST(60)
  NAMES1(6)
  NAMES2(6)
  ISS(60)
  SL(9,60)
  BACK(60)
  UNITS(2)
  E(9,60)
  APLI(30),YPLI(30,18)
COMMON / BLOCKA / NU, PI, ALD, NTYPE, INDEX, IDR, PM, MPOINT,
  ISH, IT, T1, T2, MT, INTC
COMMON / BLOCKB / DM, GA, GB, NF, NFP, MPL, MM, NM, NY
COMMON / BLOCKC / NFF, SHKA, SZERO, GO, EMP, ISS, E,
  MAX, INTPHN, INTVAL, NPP
COMMON / BLOCKD / NPANTS, PHIL, V3, NIND, NT, MT, SPRINT, VN, EYM,
  BACK, NBACK
COMMON / BLOCKE / NDE
COMMON / BLOCKF / DETERM
COMMON / BLOCKG / PLOT, PLTIME, SPLOT, PLOTP, IPLOT, YMOD, KST,
  NSAMMA, DEAD, NFN
COMMON / BLOCKH / TIME, VARTK, NVARTK
COMMON / BLOCKI / JOPLT, ALXL, ALXR, IA, IB, NOPUNC, IMPUN,
  CONVER, SI, SK, INT, IPAR, PSR, ITER, NTRY,
  MERROR, IRRM, TRYIN, INRMAX
COMMON / BLOCKJ / LEVEL1, LEVEL2
COMMON / PLYZC / XPLI, YPLI, MZC
EQUIVALENCE (VARTK(1), POINT(1))
DATA (MPO = 0.1745329252E-01)
DATA (NAME1(1) = GNDISPLA), (NAME1(5) = GNCEMENT),
  (NAME1(2) = GNFORCE),
  (NAME1(3) = GNSLOPE), (NAME1(6) = GN),
  (NAME1(4) = GNMOMENT)
DATA (MARKC = ZMYE), (MARKD = ZHNO), (MARKE = IMS),
  (MARKN = ZHNO), (MARKY = ZMYE),
  (NAME2(1) = GNCROWN), (NAME2(2) = GNCYLIND), (NAME2(3) = GNSPHERO),
  (NAME2(4) = GNSPARAB), (NAME2(5) = GNSHELLIPS), (NAME2(6) = GNSCONICA),
  (NAME2(7) = GNTORRID), (NAME2(8) = GNSVARSYL),
  (NAME2(9) = GNSWAL), (NAME2(10) = GNSWAL),
  (NAME2(11) = GNSWAL), (NAME2(12) = GNSWAL),
  (NAME2(13) = GNSWAL), (NAME2(14) = GNSWAL),
  (NAME2(15) = GNSWAL), (NAME2(16) = GNSWAL),
  (NAME2(17) = GNSWAL), (NAME2(18) = GNSWAL),
  (NAME2(19) = GNSWAL), (NAME2(20) = GNSWAL),
  (NAME2(21) = GNSWAL), (NAME2(22) = GNSWAL),
  (NAME2(23) = GNSWAL), (NAME2(24) = GNSWAL),
  (NAME2(25) = GNSWAL), (NAME2(26) = GNSWAL),
  (NAME2(27) = GNSWAL), (NAME2(28) = GNSWAL),
  (NAME2(29) = GNSWAL), (NAME2(30) = GNSWAL),
  (NAME2(31) = GNSWAL), (NAME2(32) = GNSWAL),
  (NAME2(33) = GNSWAL), (NAME2(34) = GNSWAL),
  (NAME2(35) = GNSWAL), (NAME2(36) = GNSWAL),
  (NAME2(37) = GNSWAL), (NAME2(38) = GNSWAL),
  (NAME2(39) = GNSWAL), (NAME2(40) = GNSWAL),
  (NAME2(41) = GNSWAL), (NAME2(42) = GNSWAL),
  (NAME2(43) = GNSWAL), (NAME2(44) = GNSWAL),
  (NAME2(45) = GNSWAL), (NAME2(46) = GNSWAL),
  (NAME2(47) = GNSWAL), (NAME2(48) = GNSWAL),
  (NAME2(49) = GNSWAL), (NAME2(50) = GNSWAL),
  (NAME2(51) = GNSWAL), (NAME2(52) = GNSWAL),
  (NAME2(53) = GNSWAL), (NAME2(54) = GNSWAL),
  (NAME2(55) = GNSWAL), (NAME2(56) = GNSWAL),
  (NAME2(57) = GNSWAL), (NAME2(58) = GNSWAL),
  (NAME2(59) = GNSWAL), (NAME2(60) = GNSWAL)
INTEGER VARTK, POINT, GO, TRYIN, PLOT, PLTIME, TIME, BOUNDI,
  BOUNDF, TDIST
REAL
  NU, MT, NT, NSACK, NFN

```

FOR PLOTTING USE THE FOLLOWING CODE NUMBERS TO INDICATE THE VARIABLE DESIRED.

CODE NUMBER	VARIABLE
1	W
2	O PHI
3	U PHI
4	N PHI
5	BETA PHI
6	M PHI
7	H THETA
8	M THETA
9	EPSILON THETA
10	EPSILON PHI
11	SIGMA N PHI
12	SIGMA H PHI
13	SIGMA PHI INNER INNER
14	SIGMA PHI OUTER OUTER
15	SIGMA N THETA
16	SIGMA H THETA
17	SIGMA THETA INNER INNER
18	SIGMA THETA OUTER OUTER
19	TAU PHI

C TRYIN = 0 INDICATES THAT LINEAR PROBLEM WILL BE SOLVED.
 C TRYIN = 1 INDICATES THAT LINEAR PROBLEM AND POSSIBLY ONE OR MORE
 C ITERATIONS HAVE BEEN DONE AND THE LAST RESULT IS TO BE READ IN.

C INTPRN = 0 INDICATES THAT INTERMEDIATE RESULTS FROM THE NONLINEAR
 C ANALYSIS, I.E., VALUES OF PARAMETERS AND SLOPES, WILL NOT BE
 C PRINTED OUT.

C INTVAL = 0 INDICATES THAT INTERMEDIATE RESULTS FROM INITIAL VALUE
 C INTEGRATIONS WILL NOT BE PRINTED OUT.

C NOPUNC = 0 INDICATES THAT SOLUTIONS, DM(I,NF) AND E(I,JJ) WILL
 C NOT BE PUNCHED.
 C NOPUNCH = 1 INDICATES THAT THEY WILL BE PUNCHED.

C PLOT = NUMBER OF COLUMNS OF VARIABLES TO BE PUT ON PLOT TAPE TO
 C BE MACHINE PLOTTED AT LATER TIME.

COMMENT SET NUMBER 1 (CARDS = 3)

READ(5,500) TITLE1
 IF(EOP,5) 998, 997
 CONTINUE
 READ(5,500) TITLE2, TITLE3

997

```

GO TO 402
DO 401 L = 1, IBRM
EVM(L) = YOUNG
PSR(L) = POISON
401 CONTINUE
COMMENT SET NUMBER 11
COMMENT READ IN PRESSURE LOADING, DENSITY OF MATERIAL, AND DEAD WEIGHT ONLY IF
COMMENT THEY ARE NOT THE SAME FOR EACH PART.
402 IF(NPRES.EQ.MARKC) GO TO 4025
READ(S:566) (VN(S:L), VN(6:L), VN(7:L), L = 1, IBRM)
GO TO 4026
4025 DO 963 L = 1, IBRM
VN(5:L) = PRESS
VN(6:L) = DENSITY
VN(7:L) = DEAD
963 CONTINUE
COMMENT SET NUMBER 12
COMMENT READ IN VARIABLE THICKNESSES
4024 DO 403 L = 1, IBRM
IF(VARTIKL) .EQ. 01 GO TO 403
NPNT = VARTIKL)
READ(S:551) (RPI(L), I = 1, NPNT)
READ(S:545) (RPI(L), I = 1, NPNT)
CONTINUE
IF(FLSSIERM) .GT. 11 GO TO 86
NPT = NPARTS + 1
NPART = NPARTS + 1
GO TO 87
85 NPT = NPARTS
NPART = NPARTS
COMMENT SET NUMBER 13
87 IF(IPLO) .EQ. 01 GO TO 1030
READ(S:551) (RPI(L), I = 1, NPNT)
READ(S:545) (RPI(L), I = 1, NPNT)
CONTINUE
1030
1031
1032
1033
1034
1035
1036
1037
1038
1039
1040
1041
1042
1043
1044
1045
1046
1047
1048
1049
1050
1051
1052
1053
1054
1055
1056
1057
1058
1059
1060
1061
1062
1063
1064
1065
1066
1067
1068
1069
1070
1071
1072
1073
1074
1075
1076
1077
1078
1079
1080
1081
1082
1083
1084
1085
1086
1087
1088
1089
1090
1091
1092
1093
1094
1095
1096
1097
1098
1099
1100
1101
1102
1103
1104
1105
1106
1107
1108
1109
1110
1111
1112
1113
1114
1115
1116
1117
1118
1119
1120
1121
1122
1123
1124
1125
1126
1127
1128
1129
1130
1131
1132
1133
1134
1135
1136
1137
1138
1139
1140
1141
1142
1143
1144
1145
1146
1147
1148
1149
1150
1151
1152
1153
1154
1155
1156
1157
1158
1159
1160
1161
1162
1163
1164
1165
1166
1167
1168
1169
1170
1171
1172
1173
1174
1175
1176
1177
1178
1179
1180
1181
1182
1183
1184
1185
1186
1187
1188
1189
1190
1191
1192
1193
1194
1195
1196
1197
1198
1199
1200

```



```

SIGMT(KST) = TERM1 - TERM2
SIGMB(KST) = TERM1 * TERM2
SIGTM(KST) = TERM3
SIGTH(KST) = TERM4
SIGNT(KST) = TERM3 - TERM4
SIGNB(KST) = TERM3 * TERM4
TAUPH(KST) = 1.5*V3(2)/M
IF(PLTIME .EQ. 0) GO TO 666
XPLOT(PLOTP1) = SPLOT
XPLI(PLOTP1) = XPLI(PLOTP1)
DO 665 I = 1, NLOT
  COLUMN = IPLOT(I)
  IF(COLUMN .GT. 6) GO TO 595
  VPLOT(PLOTP1,I) = V3(COLUMN)
  VPLI(KST,I) = V3(COLUMN)
  GO TO 665
595 KOLUMN = COLUMN - 6
  GO TO (600, 605, 610, 615, 620, 625,
1 630, 635, 640, 645, 650, 655, 660), KOLUMN
600 VPLOT(PLOTP1,I) = NT
  VPLI(KST,I) = NT
  GO TO 665
605 VPLOT(PLOTP1,I) = NT
  VPLI(KST,I) = NT
  GO TO 665
610 VPLOT(PLOTP1,I) = EPT
  VPLI(KST,I) = EPT
  GO TO 665
615 VPLOT(PLOTP1,I) = EPP
  VPLI(KST,I) = EPP
  GO TO 665
620 VPLOT(PLOTP1,I) = SIGMPH(KST)
  VPLI(KST,I) = SIGMPH(KST)
  GO TO 665
625 VPLOT(PLOTP1,I) = SIGMPH(KST)
  VPLI(KST,I) = SIGMPH(KST)
  GO TO 665
630 VPLOT(PLOTP1,I) = SIGMT(KST)
  VPLI(KST,I) = SIGMT(KST)
  GO TO 665
635 VPLOT(PLOTP1,I) = SIGMB(KST)
  VPLI(KST,I) = SIGMB(KST)
  GO TO 665
640 VPLOT(PLOTP1,I) = SIGTM(KST)
  VPLI(KST,I) = SIGTM(KST)
  GO TO 665
645 VPLOT(PLOTP1,I) = SIGTH(KST)
  VPLI(KST,I) = SIGTH(KST)
  GO TO 665
650 VPLOT(PLOTP1,I) = SIGNT(KST)
  VPLI(KST,I) = SIGNT(KST)
  GO TO 665
655 VPLOT(PLOTP1,I) = SIGNB(KST)
  VPLI(KST,I) = SIGNB(KST)
  GO TO 665
660 VPLOT(PLOTP1,I) = TAUPHI(KST)

```

FORTRAN Listing of Subroutine PLT

Given below is a complete listing of the FORTRAN IV version of the subroutine PLT currently operational on the CDC 6400 at Battelle-Columbus. This subroutine together with the modified versions of NONLIN, INPUT, and PRINT presented above provides the user with an improved tool for the analytical study of bellows and diaphragms.

```

SUBROUTINE PLY
DIMENSION IML(4)
DIMENSION X(100),Y(100),JOEPLI(10),IA(10),IB(10),
* SI(60),SA(60),INT(60),IPAR(60),PSR(60),
* V3(10),VM(7,60),EVM(60),BACK(60),ISS(60),
* E(9,60),XI(100),YI(100)
DIMENSION XPLI(350),YPLI(350),I0,IPL0T(10),RT(60),
* XM(350),YM(350),XS(350),YS(350)
DIMENSION YTITLE(10),XX(100),YY(100),XXI(100),YYI(100)
COMMON / BLOCKP / NFF, SMX, SZERO, GO, EMP, ISS, E,
* MAX, INTPEN, INTVAL, NPP
COMMON / BLOCKP / PLOT, PLTIME, SPLOT, PLOTP, IPL0T, YMOD, NST,
* HOAMA, DEAD, WFM
COMMON / BLOCKS / MPARTS, PHI, V3, KIND, NT, MT, SPRINT, VM, EVM,
* BACK, WBACK
COMMON / BLOCKS / JOEPLI, ALXL, ALXR, IA, IB, NODUNC, IMPUN,
* CONVER, SI, SM, INT, IPAR, PSR, ITER, NTRY,
* MERROR, IGRM, IRYIN, IGMAR
COMMON / PLKYZC / XPLY,YPLY,MCC
DATA (BPO,0,1745329252E-01)
INTEGER PLOT,PLOTP,PLTIME
REAL JSCALE,MAXI,MINI,MAXY,MINYI
IF(PLOI.EQ.0)RETURN
GO TO (1000,1001)MCC
C XY ARE COORDINATES OF POINTS ON SHELL PARTS
C XX,YY ARE COORDINATES OF INITIAL AND FINAL POINTS ON SHELL PARTS
C AND ALSO INCLUDE CENTRES OF TOROIDAL SHELLS
C BETWEEN 1000 AND 1001 XY VALUES ARE COMPUTED AFTER INPUT
C OBTAIN XY SYSTEM FOR MODEL AND STORE
1000 NBR=0
C DATA SET NUMBER 14
C READ TITLES FOR DESIRED PLOTS
READ(5,2001)((YTITLE(I),J),I=1,10),J=1,PL01)
FORMAT(10A10)
C DATA SET NUMBER 15
C READ NUMBER OF LEAF AND NO.OF PART AT END OF EACH LEAF
READ(5,2002)NLS
2002 FORMAT(I9)
READ(5,2003) (IMLS(I),I=1,NLS)
2003 FORMAT(15)
NBR=1
JBR=1
DO 1 I=1,IBRM
K=155(I)
GO TO (999,999,999,999,100,101,001K
OBTAIN XY SYSTEM FOR CYLINDRICAL PARTS
99 IF(I.EQ.1)GOTO 411
410 Y(NBR)=0.0
GO TO 412
411 Y(NBR)=Y(NBR-1)
412 X(NBR)=X(NBR-1)
XX(JBR)=X(NBR)
YY(JBR)=Y(NBR)
JBR=JBR+1
NBR=NBR+1
X(NBR)=X(NBR-1)

```

```

V(NBR)=Y(NBR-1)-VN(3,1)
X(JBR)=X(NBR)
Y(JBR)=Y(NBR)
NBR=NBR+1
JBR=JBR+1
GO TO 11
C OBTAIN XY SYSTEM FOR CONICAL PARTS.
100 IF(I.EG.1)102,103
102 V(NBR)=0.0
GO TO 104
103 V(NBR)=Y(NBR-1)
104 X(NBR)=VN(2,1)
X(JBR)=X(NBR)
Y(JBR)=Y(NBR)
JBR=JBR+1
NBR=NBR+1
X(NBR)=X(NBR-1)+VN(3,1)*COS(SI(1)*RPO)
Y(NBR)=Y(NBR-1)-VN(3,1)*SIN(SI(1)*RPO)
X(JBR)=X(NBR)
Y(JBR)=Y(NBR)
20 NBR=NBR+1
JBR=JBR+1
GO TO 11
C OBTAIN XY SYSTEM FOR CIRCLE PARTS
101 C=C*VN(2,1)
ALPHA=90.0-SI(1)
ALPHA=90.0-SI(1)
IF(I.EG.1)400,401
400 CY=0.0
GO TO 402
401 CY=Y(NBR-1)-VN(3,1)*SIN(ALPHA)*RPO)
X(JBR)=X(JBR-1)
Y(JBR)=Y(JBR-1)
JBR=JBR+1
402 A1=ABS(SI(1)-SI(1))/2.0
NPPP=2.0*A1*1.
NPPP=NPPP/2
DO 2 J=1,NPPP
IF(JJ.EG.1)3,4
4 IF(IJ.EG.NPPP)5,6
5 ALPHA=ALPHA+C
GO TO 3
6 IF(VN(3,1))200,999,201
200 ALPHA=ALPHA+2.0
GO TO 3
201 ALPHA=ALPHA-2.0
3 X(NBR)=CX+VN(3,1)*COS(ALPHA)*RPO)
Y(NBR)=CY+VN(3,1)*SIN(ALPHA)*RPO)
NBR=NBR+1
IF(I.EG.1)AND. JJ.EG.1)403,2
403 X(JBR)=X(NBR-1)
Y(JBR)=Y(NBR-1)
JBR=JBR+1
2 CONTINUE
X(JBR)=CX
Y(JBR)=CY

```

```

JBR=JBR+1
XX(JBR)=X(NBR-1)
YY(JBR)=Y(NBR-1)
JBR=JBR+1
11 IF(NBR.EQ.901)GO TO 999
IF(MLS.EQ.1)GO TO 1
IF(MLS.EQ.4)708
7 NLS1=NLS-1
GO TO 9
8 NLS1=NLS
9 CONTINUE
DO 2004 I=NLS1,NLS1
IF(I.EQ.I(NLS1MIN))22,2004
22 NBRC=NBRC+1
GO TO (23,24,25)NBRC
23 NBRI=NBRI-1
JBR1=JBR-1
GO TO 1
24 NBRI=NBRI-1
JBR2=JBR-1
GO TO 1
25 NBRI=NBRI-1
JBR3=JBR-1
GO TO 1
2004 CONTINUE
1 CONTINUE
NBRC=NBRC-1
JBR=JBR-1
RETURN
C XY VALUES HERE AFTER ARE COMPUTED AFTER PRINT
C OBTAIN XS,YS,XN,YN WHERE
C XM-I-COORDINATE OF MODEL AT PRINT POINT
C YN-Y-COORDINATE OF MODEL AT PRINT POINT
C XS AND YS ARE CORRESPONDING COORDINATES WITH VARIABLE SUPERIMPOSED
1001 DO 2000 KLM=1,PL01
NBRC=0
NMPY=0
DO 1002 I=1,ISUM
NMPY=NMPY+IPAR(I)*INT(I)
1002 CONTINUE
C FIND MAXIMUM NUMERICAL VALUE OF THE VARIABLE FROM YPLT(NMPY,KLM)
C YPLT IS THE VALUE OF VARIABLE
C XPLT IS THE MERIDIONAL COORDINATE
C KLM NO OF PLOTS,MAXIMUM OF 10
C DETERMINE BEST POSSIBLE SCALE
IJK=1
NOR=1
DO 600 I=1,IGRM
KIND=IS(I)
GO TO (999,601,999,999,999,999,601,602,601)KIND
601 IJK=IJK+IPAR(I)*INT(I)
GO TO 600
602 IJK=IJK-1+IPAR(I)*INT(I)
GO 603 J=IJK,IJMP
IF(IJK.EQ.IJK)604,605

```

```

604 YMAX=ABS(YPLT(JK,KLM))
605 IF (ABS(YPLT(JK,KLM)) .GT. YMAX) YMAX=ABS(YPLT(JK,KLM))
606 CONTINUE
   IJK=IJKP+1
   RT(NOR)=0.75*ABS(VN(3,I))/YMAX
   NOR=NOR+1
608 CONTINUE
   NOR=NOR-1
   SCALE=RT(I)
   D) 604 NO=2*NOR
   IF (RT(NO) .LT. SCALE) SCALE=RT(NO)
606 CONTINUE
   DO 1009 J=1,MPDPT
   YPLT(J,KLM)=YPLT(J,KLM)*SCALE
1009 CONTINUE
   DO 1010 I=1,IMM
   KLM=KLM+1
   GO TO (000,000,000,000,000,001,001,001,001,001)KIMD
C
998 LLL=IPAN(I)
   KKK=INT(I)
   DO 420 LL=1,LLL
   IF (I .EQ. 1 .AND. LL .EQ. 1) 421,422
   YN(NR)=0.0
   XN(NR)=VN(2,I)
   YS(NR)=XN(NR)*YPLT(NR,KLM)*SIN(VN(3,I)*RFD)
   YS(NR)=YN(NR)
   NR=NR+1
422 DO 420 KK=1,KKK
   IF (I .EQ. 1 .AND. LL .EQ. 1 .AND. KK .EQ. 1) 420 TO 420
   IF (KK .EQ. 1) 423,424
423 XN(NR)=XN(NR-1)
   YN(NR)=YN(NR-1)
   GO TO 425
424 XN(NR)=XN(NR-1)
   YN(NR)=YN(NR-1)-S(I)/(LLL*(KK-1))
425 XS(NR)=XN(NR)*YPLT(NR,KLM)*SIN(VN(3,I)*RFD)
   YS(NR)=YN(NR)
   NR=NR+1
426 CONTINUE
   GO TO 2020
C
1011 LLL=IPAN(I)
   KKK=INT(I)
   DO 1013 LL=1,LLL
   IF (I .EQ. 1 .AND. LL .EQ. 1) 1013,1015
1014 YN(NR)=0.0
   XN(NR)=VN(3,I)
   XS(NR)=XN(NR)*YPLT(NR,KLM)*SIN(VN(2,I)*RFD)
   YS(NR)=YN(NR)*YPLT(NR,KLM)*COS(VN(2,I)*RFD)
   NR=NR+1
1015 DO 1013 KK=1,KKK
   IF (I .EQ. 1 .AND. LL .EQ. 1 .AND. KK .EQ. 1) 420 TO 1013
   IF (KK .EQ. 1) 1014,1015
   XI(NR)=XN(NR)

```

```

VM(MBR)=VM(MBR-1)
GO TO 53
52 XM(MBR)=XM(MBR-1)*SI(I)*COS(VN(2,I)/RPO)/(LL*(KKK-1))
VM(MBR)=VM(MBR-1)*SI(I)*SIN(VN(2,I)/RPO)/(LL*(KKK-1))
53 XS(MBR)=XM(MBR)*YPLT(MBR,KLM)*SIN(VN(2,I)/RPO)
YS(MBR)=VM(MBR)*YPLT(MBR,KLM)*COS(VN(2,I)/RPO)
MMR=MMR+1
1013 CONTINUE
GO TO 2020
C
CIRCULAR PARTS
1012 IF(BACK(I))300,999,301
300 ALPHA=99.9*SI(I)/RPO-100.0
ALPHA=99.9*SI(I)/RPO-100.0
GO TO 302
301 ALPHA=99.9*SI(I)/RPO
ALPHA=99.9*SI(I)/RPO
302 ALPHA=ABS(ALPHA)-ALPHA
IF(I.EQ.1)404,405
404 CY=0.0
GO TO 406
405 CY=VM(MBR-1)-VN(3,I)*SIN(ALPHA/RPO)
406 CONTINUE
LLL=IPAR(I)
KKEINT(I)
DO 1016 LL=1,LLL
DO 1016 KK=1,KKK
IF(KK.EQ.1)GO TO 1020
IF(VN(3,I))1017,999,1018
1017 ALPHA=ALPHA/RPO/LLL*(KKK-1)
GO TO 1020
1018 ALPHA=ALPHA-ALPHA/LLL*(KKK-1)
XM(MBR)=CY*VN(3,I)*COS(ALPHA/RPO)
VM(MBR)=CY*VN(3,I)*SIN(ALPHA/RPO)
XS(MBR)=XM(MBR)*YPLT(MBR,KLM)*COS(ALPHA/RPO)
YS(MBR)=VM(MBR)*YPLT(MBR,KLM)*SIN(ALPHA/RPO)
MMR=MMR+1
1016 CONTINUE
2020 IF(MLS.EQ.1)GO TO 1010
DO 2005 I=1,MLS
IF(I.EQ.1)LS(I)=305,2005
305 MBR=MBR+1
GO TO (306,307,308) MBR
306 MBR=MBR-1
GO TO 1010
307 MBR=MBR-1
GO TO 1010
308 MBR=MBR-1
GO TO 1010
2005 CONTINUE
1010 CONTINUE
MMR=MMR+1
IF(MBR.EQ.0)40,31
MMR=MMR
MMR=MMR

```

```

JJJ-JBR
DO 92 NNN1,NNN
X1 (NN) SX (NN)
Y1 (NN) SY (NN)
92 CONTINUE
DO 93 J-1,JJJ
X1 (JJ) SX (JJ)
Y1 (JJ) SY (JJ)
93 CONTINUE
GO TO 41
31 IF (ML5 .EQ. 4 .AND. ELM .EQ. 1) NBRC=NBRC+1
IF (NBRC .EQ. 5) NBRC=4
DO 26 JJJ1,NBRC
GO TO (27,28,29,30) JJJ
27 NBR=0
NBR=0
JB=0
NN=NBR1
NN=NBR1
JJJ=JBR1
GO TO 32
28 NBR=NBR1
NBR=NBR1
JB=JBR1
NN=NBR2-NBR1
NN=NBR2-NBR1
JJJ=JBR2-JBR1
GO TO 32
29 NBR=NBR2
NBR=NBR2
JB=JBR2
NN=NBR3-NBR2
NN=NBR3-NBR2
JJJ=JBR3-JBR2
GO TO 32
30 NBR=NBR3
NBR=NBR3
JB=JBR3
NN=NBR-NBR3
NN=NBR-NBR3
JJJ=JBR-JBR3
32 DO 95 NNN1,NNN
X1 (NN) SX (NN) SX (NN)
Y1 (NN) SY (NN) SY (NN)
90 CONTINUE
DO 91 NNN1,NNN
X5 (NN) SX (NN) SX (NN)
Y5 (NN) SY (NN) SY (NN)
91 CONTINUE
DO 94 JJJ1,JJJ
X1 (JJ) SX (JJ) SX (JJ)
Y1 (JJ) SY (JJ) SY (JJ)
94 CONTINUE
41 IF (NBRC .EQ. 0 .OR. JJJ .EQ. 1) 42,43
42 NNN1=N1(1)
NINK1=N1(1)

```

```

MAXY1=V1(1)
MINY1=V1(1)
DO 500 MM=2,MMN
IF (X1(MM) .GT. MAXX) MAXX=X1(MM)
IF (X1(MM) .LT. MINX) MINX=X1(MM)
IF (Y1(MM) .GT. MAXY) MAXY=Y1(MM)
IF (Y1(MM) .LT. MINY) MINY=Y1(MM)
500 CONTINUE
DIFFR=MAXX-MINX
DIFFY=MAXY-MINY
IF (DIFFX .GT. DIFFY) 501,502
501 DIFF=DIFFX
JSCALE=8.0
GO TO 503
502 DIFF=DIFFY
JSCALE=6.0
KON=2
FACE=28.0
72 DIFF=DIFF*FACE
IF (DIFF1 .LE. JSCALE) 70,71
70 DX=1.0/FACE
GO TO 89
71 KON=KON+1
IF (KON .EQ. 7) 80 TO 70
FACE=FACE/2.0
IF (KON .EQ. 4) FACE=0.0
GO TO 72
80 CONTINUE
DDX=MINX-DX
DDY1=-4.0*DX
DDY2=MINY-DX
IF (DDY1 .LT. DDY2) 80,81
80 DDY=DDY1
GO TO 82
81 DDY=DDY2
82 CONTINUE
SCALE=X/SCALE
DDYCDY=7.0*DX
DO 83 JJ=2,JJJ
IF (VY1(JJ) .LT. DDY .OR. VY1(JJ) .GT. DDYCDY) 84,83
84 X1(JJ)=X1(JJ-1)
Y1(JJ)=Y1(JJ-1)
83 CONTINUE
SPECIFY LENGTH AND SCALE OF XY AXES AND VALUES OF XY AT INTERSECT.
CALL GINSET(10.0,DDX,DR,7.0,DDY,DX)
DRAW MODEL
CALL GINPLT(X1,Y1,MMN,3M0Z,0.3M0Y,0.YTITLE(1,KLM))
CALL PLOT(-11.0,1.0,-3)
SUPERIMPOSE VARIABLE COORDINATES AND FIRST-LAST PTS. OF SPELLS
CALL GLINE(XS,YS,MMN,0)
CALL GLINE(XR1,YR1,-JJJ,3)
CALL SYMBOL(6.5,1.5,0.14,14MSCALE-1IN,0.0,0.10)
ENCODE(13,60,XSCALE)SCALE
FORMAT (E13.5)
CALL SYMBOL(9.1,1.1,3.0,14,XSCALE,0.0,13)
CALL PLOT(12.0,-1.0,-3)

```

24 CONTINUE
2000 CONTINUE
RETURN
999 CALL EXIT
END

Description of Computing Program FIT

In order to ease the burden of preparing the data required by program NONLIN(1), a computing program (called FIT) has been developed which computes a mathematical model of a shell midsurface from a set of (x,y) coordinates. This appendix is intended for those who plan to use FIT for the preparation of data for NONLIN.

While NONLIN is capable of analyzing shells composed of parts having several different shapes (cylindrical, spheroidal, ellipsoidal, paraboloidal, conical, or toroidal), FIT has been designed to describe the shell in terms of cylindrical, conical, and toroidal parts only. In addition to a mathematical model of a shell midsurface, program FIT generates variable thickness data, variable elastic parameter data, and variable loading data. The information generated by FIT is punched onto cards in the sequence and format required by NONLIN. This allows the user to change the boundary conditions or make other minor changes in the data without rerunning the entire problem through FIT.

Input Preparation

The information required by FIT to produce a complete set of data for NONLIN will now be described. Although some of the following is a duplication of input data described elsewhere for NONLIN(1), for the sake of self-containment it is included here. In terms of "data-sets", FIT requires a total of eleven which are listed below:

1. Title cards (3 cards)
2. Boundary-value data at initial edge of shell (1 card)
3. Boundary-value data at final edge of shell (1 card)
4. Rotation angle between shell supports and shell centerline at initial and final edges of shell (1 card)
5. NONLIN control card (1 card)
6. Young's modulus and Poisson's ratio (1 card)
7. Loading parameters-pressure, unit weight, and dead weight (1 card)
8. FIT control card (1 card)
9. Tolerance and coordinate transformation card (1 card)
10. Pointwise description of shell (1 card for each point)
11. Vertex information (1 card).

Data Sets 1-7

With the exception of data set five, the first seven data sets are prepared exactly as described in Appendix B of Reference (1). The exception, the NONLIN control card, must have the first five columns blank. These locations are for IBRM, the number of parts in the composite shell, which is not known until the model has been developed. The other entries on data set five are as they have been.

Data Set 8 Fit Control Card

This card contains the number of points which will be used to describe the shell shape, the number of vertices in the shell (points through which the tangent is not required to turn continuously), and the total number of print points desired for the entire shell. The number of print points refers to the points at which the values of stress resultants and moments, the displacements and strains, and the surface stresses computed by NONLIN are printed out. This information was previously read in for each part. FIT computes the number of print points per segment for each part by taking the appropriate fraction of the total number of print points requested according to each parts proportion of the total arc length. Clearly this procedure does not allow the user to obtain detailed information in regions of interest on the first pass. However, the number of print points per segment for a particular region of interest can be changed on the data deck obtained from FIT.

Data Set 9 Tolerance and Coordinate Transformation Card

The first entry on this card is the tolerance which is the maximum distance any point can lie from the model. If the tolerance is set too small it may be that no model will be obtained, while too large a tolerance will yield a model which does not adequately describe the shell. A suggested tolerance is 1/10 of the average thickness, although reasonably good results have been obtained with a tolerance of 1/2 the average thickness.

The remaining entries on this card deal with transforming the arbitrary set of coordinate axes (used to measure the (x,y) coordinates of the shell midsurface) to the coordinate system needed to describe the mathematical model. In order to obtain the correct descriptions of the shell parts, the origin of coordinates must be translated so as to lie on the centerline of the shell. This also implies that the x-coordinates must all be positive. To ensure all of these conditions it may be necessary to translate and reflect in the coordinate axes.

To illustrate this point consider Figure B-2, depicting a simple encapsulated shape with a set of axes superimposed. These axes are used to measure (x,y) coordinates of the points. Table B-1 lists a set of (x,y) values which might be obtained.

TABLE B-1. COORDINATES FOR SHELL OF FIGURE B-1

Reading	Coordinates	
	x	y
1	0	0
2	0.5	0.5
3	1.0	1.0
4	1.5	1.25
5	2.0	1.4
6	2.5	1.4

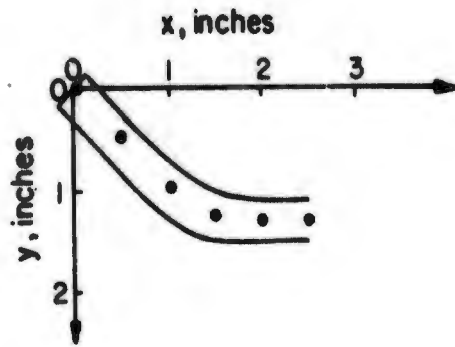


FIGURE B-2. ACTUAL ENCAPSULATED SHAPE

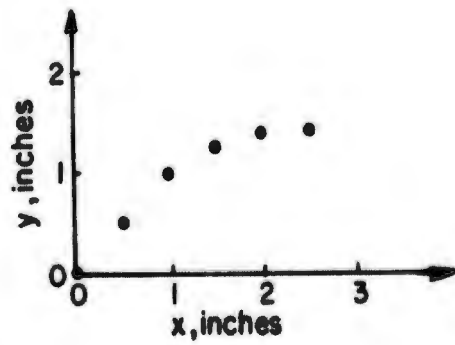


FIGURE B-3. INTERPRETATION OF MEASURED POINTS

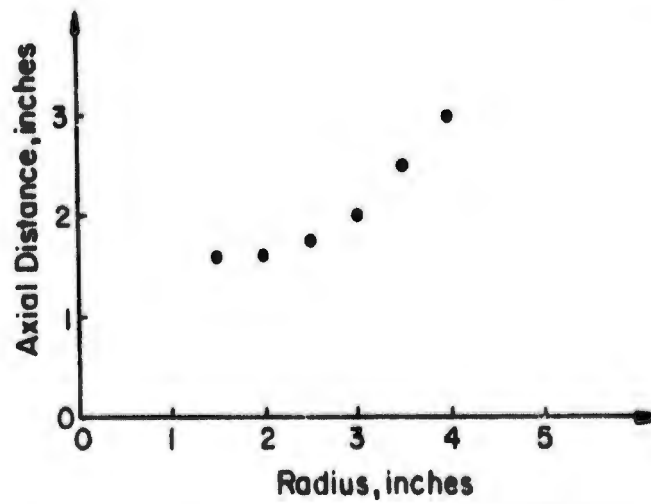


FIGURE B-4. TRANSFORMED COORDINATES

When read into FIT in the indicated order, the interpretation is as shown in Figure B-3, with the y-axis being used as the centerline of the shell. The desired interpretation is shown in Figure B-4. To transform the (x,y) coordinate system to the desired (r,z) coordinate system it is necessary to: (a) reflect in the y-axis, (b) reflect in the x-axis, and (c) translate in the positive x direction. There is no need to have the y-coordinates positive, except to enhance the appearance of any plot of the final model.

Data Set 10 Pointwise Description of the Shell

This set of data has one card for each point describing the shell midsurface. In general, each card will contain the x and y coordinates of a point and the thickness of the shell at that point. If only the first card of this set has a thickness specified, the resulting model will have constant thickness. If the thickness is not specified at a point, the last thickness value read in is assigned as the shell thickness at that point. Thus, the first card must always contain a thickness specification.

When the elastic and loading parameters are constant for a particular problem no other information need be supplied on these cards. However, if they vary along the shell, the variations are prescribed on these cards. It is anticipated that these parameters will be constant over large portions of the shell. Therefore, their values are allowed to be prescribed only at the first point and at points which are vertices. The user is allowed, however, to label as vertices points which are not "geometric" vertices when variable loading and elastic parameters require this to be done. The resulting model will probably be suitable. But, the tangent is not required to turn continuously through points which are labeled as vertices.

Data Set 11 Vertex Information

This card contains the indices (in the order of their appearance) of the points which the user calls vertices. Generally speaking, these are points on the shell generator at which the tangent is not required to turn continuously. However, if variable loading or elastic parameters change value at points which are not "geometric" vertices, the user can specify such points as vertices if he is willing to accept the loss of the continuity of the first derivative at that point.

Item-by-Item Description of Input Data

Data Set 1 Job Identification

READ (5,500) TITLE 1, TITLE 2, TITLE 3

500 FØRMAT (80A1)

Any information can be placed on these three cards. It is necessary to have three cards, although any can be left blank.

Data Set 2 Boundary Data at Initial Edge

READ (5,530) (BOUNDI(I), GA(I), I = 1,4)

530 FORMAT (4 (A6, 6X, F8.2))

BOUNDI (1) is either DISPLACEMENT or FORCE in normal or 1 direction

GA (1) is its value

BOUNDI (2) is either DISPLACEMENT or FORCE in meridional or 2 direction

GA (2) is its value

BOUNDI (3) is either SLOPE or MOMENT

GA (3) is its value

BOUNDI (4) is either DISPLACEMENT or FORCE in circumferential direction

GA (4) is its value

For an axisymmetrically loaded shell BOUNDI (4) and GA (4) need not be specified.

Data Set 3 Boundary Data at Final Edge

READ (5,530) (BOUNDF (I), GB (I), I = 5,8)

530 FORMAT (4 (A6, 6X, F8.2))

BOUNDF (5) is either DISPLACEMENT or FORCE in normal or 1 direction

GB (5) is its value

BOUNDF (6) is either DISPLACEMENT or FORCE in meridional or 2 direction

GB (6) is its value

BOUNDF (7) is either SLOPE or MOMENT

GB (7) is its value

BOUNDF (8) is either DISPLACEMENT or FORCE in circumferential direction

GB (8) is its value

For an axisymmetrically loaded shell BOUNDF (8) and GB (8) need not be specified.

Data Set 4 Boundary Rotation Angles

READ (5,565) ALXL, ALXR

565 FØRMAT (8F10.5)

ALXL is the boundary rotation angle at the initial edge of the shell

ALXR is the boundary rotation angle at the final edge of the shell

Data Set 5 Control Card

READ (5,561) IBRM, ITER, NDUMMY, PLØT, INTPRN, INTVAL, LEVEL1, LEVEL2, ERP, CØNVER, NUMHAR, (NFOURA (I), I = 1,8)

561 FØRMAT (8I5, 2E10.3, 10I2)

- IBRM = Set IBRM = 0 to use fitting subroutine. Fit determines the number of shell parts.
- ITER = number of iterations at a load level for nonlinear calculations. ITER = 0 for linear analysis.
- NDUMMY = not presently used
- INTPRN = 0 indicates that intermediate results from the nonlinear analysis, i.e., values of parameters and slopes, will not be printed out. Use 1 to obtain values.
- INTVAL = 0 indicates that intermediate results from the initial value integrations will not be printed out. Use 1 to obtain values.
- LEVEL1 = number of increments into which the loading is divided for nonlinear analysis.
- LEVEL2 = not presently used
- ERP = accuracy for integration subroutine. If left blank, it is internally set to 1.0 E-05.
- CØNVER = convergence criteria for use in nonlinear analysis.
- NUMHAR = number of FØURIER harmonics in the anlysis. For a nonlinear analysis, NUMHAR = 1. For a linear analysis, NUMHAR must not be greater than 8. If the shell is axisymmetrically loaded, NUMHAR = 1. For a nonsymmetrically loaded shell which has the same boundary conditions for all harmonics, NUMHAR can have any value up to 8.
- NFOURA(I) = FØURIER harmonic value. For an axisymmetric deformation, NFOURA (1) = 0.

Data Set 6 Elastic Parameters

READ (5,563) NELAS, YOUNG, POISSON

563 FORMAT (2X, A2, 4X, E11.4, 4X, F6.4)

NELAS is either YES or NO. YES indicates that the elastic parameters are the same for each part in the composite shell. If YES, then the values of Young's modulus and Poisson's ratio are read in on the same card. If NO, the values for each part are read in as Data Set 10.

YOUNG = Young's modulus (lb/in.²)

POISSON = Poisson's ratio (in./in.)

Data Set 7 Loading Parameters

READ (5,680) NPRES, PRESS, DENSTY, DEAD

680 FORMAT (2X, A2, 4X, 3F 14.5)

NPRES is either YES or NO. YES indicates that the distributed loadings are the same for each part in the composite shell. If YES, then the values of the normal pressure, the weight density of the material, and the dead loading on the shell are given on the same card. If NO, then the values for each part are read in as Data Set 11.

Data Set 8 Control Card For Fit (One Card)

READ (5,5010) NPTS, NV, ITNT

5010 FORMAT (3I5)

NPTS = Number of points used to describe shell midsurface.

NV = Number of vertices

ITNT = Total number of print points.

Data Set 9 Tolerance and Transformation

READ (5,5020) EPS1, XTRANS, YTRANS, XRFLCT, YRFLCT

5020 FORMAT (3F10.5, 2X, A2, 3X, A2)

EPS1 = User prescribed tolerance. No point will be more than EPS1 from the resulting model. EPS1 is a positive quantity, usually between 1/2 and 1/10 the average thickness of the shell.

XTRANS = Distance the given points are to be translated in the x direction.

- YTRANS = Distance the given points are to be translated in the y direction.
- XRFLCT = YES or NO; if YES then the given points will be reflected in the x-axis. If NO the points will be unchanged.
- YRFLCT = YES or NO. If YES then the given points will be reflected in the y-axis. If NO, the points will be unchanged.

Data Set 10 Pointwise Description of the Shell (One card is needed for each point)

READ (5,5070) X1, Y1, T1, PR, YM, PRS, DW, DNS

5070 FORMAT (8F10.5)

- X1 = x-coordinate of the point. *
- Y1 = y-coordinate of the point. *
- T1 = thickness of the shell at (X1, Y1). *
- PR = Poisson's ratio (in./in.)
- YM = Young's modulus (lb/in.²)
- PRS = Pressure loading (lb/in.²)
- DW = Dead weight loading (lb/in.²)
- DNS = Density (lb/in.³)

Data Set 11 Vertex Information

READ (5,5060) (IV(I + 1), I = 1, NV)

5060 FORMAT (16I5)

IV(I) = index of the I-th vertex.

Internally, the first and last points are required to be vertices. The user, However, must not enter these indices as vertices. IV(I) and IV(NV + 2) are set internally to 1 and NPTS, respectively.

* Note - The units used for thicknesses and coordinates should be actual dimensions in inches.

Description of Output

The main output from FIT is in the form of a punched set of data ready to be read into NONLIN. A plot of x-y coordinate and shape of model is also obtained. Since all of this standard input is described in detail in Appendix B of Reference (1), nothing more need be said about this part of the output.

In addition to the input for NONLIN, certain intermediate results which describe the fitting process are printed out. An understanding of these results is important to the user if trouble is encountered by the program in obtaining a model. Before describing these results it will be necessary to consider briefly the fitting procedure.

The fitting procedure begins by grouping the points according to whether the tangent to the fitting curve will rotate clockwise, counterclockwise, or not turn (a line), as the group of points is traversed in the positive direction. The positive direction along the curve is defined by the order in which the points are read in. This grouping of points accomplishes several important tasks. It isolates inflection points, gives a lower bound to the number of parts required in the final model, and provides an easy check on whether a given circular arc has the proper curvature. It must be emphasized here that the way in which this grouping is done requires that lines be described by at least three points. This is brought out since it may, on occasion, be necessary to add points to those obtained from the encapsulating procedure to ensure obtaining conical parts where they are desired.

Basically the fitting procedure requires the joining of two curves so that they have a common tangent and are within the prescribed tolerance of the given points. The requirement that the first derivative be continuous determines a line on which the center of a fitting circle must lie. In the case of a fitting line segment, this requirement demands that the line be tangent to any circles adjacent to it.

There are essentially four different problems associated with the fitting procedure. These are starting the fitting curve with a circle or a line and extending the fitting curve with a circle or a line.

If the fitting curve is being extended with a circle, then a line is known on which the center must lie. This line is either the normal through the last point of the preceding line or the extended diameter through the last point of the preceding circle. The next circle is then completely determined by requiring it to pass through one additional point. To fit as many points as possible the circle through the last point of the group of points being fit is tested for suitability. This test includes a check on the curvature and a check on whether or not all of the points being fit lie within the tolerance of the curve. If any point does not satisfy the tolerance the circle is judged unacceptable and the circle through the next to the last point is tested. This process is continued until a suitable circle is found. The acceptable circle is then extended as far as possible by testing successive points past the last point on the circle until one is found which exceeds the tolerance.

When the fitting curve is being extended by a line, the procedure is simply to find the appropriate line which contains the last point of the group of collinear points and is tangent to the preceding circle.

A fitting curve is begun at vertices and at the first point of the set of data points. If the first group of points being fit is not collinear, the fitting procedure requires a line on which the center of the fitting circle must lie. This line is taken to be the extended radius of the circle through the first three points.

There is one further procedure which is carried out as a matter of course when the fitting curve is extended by joining two circles of opposite curvature. This procedure is to search for a better inflection point than is offered by the last point of the preceding circle. Nine trial inflection points are created on the preceding circle between the last two points fit. Each trial point is tried and the best one is chosen according to a measure of the goodness of fit the curve from each trial point achieves.

Several things can happen to the fitting curve extended from a given trial point: (a) it can be extended from the trial point to the last point of the present group of points with one or more circular arcs, (b) it can be extended so as to fit all but a few of the points before the curvature reverses, or (c) it can only be extended one point before curvature reversal occurs. The last two cases are distinguished, because, when curvature reversal occurs, nine trial points are created between the last two points successfully fit and each is tried to obtain the best point from which to continue the fitting procedure. While this strategy is satisfactory for case (b), it will lead to uncontrolled looping in case (c).

Corresponding to each of the three cases, a number indicative of the trial points suitability is computed. For case (a), the number of circular arcs required plus the sum of the absolute values of the distances the points are from the curve is computed. This number is computed for each trial point and is placed in a vector called BSTFIT. If the fitting procedure could not go from the k^{th} trial point to the last point of the group, BSTFIT(K) is set equal to 100. In case (b), the index of the last point properly fit in extending the curve from the k^{th} trial point is stored in a vector called IFIT. Thus, if BSTFIT(K) = 100 for all nine trial points, the best trial point is chosen according to the largest entry in IFIT.

In order to discuss case (c), let us suppose that the nine trial points were created between the j^{th} and $j + 1^{\text{st}}$ points. Then IFIT(K) = $j + 1$ for all nine trial points. So that the fitting procedure may continue, the vector EP(K) is computed for each trial point. EP(K) contains the distance of the $j + 1^{\text{st}}$ point from the circle through the $j + 2^{\text{nd}}$ point, provided this circle has the proper curvature. In case the curvature does reverse, EP(K) is set equal to 100. The best trial point is chosen according to the smallest value in EP, which of course will be larger than the tolerance. A message indicating that the tolerance has been exceeded is printed out and the user can decide whether or not to accept the model.

With this brief explanation of the curve fitting procedure, the output description should now be clear. The first few pages of output are

self-explanatory, consisting of job identification, tolerance, and the translated and reflected (x,y) coordinates together with the thickness at these points.

The results of the preliminary grouping are then displaced. Each row of this output corresponds to one group of points and contains the type of the grouping and the first and last points of the grouping. The type of the grouping is a number which indicates the direction of rotation of the tangent as follows:

- | | |
|-----------------|------------------|
| a) ITYPE(I) = 1 | Clockwise |
| b) ITYPE(I) = 2 | Counterclockwise |
| c) ITYPE(I) = 3 | Line segment |

The remaining output will vary from problem to problem, but will always consist of the same type of information. The information is geared to indicate how the set of points was fit. The fitting information for each group of points is started at the top of a new page. If a group of points is collinear, no information other than the first and last points of the line is given.

For circles there are several pieces of information printed out. Whenever a set of trial points is created and tested the values of BSTFIT, IFIT, and EP are printed out for each trial point. The index of the best trial point is identified and its coordinates given. The next line gives the indices of the points the circle must pass through, the index of the last point of the group of points being fit, and the center coordinates and radius of the fitting circle. If there are any points which the circle does not contain, their coordinates and distances from the circle are then listed. The distance is a signed quantity which is positive when the point is inside the circle. When this information pertains to points fit by extending a circle, it is distinguished by the words "Following Point Check", as compared to "Intermediate Point Check".

The output described above is useful when a smaller tolerance is desired or when trouble develops during the fitting procedure. A different, better fitting model will not necessarily result from changing the tolerance. However, a glance at the actual distances the points are from the model will indicate how small the tolerance must be set to achieve a change in the model. The vectors BSTFIT, IFIT, and EP are often useful when the fitting procedure fails; as they give a good indication of what caused the failure and help in correcting the trouble.

When the fitting procedure is completed the set of (x,y) coordinates, including the various trial points used, is listed. The familiar output from NONLIN is then printed out, starting with the boundary data and followed by the geometry generated by FIT. Finally, a plot of the model versus the original set of data points is provided for visual acceptance or rejection of the model.

Sample Problem

To illustrate the preceding remarks we consider an example problem taken from Reference (2). A step-by-step explanation of input preparation and output interpretation will be given.

Table B-2 lists the (x,y) coordinates and thicknesses measured for two leafs of the 3-1/2-inch single-ply stainless steel bellows JN 136. The incapsulated bellows is shown photographed and enlarged 20X in Figure B-5. We observe that when the coordinates were measured, the positive y direction was down on the photograph. This implied that a reflection and translation about the x-axis will be required.

A decision must be made on how the weld should be modeled. It can be modeled as a short cylinder by adding one point between points 33 and 34 (three points are needed to determine a line) or it can be modeled as a sharp point (a vertex) by omitting point 34 and shifting points 35 through 65 a distance of 0.005 inch in the y direction. The second way of modeling will be used in this example, although it is not necessarily the best way.

The input data are shown prepared on coding sheets in Figure B-6. The first three cards contain the job identification desired by the user. The next three data sets contain the boundary data which are described adequately in Reference (2). Data Set 5 has the first five columns blank, since we desire to obtain a model by means of program FIT. For this problem, Young's modulus, Poisson's ratio, and the loading parameters are constant for the entire shell.

Data Set 8 is the beginning of the data for program FIT. The number of points being fit is 65. There is one vertex and we shall request 200 print points. The next card contains the tolerance, which we will specify as 0.0025 inches for a first try. We need to translate the points so that the x-coordinate represents the distance from the centerline to the point. Moreover, the points need to be reflected in x-axis. In order that the plot of the model will lie in the first quadrant, we must, also, translate the points in the y direction. From Reference (2) we find that the points need to be translated 1.4264 inches in x. To place the points in the first quadrant, a translation of 0.08 in y after reflection will suffice.

The next 65 cards comprise Data Set 10. From Figure B-5 it is clear that the first and last parts of the shell should be described by lines. To ensure this, the y-coordinate of points 2 and 64 have been changed. Each card in this set contains the coordinates and thickness of one point. The last data set contains the index of the vertices. For this problem the only vertex is the 33rd point.

The results obtained from FIT for this problem are shown in Figures B-10 to B-16. An item-by-item description is outlined below:

(a) Header page, which gives name of company. Any title appropriate to a given company can be obtained by modifying FORMAT statement Numbers 534, 535, 536, 537, 539 in subroutine input.



FIGURE 9-5. ENLARGED CROSS SECTIONAL VIEW OF A CONVENTIONAL 3.5-INCH WELDED BELLOWS JB-136

TABLE B-2. COORDINATES AND THICKNESS MEASUREMENTS
FOR 3-1/2 INCH BELLOWS JN 136

(Nominal Thickness = 0.005 in.; 1 Unit = 0.001 in.)

Reading	Coordinates		Thickness, Inch	Reading	Coordinates		Thickness, Inch
	x	y			x	y	
1	0	0	0.00527	34	365	26.5	0.00520
2	20	1.5	0.00523	35	365	29	0.00518
3	40	3	0.00535	36	335	31	0.00503
4	60	3	0.00506	37	315	31	0.00527
5	65	3.5	0.00462	38	305	30	0.00523
6	70	5	0.00466	39	295	28.5	0.00518
7	75	7.5	0.00510	40	285	26	0.00507
8	85	11	0.00503	41	275	25	0.00503
9	95	13	0.00503	42	265	26	0.00507
10	105	13	0.00494	43	255	29	0.00503
11	115	11	0.00510	44	245	34.5	0.00507
12	125	7	0.00503	45	235	40	0.00503
13	135	3.5	0.00499	46	225	43	0.00503
14	145	2	0.00523	47	215	44.5	0.00499
15	155	2	0.00527	48	205	45	0.00507
16	165	3	0.00515	49	195	42.5	0.00503
17	175	5.5	0.00499	50	185	39	0.00494
18	185	11.5	0.00515	51	175	35.5	0.00490
19	195	17	0.00523	52	165	34	0.00514
20	205	21	0.00523	53	155	34	0.00518
21	215	22.5	0.00507	54	145	35	0.00510
22	225	22.5	0.00510	55	135	38.5	0.00507
23	235	21	0.00503	56	125	44.5	0.00507
24	245	17	0.00494	57	115	49.5	0.00499
25	255	13.5	0.00494	58	105	52	0.00490
26	265	12.5	0.00503	59	95	53	0.00486
27	275	12.5	0.00494	60	85	52.5	0.00490
28	285	14.5	0.00490	61	75	50.5	0.00490
29	295	17.5	0.00503	62	70	49	0.00474
30	305	21	0.00503	63	65	48	0.00490
31	315	23	0.00523	64	60	48	0.00499
32	335	23.5	0.00510	65	40	48	0.00518
33	365	24	0.00523	66	20	49	0.00507
				67	0	50	0.00518

DATA SET 8 (control card)

NPTS					NV					ITNT				
1	2	3	4	5	6	7	8	9	10	11	12	13	14	15
				67										1
														200

DATA SET 9 (tolerance and transformation)

EPSI										XTRANS										YTRANS					XR FLCT			YR FLCT											
1	2	3	4	5	6	7	8	9	10	11	12	13	14	15	16	17	18	19	20	21	22	23	24	25	26	27	28	29	30	31	32	33	34	35	36	37	38	39	40

WATKINS MEMORIAL INSTITUTE

COLUMBUS, OHIO

STRESS ANALYSIS OF A SHELL OF REVOLUTION

ADVANCED SOLID MECHANICS DIVISION

MECHANICAL ENGINEERING DEPARTMENT

FIGURE B-7. OUTPUT DATA FROM COMPUTING
PROGRAM FIT.

3 1/2-INCH 307 STAINLESS STEEL HELLING JN 140
 COMPUTER FITTED MODEL OF ONE CIRCUMFERENCE
 SEPTEMBER 1970

COMMINUTES AS HEAD IN

	X(I)	Y(I)
1		
1	0.0000	0.0000
2	0.0200	0.0150
3	0.0400	0.0300
4	0.0600	0.0300
5	0.0500	0.0350
6	0.0800	0.0500
7	0.0750	0.0750
8	0.0500	0.1100
9	0.0500	0.1300
10	0.1500	0.1300
11	0.1150	0.1100
12	0.1750	0.0700
13	0.1350	0.0350
14	0.1450	0.0200
15	0.1550	0.0200
16	0.1650	0.0300
17	0.1750	0.0550
18	0.1450	0.1150
19	0.1450	0.1700
20	0.1500	0.2100

FIGURE B-7. (Continued)

21	.21500	.02250
22	.22500	.02250
23	.23500	.02100
24	.24500	.01750
25	.25500	.01350
26	.26500	.01250
27	.27500	.01250
28	.28500	.01450
29	.29500	.01750
30	.30500	.02100
31	.31500	.02300
32	.33500	.02350
33	.34500	.02400
34	.35500	.02650
35	.36500	.02900
36	.37500	.03100
37	.38500	.03100
38	.39500	.03000
39	.29500	.02850
40	.24500	.02690
41	.27500	.02500
42	.24500	.02600
43	.25500	.02900
44	.26500	.03450
45	.25500	.04000
46	.22500	.04300
47	.21500	.04450
48	.20500	.04500

FIGURE B-7. (Continued)

47	.14500	.04250
50	.14500	.03900
51	.17500	.03550
52	.16500	.03400
53	.15500	.03400
54	.14500	.03500
55	.14500	.03050
56	.12570	.04450
57	.11500	.04450
58	.14500	.05200
59	.04500	.05300
60	.04500	.05250
41	.07500	.05050
62	.07000	.04900
63	.06500	.04800
64	.06000	.04800
65	.04000	.04800
66	.02000	.04900
67	0.00000	.05000

FIGURE B-7. (Continued)

3 1/2-INCH 307 STAINLESS STEEL WELDS JN 136
 COMPUTER FITTED MODEL OF ONE CONVOLUTION
 SEPTEMBER 1979

NO. OF POINTS 67
 NO. OF VERTICES 2
 TOLERANCE .250E-02

COORDINATES AS MONITORED BY DATA SET 9.

I	X(I)	Y(I)	KTWICK(I)
1	1.42440	.00900	.00527
2	1.40640	.00150	.00523
3	1.39640	.00300	.00535
4	1.38640	.00300	.00500
5	1.36140	.00350	.00462
6	1.35640	.00500	.00466
7	1.35140	.00750	.00510
8	1.34140	.09100	.00503
9	1.33140	.09300	.00503
10	1.32140	.09300	.00494
11	1.31140	.09100	.00510
12	1.30140	.00700	.00503
13	1.29140	.00950	.00499
14	1.29140	.00200	.00523
15	1.27140	.00200	.00527

FIGURE B-7. (Continued)

16	1.26140	.04300	.00515
17	1.25140	.06550	.00499
18	1.24140	.09150	.00515
19	1.23140	.09700	.00523
20	1.22140	.10100	.00523
21	1.21140	.10250	.00507
22	1.20140	.10440	.00510
23	1.19140	.10100	.00503
24	1.18140	.09700	.00494
25	1.17140	.09350	.00494
26	1.16140	.09250	.00573
27	1.15140	.09250	.00494
28	1.14140	.09450	.00498
29	1.13140	.09750	.00503
30	1.12140	.10100	.00503
31	1.11140	.10300	.00523
32	1.10140	.10390	.00510
33	1.09140	.10490	.00520
34	1.08140	.10550	.00520
35	1.07140	.10700	.00510
36	1.06140	.10700	.00520
37	1.05140	.10700	.00503
38	1.04140	.10700	.00527
39	1.03140	.10800	.00523
40	1.02140	.10900	.00510
41	1.01140	.10900	.00507
42	1.00140	.10900	.00503
43	1.00140	.10900	.00507
44	1.00140	.10900	.00503

THIS POINT IS A CENTER

THIS POINT IS A CENTER

FIGURE 3-7. (Continued)

44	1.14100	.11450	.00507
45	1.19100	.12000	.00503
46	1.29100	.12300	.00503
47	1.21100	.12450	.00499
48	1.22100	.12500	.00507
49	1.23100	.12750	.00503
50	1.24100	.11900	.00494
51	1.25100	.11550	.00490
52	1.26100	.11400	.00514
53	1.27100	.11400	.00514
54	1.28100	.11500	.00510
55	1.29100	.11050	.00507
56	1.30100	.12450	.00507
57	1.31100	.12950	.00499
58	1.32100	.13200	.00490
59	1.33100	.13300	.00406
60	1.40100	.13250	.00490
61	1.35100	.13050	.00490
62	1.35600	.12900	.00474
63	1.36100	.12400	.00470
64	1.36600	.12400	.00499
65	1.36600	.12400	.00510
66	1.40600	.12900	.00507
67	1.40600	.13000	.00510

FIGURE B-7. (Continued)

3 1/2-INCH 317 STAINLESS STEEL BELLONS JM 136
 COMPUTED FITTED MODEL OF ONE CONVOLUTION
 SEPTEMBER 1978

PRELIMINARY GROUPING OF POINTS

I	ITYPE(I)	FIRST POINT		LAST POINT	
		A	Y	A	Y
1	3	1.4200	.0800	1.3060	.0830
2	2	1.4060	.0830	1.3060	.0830
3	1	1.3060	.0830	1.3510	.0875
4	2	1.3510	.0875	1.3010	.0870
5	1	1.3010	.0870	1.2410	.0915
6	2	1.2410	.0915	1.1810	.0970
7	1	1.1810	.0970	1.1210	.1010
8	2	1.1210	.1010	1.0610	.1040
9	3	1.0610	.1040	1.0010	.1090
10	1	1.0010	.1090	1.0410	.1060
11	2	1.0410	.1060	1.1710	.1090
12	3	1.1710	.1090	1.1910	.1200
13	1	1.1910	.1200	1.2310	.1225
14	3	1.2310	.1225	1.2510	.1155
15	2	1.2510	.1155	1.3010	.1245
16	1	1.3010	.1245	1.3500	.1290
17	2	1.3500	.1290	1.3610	.1280
18	3	1.3610	.1280	1.3060	.1240
19	3	1.3060	.1240	1.4200	.1300

FIGURE B-7. (Continued)

3 1/2-INCH 307 STAINLESS STEEL WELLS JM 116
COMPUTER FITTED MODEL OF ONE CONVOLUTION
SEPTEMBER 1970

FITTING DATA FOR GROUP OF POINTS NO. 1

THIS GROUP OF POINTS IS COLINEAR. IT EXTENDS FROM POINT 1 TO POINT 3.

FIGURE B-7. (Continued)

3 1/2-INCH 307 STAINLESS STEEL BELLOWS JM 134
COMPUTER FITTED MODEL OF ONE CYCLOSTATION
SEPTEMBER 1970

FITTING DATA FOR GROUP OF POINTS NO. 2

L1 = 2 L2 = 4 L = 4 K3 = 1.37640 V3 = -.05039 W = .13371

FIGURE B-7. (Continued)

3 1/2-INCH 307 STAINLESS STEEL BELLOWS JW 134
 COMPUTED FITTED MODEL OF ONE CONVOLUTION
 SEPTEMBER 1978

FITTING DATA FOR GROUP OF POINTS NO. 3

MSFIT	ICFIT	FP
1.00017	0	0.F.000
1.00009	M	0.E.000
1.00101	M	0.E.000
1.00027	0	0.E.000
1.00024	0	0.F.000
1.00092	0	0.E.000
1.00051	0	0.E.000
1.00009	0	0.E.000
1.00050	0	0.E.000
1.00050	0	0.E.000

LL = 1 IS THE BEST TRIAL POINT.

L1 = 4 L2 = 8 L3 = 1.00000 V3 = .01179 M = .02065

J = 1 WP = 3 X4 = 1.30440 V4 = .00307 RMS = -.00799312E-00 INTERMEDIATE POINT CHECK

J = 2 WP = 3 X4 = 1.30440 V4 = .00351 RMS = -.7330937E-00 INTERMEDIATE POINT CHECK

J = 3 WP = 3 X4 = 1.30000 V4 = .00500 RMS = .7202705E-05 INTERMEDIATE POINT CHECK

FIGURE B-7. (Continued)

3 1/2-INCH 307 STAINLESS STEEL HELLOYS JW 17A
 COMPUTER FITTED MODEL OF ONE CONVOLUTION
 SEPTEMBER 1978

FITTING DATA FOR GROUP OF POINTS NO. 4

	MSFIT	IPIT	EP
	1.04336	14	0.2.00
	1.04205	14	0.2.00
	1.04074	14	0.2.00
	1.03947	14	0.2.00
	1.03814	14	0.2.00
	1.03687	14	0.2.00
	1.03554	14	0.2.00
	1.03421	14	0.2.00
	1.03288	14	0.2.00
	1.03155	14	0.2.00
	1.03022	14	0.2.00
	1.02889	14	0.2.00
	1.02756	14	0.2.00
	1.02623	14	0.2.00
	1.02490	14	0.2.00

LL	1	2	3	4	5	6	7	8	9	10	11	12	13	14	15	16	17	18	19	20
L1	1.02640	1.02640	1.02640	1.02640	1.02640	1.02640	1.02640	1.02640	1.02640	1.02640	1.02640	1.02640	1.02640	1.02640	1.02640	1.02640	1.02640	1.02640	1.02640	1.02640
J	1	2	3	4	5	6	7	8	9	10	11	12	13	14	15	16	17	18	19	20
MS	0.00750	0.00750	0.00750	0.00750	0.00750	0.00750	0.00750	0.00750	0.00750	0.00750	0.00750	0.00750	0.00750	0.00750	0.00750	0.00750	0.00750	0.00750	0.00750	0.00750
EP	0.00750	0.00750	0.00750	0.00750	0.00750	0.00750	0.00750	0.00750	0.00750	0.00750	0.00750	0.00750	0.00750	0.00750	0.00750	0.00750	0.00750	0.00750	0.00750	0.00750
MS	0.00750	0.00750	0.00750	0.00750	0.00750	0.00750	0.00750	0.00750	0.00750	0.00750	0.00750	0.00750	0.00750	0.00750	0.00750	0.00750	0.00750	0.00750	0.00750	0.00750
EP	0.00750	0.00750	0.00750	0.00750	0.00750	0.00750	0.00750	0.00750	0.00750	0.00750	0.00750	0.00750	0.00750	0.00750	0.00750	0.00750	0.00750	0.00750	0.00750	0.00750
MS	0.00750	0.00750	0.00750	0.00750	0.00750	0.00750	0.00750	0.00750	0.00750	0.00750	0.00750	0.00750	0.00750	0.00750	0.00750	0.00750	0.00750	0.00750	0.00750	0.00750
EP	0.00750	0.00750	0.00750	0.00750	0.00750	0.00750	0.00750	0.00750	0.00750	0.00750	0.00750	0.00750	0.00750	0.00750	0.00750	0.00750	0.00750	0.00750	0.00750	0.00750
MS	0.00750	0.00750	0.00750	0.00750	0.00750	0.00750	0.00750	0.00750	0.00750	0.00750	0.00750	0.00750	0.00750	0.00750	0.00750	0.00750	0.00750	0.00750	0.00750	0.00750
EP	0.00750	0.00750	0.00750	0.00750	0.00750	0.00750	0.00750	0.00750	0.00750	0.00750	0.00750	0.00750	0.00750	0.00750	0.00750	0.00750	0.00750	0.00750	0.00750	0.00750

(FIGURE B-7. (Continued))

3 1/2-INCH 307 STAINLESS STEEL MELLOWS JM 145
 COMPUTER FITTED MODEL OF ONE CORRUPTION
 SEPTEMBER 1979

FITTING DATA FOR GROUP OF POINTS NO. 4

WSTFII	IP11	E0
1.00431	24	0.000
1.00454	24	0.000
100.00001	21	.1000000E+03
100.00001	21	.1000000E+03
100.00001	21	.1000000E+03
100.00001	21	.1000000E+03
100.00001	21	.1000000E+03
100.00001	21	.1000000E+03
100.00001	21	.1000000E+03
100.00001	21	.1000000E+03

LL = 1 TO THE WEST TAIL POINT.

L1 = 21	L2 = 24	L3 = 1.02050	V3 = .03015	R = .07107	
J = 1	WP = 6	K4 = 1.24100	V4 = .09151	EPS = -.19430095E-04	INTERMEDIATE POINT CHECK
J = 2	WP = 4	K4 = 1.23100	V4 = .09700	EPS = -.63020105E-03	INTERMEDIATE POINT CHECK
J = 3	WP = 4	K4 = 1.22100	V4 = .10100	EPS = -.15507552E-02	INTERMEDIATE POINT CHECK
J = 4	WP = 6	K4 = 1.21100	V4 = .10250	EPS = -.152000257E-02	INTERMEDIATE POINT CHECK
J = 5	WP = 6	K4 = 1.20100	V4 = .10250	EPS = -.10007700E-02	INTERMEDIATE POINT CHECK
J = 6	WP = 6	K4 = 1.19100	V4 = .10100	EPS = -.11100047E-02	INTERMEDIATE POINT CHECK

FIGURE B-7. (Continued)

3 1/2-INCH 307 STAINLESS STEEL WFL005 .JM 145
 COMPUTER FITTED MODEL OF ONE CONVOLUTION
 SEPTEMBER 1979

FITTING DATA FOR GROUP OF POINTS NO. 7

MSPLI	IFIT	EP
1.00203	35	0.0000
1.00340	35	0.0000
1.00527	35	0.0000
1.00704	35	0.0000
1.00885	35	0.0000
100.00000	24	-1.00000E+03
100.00000	26	-1.00000E+03
100.00000	24	-1.00000E+03
100.00000	24	-1.00000E+03

LL	1	1c	THE	BEST	TOTAL	POINT.						
L1	=	20	L2	=	35	L = 35	R3 =	1.015433	VJ =	-0.17329	R =	-0.00022
J = 1	WP	=	6	XP	=	1.01100	V4 =	0.02700	EPS =	-0.14005422E-04	INTERMEDIATE	POINT CHECK
J = 2	WP	=	6	XP	=	1.17140	V4 =	-0.03350	EPS =	-0.99954700E-03	INTERMEDIATE	POINT CHECK
J = 3	WP	=	6	XP	=	1.10140	V4 =	-0.02250	EPS =	-0.05000715E-03	INTERMEDIATE	POINT CHECK
J = 4	WP	=	6	XP	=	1.15100	V4 =	-0.02250	EPS =	-0.04750772E-03	INTERMEDIATE	POINT CHECK
J = 5	WP	=	6	XP	=	1.10100	V4 =	0.04051	EPS =	-0.99770700E-04	INTERMEDIATE	POINT CHECK
J = 6	WP	=	6	XP	=	1.13100	V4 =	-0.02750	EPS =	-0.50005500E-03	INTERMEDIATE	POINT CHECK

FIGURE B-7. (Continued)

3 1/2-INCH 307 STAINLESS STEEL BELLWAS JM 136
 COMPUTER FITTED MODEL OF THE CORROSION
 SEPT-NOV 1970

FITTING DATA FOR GROUP OF POINTS NO. 9

RESTIT	IPIT	LP
100.00000	35	.1000000E+03
100.00000	35	.1000000E+03
100.00000	35	.1000000E+03
100.00000	35	.1000000E+03
100.00000	35	.1000000E+03
100.00000	35	.1000000E+03
1.00207	34	0.5000
1.00201	39	0.5000
1.00301	34	0.5000

LL = 9 IS THE BEST TOTAL POINT.

L1 = 3 L2 = 39 L = 39 R3 = 1.00311 R3 = -.03007 M = .13057
 J = 1 WP = 3 RA = 1.12100 RA = .10100 PWS = -.71216693E-03 INTERMEDIATE POINT CHECK
 J = 2 WP = 3 RA = 1.11100 RA = .10300 PWS = -.22135743E-03 INTERMEDIATE POINT CHECK
 J = 3 WP = 3 RA = 1.09100 RA = .10350 PWS = .19007305E-02 INTERMEDIATE POINT CHECK

FIGURE B-7. (Continued)

3 1/2-INCH 307 STAINLESS STEEL BELLNES JM 136
COMPUTER FITTED MODEL OF ONE CONVOLUTION
SEPTEMBER 1979

FITTING DATA FOR GROUP OF POINTS NO. 9

THIS GROUP OF POINTS IS COLLINEAR. IT EXTENDS FROM POINT 39 TO POINT 41.

FIGURE B-7. (Continued)

3 1/2-INCH 307 STAINLESS STEEL WELLS JN 136

COMPUTER FITTED MODEL OF ONE CONVOLUTION

SEPTEMBER 1974

FITTING DATA FOR GROUP OF POINTS NO. 19

L1 = 61	L2 = 66	L = 66	K3 = 1.00196	V3 =	-0.14430	R =	.27004
J = 1	MP = 6	K4 = 1.00100	V4 =	.11104	EPS =		-0.01075302E-03 INTERMEDIATE POINT CHECK
J = 2	MP = 6	K4 = 1.11100	V4 =	.11100	EPS =		-0.11503750E-02 INTERMEDIATE POINT CHECK
J = 3	MP = 6	K4 = 1.12100	V4 =	.11000	EPS =		-0.10677510E-02 INTERMEDIATE POINT CHECK
J = 4	MP = 6	K4 = 1.13100	V4 =	.10500	EPS =		-0.00200330E-03 INTERMEDIATE POINT CHECK

FIGURE B-7. (Continued)

3 1/2-INCH 307 STAINLESS STEEL WELLS J# 136
 COMPUTER FITTED MODEL OF ONE CONVOLUTION
 SEPTEMBER 1970

FITTING DATA FOR GROUP OF POINTS NO. 11

MS117	IF17	EP
1.00051	50	0.E+00
1.00002	50	0.E+00
1.00110	50	0.E+00
1.00149	50	0.E+00
1.00103	50	0.E+00
1.00217	50	0.E+00
1.00251	50	0.E+00
1.00205	50	0.E+00
1.00319	50	0.E+00

LL = 1 IS THE BEST INITIAL POINT.

L1 = 44 2 = 50 L = 90 K3 = 1.15070 Y3 = .16394 R = .05070
 J = 1 NP = 3 K4 = 1.14100 Y4 = .10600 EPS = -.10000030E-04 INTERMEDIATE POINT CHECK
 J = 2 NP = 3 K4 = 1.15140 Y4 = .10500 EPS = -.20000100E-03 INTERMEDIATE POINT CHECK
 J = 3 NP = 3 K4 = 1.10100 Y4 = .10600 EPS = -.2231000E-03 INTERMEDIATE POINT CHECK

FIGURE B-7. (Continued)

3 1/2-INCH 307 STAINLESS STEEL WELDS J4114
COMPUTER FITTED MODEL OF ONE CONVOLUTION
SEPTEMBER 1970

FITTING DATA FOR GROUP OF POINTS NO. 12

THIS GROUP OF POINTS IS COLINEAR. IT EXTENDS FROM POINT 50 TO POINT 52.

FIGURE B-7. (Continued)

3 1/2-INCH 307 STAINLESS STEEL WELLS JW 176
 COMPUTER FITTED MODEL OF ONE CONVOLUTION
 SEPTEMBER 1974

FITTING DATA FOR GROUP OF POINTS NO. 13

L1 = 57	L2 = 56	L = 56	HJ = 1.21376	VJ = .00307	H = .04203
J = 1	NP = 3	K4 = 1.20140	V4 = .12300	EPS = .14120676E-02	INTERMEDIATE POINT CHECK
J = 2	NP = 3	K4 = 1.21140	V4 = .12450	EPS = .17325736E-02	INTERMEDIATE POINT CHECK
J = 3	NP = 3	K4 = 1.22140	V4 = .12500	EPS = .60300822E-03	INTERMEDIATE POINT CHECK

FIGURE B-7. (Continued)

3 1/2-INCH 307 STAINLESS STEEL WELLS JW 130
COMPUTER FITTED MODEL OF ONE CONVICTION
SEPTEMBER 1978

FITTING DATA FOR GROUP OF POINTS NO. 14

THIS GROUP OF POINTS IS COLINEAR. IT EXTENDS FROM POINT 56 TO POINT 58.

FIGURE B-7. (Continued)

3 1/2-INCH 307 STAINLESS STEEL WELLS JM 13A
 COMPUTER FITTED MODEL OF ONE CIRCVOLUTION
 SEPTEMBER 1970

FITTING DATA FOR GROUP OF POINTS NO. 14

L1 = 50	L2 = 63	L = 63	X3 =	1.26057	Y3 =	.18752	H =	.05100
J = 1	WP = 6	X4 =	1.26140	Y4 =	.11400	EPS =	.96022352E-03	INTERMEDIATE POINT CHECK
J = 2	WP = 4	X4 =	1.27160	Y4 =	.11000	EPS =	.13050575E-02	INTERMEDIATE POINT CHECK
J = 3	WP = 6	X4 =	1.28140	Y4 =	.11500	EPS =	.80749070E-03	INTERMEDIATE POINT CHECK
J = 4	WP = 4	X4 =	1.29160	Y4 =	.11500	EPS =	.51000402E-03	INTERMEDIATE POINT CHECK

FIGURE B-7. (Continued)

3 1/2-INCH 307 STAINLESS STEEL WELLS JM 136
 COMPUTED FITTED MODEL OF ONE CONVECTION
 SEPTEMBER 1970

FITTING DATA FOR GROUP OF POINTS NO. 16

MSFIT	IFIT	EP
1.00704	70	0.2E+00
1.00454	70	0.2E+00
1.00232	70	0.2E+00
1.00144	70	0.2E+00
1.00134	70	0.2E+00
1.00614	70	0.2E+00
1.00271	70	0.2E+00
100.00000	63	.1000000E+03
100.00000	63	.1000000E+03

LL = 4 IS THE BEST INITIAL POINT.

L1 = 63	L2 = 70	L3 = 70	L4 = 1.33005	V3 = .06037	R = .06373
J = 1	WP = 6	X4 = 1.30140	V4 = .12450	EPS = -.30750122E-03	INTERMEDIATE POINT CHECK
J = 2	WP = 4	X4 = 1.31140	V4 = .12450	EPS = -.57301171E-03	INTERMEDIATE POINT CHECK
J = 3	WP = 6	X4 = 1.32140	V4 = .13200	EPS = -.21500402E-03	INTERMEDIATE POINT CHECK
J = 4	WP = 6	X4 = 1.33140	V4 = .13300	EPS = -.71240724E-05	INTERMEDIATE POINT CHECK
J = 5	WP = 6	X4 = 1.34140	V4 = .13240	EPS = .12174153E-03	INTERMEDIATE POINT CHECK
J = 6	WP = 6	X4 = 1.35140	V4 = .13050	EPS = .13520959E-03	INTERMEDIATE POINT CHECK

FIGURE B-7. (Continued)

3 1/2-INCH 307 STAINLESS STEEL WELLS IN 136
 COMPUTER FITTED MODEL OF ONE CONVOLUTION
 SEPT-NOV 1970

FITTING DATA FOR GROUP OF POINTS NO. 17

WSTF11	IFIT	EP
1.00901	72	0.0000
1.00903	72	0.0000
1.00904	72	0.0000
1.00906	72	0.0000
1.00912	72	0.0000
1.00914	72	0.0000
1.00916	72	0.0000
1.00921	72	0.0000
1.00926	72	0.0000

LL = 1 IS THE BEST TOTAL POINT.

L1 = 7 L2 = 72 L3 = 72 L4 = 1.36240 V3 = 0.14033 H = 0.02030

J = 1 WP = 1 SA = 1.35000 VA = 0.12009 EPS = -0.0030523E-05 INTERMEDIATE POINT CHECK

FIGURE B-7. (Continued)

3 1/2-INCH 307 STAINLESS STEEL WELLS JM 196
COMPUTER FITTED MODEL OF ONE CONVOLUTION
SEPTEMBER 1970

FITTING DATA FOR GROUP OF POINTS NO. 14

THIS GROUP OF POINTS IS COLINEAR. IT EXTENDS FROM POINT 72 TO POINT 74.

FIGURE B-7. (Continued)

3 1/2-INCH 307 STAINLESS STEEL WELLOWS JM 176
COMPUTER FITTED MODEL OF ONE CONVOLUTION
SEPTEMBER 1970

FITTING DATA FOR GROUP OF POINTS NO. 10

THIS GROUP OF POINTS IS COLINEAR. IT EXTENDS FROM POINT 74 TO POINT 76.

FIGURE B-7. (Continued)

• • • PRINTOUT OF INPUT DATA • • •

• BOUNDARY DATA •

INITIAL EDGE		FINAL EDGE	
DISPLACEMENT =	0.00000	DISPLACEMENT =	-1.00000
DISPLACEMENT =	0.00000	DISPLACEMENT =	0.00000
SLOPE =	0.00000	SLOPE =	0.00000
BOUNDARY ANGLE =	0.70000	BOUNDARY ANGLE =	0.00000

ELASTIC PARAMETERS ARE THE SAME FOR EVERY PART IN THIS SHELL. THEIR VALUES ARE
YOUNG'S MODULUS = .30000E+08 POUNDS PER SQUARE INCH
POISSON'S RATIO = .30000

LOADING PARAMETERS ARE THE SAME FOR EVERY PART IN THIS SHELL. THEIR VALUES ARE
PRESSURE = 0.00000 POUNDS PER SQUARE INCH
UNIT WEIGHT OF MATERIAL = 0.00000 POUNDS PER CUBIC INCH
DEAD WEIGHT = 0.00000 POUNDS PER SQUARE INCH

FIGURE B-7. (Continued)

3 1/2-INCH 307 STAINLESS STEEL HELLO-S JM 116
 COMPUTER FITTED MODEL OF ONE CONVOLUTION
 SEPTEMBER 1979

PART	TYPE	NO. OF SEGMENTS	C O O R D I N A T E S		D I M E N S I O N S	A I N C H E S	R. I N C H E S	C. I N C H E S	T H I C K N E S S. I N C H E S	I N C R E M E N T V A L U E
			INITIAL	FINAL						
1	CONICAL	1	-175.71045	-103.043132	INCHES	1.42600	.04011			
2	TRUNCAL	1	-175.71045	-151.12167	INCHES	1.37600	-.13371			
3	TRUNCAL	1	-151.12167	-203.70579	INCHES	1.36600	-.02865			
4	TRUNCAL	1	-203.70579	-148.73357	INCHES	1.27500	-.05394			
5	TRUNCAL	1	-148.73357	-198.96491	INCHES	1.20500	-.04307			
6	TRUNCAL	1	-198.96491	-148.73357	INCHES	1.15600	-.07167			
7	TRUNCAL	1	-148.73357	-198.96491	INCHES	1.00300	-.00022			
8	TRUNCAL	1	-198.96491	-148.73357	INCHES	1.06100	-.13657			
9	TRUNCAL	1	-148.73357	-198.96491	INCHES	1.09100	-.09500			
10	TRUNCAL	1	-198.96491	-148.73357	INCHES	1.15000	-.27600			
11	TRUNCAL	1	-148.73357	-198.96491	INCHES	1.15000	-.05070			
12	CONICAL	1	-31.07100	10.14010	INCHES	1.01100	-.01170			
13	CONICAL	1	-31.07100	19.67006	INCHES	1.01100	-.01170			
14	CONICAL	1	19.67006	34.00000	INCHES	1.22010	-.04203			
15	TRUNCAL	1	19.67006	20.00000	INCHES	1.26000	-.02000			
16	TRUNCAL	1	34.00000	20.00000	INCHES	1.33000	-.05373			
17	TRUNCAL	1	20.00000	-0.13012	INCHES	1.36000	-.02030			
18	CONICAL	1	-0.13012	-2.00000	INCHES	1.40000	-.02305			
19	CONICAL	1	-2.00000		INCHES	1.50000	-.04005			

FIGURE B-7. (Continued)

3 1/4-INCH 907 STAINLESS STEEL WELLOWS JM 136
 COMPUTER FITTED MODEL OF ONE CIRCUMFERENCE
 SEPTEMBER 1970

• VARIABLE THICKNESS •

PART 1 COORDINATE THICKNESS	0.0000 .00527	.02004 .00523	.00011 .00535					
PART 2 COORDINATE THICKNESS	-175.71005 .00535	-107.43132 .00504						
PART 3 COORDINATE THICKNESS	-103.43132 .00504	-179.43450 .00504	-164.48147 .00442	-154.90044 .00406	-121.12167 .00407			
PART 4 COORDINATE THICKNESS	-151.12167 .00407	-157.08206 .00510	-164.10301 .00503	-175.00227 .00503	-185.75101 .00494	-196.61936 .00510	-205.79574 .00506	
PART 5 COORDINATE THICKNESS	-205.79574 .00506	-203.46700 .00503	-194.35066 .00499	-185.20003 .00523	-174.27505 .00527	-167.25407 .00515	-159.08308 .00499	-148.73257 .00513
PART 6 COORDINATE THICKNESS	-148.73257 .00513	-146.66694 .00515	-150.02317 .00523	-167.35219 .00523	-175.32847 .00507	-183.20301 .00510	-191.25500 .00503	-198.90691 .00495
PART 7 COORDINATE THICKNESS	-198.90691 .00495	-190.20400 .00404	-197.70503 .00404	-183.59336 .00403	-174.50602 .00494	-169.26230 .00490	-161.77709 .00403	-148.26005 .00503
PART 8 COORDINATE THICKNESS	-168.26005 .00503	-163.40330 .00503	-164.00300 .00523	-174.46702 .00510	-189.16042 .00523			
PART 9 COORDINATE THICKNESS	0.0000 .00523	.00250 .00520	.00500 .00510					
PART 10 COORDINATE THICKNESS	-6.16660 .00514	.07024 .00503	.00573 .00527	4.22274 .00523	9.29229 .00510	10.10910 .00500		
PART 11 COORDINATE THICKNESS	19.10010 .00510	0.10000 .00507	-.00710 .00513	-1.30701 .00517	-31.07100 .00503			

FIGURE B-7. (Continued)

- (b) (1) First three printed lines are the job identification cards supplied by the user.
- (2) The number of points, vertices, and the tolerance are then listed.
- (3) The coordinates and thicknesses read in are then given. Vertices, if any are specified, are identified.
- (c) (1) First three lines are the job identification cards supplied by the user.
- (2) The preliminary grouping of points is given. This includes the type and first and last point of each group.

The following information is provided for each group of points.

- (d) (1) First three lines are the job identification cards supplied by the user.
- (2) If trial inflection points are tested for a group of points, the vectors BSTFIT, IFIT, and EP are printed out and the best trial point identified.
- (3) The indices of the two points which determine a fitting circle (L1 and L) are identified along with the index of the last point of the group of points (L2) and the center coordinates and radius of the circle.
- (4) Intermediate point checks are given for each point between K(L1) and K(L). The distance each point is from the circle is also given.
- (5) Following point checks are given if the circle is extended.

The input data for NONLIN generated by FIT is then given.

- (e) (1) First three printed lines are the job identification cards supplied by user.
- (2) Boundary conditions are then listed along with boundary rotation angles.
- (3) If elastic parameters are the same for every part in the shell, their values are given.
- (4) If loading parameters are the same for every part in the shell, their values are given.
- (f) (1) First three printed lines are the job identification cards.
- (2) Geometry of shell is now listed. The following items are given: part number, type of part, number of segments,

coordinates, radii a, b, and c, and thickness data. If thickness is constant, a YES is printed along with the value. If thickness is variable, a NO is printed and entry under value is left blank. If there are more than 40 parts in the composite shell, the numbers over 40 are listed on the next page.

- (g) If Young's modulus and Poisson's ratio are not constant for the shell, then the following is printed out. Otherwise go to (h).
- (1) First three printed lines are the job identification cards.
 - (2) The part number, type, Young's modulus, and Poisson's ratio are then given.

If there are more than 40 parts in the composite shell, the numbers over 40 are listed on the next page.

- (h) If the heading parameters are not constant then the following is printed out. Otherwise go to (i).
- (1) First three printed lines are the job identification cards.
 - (2) The part number, type, normal pressure, weight density, and dead loading are then given.

If there are more than 40 parts in the composite shell, the numbers over 40 are listed on the next page.

- (i) If at least one of the parts has variable thickness, then the following is printed out.
- (1) First three printed lines are the job identification cards.
 - (2) The part number, independent coordinates, and thickness for each part which has variable thickness are then listed.

Listings of FIT and Associated Program and Subroutines

The basic total computational package associated with the subroutine FIT consists of the program DATA and the subroutines FIT, EXITD, and ANGLE. DATA is the name given to a version of the program NONLIN modified for use with FIT. EXITD and ANGLE are smaller subroutines called from FIT to facilitate numerous routine calculations required during the fitting process described above. This set of programs, the FORTRAN IV listings of which follow, allows the user to generate a complete and accurate set of input data which can in turn be used with NONLIN (and/or the PLT version of NONLIN) to obtain a detailed theoretical analysis of a bellows or diaphragm.


```

00011 IF (END=5) GO=, 947
00012 CONTINUE
00013 KFIT = A
00014
00015 MFAD(5,53n) TITLE2, TITLE3
00025 WRITE(6,53n)
00031 WRITE(6,53n)
00035 WRITE(6,53n)
00041 WRITE(6,53n)
00045 WRITE(6,53n)
00051 WRITE(6,53n)
00052 WRITE(6,53n)
00066 GO TO (35%, 36%, 34%, 37%, 37%), NTIME

C
COMMENT SET NUMBER 2 ( CARDS = 1 )
COMMENT BOUNDARY DATA AT INITIAL EDGE
C
35% MFAD(5,53n) (ROUND(I), 6A(I), I = 1, 4)
COMMENT SET NUMBER 3 ( CARDS = 1 )
COMMENT BOUNDARY DATA AT FINAL EDGE
C
HEAD(5,53n) (ROUND(I), 6A(I), I = 5, 8)
COMMENT SET NUMBER 4 ( CARDS = 1 )
COMMENT ANGLE IN DEGREES AT INITIAL AND FINAL BOUNDARIES
C
READ(5,56%) ALL, ALIA
IF (ROUND(1)) -EQ. NAME1(1) -OR. ROUND(1) -EQ. NAME1(2) 015.000
01% IF (ROUND(2)) -EQ. NAME1(1) -OR. ROUND(2) -EQ. NAME1(2) 016.000
01% IF (ROUND(3)) -EQ. NAME1(1) -OR. ROUND(3) -EQ. NAME1(2) 017.000
01% IF (ROUND(4)) -EQ. NAME1(1) -OR. ROUND(4) -EQ. NAME1(2)
01% IF (ROUND(5)) -EQ. NAME1(1) -OR. ROUND(5) -EQ. NAME1(2) 018.000
01% IF (ROUND(6)) -EQ. NAME1(1) -OR. ROUND(6) -EQ. NAME1(2) 019.000
01% IF (ROUND(7)) -EQ. NAME1(1) -OR. ROUND(7) -EQ. NAME1(2) 020.000
01% IF (ROUND(8)) -EQ. NAME1(1) -OR. ROUND(8) -EQ. NAME1(2) 021.000
01% CONTINUE
C
COMMENT CONTROL CARD
COMMENT SET NUMBER 5 ( CARDS = 1 )
READ(5,56) IRR4, ITER, NOUNUM, PLOT, INTRON, INTVAL,
LEVEL1, LEVEL2, FRP, CONVER, NUMBAR, (INFOUA(1),
I = 1, 8)
IF (IRR4 -EQ. 0) KFIT = 5
MDFUNC = A
INPUN = 0
TPVIN = 0
NDE = 6
IF (INFOUA(1) -GT. 0) NDE = 8
MPL = NDE + 1
MFM = FLOAT(INFOUA(1))
IF (ABS(ERP) -EQ. 0.0) ERP = 1.E - 05
IF (PLOT -RT. 10) GO TO 003

```

```

C COMMENT SET NUMBER 6 ( CARDS = 1 )
C COMMENT INDICATE BY YES OR NO WHETHER ELASTIC PARAMETERS ARE SAME FOR EACH
C COMMENT PART. IF YES, ON SAME CARD, GIVE VALUES. IF NO, READ THEM IN AFTER SET
C COMMENT NUMBER 6.
C
000327 READ(S,6) MELAS, YOUNG, VUISON
000340 IF(MELAS.EQ. MARKC .OR. MELAS.EQ. MARKD) RPT6, H09
000350 CONTINUE
C
C COMMENT SET NUMBER 7 ( CARDS = 1 )
C COMMENT INDICATE BY YES OR NO WHETHER PRESSURE LOADINGS, DENSITY OF MATERIAL,
C COMMENT OR DEAD LOAD ON SHELL IS THE SAME FOR EACH PART. IF YES, ON SAME
C COMMENT CARD, GIVE VALUES. IF NO, READ THEM IN AFTER SET NUMBER 10.
C
000350 READ(S,7) MPRES, PRESS, DENSITY, DEAN
000364 IF(MPRES.EQ. MARKC .OR. MPRES.EQ. MARKD) R225, 010
000374 CONTINUE
C
C COMMENT SET NUMBER 8 ( CARDS = NUMBER OF PARTS )
C COMMENT TYPE OF SHELL, INITIAL AND FINAL COORDINATES, NUMBER OF SEGMENTS,
C COMMENT NUMBER OF POINTS, YES OR NO FOR THICKNESS DISTRIBUTION, IF
C COMMENT YES, THEN SPECIFY VALUE. IF NO, SPECIFY NUMBER OF POINTS WHICH
C COMMENT SPECIFICS DISTRIBUTION.
C
C COMMENT FOR CYLINDER S(L) IS EITHER 90.0 DEGREES (NORMAL OUT) OR
C COMMENT 270.0 DEGREES (NORMAL IN). S(L) IS LEFT BLANK.
C
C COMMENT FOR CONE S(L) IS THE ANGLE (DEGREES) WHICH THE NORMAL MAKES WITH
C COMMENT THE AXIS OF THE SHELL. S(L) IS LEFT BLANK.
C
000374 IF(INFIT.EQ. 0) GO TO 000409
000375 CALL FIT (VN,IPAR,S1,SK,ISS,INT,VANTIK,TDIST,RP,YP,EYN,PSR,IBRM,
* MPRES,MELAS,TITLE1,TITLE2,TITLE3)
000417 CONTINUE
000417 IF(IARM .GT. 60) GO TO 002
000421 IF(INFIT .GT. 0) GO TO 00000
000425 READ(S,8) (NAME2(L), S(L), SK(L), IPAR(L), INT(L),
* TDIST(L), VMI(L), VANTIK(L), L = 1, IBRM)
C
C COMMENT DETERMINE IF SPELLING OF SHELL PARTS IS CORRECT.
C
DO 325 L = 1, IBRM
IF(NAME2(L).EQ. NAME1(L)) .OR.
* NAME2(L).EQ. NAME1(2)) .OR.
* NAME2(L).EQ. NAME1(3)) .OR.
* NAME2(L).EQ. NAME1(4)) .OR.
* NAME2(L).EQ. NAME1(5)) .OR.
* NAME2(L).EQ. NAME1(6)) .OR.
* NAME2(L).EQ. NAME1(7)) .OR.
* NAME2(L).EQ. NAME1(8)) 325, 001
325 CONTINUE
000522 CONTINUE
000525 CONTINUE
C

```

```

000525 COMMENT DETERMINE IF INIST(L) CONTAINS CORRECT SPLI TAG.
000527 C
000537 DO 326 L = 1, IHRM
000542 IF (INIST(L) .EQ. MARKC .OR. TUIST(L) .EQ. MARKU) 326, 804
000543 CONTINUE
000544 PLOPT = A
000545 DO 123 I = 1, IHRM
000546 PLOPT = PLOPT + IPAN(I) + INI(I)
000547 CONTINUE
000548 IF (PLOPT .GT. 340) GO TO 805
000549 MPARTS = A
000550 DO 85 J = 1, IHRM
000551 MPARTS = MPARTS + IPAN(J)
000552 CONTINUE
000553 IF (MPARTS .GT. 60) GO TO 806
000554 DO 327 L = 1, IHRM
000555 VARTIK(L) = IANS * VARTIK(L)
000556 CONTINUE
000557 DO 300 L = 1, IHRM
000558 IF (IDIST(L) .EQ. MARKC) GO TO 329
000559 IF (VARTIK(L) .LT. 2 .OR. VARTIK(L) .GT. 10) GO TO 807
000560 GO TO 300
000561 IF (VARTIK(L) .NE. 0) GO TO 808
000562 CONTINUE
000563 C
000564 COMMENT SET ISS(L) MATRIX. THIS SPECIFES CODE NUMBER FOR SHELL TYPES.
000565 C
000566 COMMENT CROWN = 1
000567 COMMENT CYLINDRICAL = 2
000568 COMMENT SPHERICAL = 3
000569 COMMENT PARABOLOIDAL = 4
000570 COMMENT ELLIPSOIDAL = 5
000571 COMMENT CONICAL = 6
000572 COMMENT TOROIDAL = 7
000573 COMMENT VARCHLINDER = 8
000574 C
000575 IF (KFIT .GT. 0) GO TO 8910
000576 DO 150 L = 1, IHRM
000577 DO 150 I = 1, A
000578 IF (NAME2(L) .NE. NAME3(I)) GO TO 150
000579 ISS(L) = I
000580 CONTINUE
000581 P(0) CONTINUE
000582 C
000583 COMMENT DETERMINE IF CYLINDRICAL SHELL 2 HAS VARTIK(L) .EQ. 0 AND IF
000584 COMMENT VARCHLINDER SHELL 8 HAS VARTIK(L) .NE. 0.
000585 C
000586 DO 994 L = 1, IHRM
000587 ISM = ISS(L)
000588 GO TO (994, 995, 994, 994, 994, 994, 994, 994, 994, 994), ISM
000589 IF (VARTIK(L) .NE. 0) GO TO 808
000590 GO TO 994
000591 IF (VARTIK(L) .EQ. 0) GO TO 807
000592 CONTINUE
000593 C

```

```

C          SET NUMBER 9          ( CAMDS = NUMBER OF PARTS )
COMMENT   READ IN A. D. C
C
COMMENT   FUM (MINI AND) SOMEONE ONLY SPECIFY A
C
COMMENT   FOM CYLINDER A IS RADIUS, B IS LENGTH
C
COMMENT   FUM CONE A IS RADIUS AT INITIAL, R IS SLANT LENGTH
C
COMMENT   FOM ELLIPSE C .ST. 0.0 INDICATES TORNIUAL SHPLL OF ELLIPTICAL CROSS
COMMENT   SECTION PROVIDED A .WE. R.
C
000661   IF (KPI1 .GT. 0) GO TO 89020
000662   RFAD(S,562) (VN(20L), VN(30L), VN(40L), L = 1, IRRM)
000704   CONTINUE
C
COMMENT   SET NUMBER 10
COMMENT   READ IN YOUNG'S MODULUS AND POISSON'S RATIO ONLY IF NOT THE SAME FOR
COMMENT   EACH PART.
C
000704   IF (NFLAS .EQ. MARKC) GO TO 400
000706   IF (KPI1 .GT. 0) GO TO 89030
000711   READ(S,564) (EYM(L), PSR(L), L = 1, IRRM)
000725   CONTINUE
000725   GO TO 402
000726   UN 401 L = 1, IRRM
000730   EYM(L) = YOUNG
000732   PSR(L) = POISON
000733   CONTINUE
C
COMMENT   SET NUMBER 11
COMMENT   READ IN PRESSURE LOADING, DENSITY OF MATERIAL, AND DEAD WEIGHT ONLY IF
COMMENT   THEY ARE NOT THE SAME FOR EACH PART.
C
000735   IF (UPRES .EQ. MARKC) GO TO 4025
000737   IF (KPI1 .GT. 0) GO TO 89040
000742   READ(S,564) (VN(50L), VN(60L), VN(70L), L = 1, IRRM)
000763   CONTINUE
000763   GO TO 4024
000764   UN 503 L = 1, IRRM
000766   VN(50L) = PRESS
000771   VN(60L) = DENSITY
000773   VN(70L) = DEAD
000776   CONTINUE
C
COMMENT   SET NUMBER 12
COMMENT   READ IN VARIABLE THICKNESSES
C
001000   CONTINUE
001000   IF (KPI1 .GT. 0) GO TO 89050
001003   DO 403 L = 1, IRRM
001004   IF (VARTK(L) .EQ. 0) GO TO 403
001005   NPNT = VARTK(L)
001007   RFAD(S,565) (RPI(L), I = 1, NPNT)

```

```

00102J      WFAU(5,565) (V(L), I = 1, NPNT)
00100      CONTINUE
00104J      CONTINUE
00104J      IF (ISS(I,MPM) .GT. 1) GO TO 86
00104J      NTRY = NPARTS + 1
00105J      APMOR = NPARTS - 1
00105J      GO TO 47
00105J      NTRY = NPARTS
00105J      NERRR = NPARTS
C
C      COMMENT SET NUMBER 13
C
001054      A7 IF (PLOT .EQ. 0) GO TO 1238
001055      WFAU(5,525) (PLOT(I), I = 1, PLOT)
001076      WFAU(5,526) (JMPNT(I), I = 1, PLOT)
001103      CONTINUE
001104      IA(1) = 1
001105      IA(2) = 3
001106      IA(3) = 5
001106      IA(4) = 7
001107      IM(S) = 1
001116      IA(6) = 3
001111      IA(7) = 5
001112      IA(8) = 7
001113      IF (BOUND(1)) .NE. NAMEH(1)) IA(1) = 2
001116      IF (BOUND(2)) .NE. NAMEH(2)) IA(2) = 4
001121      IF (BOUND(3)) .NE. NAMEH(3)) IA(3) = 6
001124      IF (BOUND(4)) .NE. NAMEH(4)) IA(4) = 8
001127      IF (BOUND(5)) .NE. NAMEH(5)) IA(5) = 2
001132      IF (BOUND(6)) .NE. NAMEH(6)) IA(6) = 4
001135      IF (BOUND(7)) .NE. NAMEH(7)) IA(7) = 6
001140      IF (BOUND(8)) .NE. NAMEH(8)) IA(8) = 8
001143      WRITE(6,543)
001147      WRITE(6,546)
001154      WRITE(6,545)
001157      IF (IA(1)) .EQ. 1 .AND. IA(5) .EQ. 1) GO TO 121
001164      IF (IA(1)) .EQ. 1 .AND. IA(5) .EQ. 2) GO TO 122
001174      IF (IA(1)) .EQ. 2 .AND. IA(5) .EQ. 1) GO TO 123
001203      IF (IA(1)) .EQ. 2 .AND. IA(5) .EQ. 2) GO TO 124
001221      WRITE(6,551) 6A(1), 6B(5)
001222      GO TO 125
001232      WRITE(6,542) 6A(1), 6B(5)
001233      GO TO 125
001243      WRITE(6,543) 6A(1), 6B(5)
001244      GO TO 125
001244      WRITE(6,544) 6A(1), 6B(5)
001254      IF (IA(2)) .EQ. 3 .AND. IA(6) .EQ. 3) GO TO 126
001263      IF (IA(2)) .EQ. 3 .AND. IA(6) .EQ. 4) GO TO 127
001271      IF (IA(2)) .EQ. 4 .AND. IA(6) .EQ. 3) GO TO 128
001306      IF (IA(2)) .EQ. 4 .AND. IA(6) .EQ. 4) GO TO 129
001306      WRITE(6,543) 6A(2), 6B(6)
001316      GO TO 130
001317      WRITE(6,542) 6A(2), 6B(6)
001327      GO TO 130
001334      WRITE(6,543) 6A(2), 6B(6)

```

```

001340      GO TO 131
001341      WRITE(4,540)  W(2), G(16)
001342      IF (IA(3) .EQ. 5 .AND. I(7) .FO. 5) GO TO 131
001343      IF (IA(3) .EQ. 5 .AND. I(7) .FO. 6) GO TO 132
001344      IF (IA(3) .EQ. 5 .AND. I(7) .FO. 5) GO TO 133
001345      IF (IA(3) .EQ. 6 .AND. I(7) .FO. 6) GO TO 134
001346      WRITE(4,551)  G(13), G(17)
001347      GO TO 135
001348      WRITE(4,540)  G(13), G(17)
001349      GO TO 135
001350      WRITE(4,547)  G(13), G(17)
001351      GO TO 135
001352      WRITE(4,550)  G(13), G(17)
001353      IF (I(4) .EQ. 4) GO TO 140
001354      IF (IA(4) .EQ. 7 .AND. I(8) .EQ. 7) GO TO 134
001355      IF (IA(4) .EQ. 7 .AND. I(8) .EQ. 8) GO TO 137
001356      IF (IA(4) .EQ. 8 .AND. I(8) .EQ. 7) GO TO 138
001357      IF (IA(4) .EQ. 8 .AND. I(8) .FO. 8) GO TO 139
001358      WRITE(4,541)  G(14), G(14)
001359      GO TO 141
001360      WRITE(4,542)  G(14), G(14)
001361      GO TO 140
001362      WRITE(4,543)  G(14), G(14)
001363      GO TO 140
001364      WRITE(4,544)  G(14), G(14)
001365      WRITE(4,549)  A(L), A(L)
001366      IF (NDE .EQ. 4) GO TO 100
001367      I(4) = I(4)
001368      I(5) = I(4)
001369      I(6) = I(7)
001370      G(4) = G(5)
001371      G(5) = G(4)
001372      G(6) = G(7)
001373      MM = NDE/?
001374
001375      C
001376      COMMENT THIS LOOP SETS UP IA(4), IA(5), IA(6) FOR NDE = 6 AND
001377      COMMENT IA(5), IA(6), IA(7), IA(8) FOR NDE = 8.
001378      C
001379      M = MM + 1
001380      L = 1
001381      DO 104 IK = M, NDE
001382      DO 102 N = L, NDE
001383      DO 101 J = 1, MM
001384      IF (IA(J) .EQ. N) GO TO 102
001385      CONTINUE
001386      GO TO 103
001387      CONTINUE
001388      L = M + 1
001389      IA(4) = M
001390      CONTINUE
001391
001392      C
001393      COMMENT THIS LOOP SETS UP IB(4), IB(5), IB(6) FOR NDE = 6 AND
001394      COMMENT IB(5), IB(6), IB(7), IB(8) FOR NDE = 8.
001395      C
001396      L = 1

```



```

002170 WRITE(6,7A1) L, NAME$1(15M), NAME$2(15M), IPAR(1), SI(1), SK(1),
002230 GO TO 395
002235 IF (VARTIC(L) .EQ. 0) GO TO 4045
002240 WRITE(6,7A2) L, NAME$1(15M), NAME$2(15M), IPAR(1), SI(1), SK(1),
002245 UNIT(1), UNIT(2), VN(2), VN(3), VN(4),
002250 MARK$
002255 GO TO 395
002300 WRITE(6,7A3) L, NAME$1(15M), NAME$2(15M), IPAR(1), SI(1), SK(1),
002305 UNIT(1), UNIT(2), VN(2), VN(3), VN(4),
002310 MARK$, VN(5)
002315 CONTINUE
002320 CONTINUE
002325 CONTINUE
002330 CONTINUE
C
C COMMENT INFORMATION IF SMALL PRINTS ARE CONTINUOUS.
C
002340 WRITE(6,7A4)
002345 L=0
002350 IF (L .GT. 1000) GO TO 13
002355 ISMISS(L)
002360 ALFA = SIN(1000)
002365 ALFA = SIN(1000)
002370 A = VN(2)
002375 A = VN(3)
002380 GO TO (3, 4, 5, 6, 7, 8, 9, 0), ISM
002385 RI = A
002390 RF = RI
002395 GO TO 10
002400 RI = A*SIN(ALFA)
002405 RF = A*SIN(ALFA)
002410 GO TO 10
002415 RI = A
002420 RF = A*TAN(ALFA)/TAN(ALFA)
002425 GO TO 10
002430 RI = 1
002435 IF (1 .EQ. 2) GO TO 70
002440 SIN = SIN(ALFA)
002445 GO TO 77
002450 SIN = SIN(ALFA)
002455 RI = VN(4) * COS(1/(A/1000) * (1.0 - (A/1000)*SIN(SIN)
002460 IF (1 .EQ. 2) GO TO 70
002465 RI = R
002470 GO TO 75
002475 RF = R
002480 CONTINUE
002485 GO TO 10
002490 RI = A * COS(ALFA)
002495 RF = A * COS(ALFA)
002500 GO TO 10
002505 RI = A * COS(ALFA)
002510 IF (TIME .EQ. 1) GO TO 11
002515 WRITE

```

```

002507      RTIME=1
002510      GO TO 3
002511      II = 1
002512      RTIME=1
002513      IF (AMS(MF1 - M12) .GT. 0.0025) GO TO 012
002514      RTIME=2
002515      M11=M12
002516      GO TO 3
002517      13 CONTINUE
002518      IF (NELAS .EQ. MARKC) GO TO 000
002519      IN 442 II * 1. 2
002520      IF (II .EQ. 1) GO TO 403
002521      IF (IRRM .LT. 41) GO TO 400
002522      RTIME = 3
002523      GO TO 340
002524      WRITE(6,540)
002525      WRITE(6,577)
002526      GO TO (3600, 3600), II
002527      IMIN = 1
002528      IMAZ = IRRM
002529      IF (IRRM .GT. 40) IMAZ = 40
002530      GO TO 401
002531      IMIN = 41
002532      IMAZ = IRRM
002533      DO 300 L = IMIN, IMAZ
002534      ISM = ISS(L)
002535      WRITE(6,576) L, NAMES(IISM), NAMES2(IISM), EYM(L), PSA(L)
002536      CONTINUE
002537      IF (MPRES .EQ. MARKC) GO TO 4005
002538      ON 1702 IT = 1, 2
002539      IF (II .EQ. 1) GO TO 1703
002540      IF (IRRM .LT. 41) GO TO 4005
002541      RTIME = 4
002542      GO TO 350
002543      WRITE(6,603)
002544      WRITE(6,584)
002545      GO TO (7030, 7031), II
002546      IMIN = 1
002547      IMAZ = IRRM
002548      IF (IRRM .GT. 40) IMAZ = 40
002549      GO TO 7032
002550      IMIN = 41
002551      IMAZ = IRRM
002552      DO 700 L = IMIN, IMAZ
002553      ISM = ISS(L)
002554      WRITE(6,605) L, NAMES(IISM), NAMES2(IISM), (VMT(L), I = 9, 7)
002555      CONTINUE
002556      1703 CONTINUE
002557      C
002558      COMMENT PUT YP(1,1) IN VP(1,1)
002559      C
002560      ON 955 L = 1, IRRM
002561      IF (VARTIM(L) .EQ. 0) GO TO 950

```



```

000025 SIMULATING FIT (VM,IPAR,SI,SH,ISS,INT,VARTIK,TOJCT,ED,YP,ETM,PSA,I
1 NAME,NAME,S,NFLAS,TITLE1,TITLE2,TITLE3)
DIMENSION
1 INT(40) • VARTIK(60) • TOJCT(60) •
2 EP(10,50) • VP(10,60) • EYM(40) •
3 VMOD(10) • PRAT(10) • JPLAS(60) •
4 NAME$1(10) • NAME$1(10) • NFU(10) •
5 NAME$1(10) • FP(4) • ZI(PT) •
6 AT(2M) • IF(1,1) • PSK(40) •
7 ATWICK(400) • KTY(10) • VMV(9) •
8 RSTPT(10) • LPC(3) • LPH(3) •
9 TITLE1(20) • TITLE2(20) • TITLE3(20) •
10 QPJM(62) • A(3,3) • A(3) •
11 LTEMP(7) • IPAR(40) • K(60) •
12 Y(400) • IV(20) • IPMT(400) •
13 ITYPE(60) • ISF(62) • ISF(62) •
14 UNITD(2) • VM(7,60) • SI(60) •
15 SA(60) • ISS(60) • NAME$1(10) •
16 NAME$2(8) • EX(400) • VV(400) •
17 X(400) • VO(400) • ITITLE(10) •
DATA ( MARKC = 2*VE ), ( MARKD = 2*MD )
DATA ( RPO = 0.1745329252E-01 ), ( DPR = 57.29577951 )
REAL NCOMP
INTEGER VARTIK,TOJST,NFLCT,VNPLCT, TITLE1, TITLE2, TITLE3
C
C COMMENT INPUT OF DATA
C
000025 READ (5,2430) NPTS,NV,ITNT
000025 READ (5,2440) EPSI,XTRANS,VTRANS,NFLCT,VNPLCT
000025 READ (5,2450) H1,V1,V1,PR,VM,PRS,DW,DWS
000025 X(1),X(1)
000025 V(1),V(1)
000025 ATWICK(1),AT(1)
000025 JPLAS(1),JPLAS(1)
000025 VMOD(1),VM(1)
000025 PRAT(1),PRAT(1)
000025 NAME$1(1),NAME$1(1)
000025 NAME$2(1),NAME$2(1)
000025 DF(1),DF(1)
000025 L=2
000025 K=2
000025 DO 40 I=2,NPTS
000025 READ (5,2450) H1,V1,V1,PR,VM,PRS,DW,DWS
000025 X(I),X(I)
000025 V(I),V(I)
000025 ATWICK(I),ATWICK(I-1)
000025 IF (V1,NE,0) ATWICK(I)=1
000025 IF (NAME$.EQ,MARKC) GO TO 20
000025 IF (PR,EG,0.0) GO TO 20
000025 JPLAS(L)=J
000025 VMOD(L)=VM
000025 PRAT(L)=PR
000025 L=L+1

```

```

5
10
14
20
25
30
35
40
45
50
55
60
65
70
75
80
85
90
95
100
105
110
115
120
125
130
135
140
145
150
155
160
165
170
175
180
185
190
195
200
205
210
215
220
225
230
235
240
245
250
255
260
265
270

```

```

003004 26.4 DR. 295 I = 1. MMWT
003006 XP(1,0) = AP(1,0)ORAC
003013 26C CONTINUE
003017 47C CONTINUE
003020 DR 405 L = 1. MMWT
003021 IF VARTIK(L) .EQ. 0) GO TO 405
003022 NEXT = VARTIK(L)
003024 DR 304 I = 2. MMWT
003025 SL(I - 1,0) = (VP(I,0) - VP(I - 1,0)) /
      * (XP(I,0) - XP(I - 1,0)) - SL(I - 1,0)EXP(I - 1,0)
003027 CONTINUE
003028 CONTINUE
003029 GO TO 999
003030 WRITE(6,670)
003031 GO TO 999
003032 WRITE(6,671) L
003033 GO TO 999
003034 WRITE(6,646)
003035 GO TO 999
003036 WRITE(6,644) PL01
003037 GO TO 999
003038 WRITE(6,672) L
003039 GO TO 999
003040 WRITE(6,663) PL01PT
003041 GO TO 999
003042 WRITE(6,645) NPARTS
003043 GO TO 999
003044 WRITE(6,673) L, VARTIK(L)
003045 GO TO 999
003046 WRITE(6,674) L, VARTIK(L)
003047 GO TO 999
003048 WRITE(6,675)
003049 GO TO 999
003050 WRITE(6,676)
003051 GO TO 999
003052 WRITE(6,677)
003053 *12 WRITE(6,641) L
003054 WRITE(6,649)
003055 GO TO 999
003056 FINMAT(2000)
003057 FORMAT(1M1, '//////////541, 27M0ATIELLE MEMORIAL INSTITUTE)
003058 534 FORMAT(//40X, 14-COLUMBUS, OHIO)
003059 534 FORMAT(//47X, 47X, STRESS ANALYSIS OF A SHELL OF REVOLUTION)
003060 537 FORMAT(// 50X, 33M0ADVANCED SOLID MECHANICS DIVISION)
003061 539 FORMAT(// 50X, 33M0MECHANICAL ENGINEERING DEPARTMENT)
003062 501 FORMAT(1M1, 2000(1M3, 2000))
003063 534 FORMAT(0, 4X, 09-20 46, 0X, 09-20 46, 0X, 09-20 46, 0X, 09-20 46)
003064 501 FORMAT(1M1, 2010.3, 1012)
003065 547 FORMAT(2X, 42, 0X, 211.4, 0X, 06.4)
003066 441 FORMAT(2X, 42, 0X, 314.5)
003067 517 FORMAT(4X, 46, 0X, 011.0, 012.0, 215, 2X, 42, 1X, 010.0, 15)
003068 547 FORMAT(3X, 2012.0)

```

000175	PP	CONTINUE	275
000176		IF (MPRES.EQ.MARKC) GO TO 30	280
000200		IFSTAMPSTORMS	285
000201		IF (AMPTSTL.L.J.ME-12) GO TO 30	290
000204		MPRES(I)	295
000210		MPRES(K)MPRES	300
000211		MPRES(M)	305
000212		MPRES(N)MPRES	310
000214		KEND	315
000216	30	CONTINUE	320
000217	60	CONTINUE	325
000221		WRITE (5,244)I	330
000224		WRITE (6,247) (I,X(I),Y(I),I=1,MPYS)	335
000242		RELASL=1	340
000244		MPRESM=1	345
000246		READ (5,2,80) (IV(I),I=1,MV)	350
000249		IV(I)=1	355
000261		IV(MV+2)MPYS	360
000264		MV=MV+2	365
000265		IF (XMPCT.EQ.MARKD) GO TO 60	370
000272		DO 50 I=1,MPYS	375
000274		Y(I)=Y(I)	380
000276	50	CONTINUE	385
000309	60	IF (XMPCT.EQ.MARKD) GO TO 80	390
000302		DO 70 I=1,MPYS	395
000304		X(I)=X(I)	400
000306	70	CONTINUE	405
000310	80	CONTINUE	410
000311		IF (RELAS.EQ.MARKC) GO TO 110	415
000313		DO 100 J=1,RELAS	420
000314		IFLAG=1	425
000315		DO 90 L=1,MV	430
000317		IF (IV(L).NE.JELAS(J)) GO TO 90	435
000322		IFLAG=2	440
000323	90	CONTINUE	445
000324		IF (IFLAG.EQ.2) GO TO 100	450
000330		CALL EAITN (12,J)	455
000332		GO TO 242	460
000336	100	CONTINUE	465
000341	110	CONTINUE	470
000341		IF (MPRES.EQ.MARKC) GO TO 140	475
000344		DO 130 J=1,MPRES	480
000345		IFLAG=1	485
000346		DO 120 L=1,MV	490
000350		IF (IV(L).NE.JPRES(J)) GO TO 120	495
000354	120	IFLAG=2	500
000354		CONTINUE	505
000357		IF (IFLAG.EQ.2) GO TO 130	510
000361		CALL EAITN (13,J)	515
000364		GO TO 242	520
000367	130	CONTINUE	525
000372	140	CONTINUE	530
	C	COMMENT PRINT OF INPUT	535
	C		540
			545

```

000774 NVZ=44-2
000775 FMSLEPSI
000776 M=.01
000777 ITES=2
000778 MPTS=40
000779 WRITE (4,2400) TITLE1,TITLE2,TITLE3
000780 WRITE (4,2500) MPTS,NVZ,EPSI
000781 IW, IY, IZ=PTS
000782 X(I)=X(I)+ITRANS
000783 Y(I)=Y(I)+YTRANS
000784 IF (X(I)-GE.0.0) GO TO 150
000785 CALL EXIT( I,I )
000786 GO TO 240
000787 CONTINUE
15-
C
C COMMENT STORE X,Y VALUES FOR LATER PLOT
C
000455 X(I)=X(I)
000456 Y(I)=Y(I)
000457 IF (I.EQ.MPTS) GO TO 100
000458 X(I)=I*EPSI
000459 IF (M-I) 100,170,100
000460 WRITE (4,2520) M
000461 CALL EXIT
000462 WRITE (4,2530) I,X(I),Y(I),X(I)*MICK(I)
000463 ITES=ITES+1
000464 GO TO 100
000465 WRITE (4,2540) I,X(I),Y(I),X(I)*MICK(I)
000466 CONTINUE
000467 DO 200 I=2,MPTS
000468 IF (X(I)-L.I*MIN) XMIN=X(I)
000469 CONTINUE
000470 XTRANS=XMIN-.01
000471 DO 210 I=1,MPTS
000472 X(I)=X(I)-XTRANS
000473 CONTINUE
000474 WRITE (6,2400) TITLE1,TITLE2,TITLE3
C
C COMMENT COMPUTE THE DIRECTION OF ROTATION OF THE TANGENT FOR
C COMMENT CONSECUTIVE TRIPLES OF POINTS
C
C C IPHI(I) DESIGNATES ROTATION DIRECTION AS FOLLOWS
C C IPHI(I) = 1 CLOCKWISE
C C IPHI(I) = 2 COUNTER-CLOCKWISE
C C IPHI(I) = 3 NO ROTATION ( STRAIGHT LINE )
C C IPHI(I) = 4 (X(I),Y(I)) IS A VERTEX
C
000401 MPTS=
000402 L1=1
000403 M=420 L2=0
000404 L2=IV(L)-2
000405 DX1=X(L)-X(L1)

```

```

550
555
560
565
570
575
580
585
590
595
600
605
610
615
620
625
630
635
640
645
650
655
660
665
670
675
680
685
690
695
700
705
710
715
720
725
730
735
740
745
750
755
760
765
770
775
780
785
790
795
800
805
810
815
820

```



```

001021 430 IF (IPI=1).EQ.4) GO TO 450
C COMMENT TYPE IS A VERTEX
C
440 ISF(MS)I=1
MS=MS+1
ISF(MS)I=1
IYPE(I)=IYPE(I)+1
GO TO 460
450 ISF(MS)I=1
MS=MS+1
ISF(MS)I=1
IYPE(I)=IYPE(I)+1
IF (MS.GT.60) 470,480
CALL CALLN (3,1)
GO TO 242
460 IF (I.EQ.NPT) 490,500
ISF(MS)I=1
CONTINUE
IF (MS.EV.1) GO TO 520
LS=1
LS=LS+1
IF (LS.EQ.MS-1) GO TO 520
IF (IYPE(LS)=ME.2) GO TO 510
M=I(LS)-1
M=I(M)+1
IF (M.EQ.4) GO TO 510
I(LS)=I(LS)-1
ISF(LS-1)=ISF(LS)
GO TO 510
520 CONTINUE
LS=1
530 LS=LS+1
IF (LS.EQ.MS-1) GO TO 550
JTEST=ISF(LS)-ISF(LS-1)
IF (JTEST.NE.0) GO TO 530
IF (IYPE(LS-1).EQ.3 .AND. IYPE(LS-1).EQ.3)3001,3002
3001 M=I(M)+1
3003 IF (IYPE(LS).EQ.1) I(VI)=I GO TO 3003
M=MS-1
DO 3004 I=1,M
J=J+1-1
IF (J.EQ. M) GO TO 3005
I(VI)=I(J)-1
3004 CONTINUE
3005 I(VI)=I(I)+1
3002 CONTINUE
MS=MS-1
DO 540 I=LS,MS
IYPE(I)=IYPE(I)+1
ISF(I)=ISF(I)+1
ISF(I)=ISF(I)+1
GO TO 530
540 CONTINUE
550 CONTINUE

```

1100
1105
1110
1114
1120
1125
1130
1135
1140
1145
1150
1155
1160
1165
1170
1175
1180
1185
1190
1195
1200
1205
1210
1215
1220
1225
1230
1235
1240
1245
1250
1255
1260
1265
1270
1275

1280
1285
1290
1295
1300
1305
1310

```

001201          C      COMMENT PRINT OF PRELIMINARY GROUPING OF POINTS
001202          C
001203          WRITE (4,255.7)
001204          DO 546 L=1,MS
001205          WRITE(L)
001206          WRITE(L)
001207          WRITE (6,256.1) L,TYPE(L),A(M),Y(M),S(M),T(M)
001208          CONTINUE
001209          546
001210          C
001211          C      COMMENT FIT GIVEN SET OF POINTS WITH CIRCLES AND STRAIGHT LINES
001212          C
001213          PC=6.0
001214          PCY=6.0
001215          S=1.0
001216          W=6.0
001217          I=1
001218          I=1
001219          DO 221 I=1,MS
001220          DO 570 J=1,MS
001221          EP(J)=0
001222          CONTINUE
001223          WRITE (6,249.7) TITLE,TITLE2,TITLE3
001224          WRITE (6,257A) I
001225          ADJUST
001226          IF (1.E0.1) 580,610
001227
001228          C      COMMENT IS THE FIRST SEGMENT A LINE OR A CIRCLE
001229          C
001230          564 IF (ITYPE(I).EQ.3) 630,590
001231          564 J=1
001232          C
001233          C      COMMENT OBTAIN THE LINE ON WHICH THE CENTER OF THE STARTING CIRCLE
001234          C      COMMENT IS TO LIE
001235          C
001236          C      COMMENT SOLVE THE SYSTEM
001237          DO 600 M=1,3
001238          LTEMP(M)=1
001239          A(M)=1
001240          A(M,2)=Y(J)
001241          A(M,3)=1.0
001242          B(M)=X(J)-OXP(Y(J))
001243          J=J+1
001244          CONTINUE
001245          CALL LINEZ (A,3,3,0,0,0,1,3,LTEMP,TEMP,DET,MPV,PTV,LPH,LPC)
001246          D=M(1)
001247          F=M(2)
001248          P=M(3)
001249          C=C*0.72
001250          C=C*E/2.0
001251          C=C*(SUNT(M*0.72-0.047)/2.0)
001252          L=1
001253          L=1
001254          DO 600 TO 660
001255
001256
001257
001258
001259
001260
001261
001262
001263
001264
001265
001266
001267
001268
001269
001270
001271
001272
001273
001274
001275
001276
001277
001278
001279
001280
001281
001282
001283
001284
001285
001286
001287
001288
001289
001290
001291
001292
001293
001294
001295
001296
001297
001298
001299
001300
001301
001302
001303
001304
001305
001306
001307
001308
001309
001310
001311
001312
001313
001314
001315
001316
001317
001318
001319
001320
001321
001322
001323
001324
001325
001326
001327
001328
001329
001330
001331
001332
001333
001334
001335
001336
001337
001338
001339
001340
001341
001342
001343
001344
001345
001346
001347
001348
001349
001350
001351
001352
001353
001354
001355
001356
001357
001358
001359
001360
001361
001362
001363
001364
001365
001366
001367
001368
001369
001370
001371
001372
001373
001374
001375
001376
001377
001378
001379
001380
001381
001382
001383
001384
001385
001386
001387
001388
001389
001390
001391
001392
001393
001394
001395
001396
001397
001398
001399
001400
001401
001402
001403
001404
001405
001406
001407
001408
001409
001410
001411
001412
001413
001414
001415
001416
001417
001418
001419
001420
001421
001422
001423
001424
001425
001426
001427
001428
001429
001430
001431
001432
001433
001434
001435
001436
001437
001438
001439
001440
001441
001442
001443
001444
001445
001446
001447
001448
001449
001450
001451
001452
001453
001454
001455
001456
001457
001458
001459
001460
001461
001462
001463
001464
001465
001466
001467
001468
001469
001470
001471
001472
001473
001474
001475
001476
001477
001478
001479
001480
001481
001482
001483
001484
001485
001486
001487
001488
001489
001490
001491
001492
001493
001494
001495
001496
001497
001498
001499
001500
001501
001502
001503
001504
001505
001506
001507
001508
001509
001510
001511
001512
001513
001514
001515
001516
001517
001518
001519
001520
001521
001522
001523
001524
001525
001526
001527
001528
001529
001530
001531
001532
001533
001534
001535
001536
001537
001538
001539
001540
001541
001542
001543
001544
001545
001546
001547
001548
001549
001550
001551
001552
001553
001554
001555
001556
001557
001558
001559
001560
001561
001562
001563
001564
001565
001566
001567
001568
001569
001570
001571
001572
001573
001574
001575
001576
001577
001578
001579
001580
001581
001582
001583
001584
001585
001586
001587
001588
001589
001590
001591
001592
001593
001594
001595
001596
001597
001598
001599
001600
001601
001602
001603
001604
001605
001606
001607
001608
001609
001610
001611
001612
001613
001614
001615
001616
001617
001618
001619
001620
001621
001622
001623
001624
001625
001626
001627
001628
001629
001630
001631
001632
001633
001634
001635
001636
001637
001638
001639
001640
001641
001642
001643
001644
001645
001646
001647
001648
001649
001650
001651
001652
001653
001654
001655
001656
001657
001658
001659
001660
001661
001662
001663
001664
001665
001666
001667
001668
001669
001670
001671
001672
001673
001674
001675
001676
001677
001678
001679
001680
001681
001682
001683
001684
001685
001686
001687
001688
001689
001690
001691
001692
001693
001694
001695
001696
001697
001698
001699
001700
001701
001702
001703
001704
001705
001706
001707
001708
001709
001710
001711
001712
001713
001714
001715
001716
001717
001718
001719
001720
001721
001722
001723
001724
001725
001726
001727
001728
001729
001730
001731
001732
001733
001734
001735
001736
001737
001738
001739
001740
001741
001742
001743
001744
001745
001746
001747
001748
001749
001750
001751
001752
001753
001754
001755
001756
001757
001758
001759
001760
001761
001762
001763
001764
001765
001766
001767
001768
001769
001770
001771
001772
001773
001774
001775
001776
001777
001778
001779
001780
001781
001782
001783
001784
001785
001786
001787
001788
001789
001790
001791
001792
001793
001794
001795
001796
001797
001798
001799
001800
001801
001802
001803
001804
001805
001806
001807
001808
001809
001810
001811
001812
001813
001814
001815
001816
001817
001818
001819
001820
001821
001822
001823
001824
001825
001826
001827
001828
001829
001830
001831
001832
001833
001834
001835
001836
001837
001838
001839
001840
001841
001842
001843
001844
001845
001846
001847
001848
001849
001850
001851
001852
001853
001854
001855
001856
001857
001858
001859
001860
001861
001862
001863
001864
001865
001866
001867
001868
001869
001870
001871
001872
001873
001874
001875
001876
001877
001878
001879
001880
001881
001882
001883
001884
001885
001886
001887
001888
001889
001890
001891
001892
001893
001894
001895
001896
001897
001898
001899
001900
001901
001902
001903
001904
001905
001906
001907
001908
001909
001910
001911
001912
001913
001914
001915
001916
001917
001918
001919
001920
001921
001922
001923
001924
001925
001926
001927
001928
001929
001930
001931
001932
001933
001934
001935
001936
001937
001938
001939
001940
001941
001942
001943
001944
001945
001946
001947
001948
001949
001950
001951
001952
001953
001954
001955
001956
001957
001958
001959
001960
001961
001962
001963
001964
001965
001966
001967
001968
001969
001970
001971
001972
001973
001974
001975
001976
001977
001978
001979
001980
001981
001982
001983
001984
001985
001986
001987
001988
001989
001990
001991
001992
001993
001994
001995
001996
001997
001998
001999
002000

```

```

001400      C
001401      C COMMENT IS (A(L1),V(L1)) A CENTER ON AN INFLECTION POINT
001402      C
001403      C 61* IF (IV(L1),FO(L1)) 620.600
001404      C
001405      C COMMENT IS CURVE FROM CENTER (A(L1),V(L1)) A LINE OR A CIRCLE
001406      C
001407      C 62* IF (ITYPE(L1),EQ.3) 630.500
001408      C
001409      C 63* L1=J(L1)
001410      C LP=ISF(L1)
001411      C 64* IF (L1=SM) L1=L2
001412      C
001413      C 65* GO TO 1415
001414      C
001415      C 66* IF (ITYPE(L1),EQ.3) 620.600
001416      C
001417      C 67* L2=ISF(L1)
001418      C
001419      C 68* L2=L2
001420      C
001421      C 69* X1=X(L1)
001422      C
001423      C 70* Y1=Y(L1)
001424      C
001425      C 71* X2=X(L2)
001426      C
001427      C 72* Y2=Y(L2)
001428      C
001429      C 73* DX=X2-X1
001430      C
001431      C 74* DY=Y2-Y1
001432      C
001433      C 75* R=SQRT(DX**2+DY**2)
001434      C
001435      C 76* SUM=0.
001436      C
001437      C COMMENT PASS CIRCLE THROUGH (X1,Y1), (X2,Y2) WITH CENTER ON
001438      C
001439      C 77* X=CX
001440      C
001441      C 78* Y=CY
001442      C
001443      C 79* IF (ABS(Y1)-L1).LE-.05) 600.600
001444      C
001445      C 80* E=2.00Y1
001446      C
001447      C 81* D=(1.42002-X1**2)-(Y2-Y1)**2)/(X1-X2)
001448      C
001449      C 82* F=Y1**2-X1**2-D**2
001450      C
001451      C 83* ON T0 720
001452      C
001453      C 84* IF (ABS(D)-L1).LE-.05) 700.710
001454      C
001455      C 85* D=2.30X1
001456      C
001457      C 86* F=(X1-X2)**2-(Y2**2-Y1**2)/(Y1-Y2)
001458      C
001459      C 87* F=X1**2-Y1**2-C**2
001460      C
001461      C 88* ON T0 720
001462      C
001463      C 89* SL=D*Y1/DX1
001464      C
001465      C COMMENT SOLVE THE SYSTEM
001466      C
001467      C
001468      C A(1,1)=X1
001469      C
001470      C A(1,2)=Y1
001471      C
001472      C A(1,3)=1.0
001473      C
001474      C A(2,1)=X2
001475      C
001476      C A(2,2)=Y2
001477      C
001478      C A(2,3)=1.0
001479      C
001480      C A(3,1)=SL/2.0
001481      C
001482      C A(3,2)=1.0/2.0
001483      C
001484      C A(3,3)=0.0
001485      C
001486      C R(1,1)=X1**2+Y1**2
001487      C
001488      C R(2,1)=X2**2+Y2**2
001489      C
001490      C R(3,1)=SL**2
001491      C
001492      C CALL LINE (A,3,3,0.0,0.1,3,0,TRMP,IERM,NET,MP IV,PIV,LPH,LMC)
001493      C
001494      C
001495      C
001496      C
001497      C
001498      C
001499      C
001500      C
001501      C
001502      C
001503      C
001504      C
001505      C
001506      C
001507      C
001508      C
001509      C
001510      C
001511      C
001512      C
001513      C
001514      C
001515      C
001516      C
001517      C
001518      C
001519      C
001520      C
001521      C
001522      C
001523      C
001524      C
001525      C
001526      C
001527      C
001528      C
001529      C
001530      C
001531      C
001532      C
001533      C
001534      C
001535      C
001536      C
001537      C
001538      C
001539      C
001540      C
001541      C
001542      C
001543      C
001544      C
001545      C
001546      C
001547      C
001548      C
001549      C
001550      C
001551      C
001552      C
001553      C
001554      C
001555      C
001556      C
001557      C
001558      C
001559      C
001560      C
001561      C
001562      C
001563      C
001564      C
001565      C
001566      C
001567      C
001568      C
001569      C
001570      C
001571      C
001572      C
001573      C
001574      C
001575      C
001576      C
001577      C
001578      C
001579      C
001580      C
001581      C
001582      C
001583      C
001584      C
001585      C
001586      C
001587      C
001588      C
001589      C
001590      C
001591      C
001592      C
001593      C
001594      C
001595      C
001596      C
001597      C
001598      C
001599      C
001600      C
001601      C
001602      C
001603      C
001604      C
001605      C
001606      C
001607      C
001608      C
001609      C
001610      C
001611      C
001612      C
001613      C
001614      C
001615      C
001616      C
001617      C
001618      C
001619      C
001620      C
001621      C
001622      C
001623      C
001624      C
001625      C
001626      C
001627      C
001628      C
001629      C
001630      C
001631      C
001632      C
001633      C
001634      C
001635      C
001636      C
001637      C
001638      C
001639      C
001640      C
001641      C
001642      C
001643      C
001644      C
001645      C
001646      C
001647      C
001648      C
001649      C
001650      C
001651      C
001652      C
001653      C
001654      C
001655      C
001656      C
001657      C
001658      C
001659      C
001660      C
001661      C
001662      C
001663      C
001664      C
001665      C
001666      C
001667      C
001668      C
001669      C
001670      C
001671      C
001672      C
001673      C
001674      C
001675      C
001676      C
001677      C
001678      C
001679      C
001680      C
001681      C
001682      C
001683      C
001684      C
001685      C
001686      C
001687      C
001688      C
001689      C
001690      C
001691      C
001692      C
001693      C
001694      C
001695      C
001696      C
001697      C
001698      C
001699      C
001700      C
001701      C
001702      C
001703      C
001704      C
001705      C
001706      C
001707      C
001708      C
001709      C
001710      C
001711      C
001712      C
001713      C
001714      C
001715      C
001716      C
001717      C
001718      C
001719      C
001720      C
001721      C
001722      C
001723      C
001724      C
001725      C
001726      C
001727      C
001728      C
001729      C
001730      C
001731      C
001732      C
001733      C
001734      C
001735      C
001736      C
001737      C
001738      C
001739      C
001740      C
001741      C
001742      C
001743      C
001744      C
001745      C
001746      C
001747      C
001748      C
001749      C
001750      C
001751      C
001752      C
001753      C
001754      C
001755      C
001756      C
001757      C
001758      C
001759      C
001760      C
001761      C
001762      C
001763      C
001764      C
001765      C
001766      C
001767      C
001768      C
001769      C
001770      C
001771      C
001772      C
001773      C
001774      C
001775      C
001776      C
001777      C
001778      C
001779      C
001780      C
001781      C
001782      C
001783      C
001784      C
001785      C
001786      C
001787      C
001788      C
001789      C
001790      C
001791      C
001792      C
001793      C
001794      C
001795      C
001796      C
001797      C
001798      C
001799      C
001800      C
001801      C
001802      C
001803      C
001804      C
001805      C
001806      C
001807      C
001808      C
001809      C
001810      C
001811      C
001812      C
001813      C
001814      C
001815      C
001816      C
001817      C
001818      C
001819      C
001820      C
001821      C
001822      C
001823      C
001824      C
001825      C
001826      C
001827      C
001828      C
001829      C
001830      C
001831      C
001832      C
001833      C
001834      C
001835      C
001836      C
001837      C
001838      C
001839      C
001840      C
001841      C
001842      C
001843      C
001844      C
001845      C
001846      C
001847      C
001848      C
001849      C
001850      C
001851      C
001852      C
001853      C
001854      C
001855      C
001856      C
001857      C
001858      C
001859      C
001860      C
001861      C
001862      C
001863      C
001864      C
001865      C
001866      C
001867      C
001868      C
001869      C
001870      C
001871      C
001872      C
001873      C
001874      C
001875      C
001876      C
001877      C
001878      C
001879      C
001880      C
001881      C
001882      C
001883      C
001884      C
001885      C
001886      C
001887      C
001888      C
001889      C
001890      C
001891      C
001892      C
001893      C
001894      C
001895      C
001896      C
001897      C
001898      C
001899      C
001900      C
001901      C
001902      C
001903      C
001904      C
001905      C
001906      C
001907      C
001908      C
001909      C
001910      C
001911      C
001912      C
001913      C
001914      C
001915      C
001916      C
001917      C
001918      C
001919      C
001920      C
001921      C
001922      C
001923      C
001924      C
001925      C
001926      C
001927      C
001928      C
001929      C
001930      C
001931      C
001932      C
001933      C
001934      C
001935      C
001936      C
001937      C
001938      C
001939      C
001940      C
001941      C
001942      C
001943      C
001944      C
001945      C
001946      C
001947      C
001948      C
001949      C
001950      C
001951      C
001952      C
001953      C
001954      C
001955      C
001956      C
001957      C
001958      C
001959      C
001960      C
001961      C
001962      C
001963      C
001964      C
001965      C
001966      C
001967      C
001968      C
001969      C
001970      C
001971      C
001972      C
001973      C
001974      C
001975      C
001976      C
001977      C
001978      C
001979      C
001980      C
001981      C
001982      C
001983      C
001984      C
001985      C
001986      C
001987      C
001988      C
001989      C
001990      C
001991      C
001992      C
001993      C
001994      C
001995      C
001996      C
001997      C
001998      C
001999      C
002000      C

```



```

002056      4243-T
002057      GO TO MR3
002063      2430020Y000-03002-0013-00V3
002073      T0(23-H)/(V3-S)
002075      T0V3-S
002077      U01.001000
002102      V02.0010V3-Z/T01-2.0043
002107      V02.002/T00P-2.00V3-Z/T0-V300P-03002-03002
002124      019002-4.0000
002130      IF (M)0E.0.) GO TO 070
002131      CALL EALIN (10.1)
002134      GO TO 2420
002137      CONTINUE
002137      RESORT (0002-4.0000)
002140      H1=(-V01)/(2.000)
002152      X2=(-V01)/(P.000)
002156      Y1=Z/T0-T0X1
002161      Y2=Z/T0-T0X2

C
C COMMENT CHOOSE THE POINT OF TANGENCY CLOSEST TO POINT (X(L1),Y(L1))
C
002164      AA= D1=SQRT((V1-X(L1))002+(V1-Y(L1))002)
002175      02=SQRT((X2-X(L1))002+(Y2-Y(L1))002)
002205      IF (01.LT.02) 000000
002214      X(L1)=X1
002216      Y(L1)=Y1
002220      L2=L
002221      GO TO 016
002222      X(L1)=X2
002224      Y(L1)=Y2
002226      L2=L

C
C COMMENT ADJUST FINAL ANGLE OF PRECEDING PART
C
002227      T1=XT-X(L1)
002232      T2=YT-Y(L1)*1)
002236      T1=10T2
002237      01=XT-C4
002241      0Y1=YT-CY
002243      C=001/CH
002245      S=001/CR
002249      NX2=X(L1)-CX
002250      DY2=Y(L1)-CY
002252      AT=0X2-SA-0Y2*CA
002256      VT=0X2-CA-0Y2*SA
002260      CALL ANGLE (1.0T,VT,0.00.000L2-2.ANGL0.0,IF (00.0L)
002271      0YMETASMS (AVGLE0)
002273      JM=2
002274      ID=2
002275      IF (T1.LT.0.0) JM=3
002304      IF (11TPE(1-1).EQ.2) 10=3
002307      JM=JM-ID
002311      GO TO (2420,2420,2420,030,020,030), JM
002322      0YMETAS=0YMETAS
002324      SH(IP-1)=SX(IP-1)+0YMETAS

```

```

2134
2140
2145
2150
2155
2165
2170
2175
2180
2185
2190
2195
2200
2205
2210
2215
2220
2225
2230
2235
2240
2245
2250
2255
2260
2265
2270
2275
2280
2285
2290
2295
2300
2305
2310
2315
2320
2325
2330
2335
2340
2345
2350
2355
2360
2365
2370
2375
2380
2385
2390
2395
2400
2405

```

```

002324      GO TO 1010
002327      J=1
002330      MP(L-1)=1
C
C      COMMENT CHECK TO SEE WHETHER POINTS BETWEEN (A1,V1) AND (A2,V2) ARE
C      COMMENT CLOSE ENOUGH TO THE CIRCLE
C
      ETEMP=EPS1
      IFLAG=1
      DO 949 J=1,MP
      X=X1(L1+J)
      Y=Y1(L1+J)
      EPS=MP-SORT((X3-X4)**2+(Y3-Y4)**2)
      SUM=SUM+ABS(EPS)
      IF (IADJUST.NE.0) GO TO 950
      WRITE (6,2600) J,MP,X4,Y4,EPS
C
950      CONTINUE
      IF (ABS(EPS).LE.EPS1) GO TO 960
      IFLAG=10
      IF (ETEMP.LT.AMSTEPS) ETEMP=ABS(EPS)
      CONTINUE
960      IF (IFLAG.EQ.1) GO TO 969
      IF (IADJUST.EQ.0) GO TO 970
      IF (L-L1.FO.2) E(IADJUST)=ETEMP
      L=L+1
      IF (L.NE.L1+1) GO TO 670
      IF (L.EQ.1) GO TO 670
      IF (IYEQ11-1).EQ.3.AND.IADJUST.NE.0) GO TO 980
      GO TO 670
980      IF (L.EQ.L2) I190=990
990      J=1
C
C      COMMENT EXTERN CIRCLE AS FAR AS POSSIBLE
C
1000      X=X1(L+J)
      Y=Y1(L+J)
      EPS2=ABS(SUM+(X3-X4)**2+(Y3-Y4)**2)
      IF (IADJUST.NE.0) GO TO 1010
      WRITE (6,2610) J,X4,Y4,EPS2
      CONTINUE
1010      IF (EPS2.LT.0.0) I020=1070
      IF (J.EQ.1) I030=1060
      IF (EPS.LT.0.0) I190=1040
      IF (L-L1).EQ.1) I110=1050
      L=L+1
      GO TO 1110
1040      L=L+J-2
      IF (J.EQ.1) L=L+1
      GO TO 1110
1070      IF (ABS(EPS2).LT.EPS1) I100=1060
1080      SUM=SUM+ABS(EPS2)
      IF (L+J).EQ.L2) I100=1090
      J=J+1
      GO TO 1000
1100      L=L2
002331
002334
002335
002337
002342
002344
002354
002357
002363
002401
002401
002410
002411
002415
002420
002422
002423
002427
002431
002433
002435
002443
002443
002450
002451
002454
002456
002460
002473
002473
002490
002500
002515
002522
002526
002533
002535
002535
002540
002542
002543
002551
002554
002561
002563
002563
2410
2415
2420
2424
2430
2435
2440
2445
2450
2455
2460
2465
2470
2475
2480
2485
2490
2495
2500
2505
2510
2515
2520
2525
2530
2535
2540
2545
2550
2555
2560
2565
2570
2575
2580
2585
2590
2595
2600
2605
2610
2615
2620
2625
2630
2635
2640
2645
2650
2655
2660
2665
2670
2675
2680

```

```

002565      1114  DMAX3=4(L)
002570      UVV3=V(L)

C
C COMMENT PLACE LAST POINT ON OBTAINED CIRCLE
C
002573      1179  A1=Z3
002581      ZP=Z3
002583      V1=V3+H
002589      V2=V3-H
002596      GO TO 1164
002607      1188  IF (ABS(OV)-L.T.1.EE-05) 1180,1150
002610      1188  V1=V3
002614      V2=V3
002620      A1=Z3+R
002621      A2=Z3-R
002622      GO TO 1164
002624      SL=OV/VA
002627      T=2/507(1-SL**2)
002632      A1=Z3+T
002637      ZP=Z3-T
002643      V1=V3+SL*V
002644      V2=V3-SL*V
002645      D1=SQRT((H1-Z(L))**2-(V1-V(L))**2)
002656      D2=SQRT((H2-Z(L))**2-(V2-V(L))**2)
002660      IF (D1.LT.D2) 1170,1180
002675      K(L)=H1
002677      V(L)=V1
002701      GO TO 1194
002701      K(L)=Z2
002703      V(L)=V2

C
C COMMENT CHECK CURVATURE TO SEE IF IT IS CORRECT I.E., IF TWO CIRCLES
C COMMENT JOIN AND BOTH HAVE A TANGENT TURNING IN THE SAME DIRECTION.
C
002705      1198  GO TO 1414
002706      1200  IF (IADJST.EQ.0) GO TO 1230
002707      WSTPT(IADJST)=140.0
002711      IFIT(IADJST)=L1
002712      IF (EPS.EQ.0.0) GO TO 1210
002713      EPI(IADJST)=100.
002715      CONTINUE
002715      1210  IF (IADJST.EQ.0) GO TO 1440
002717      IADJST=IADJST+1
002720      L1=J1
002722      K(L)=STBY(IADJST)
002725      V(L)=VTV(IADJST)
002727      L=Z
002730      K=L
002731      I=I+1
002733      DO 1225 J=I,NOL
002734      K(I)=ZT(K)
002737      V(I)=VT(K)
002741      K=K+1
002742      1225  CONTINUE

```

```

2689
2690
2695
2700
2705
2710
2715
2720
2725
2730
2735
2740
2745
2750
2755
2760
2765
2770
2775
2780
2785
2790
2795
2800
2805
2810
2815
2820
2825
2830
2835
2840
2845
2850
2855
2860
2865
2870
2875
2880
2885
2890
2895
2900
2905
2910
2915
2920
2925
2930
2935
2940
2945
2950
2955

```



```

003276      DN 1407 JMT,MS
003277      ISIJMIS(J-1)
003303      ISIJMIS(I-1)

C          COMMENT  INITIALIZE THE VARIOUS COUNTERS FOR INITIAL OF FIRST TRIAL POINT
C
C          MC OF PARTS TO GET TO THE END OF THE ARC
C          IADJUST  INDEX OF CURRENT INITIAL POINT
C          L2       INDEX OF THE LAST POINT OF THE PRESENT ARC
C          I1 AMN L  INDICES OF THE FIRST AND LAST POINTS OF THE
C          PRESENT CIRCLE BEING TESTED FOR SUITABILITY
C          CX AMN CY COORDINATES OF THE CENTER OF THE PRECEDING
C          CIRCLE

003300      APPA=1
003307      IADJUST=1
003310      L2=ISIJM(I)
003311      L=2
003312      L=J
003314      X(L1)=AMN(I)
003316      V(L1)=VTV(I)
003317      CVM(2,J)=IADJUST+C
003325      CVM(1,J)=IADJUST+C
003331      PC=MC
003333      PC=CY
003334      GO TO 670
003335      CONTINUE
003336      IF (IADJUST.EQ.0) GO TO 1499
003337      IF (L.LO.1) GO TO 1420
003340      C=I1
003342      C=V2
003343      L=L2
003344      L=L2
003346      APPA=APPA+1
003348      SIMP=SIMP+SIM
003350      GO TO 670
003351      MSF=1/(IADJUST)*APPA*SUM1*SUM
003352      ISIJM(I)=L2
003355      APPA=1
003357      IF (IADJUST.EQ.0) GO TO 1400
003361      IADJUST=IADJUST+1
003362      SIMP=0
003363      L=J
003364      L=L2
003366      I1=L+1
003371      V(L1)=VTV(IADJUST)
003373      K=1
003374      MIN=L1+1
003376      GO TO 1437
003377      X(J)=X(I)
003382      V(J)=V(I)
003384      K=K+1
003385      CONTINUE
003387      CVM(2,J)=IADJUST+C
003388      CVM(1,J)=IADJUST+C

```

```

3510
3515
3520
3525
3530
3535
3540
3545
3550
3555
3560
3565
3570
3575
3580
3585
3590
3595
3600
3605
3610
3615
3620
3625
3630
3635
3640
3645
3650
3655
3660
3665
3670
3675
3680
3685
3690
3695
3700
3705
3710
3715
3720
3725
3730
3735
3740
3745
3750
3755
3760
3765
3770
3775
3780

```

```

003421 003421
003422 003422
003424 003424

PCACR
PCVDCY
G4 TO 674

C COMMENT THE FIRST OF THE NINE TRIAL POINTS IS CHOSEN ACCORDING TO THE
C VECTORS MSFIT, FIT, AND EP
C
C MSFIT(IADJUST) THE NUMBER OF PARS PLUS THE SUM OF
C THE ABSOLUTE VALUES OF THE DISTANCES OF THE
C POINTS FROM THE OBTAINED CIRCLES. IF NO
C SEQUENCE OF CIRCLES CAN BE FOUND WHICH GO FROM
C THE INITIAL VALUE OF LI TO LP, THEN
C MSFIT IS SET EQUAL TO 100
C IFIT(IADJUST) TESTED ONLY IF ALL PATHS OF MSFIT
C ARE 100. IF CONTAINS THE INDEX OF THE LAST
C POINT SUCCESSFULLY FOUND, STARTING FROM
C (IADJUST).Y(IADJUST)
C EP
C SEARCHED FOR THE BEST TRIAL POINT
C ONLY IF THE MAXIMUM VALUE IN IFIT IS 101.
C THAT IS, NONE OF THE TRIAL POINTS ENABLED THE
C PROGRAM TO DO CALCULATIONS ANY FURTHER THAN IT
C DID BEFORE THE CREATION OF THE TRIAL POINTS.
C IN THIS CASE, EP(IADJUST) CONTAINS THE DISTANCE
C FROM THE CIRCLE THROUGH POINTS INDEXED BY LI
C AND LI+2 OF POINT WITH INDEX LI+1. THE BEST
C TRIAL POINT IS THEN THE POINT WITH THE SMALLEST
C EP VALUE

146P J00
003424 POINT 2624
003425 DO 1459 K=1,9
003431 POINT 2630 MSFIT(K)=IFIT(K)+EP(K)
003436 CONTINUE
003447 TEST=54.
003455 L=56.
003456 J=J01
003461 IF (J.GT.0) GO TO 1469
003464 TEST=MSFIT(J)
003465 IF (TEST.LT.TEST1) GO TO 1474
003467 GO TO 1469
003474 L=J
003475 TEST=TEST2
003476 GO TO 1469
003477 IF (L.LT.56) GO TO 1530
003484 J=J1
003485 TEST=I
003491 L=L191
003501 J=J01
003502 IF (J.GT.0) GO TO 1510
003504 TEST=IFIT(J)
003510 IF (TEST.LT.TEST2) GO TO 1504
003512 GO TO 1469
003514 L=LJ
003515 TEST=ITST2
003516 GO TO 1469

```

```

3764
3790
3795
3800
3805
3810
3815
3820
3825
3830
3835
3840
3845
3850
3855
3860
3865
3870
3875
3880
3885
3890
3895
3900
3905
3910
3915
3920
3925
3930
3935
3940
3945
3950
3955
3960
3965
3970
3975
3980
3985
3990
3995
4000
4005
4010
4015
4020
4025
4030
4035
4040
4045
4050
4055

```

003517	1510	IF (LL-L7.100) GO TO 153.	0060
003522	1520	CALL EXITM (7,1)	0065
003526		GO TO 2024	0070
003530	1520	CONTINUE	0075
003533		IF (IF17(LL).GT.JJ*) GO TO 1570	0080
003537		TEST15A.	0085
003540		DO 1550 J=1,9	0090
003543		IF (EP1J).LT.(TEST1) GO TO 1540	0095
003546		GO TO 1550	0100
003549	1540	LL=J	0105
003550		TEST1=EP1J	0110
003557	1540	CONTINUE	0115
003551		IF (EP1LL).GT.(EP100) GO TO 1520	0120
003554		IF (LL-EP10) GO TO 1500	0125
003557	1540	LL=LL+1	0130
003557		EP1=EP1LL+.000000001	0135
003562		CALL EXITM (7,JJ)	0140
003564		PRINT 2040, PPG1	0145
003572	1570	TEST1=J	0150
003573		PRINT 2050, LL	0155
003601		LAUJSTED	0160
003602		LL=J	0165
003606		X(1)=X1MY(1LL)	0170
003607		V(1)=V1MY(1LL)	0175
003611		X(MICK(1))=X(MICK(1)-1)+.1*(X-LL)*(X(MICK(1)-1)-X(MICK(1)-1))	0180
003623		X(MICK(1))=X(MICK(1)-1)+.1*(X-LL)*(X(MICK(1)-1)-X(MICK(1)-1))	0185
003623		CRVNI2=J*21-LL*0.000000001	0190
003626		CRVNI=J*21-LL*0.000000001	0195
003641		PCVACV	0200
003642		PCVACV	0205
003644		SZ(J*21+SZ(J*21)-1)+.000000001*DELTIME	0210
003650		L2=15*(1)	0215
003660		K=1	0220
003661		K=1	0225
003662		M1=1+1	0230
003664		DO 1560 J=1,M1	0235
003665		X(J)=X1(K)	0240
003670		V(J)=V1(K)	0245
003672		K=K+1	0250
003673		CONTINUE	0255
003675	1500	IF (155(J*2).E7) GO TO 070	0260
003700		V(12)=J*21+V12	0265
003704		V(16)=J*21+V14	0270
003705		DAT=SUM(DIC002+UYC002)	0275
003712		V(13)=J*21+V13+J*21-LL*0.000000001	0280
003722		GO TO 070	0285
		COMMENT PANTS DESCRIBED BY STRAIGHT LINES	0290
		C	0295
003723	1500	IF (11*PE(1).NE.3) GO TO 1770	0300
003726		0.1*(X(1)-V(1))	0305
003731		V(10)=11-V(1)	0310
003734		1.5*(11*PE)	0315
003736		IF (ABS(DN1).LT.1.0E-05) 1600.1630	0320
		COMMENT PANTS DESCRIBED BY CURVED LINES	0325
		C	0330

004230	GO TO 2424	0610
004241	IPAR(IP)MS	0615
004244	W(3,IP)ARCL	0620
004246	R3P(ARCL)	0625
004251	V2V(L)-A(L)/24	0630
004254	IF (IV(IV).EQ.L1) GO TO 1760	0635
004257	SI(IP)S(IP-1)	0640
004262	SI(IP)S(IP)	0645
004264	GO TO 2424	0650
004265	RTAR(L)	0655
004267	VIVAR(L)	0660
004271	IV=110.1	0665
004272	NOI	0670
004273	IF(SIG=0)VI	0675
004275	IF (TEST.LT.1.0) K=2	0680
004277	CALL A=GLF (M=1,V=23.7,AN=1,ER=ANGLC,IP (M),SL)	0685
004310	SI(IP)ARWLEN	0690
004314	SI(IP)S(IP)	0695
004321	GO TO 2424	0700
C		
COMMENT PARTS DESCRIBED BY CIRCLES		
C		
004321	W(2,IP)M23	0710
004324	W(4,IP)M73	0715
004327	W(1M(L))-M3	0720
004332	W(1M(L))-V3	0725
004334	W(2M(L))-V3	0730
004337	W(2M(L))-V3	0735
004341	W(4M(L))-M(L)	0740
004344	W(2M(L))-V(L)	0745
004346	ISS(IP)M7	0750
004350	IF (ANS(IV)) .LT. 1.0E-05) 1700.1700	0755
004354	M(1,RE)14	0760
004360	GO TO 1424	0765
004366	IF (ANS(OV)) .LT. 1.0E-05) 1400.1010	0770
004367	W(2M)	0775
004367	GO TO 1424	0780
004374	M(OV)I/OVI	0785
004372	1424 IF (ANS(OV2)) .LT. 1.0E-05) 1439.1440	0790
004400	M2=1.4E+14	0795
004402	GO TO 1474	0800
004402	IF (ANS(OV2)) .LT. 1.0E-05) 1450.1460	0805
004410	M2=0.9	0810
004411	GO TO 1474	0815
004412	M2=OV2/OH2	0820
004414	IF (IV(IV).EQ.L1) 1490.1400	0825
004421	SI(IP)S(IP-1)	0830
004424	GO TO 1944	0835
004425	IV=110.1	0840
004427	IF (M(1,RE).GT.1) 1400.1930	0845
004433	IF (OH(O).EQ.1) 1417.1923	0850
004440	SI(IP)M-0.0	0855
004443	GO TO 1944	0860
004443	SI(IP)M=0	0865
004446	GO TO 1944	0870
004446		0875

```

004460 1039 IF (M1.EQ.1.ME-1) 1040,1070
004461 1041 IF (M2.GT.0.0) 1050,1060
004462 1042 STIP)00.0
004463 1043 GO TO 1044
004464 1044 STIP)0100.0
004465 1045 GO TO 1046
004466 1046 K=TYPE(1)
004467 1047 X=X(L)
004468 1048 Y=Y(L)
004469 1049 CALL ANGLE (KOT,YT,Y3,ANGLE,ANGLE,ANGLE,IFIND,SL)
004470 1050 STIP)ANGLE
004471
004472
004473
004474
004475
004476
004477
004478
004479
004480
004481
004482
004483
004484
004485
004486
004487
004488
004489
004490
004491
004492
004493
004494
004495
004496
004497
004498
004499
004500
004501
004502
004503
004504
004505
004506
004507
004508
004509
004510
004511
004512
004513
004514
004515
004516
004517
004518
004519
004520
004521
004522
004523
004524
004525
004526
004527
004528
004529
004530
004531
004532
004533
004534
004535
004536
004537
004538
004539
004540
004541
004542
004543
004544
004545
004546
004547
004548
004549
004550
004551
004552
004553
004554
004555
004556
004557
004558
004559
004560
004561
004562
004563
004564
004565
004566
004567
004568
004569
004570
004571
004572
004573
004574
004575
004576
004577
004578
004579
004580
004581
004582
004583
004584
004585
004586
004587
004588
004589
004590
004591
004592
004593
004594
004595
004596
004597
004598
004599
004600
004601
004602
004603
004604
004605
004606
004607
004608
004609
004610
004611
004612
004613
004614
004615
004616
004617
004618
004619
004620
004621
004622
004623
004624
004625
004626
004627
004628
004629
004630
004631
004632
004633
004634
004635
004636
004637
004638
004639
004640
004641
004642
004643
004644
004645
004646
004647
004648
004649
004650
004651
004652
004653
004654
004655
004656
004657
004658
004659
004660
004661
004662
004663
004664
004665
004666
004667
004668
004669
004670
004671
004672
004673
004674
004675
004676
004677
004678
004679
004680
004681
004682
004683
004684
004685
004686
004687
004688
004689
004690
004691
004692
004693
004694
004695
004696
004697
004698
004699
004700
004701
004702
004703
004704
004705
004706
004707
004708
004709
004710
004711
004712
004713
004714
004715
004716
004717
004718
004719
004720
004721
004722
004723
004724
004725
004726
004727
004728
004729
004730
004731
004732
004733
004734
004735
004736
004737
004738
004739
004740
004741
004742
004743
004744
004745
004746
004747
004748
004749
004750
004751
004752
004753
004754
004755
004756
004757
004758
004759
004760
004761
004762
004763
004764
004765
004766
004767
004768
004769
004770
004771
004772
004773
004774
004775
004776
004777
004778
004779
004780
004781
004782
004783
004784
004785
004786
004787
004788
004789
004790
004791
004792
004793
004794
004795
004796
004797
004798
004799
004800
004801
004802
004803
004804
004805
004806
004807
004808
004809
004810
004811
004812
004813
004814
004815
004816
004817
004818
004819
004820
004821
004822
004823
004824
004825
004826
004827
004828
004829
004830
004831
004832
004833
004834
004835
004836
004837
004838
004839
004840
004841
004842
004843
004844
004845
004846
004847
004848
004849
004850
004851
004852
004853
004854
004855
004856
004857
004858
004859
004860
004861
004862
004863
004864
004865
004866
004867
004868
004869
004870
004871
004872
004873
004874
004875
004876
004877
004878
004879
004880
004881
004882
004883
004884
004885
004886
004887
004888
004889
004890
004891
004892
004893
004894
004895
004896
004897
004898
004899
004900
004901
004902
004903
004904
004905
004906
004907
004908
004909
004910
004911
004912
004913
004914
004915
004916
004917
004918
004919
004920
004921
004922
004923
004924
004925
004926
004927
004928
004929
004930
004931
004932
004933
004934
004935
004936
004937
004938
004939
004940
004941
004942
004943
004944
004945
004946
004947
004948
004949
004950
004951
004952
004953
004954
004955
004956
004957
004958
004959
004960
004961
004962
004963
004964
004965
004966
004967
004968
004969
004970
004971
004972
004973
004974
004975
004976
004977
004978
004979
004980
004981
004982
004983
004984
004985
004986
004987
004988
004989
004990
004991
004992
004993
004994
004995
004996
004997
004998
004999
005000

```

004717	2070	METAINFOFAS	5155
004721	2070	GO TO 2090	5160
004721	2090	METAINFOFAS000	5165
004723	2090	EX (MAM)MAM5 (M(3,IP))CUCS (METAINFOFAS) - 516005	5170
004744		VT (MAM)MAM5 - 516005A (METAINFOFAS)	5175
004741		MAM50001	5180
004742	2100	CONTINUE	5185
004743		GO TO 2174	5190
004745	2110	METAINFOFAS000.0	5195
004774		METAINFOFAS000.0	5200
004772		ALPHAS (METAINFOFAS) / 4.03	5205
004773		MAM50002.0ALPHAS01.0	5210
005000		MAM50007.2	5215
005402		DO 2160 MAM5.MAM5	5220
005003	2120	IF (MAM5.1) 2150,2120	5225
005007	2130	IF (MAM5.MAM5) 2130,2140	5230
005010	2130	METAINFOFAS	5235
005016		GO TO 2154	5240
005010	2140	METAINFOFAS000	5245
005020	2140	EX (MAM)MAM5 (M(3,IP))CUCS (METAINFOFAS) - 516005	5250
005001		VT (MAM)MAM5 - 516005A (METAINFOFAS)	5255
005050		MAM50001	5260
005057	2140	CONTINUE	5265
005042	2150	CONTINUE	5270
005062		IPALPOL	5275
005060		IF (MAM5.07.00) 2220,2100	5280
005071	2160	MAM50001 (IPAL)	5285
005073		PCAM3	5290
005075		PCAM3	5300
005100		PCAM3	5305
005101		PCAM3	5310
005105	2190	IF (L.EO.L2) 2200,2100	5315
005107		LIML	5320
005110		LAL2	5325
005111		2200 (L2)	5330
005113		2200 (L2)	5335
005114		CVX3	5340
005116		CVX3	5345
005117		CVX3	5350
005120	2200	GO TO 070	5355
005122		CVX3	5360
005124		CVX3	5365
005125		CVX3	5370
005126		LIML	5375
005131	2220	CONTINUE	5380
005133		MAM50001	5385
005134		MAM50002	5390
005136		GO 2200,2100	5395
005141		IF (MAM5.07.07) GO TO 2230	5400
005145		EX (MAM)MAM5 (M(3,IP))CUCS (METAINFOFAS) - 516005	5405
005145		VT (MAM)MAM5 - 516005A (METAINFOFAS)	5410
005146		MAM50001	5415
005146	2240	CONTINUE	5420
005141		GO 2200,2100	5425

005162	IF (ISS(J),RN,7) GO TO 2250	5430
005163	SAVE(SUM(SJ))	5435
005170	RATE5/SUM	5440
005172	APPENDATE(TMT)	5445
005174	IF (APP-ITL,9) APPEND-1	5450
005200	INT(J)0-APP/TPEN(J)	5455
005217	GO TO 2240	5460
005214	SAVE(SJ0(SJ1)-SI(J)00PU	5465
005217	APPEND(SI)/SUM	5470
005221	APPENDATE(TMT)	5475
005223	IF (APP-ITL,9) APPEND-1	5480
005227	INT(J)0-APP/TPEN(J)	5485
005230	CONTINUE	5490
005241	DO 233, I=1,100M	5495
005242	CALLS(I)	5500
005240	JUMPPOINT(I)	5505
005240	JUMPPOINT(I+1)	5510
005247	IVANNI	5515
005250	TWENTY(CX(J))	5520
005252	J11(J)01	5525
005253	ON 227, J=J11,02	5530
005253	TWENTY(CX(J))	5535
005257	IF (TMT,RN,TM2) GO TO 2270	5540
005261	IVAN02	5545
005262	J=J2	5550
005263	CONTINUE	5555
005260	IF (IVAN,RN,2) GO TO 2280	5560
005270	THISILLIENWE	5565
005270	WILLIETHU	5570
005273	GO TO 2330	5575
005277	CONTINUE	5580
005300	IF (J2-J1,67,1) CALL EXITD (11,1)	5585
005300	IF (K,64,7) GO TO 2310	5590
005312	CP(I),I)0,6	5595
005310	VP(I),I)0,6	5600
005320	VP(I),I)0,6	5605
005320	VP(I),I)0,6	5610
005327	VP(I),I)0,6	5615
005327	VP(I),I)0,6	5620
005333	CALL	5625
005334	GO 229, J=J1,02	5630
005336	ON 229, J=J1,02	5635
005341	ON 229, J=J1,02	5640
005343	ON 229, J=J1,02	5645
005351	ON 229, J=J1,02	5650
005352	ON 229, J=J1,02	5655
005361	ON 229, J=J1,02	5660
005365	ON 229, J=J1,02	5665
005373	ON 229, J=J1,02	5670
005377	ON 229, J=J1,02	5675
005400	ON 229, J=J1,02	5680
005405	ON 229, J=J1,02	5685
005411	ON 229, J=J1,02	5690
005410	ON 229, J=J1,02	5695
005420	ON 229, J=J1,02	5700
005421	ON 229, J=J1,02	5705


```

00014 SUMPTIME ANGLE (1.0101) 4C.VC.ANGLER.ANGLER.IFINU.SL)
00015 INRMS7.2997735)
00016 PR3.1159264
00017 XE1-BC
00018 YV1-VC
00019 IF (1.0101) GO TO 10
00020 IS=1
00021 Y=7
00022 IF (AMS(X1)LT.1."E-05.CH.AMS(Y)LT.1.0F-05) ANZ=
00023 11=2
00024 IF (XLT.0) 11=3
00025 IF (YLT.0) 12=3
00026 IF INM11012
00027 IF (IPIN.2.0.4) IF INCE1
00028 IF (IPIN.2.0.4) IF INCE4
00029 IF (IPIN.2.0.4) IF INCE2
00030 IF (IPIN.2.0.4) IF INCE3
00031 S=AMS(Y/Y)
00032 SL=PI/2.1-ATAN(SL)
00033 GO TO (30.40.50.60), IF INU
00034 ANGLESL
00035 GO TO 70
00036 ANGLE=SL
00037 GO TO 70
00038 ANGLESL=PI
00039 GO TO 70
00040 ANGLE=PI-SL
00041 ANGLE=ANGL
00042 ANGLE=ANGL*PI/PI
00043 GO TO 100
00044 CUMTIME
00045 IF (AMS(X1)LT.1.0E-05) GO TO 100
00046 ANGLE=PI
00047 GO TO 100
00048 IF (X) 12=130.110
00049 ANGLE=PI/2.
00050 GO TO 100
00051 ANGLE=3.001/2.
00052 GO TO 100
00053 CALL EATM (4,1)
00054 CALL EATM (4,1)
00055 IF INDE1
00056 GO TO 70
00057 PFT,MM
00058 END
00059
00060
00061
00062
00063
00064
00065
00066
00067
00068
00069
00070
00071
00072
00073
00074
00075
00076
00077
00078
00079
00080
00081
00082
00083
00084
00085
00086
00087
00088
00089
00090
00091
00092
00093
00094
00095
00096
00097
00098
00099
00100
00101
00102
00103
00104
00105
00106
00107
00108
00109
00110
00111
00112
00113
00114
00115
00116
00117
00118
00119
00120
00121
00122
00123
00124
00125
00126
00127
00128
00129
00130
00131
00132
00133
00134
00135
00136
00137
00138
00139
00140
00141
00142
00143
00144
00145
00146
00147
00148
00149
00150
00151
00152
00153
00154
00155
00156
00157
00158
00159
00160
00161
00162
00163
00164
00165
00166

```

REFERENCES

1. "Final Report on the Development of Analytical Techniques for Bellows and Diaphragm Design", by T. M. Trainer et al., Technical Report No. AFRPL TR-68-22, Air Force Rocket Propulsion Laboratory, March, 1968, AD828243
2. "Study of Zero-Gravity Positive Expulsion Techniques", Interim Report No. 8230-933007, Bell Aerosystems Co., April, 1964, (Contract NAS7-149) NASA Accession No. N64-27307.
3. "Finite Element Stress Analysis of Axisymmetric Solids with Orthotropic, Temperature-Dependent Material Properties", by E. L. Wilson and R. M. Jones, Air Force Report No. BSD-TR-67-228, Aerospace Corporation, September, 1967, AD820991.

Unclassified

Security Classification

DOCUMENT CONTROL DATA - R&D

(Security classification of title, body of abstract and indexing annotation must be entered when the overall report is classified)

1. ORIGINATING ACTIVITY (Corporate author) Battelle Memorial Institute Columbus Laboratories, 505 King Avenue Columbus, Ohio 43201		2a. REPORT SECURITY CLASSIFICATION Unclassified	
		2b. GROUP	
3. REPORT TITLE Final Report on the Development of the Tilt-Edge Bellows Concept			
4. DESCRIPTIVE NOTES (Type of report and inclusive dates) Summary of program activities from January 1, 1970 to September, 1970, under USAF Contract No. F04611-68-C-0031			
5. AUTHOR(S) (Last name, first name, initial) L. E. Hulbert, T. M. Trainer, N. D. Ghadiali			
6. REPORT DATE September, 1970		7a. TOTAL NO. OF PAGES 254	7b. NO. OF REFS 3
8a. CONTRACT OR GRANT NO. F04611-68-C-0031 <i>man</i>		9a. ORIGINATOR'S REPORT NUMBER(S)	
a. PROJECT NO. AFPPS. NO. 623058			
c. AFSC Project No. 3058		9b. OTHER REPORT NO(S) (Any other numbers that may be assigned this report) AFRPL-70-115	
d. Program Element No. 6.24.05.18.F			
10. AVAILABILITY/LIMITATION NOTICES This document is subject to special export controls and each transmittal to foreign governments or foreign nationals may be made only with prior approval of AFRPL (RPPR/STINFO), Edwards, California 93523			
11. SUPPLEMENTARY NOTES		12. SPONSORING MILITARY ACTIVITY Air Force Rocket Propulsion Laboratory Directorate of Laboratories Air Force Systems Command	
13. ABSTRACT <p>A two and one-half year program was conducted to investigate the tilt-edge bellows concept. This involved the idea that the stresses at the convolution root and crown welds of a welded bellows could be minimized by appropriately tilting the convolution mid surfaces near the root and crown. The research program involved an extensive theoretical analysis of various convolution cross-sectional shapes to optimize the shape with respect to the maximum stress as well as the weld bead stresses. A particular optimized bellows with a 3.5-inch OD was fabricated and tested. The results of the tests verified that the tilt-edge bellows had superior fatigue resistance. Further, the fatigue failures occurred at positions away from the welds which verified that the weld bead stresses were small. Elimination of fatigue failures at the convolution and end fitting welds also resulted in reduced scatter in bellows fatigue life. This should allow fatigue life predictions to be made with greater confidence for tilt-edge bellows than for conventional welded bellows designs.</p>			

DD FORM 1473
1 JAN 64

Unclassified
Security Classification

14. KEY WORDS	LINK A		LINK B		LINK C	
	ROLE	WT	ROLE	WT	ROLE	WT
Bellows Bellows Analysis Bellows Configuration Bellows Design Bellows Evaluation Bellows Manufacturing Elastic Analysis Linear Shell Analysis Metallic Bellows Nonlinear Shell Analysis Stress Analysis Welded Bellows						